

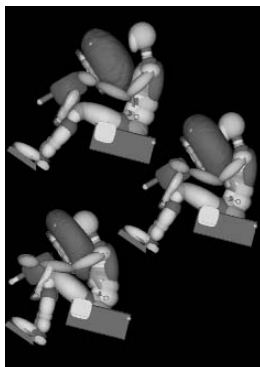


# TECHNICAL REVIEW

**2007 NO. 19**



**MITSUBISHI MOTORS**



- **Cover Photograph**

The cover photograph shows a simulation of the behavior of the driver side dummy of a vehicle equipped with a SRS knee airbag during a frontal impact. The driver side SRS knee airbag instantaneously deploys between the instrument panel and the driver's knees, directly restraining the driver's legs at the very beginning of the collision. Together with the upper-extremity restraint provided by the seatbelt and SRS front airbag, it enhances the efficiency of ride-down (absorption of the kinetic energy conferred on the driver by deformation of the vehicle body). As a result, the driver's kinetic energy is more effectively absorbed.

Published by Editorial Committee for the Technical Review  
c/o Environment & Recycling Affairs Dept.  
MITSUBISHI MOTORS CORPORATION,  
33-8, Shiba 5-chome, Minato-ku, Tokyo 108-8410, Japan  
Phone: +81-3-3456-1111  
Fax: +81-3-6852-5420

We welcome e-mail inquiries about this publication at:  
[technicalreview.et@mitsubishi-motors.com](mailto:technicalreview.et@mitsubishi-motors.com)



# MITSUBISHI MOTORS TECHNICAL REVIEW

2007 NO.19

## Contents

<b>Foreword</b> .....	4
-----------------------	---

### Technical Perspective

Continuously Providing Safety through the "Utmost Security" Efforts .....	6
---	---

### Technical Papers

Valve Jump Prediction Using Dynamic Simulation on Direct Acting Valve Train .....	19
Modeling and Control of Catalytic Reactions .....	25
Knowledge-Based Diagnosis – Failure Detection and Isolation by State Comparison with Model Behavior – .....	33
A Method for Analyzing Car Driver's Sensitivity to Stress and Comfort .....	40

### New Technologies

#### Special Feature Safety

Development of Inter-Vehicle Communication Type Driving Support System in the ASV-3 Project .....	46
GRANDIS ASV-3 – Unlikely to Strike, or Be Struck by, Another Vehicle – .....	51
Multi-around Monitor System .....	55
Development of Active Cornering Light System .....	59
Development of Driver Side SRS Knee Airbag .....	62
Development of Next-Generation Electric Vehicle "i-MiEV" .....	66
Newly Developed V6 MIVEC Gasoline Engine .....	71
Development of OUTLANDER's Emission Control System to Meet North American Super-Ultra-Low Emission Vehicle (SULEV) Standards .....	75
Newly Developed Six-Speed Automatic Transmission .....	80
Development of Inner Rail Type Power Sliding Door .....	85
New Aluminum Hairline Finish Decoration Process .....	89
Development of Plastic Fender for New DELICA D:5 .....	95
Development of Aluminum Space-Frame Body with New Structure in Front .....	101
Development of High-Efficiency MAC System .....	107

Photo on first page

The "Car School – Sporty Driving Course" is a hands-on safe-driving lesson for customers who drive sporty vehicles. It was held for the first time on October 15, 2006 at Mitsubishi Motors Corporation's R&D Center – Okazaki. The curriculum included full-force braking from high speeds and vehicle control on a slippery surface.



---

Digital Evaluation Method with VR Technology .....	111
Quick Heating Rear Heater System for the New DELICA D:5 .....	119
Comprehensive ECU Testing Using Simulation Tools .....	124
Development of High-Grade Sound System for Minicars .....	127
Development of High-Quality 5.1-channel Theater Surround System .....	130

### **Technical Topics**

“Car School” – Sporty Driving Course .....	134
--	-----

### **New Facilities**

Construction of Large Anechoic Chamber .....	136
--	-----

### **New Products**

eK WAGON and eK SPORT .....	141
PAJERO .....	144
DELICA D:5 .....	148
LANCER EVOLUTION IX MR and LANCER EVOLUTION WAGON MR .....	152

---



### **‘Pursuing the Origins of Car Engineering’ is Synonymous with ‘Striving to Satisfy Others’**

**Tetsuro AIKAWA**

Managing Director

Two years ago, we at Mitsubishi Motors Corporation (MMC) established the customer-communication phrase “Pursuing the Origins of Car Engineering” as a way to declare to society and ourselves that we are committed to providing “the utmost driving pleasure and safety” as stated in our corporate philosophy. Here, “the origins” refers to our customer-first approach, our corporate responsibility to society, the car engineering expertise that we have built over the years, and the Mitsubishi uniqueness that our customers expect. And “Pursuing the Origins” reflects our commitment to continuing to offer vehicles and services that meet customer expectations by focusing on what our customers really seek from our products while carrying forward the great resources we have created.

My personal interpretation of our customer-communication phrase is “a quest for the satisfaction of others” or “striving to satisfy everyone around you”, and I characterize the means to achieve this goal as “tireless pursuit of knowledge and technologies”.

I believe the origins of car engineering are all about focusing on how we at MMC can delight and satisfy those around us through the cars that we make. On an in-house level, each employee needs to consider how best to please his or her colleagues at all levels of the company. And on a wider level, each employee needs to consider how best to please customers, distributors, shareholders, and society as a whole.

To turn ideas into vehicles, all of us at MMC need to constantly try new approaches and technologies. New technologies are particularly important; even if we identify new customer needs, we can’t satisfy those needs without the necessary new technologies. In other words, new technologies are crucial for customer satisfaction.

Satisfying other people is far more pleasing than satisfying oneself. In this sense, too, then, satisfying everyone around oneself needs to be fundamental to the way everyone at MMC works. If we are ever in doubt as to which of two options is better, we must take the one that satisfies more people. And if we were ever to make a particular kind of car simply because it was the kind of car we wanted to make, we would probably be the only people satisfied by it. The only way to avoid this outcome is for each of us to be open-minded enough to listen to the opinions of others. The mistaken pursuit of self-satisfaction begins the moment any of us believes we are absolutely right. It is only when we focus on the basic goal of satisfying those around us that our work is worthwhile for our customers.

---

Today's automotive technologies offer a host of user benefits. But automobiles are also major causes of traffic accidents and environmental problems. We cannot say that we offer vehicles that satisfy our customers unless we strive to tackle these issues with all our resources. Traffic-accident deaths in Japan are declining thanks to efforts by concerned parties, but there are still more than a million casualties every year. Everyone engaged in automotive development has an obligation to make vehicles that help reduce traffic accidents even further; every accident prevented is a step in the right direction.

This issue of **MITSUBISHI MOTORS TECHNICAL REVIEW** contains a special feature about MMC's safety initiatives and latest safety technologies.

On the environmental front, global warming is as pressing an issue as exhaust emissions. We at MMC will continue with our efforts to develop cleaner and more fuel-efficient powertrains while accelerating our development of the MiEV electric cars, which we see as the ultimate clean vehicles.

By striving to please our customers with unique vehicles that are built upon our safety technologies, our environmental technologies, and the all-wheel-control technologies that we have used in vehicles such as the LANCER EVOLUTION and PAJERO, we at MMC are truly focusing on the origins of car engineering.

# Continuously Providing Safety through the “Utmost Security” Efforts

Hiroyuki ASADA\* Tetsushi MIMURO\*\*  
Toshiaki FUJINO\*\*

## Abstract

Mitsubishi Motors Corporation (MMC) is making efforts in various aspects of safety to continue providing our customers and society with “utmost security”, the company philosophy. Outlined here are recent automobile safety technologies in the fields of active safety and passive safety, as well as important social issues and activities for promoting safe driving habits.

**Key words:** Traffic Accident, Active Safety, Passive Safety, Education

## 1. Introduction

According to data from the World Health Organization (WHO), almost 1.2 million people die annually (over 3,000 people die each day) in road traffic accidents around the world, and another 20 – 50 million people suffer from injuries. This accounts for 2.2 % of deaths in the world and the estimated cost of traffic accidents on the roads is 518 billion US dollars. With automobile usage continuing to rise, especially in developing countries, road traffic accident deaths are forecast to rise to 2.3 million by 2020, placing it as the third most likely cause of death and injury, above both war and HIV<sup>(1)</sup>. (Table 1)

As realized from the above data, the road traffic accident is the most life threatening manmade disaster, not including disease. In its publication entitled “A 5-year WHO Strategy for Road Traffic Injury Prevention”, the WHO states “Countries need greater commitment to prevention. Provided there is adequate political will, millions of lives could be saved in the coming years”.

## 2. Activities by leading countries and the present status of road traffic accidents

In order to reduce traffic accidents, understanding their main contributing factors, which are interactions between road users, vehicles and the road environment, is necessary and taking a unified approach from all aspects including joint actions of all involved, starting with the government and on through the industry, medical professionals and citizens. Aiming at this goal, the governments of developed countries are now taking the lead in making a strong drive to implement political measures for the reduction of road traffic accidents. In the 50 signatory countries of the Organization for Economic Cooperation and Development (OECD) and European Conference of Ministers of Transport (ECMT), there has been a significant improvement in the conditions of road accidents since 1990. In the period from 1990 to 2004, despite a 30 % increase in the number of

**Table 1** Change in rank order for the world’s 10 leading causes of death between 1998 and 2020

1998	2020
1. Lower respiratory infections	1. Ischaemic heart disease
2. HIV/AIDS	2. Unipolar major depression
3. Perinatal conditions	3. Road traffic accidents
4. Diarrheal diseases	4. Cerebrovascular disease
5. Unipolar major depression	5. Chronic obstructive pulmonary disease
6. Ischaemic heart disease	6. Lower respiratory infections
7. Cerebrovascular disease	7. Tuberculosis
8. Malaria	8. War
9. Road traffic injuries	9. Diarrheal disease
10. Chronic obstructive pulmonary disease	10. HIV/AIDS

registered vehicles in these countries, there has been a 26 % decrease in fatalities and an 8 % decrease in injuries across all the 50 member countries<sup>(2)</sup> (Figs. 1 and 2). However, differences in culture, traffic conditions, and circumstances of the road have given rise to particularities in the accidents occurring across the countries (Fig. 3) despite similarities between them. For the areas of similarities, the United Nations ECE/WP.29 has adopted the global technical regulation (gtr) on vehicle safety, and the individual countries are resolving those areas that are particular to each country through individually planned measures.

### (1) European efforts

In 2002, the ECMT unanimously adopted the program to cut the fatalities caused by traffic accidents to 50 % of the level of 2000 by 2012 (Fig. 1). In response to this, the EU disclosed in 2003 a concrete action program entitled “European Road Safety Action Programme”, which aimed to cut the number of fatalities to 50 % of the 2000 level by the year 2010<sup>(6)</sup>. The program includes the following action items: road safety education and campaigns; implementation of political measures aimed at road users such as license sys-

\* Safety Testing Dept., Development Engineering Office

\*\* Environment & Recycling Affairs Dept., Corporate Planning Office

\*\* Advanced Vehicle Engineering Dept., Development Engineering Office

tems; implementation of political measures aimed at vehicles such as vehicle inspection systems and active and passive safety technologies; and implementation of political measures concerning road environment maintenance and accident analysis. These action items were updated by the 2006 mid-term follow up review. Especially noteworthy is the initiative called "eSafety" to promote the active safety using advanced communications and electronics technologies. This initiative aims at, amongst other things, increased installation of electronic stability control (ESC) systems as well as promotions for research and introduction of automated electronic accident emergency notification systems (eCall), intelligent speed adaptation (ISA) systems which give a warning when a vehicle exceeds the pre-established speed limit, collision warning/alleviating systems utilizing a 24 GHz short range radar, event data recorder (EDR, see Section 5.3), and a new and improved artificial satellite (Galileo) for fixing vehicles positions accurately.

Also, the EU is leading in making a new pedestrian protection gtr in cooperation with Japan as the second stage action following the directive that came into effect in 2003.

#### (2) US efforts

The US Transportation Secretary has taken on the challenge of "decreasing the mortality rate on US roads to 1.0 person (per one hundred million vehicle miles) by 2008" (Fig. 1), and in January 2005 the National Highway Traffic Safety Administration (NHTSA) re-released the five-year (2005 – 2009) plan for automobile road safety rules<sup>(7)</sup>. This plan puts forward eight priorities, the main five of which are as listed below:

- ① Decreasing risks to passenger cars due to the increase in sport utility vehicle (SUV) and small truck ownership, and lessening damage from sideways collision with such things as

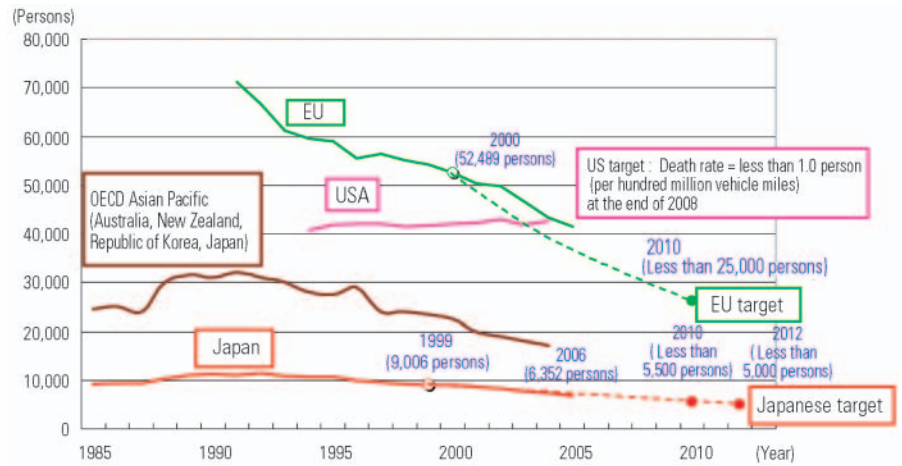


Fig. 1 Change in fatalities and their reduction targets in the three world regions<sup>(2)(3)(4)(5)</sup>

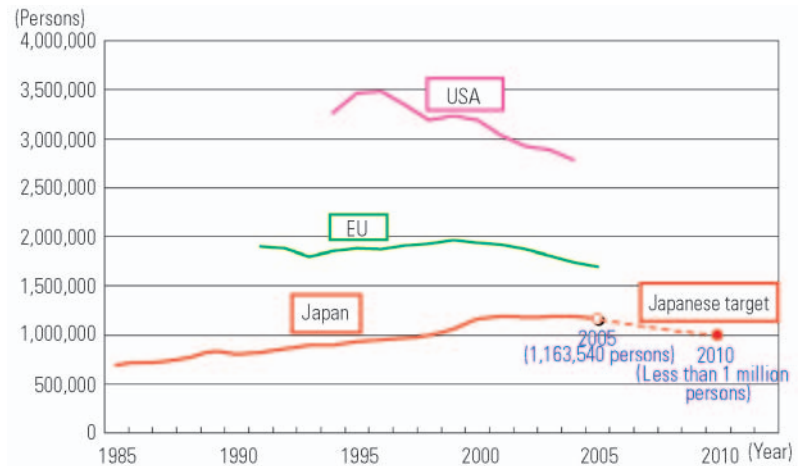


Fig. 2 Change in fatalities and injury accidents and their reduction targets in the three world regions<sup>(2)(3)(4)(5)</sup>

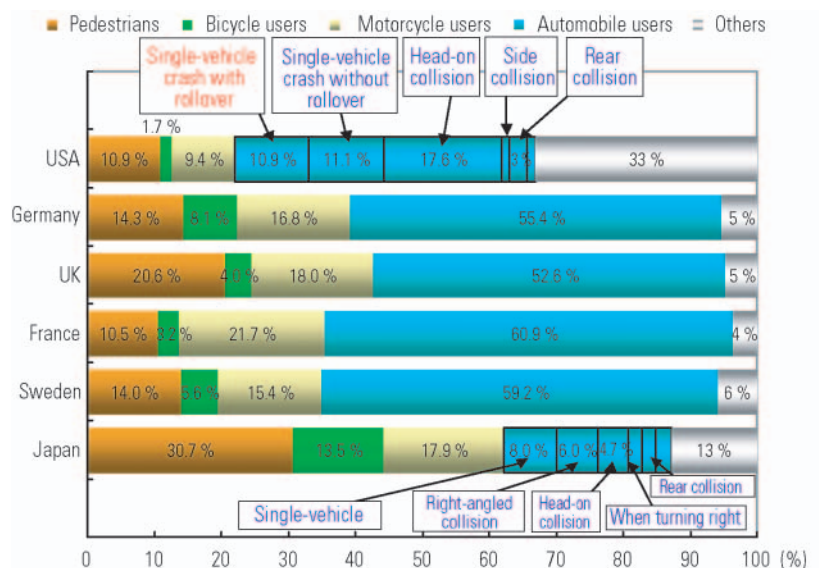


Fig. 3 Fatality by accident type in the six countries (2004)<sup>(5)</sup>



trees and utility poles.

- ② Preventing rollover accidents, the fatalities from which account for 30 % of all deaths, and preventing the ejection of passengers as well as protecting those not ejected during a rollover.
- ③ Accident avoidance and warning functions for passenger cars, improvement of visibility, tire safety, and limiting the decline of drivers' awareness.
- ④ Protection for children in vehicles.
- ⑤ Data collection as a measure to avoid collisions and standard equipment of EDR for later analysis of accident causes.

Also, the USA has taken the initiative in finalizing the world's first global technical regulation (gtr) regarding door latches, and is engaging itself in developing other global technical regulations for headrests and fuel cell powered vehicles.

#### (3) Japanese efforts

In 2003, former Prime Minister Junichiro Koizumi declared "Japan aims towards having 'the world's safest' roads (...) with the number of deaths from road accidents halved in 10 years from now". In 2006, the number of deaths was 6,352, the first time in 51 years that this figure has been in the low 6,000s and injuries also decreased showing a trend towards improvement. However, the number of deaths and injuries still showed a high standard (**Figs. 1 and 2**). In March 2003, the Japanese government produced the Eighth Fundamental Traffic Safety Program, in which it set up a program aiming at the following numerical objectives from the viewpoint of a transition into aging of the population with a low birth rate, securing pedestrian safety, raising awareness of traffic safety among citizens, and more utilization of information technologies<sup>(8)</sup>:

- By 2012, to reduce annual road traffic fatalities to less than 5,000 and make Japan's roads the safest in the world.
- By 2010, to reduce annual road traffic fatalities to less than 5,500.
- By 2010, to reduce annual road traffic casualties (fatalities and injuries) to less than 1 million.

In response to setting up of this program, the Automobile Traffic Subcommittee Meeting, Advisory Panel of Road Traffic Policy of the Ministry of Land Infrastructure and Transport of Japan published a report in June 2006, in which the meeting states that it is looking to "have a marked increase in the effectiveness of the active safety measures from 2010 and have a continued decrease in the annual death rate by 2015". In order to come up to this expectation, the following points were decided as vehicle safety plans to be implemented in the coming years:

- ① Dissemination and promotion for increased application of active safety technologies
  - Dissemination of collision mitigation brake systems and promotion for their increased application to large-sized vehicles
  - Full use of drive recorders for analysis of accidents and for effective evaluation of safety technologies (Section 6.2)

- ② Promotion of the development of advanced safety vehicles (ASV) using communications technologies (Section 4.4).
- ③ Promotion of measures against neck injuries (Section 5.1).
- ④ Promotion of the correct use of safety devices
  - ASV technologies (Section 4.4), rear seatbelts, headrests and tire pressure.
- ⑤ Measures for protecting pedestrians and elderly people (Sections 5.1 and 5.2)
  - Promoting development and introduction of global technical regulations (gtr) for pedestrian safety
  - Increased application of brake assist systems and its promotion
  - Promoting development of vehicles that can accommodate the varied physiques and builds of people including elderly drivers.
- ⑥ Introduction of compatibility standards and reinforcing accident analysis means through the use of EDR (Sections 5.1 and 5.3).

The Ministry of Land, Infrastructure and Transport will examine the best methods to implement the above points of the plan (while maintaining an organic unity between the safety standard, ASV promotional plans and car assessment). To the above list, the "measures against drunk driving" was added following the frequency with which tragic accidents have occurred since August 2006 due to drivers under the alcoholic influence.

#### (4) Efforts by other countries

As much as 90 % of road traffic accidents that occur around the world are in developing countries. In these countries, the loss and consequential cost to the society constitutes one of the contributing factors to stunting progress. In order to improve the road traffic safety on a world level, the leaders of the eight vehicle manufacturers (including MMC) held a summit meeting as part of cooperation to safety from the private sector at the Geneva Motor Show in February 2006, and agreed that by July 2008 (or by the next vehicle redesign stage) seatbelts are to be installed on all seats in all vehicles sold the world over<sup>(9)</sup>. It is expected that this will substantially improve road traffic safety, particularly in the developing countries where the motorization goes on growing rapidly.

### 3. MMC efforts for road traffic safety

"We are committed to providing the utmost driving pleasure and safety for our valued customers and our community". With this corporate philosophy in mind, MMC is aiming towards a society with minimum traffic accidents. To this end, MMC is developing new technologies in order to provide customers with the safest vehicles and is performing a variety of promotional activities to increase awareness in the safe use of vehicles. It is said that traffic accidents are caused by the 'human', 'traffic environment' and 'vehicle' factors, and out of these, the 'human' factor is mostly contributory to accidents, followed by the 'traffic environment' (**Fig.**

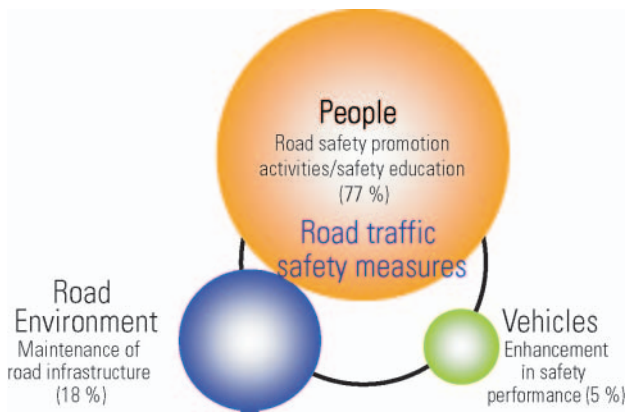


Fig. 4 Factors making up road traffic safety measures<sup>(10)</sup>

4). Having this notion as the base, MMC classified its products according to the class of customer, the destinations where vehicles are used differently, and the vehicle type segments, and the company then analyzed the accident data from markets for each vehicle segment to find the particularities attributable to the segment. Not limited to those accident types that are subject to regulations or car assessments, MMC has been and is now making constant effort toward achievement of its safety performance objectives. Also, MMC uses a special approach for enhancement of safety performance to deal with accidents specific to a particular vehicle segment. For example, most frequently occurring accidents common to all vehicle segments are those resulting from head-on collisions and leading to death of pedestrian, while the rate of driver fatalities from collisions between a mini-sized car and a heavier vehicle ranks highest when a female drivers drove the mini-sized car. Also, fatal accidents involving sporty cars most often occur without involving other vehicles and when they are running at high speeds, while a vehicle-to-vehicle collision involving an SUV most often cause fatalities on the part of the other vehicle.

The efforts mentioned above by MMC on the vehicle safety aspects, in conjunction with the intensification of traffic regulations as well as the improvement in road environment and medical technology proved to be effective. Fatalities from accidents involving MMC vehicles have been on a downward trend since 1995 in Japan (Fig.5). While concentrating on reducing fatalities from accidents, MMC is also making efforts, following the new objectives set out by the Japanese government, into reducing the number of traffic accidents and finding ways of lessening the incidents of whiplash or pedestrian leg injuries that can cause lasting disabilities.

#### 4. Active safety efforts

In the field of active safety, technology items that are subject to regulations and car assessment are continuing to increase, from which it seems that the trend of the safety interest is toward active safety rather than passive safety. One of the typical modern active safety

technologies is the Electronic Stability Control or ESC system (ESC will be used hereafter to represent this type of system because this acronym is becoming the standard name throughout the world although the system is called Active Stability Control or ASC at MMC). For external lighting, discharge headlights are becoming more prevalent and LEDs are used increasingly frequently as stop lamps and other small lamps. These lighting means contribute to enhancement in visibility both when they provide views and when they are seen. In recent years, driver assist systems using high tech solutions such as radar or cameras are attracting more attention in the active safety area. It is still hard to say if these high cost driver assist systems will become a legitimate part of the market, yet some of them will probably become standard safety installations in the near future.

##### 4.1 Vehicle motion control systems

###### (1) Accident reduction effect provided by ESC

The anti-lock brake system (ABS) is a most popular brake control system already being installed even in mini-sized cars. Recently, ABS is frequently combined with the electronic brake-force distribution (EBD) system for more effective braking. ESC is most effective when a vehicle is about to lose directional stability because the system can automatically apply an appropriate braking force independently to each of the four wheels to help regain the directional control. The effectiveness in reducing accidents of ESC is being studied all across the market in every area. Fig. 6 shows an example of the results from such a survey. Vehicles with ESC are about an average of 36 % less likely to be involved in accidents than vehicles without ESC for both single-vehicle crashes and head-on collision accidents for which ESC is believed to effective to prevent<sup>(12)</sup>. ESC is one of the few safety systems that have clearly demonstrated to be effective in making a marked decrease in accidents. A few years ago, ESC was an expensive piece of equipment but it is now becoming more affordable. The Mitsubishi OUTLANDER, which was launched into Japanese market in December 2005, has ESC fitted as standard. MMC endeavors to increase standard equipment of ESC on other models (Fig. 7).

###### (2) Mandatory installation of brake-assist systems and ESC

From around 2008, it is expected that the brake assist system, a device for providing more brake power during emergency braking, will be made a mandatory addition to vehicles in the European Union countries. Even now in Japan, a majority of vehicles are fitted with a brake assist system as standard equipment, but it may become necessary for automotive manufacturers to make new developments to meet the performance standards required by the relevant EU law in the not so distant future.

In the USA, ESC is finding increasing installation, especially on SUVs, as a measure to prevent rollover crashes. A law will soon be passed in the country demanding that all passenger cars, multi-purpose vehicles, trucks and buses with a 4,536 kg (10,000 pounds)

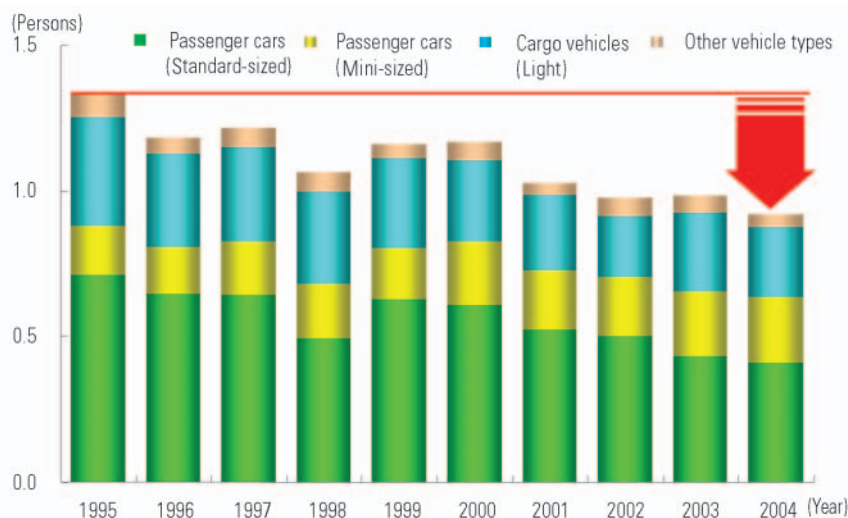
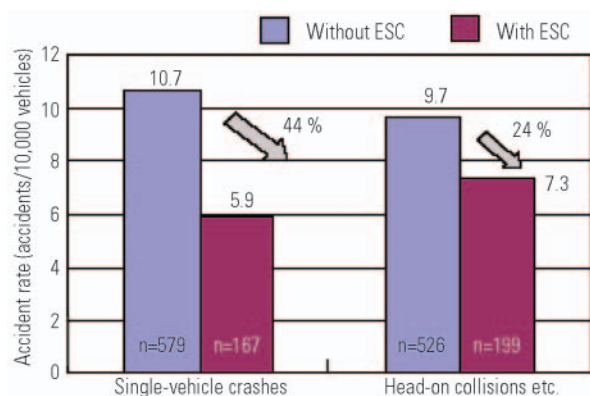


Fig.5 Change in fatalities involving MMC vehicles (per one million vehicles owned)<sup>(11)</sup>



The data are on the single-vehicle crashes and the head-on collisions etc. involving parties of the first part on regular roads and highways between 1992 and 2003. Alcohol or doze induced accidents are excluded. Head-on collisions etc. means "head-on collisions" on regular roads, and "impacting or contact accidents" excluding rear-end collisions on highways.

Fig. 6 Effects of ESC in reducing accidents<sup>(12)</sup>

or lighter gross vehicle weight (GVW) are to have ESC fitted as standard equipment, and it is expected that 100 % of vehicles will be required to be equipped with the device in the next few years (Fig. 8).

### (3) ESC as evaluated in car assessment

Until now, European car assessment did not have any active safety items in its rating items. However, the European car assessment homepage strongly recommends that users have ESC fitted<sup>(13)</sup>. Indeed, the homepage of Thatcham (the common name for The Motor Insurance Repair Research Centre, a member of the Association of British Insurers)<sup>(14)</sup> includes information concerning the availability of ESC on the car models from each manufacturer. In Japan, the braking distances on both dry and wet road surfaces of every car model have been published as car assessment test results. In addition to them, car assessment brochures published recently contain a list indicating the availabil-

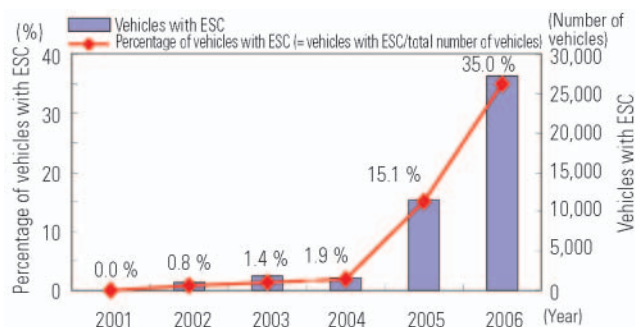


Fig.7 Increase in ESC equipped MMC vehicles in Japan (passenger cars and light trucks, not including mini-sized cars)

ity of safety devices, such as ESC, brake-assist systems, and ASV technologies for the vehicle models from each manufacturer.

## 4.2 Lighting systems

### (1) Emergency stop signal (ESS)

ESS is a system that causes the stop lights or hazard warning lights to flash rapidly (at a frequency of about 4 Hz) during an emergency braking maneuver to alert the drivers of following vehicles. The system is considered to be effective to reduce rear-end collisions, the most common type of accident. As a member of the Advanced Safety Vehicle projects ASV-2<sup>(15)</sup> and ASV-3 (see "GRANDIS ASV-3 – Unlikely to Strike, or Be Struck by, Another Vehicle – " in this issue of Mitsubishi Motors Technical Review), MMC has carried out the development of a system similar to ESS. In November 2006, the United Nations Economic Commission for Europe (ECE) adopted the regulation that approved ESS. Since the regulation will come into effect in the middle of 2007, Japanese automobile markets will soon see vehicles with ESS fitted.



**Fig. 8 Percentage of ESC equipped vehicles in the USA (Midsize moderately priced SUVs and Sedans)**

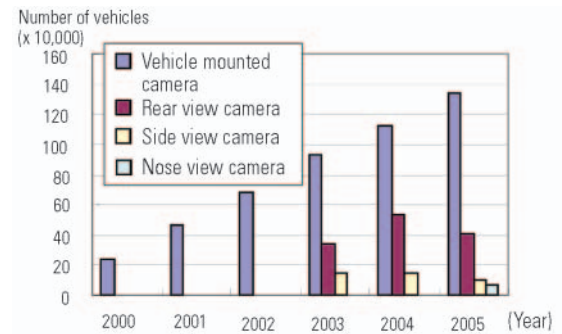
## (2) Adaptive front-lighting system (AFS) for winding roads

AFS automatically directs the headlamp beam in the direction of the driver's vision when driving on winding roads or turning a corner. The system is being commercialized recently. MMC has been developing AFS through the ASV-2 project<sup>(15)</sup>, while the company adopted a highly useful system named "Active Cornering Light System" on the DELICA D:5 which lights an inside cornering light also when turning the steering wheel (see "Development of Active Cornering Light System" in this issue of Mitsubishi Motors Technical Review).

### 4.3 Visibility and parking support systems

#### (1) Blind-spot cameras

The use of rear-view cameras for assisting the driver's rear vision when parking is continuing to spread. Nose cameras useful at junctions and side view cameras providing the driver with lower views on the opposite side are beginning to be fitted on certain vehicles (Fig. 9). The DELICA D:5 is equipped with a visibility assist system consisting of a nose-view camera (also capable of providing a downward view), side view cameras and a rear-view camera, in addition to an ultrasonic cornering sensor, also known as the "Multi Around Monitor". (See "Multi-Around Monitor System" in this



The data on vehicle-mounted cameras is from JEITA produced in Japan each year. Predicted numbers are shown for 2004 and 2005. The number of vehicles equipped with rear view and other cameras (passenger cars with manufacturer installed cameras) depends on such data as the announcement from the Ministry of Land, Infrastructure and Transport for each calendar year. The numbers of vehicles with side view cameras for 2003 and 2004 include those of the vehicles also equipped with nose view cameras.

**Fig. 9 Increase in number of onboard-camera-equipped vehicles**

issue of Mitsubishi Motors Technical Review.)

#### (2) Parking support systems

While primitive parking support systems only provide support to human perception using corner sensors and rear view cameras, recent systems provide judgments about the parking space and the timing of the driver's steering maneuver. Further advanced systems even provide automatic steering for movement into the parking place. Raising the parking space sensing accuracy is one of the most difficult challenges when developing such a system. Mitsubishi GRANDIS employs an arrangement that uses a nose view camera to determine positions, which is highly accurate and, in conjunction with audio guidance, makes the system very practical<sup>(16)</sup>.

### 4.4 Advanced driving support systems

Pre-crash safety systems using radar and cameras (such as collision mitigation brakes), adaptive cruise control (ACC) systems, lane keeping assistance systems, night vision assistance systems and other advanced driving support systems are arousing users' interests, especially in the Japanese market. These systems are also known as Advanced Safety Vehicle (ASV) technologies and the Ministry of Land, Infrastructure and Transport of Japan is working to promote their increased application. The 1995 model Mitsubishi DIAMANTE carried the world's first ACC system, using a combination of a laser sensor and a camera. The PROUDIA, the model MMC launched into the market in 2000, boasted a driver support system formed of the three functions, namely ACC, lane departure warning and side-rear monitor. Development of these systems made MMC a forerunner in the field. The ASV systems now on the market are the most often supplied as high-price options and although their installation is increasing, the actual number of vehicles with such systems is still extremely small (Fig. 10) and users' attention to them is as yet low. Development of ASV technologies is progressing at MMC (see "GRANDIS ASV-3 – Unlikely



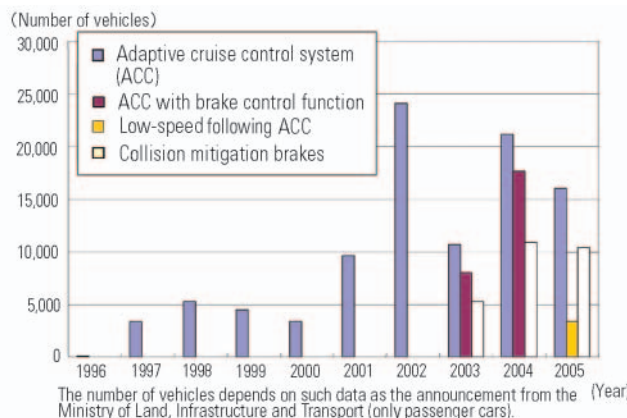


**Fig. 10 Increase in use of ACC and collision mitigations brake systems in Japan**

to Strike, or Be Struck by, Another Vehicle – ” in this issue of Mitsubishi Motors Technical Review) and they will be released at the best timing for commercialization.

#### (1) Collision mitigation brakes

Pre-crash safety systems are designed to set up seatbelts and other passive safety devices before a crash happens when they determine that a collision is unavoidable based on the traffic conditions in the road ahead as monitored with radars and other types of sensor. They also activate an automatic braking system known as “collision mitigation brakes” to reduce the crash speed of the vehicle to a certain extent. As the name “damage mitigation” suggests, the concept behind the system is to reduce the crash speed to a possible minimum when a collision is unavoidable. This system is developed on the base of the studies in the Phase 3 ASV project and turned into product under the 2003 technical guidelines of the Ministry of Land, Infrastructure and Transport of Japan. Emergency braking should occur 0.6 seconds before a crash (as roughly expressing the guideline). This timing was too imminent to the crash and thus the time is too short to produce an expected speed reduction. The later revision to the guideline allowed braking to start earlier, but in order to prevent the risk of accidental operation of the system, further development for higher sensing performance is necessary.

#### (2) Full speed range ACC

ACC measures the distance to the vehicle in front using laser sensors or extremely high frequency radar to always maintain an adequate distance to the preceding vehicle. It was originally intended for application in cruise-speed driving on a highway, so such an ACC is also known as a high-speed ACC. Recently, this system has begun finding applications expanded to low-speed operation areas such as following of the preceding vehicle in a traffic jam. However, about ACC for low-speed applications, there are differences between manufacturers in the opinion about system control methodology, such as whether the system should control the brakes until the vehicle comes to a complete stop; until when

the automatic braking should keep the vehicle stopped; and whether the vehicle should be restarted under the control of the system. Lacking in unity in manufacturer’s way of thinking about the system control design may be the concern that has influence on acceptability of the system by users. The International Standardization Organization is now in the process of working for integrating observations (ISO/TC204/WG14); it is important to pay attention to the process as the system is useful and contributes to safety (Fig. 11).

#### (3) Safe driving support systems using communications technologies

The autonomous systems installed on individual vehicles described until now have difficulty in preventing those accidents that result from running a car into another at right angles at an intersection, involve pedestrians suddenly moving onto the road, occur just after turning a curve, or are caused by other random events. Safety systems most expected against such types of accident are cooperative safe driving support systems in which on-vehicle systems coordinate with roadside systems or with other on-vehicle systems using communications technologies. In its New Information Technology Reforming Strategy of January 2006, the Japanese government announced a basic policy to “expand safe driving support systems using communications technologies to the whole of Japan by 2010”. Both the EU and the USA are also advancing the study of safe driving systems utilizing communications technologies.

MMC participated in the development of the Phase 3 ASV project, making the most of experience gained through building an information hotspot in the Mitsubishi IT-GRANDIS using communications technologies<sup>(17)</sup> (see “Development of Inter-Vehicle Communication Type Driving Support System in the ASV-3 Project ” in this issue of Mitsubishi Motors Technical Review). Its efforts will be continued in the Phase 4 ASV project that started from 2006.

## 5. Passive safety efforts

Regarding the passive safety of vehicles, each country stipulates performance standards as legislation for typical collision types, such as frontal, side and rear collisions, requiring manufacturers to comply with these standards. However, recently required of automotive manufacturers is not only compliance with these standards but also setting up their own policies to come up with the government’s objectives for reduction in road accident fatalities, through which they make a positive contribution to society. In line with this, MMC is aiming to set its standards even more strictly than those already laid out by legislation in order to reduce occupant injuries and damages as well as to give rescue and first aid for a one-level higher safety performance. Also, MMC’s efforts toward safety now being made is to adapt its originally developed technologies optimally to its products using the accident characteristic analysis results for every vehicle segment as mentioned earlier.



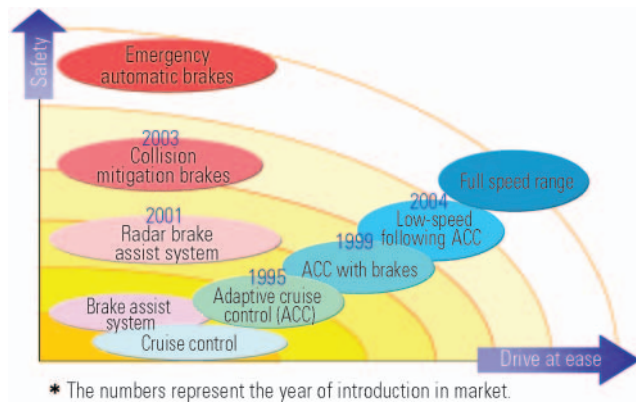


**Fig. 11 Development of longitudinal driving support systems**

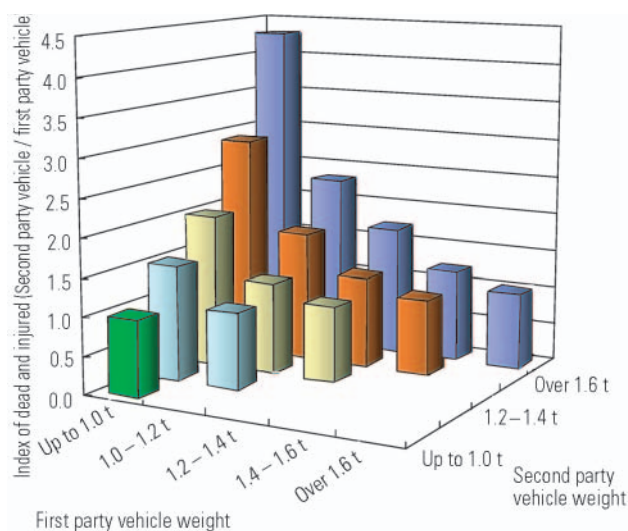


**Fig. 12 Fatalities and injury accidents caused by collisions between differently weighing vehicles (1993)<sup>(18)</sup>**

### 5.1 Vehicle occupant protection

#### (1) Enhancement of compatibility performance

Relieving the shock received by vehicle occupants during a crash as well as maintaining enough survival space in the cabin is most important when enhancing the passive safety. The Reinforced Impact Safety Evolution (RISE) body design MMC has employed since 1996 is one of the passive safety solutions based on this concept. Recently drawing increased attention as an additional regulatory measure to reduce the number of road traffic fatalities of which implementation is expected is the measure that deals with collisions of vehicles of different height and/or weight (compatibility), in addition to collisions of vehicles of the same class that are already covered by legislation (Fig. 12). The results of accident analyses revealed that the following types of collision lead to most serious consequences<sup>(18)</sup>:

- ① Sedans being forced under RVs because of the difference in height of the side members.
- ② Collisions involving a lightweight vehicle and a vehicle 1.5 times heavier.

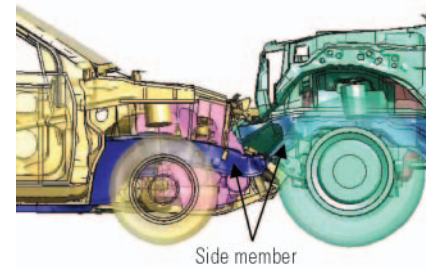


**Fig. 13 Partner protection design of new PAJERO**

In light of the above analysis results, MMC has been employing a partner protection design (a design to protect the other vehicle involved in an accident) for all SUVs from the OUTLANDER inclusive as measures against point ① above. Also, the New Model PAJERO has enlarged side member ends, which is an MMC original design to prevent the side members of all vehicles of a different height, from sedans to SUVs, from getting under the PAJERO's side members in a collision (Fig. 13).

As measures against point ② above, MMC has checked its mini-sized cars for self-protection performance through conducting offset impact tests using a vehicle 1.5 times heavier. The Mitsubishi "i" employs a rear midship-engine layout having the engine positioned in front of the rear wheels. This design allows for an increase in the side member cross section and employment of a trapezoidal cross member, both of which contribute to enhancement in strength of the passenger compartment and would otherwise not be realizable in a mini-sized car of the conventional design due to limited width. Having thus enhanced self-protection performance despite a short nose body uncommon to conventional cars of the same size, MMC realized a sort of "antinomy" with the Mitsubishi "i" (Fig. 14).

Another self-protection feature of the Mitsubishi "i" is the engine being located further back than the fuel tank. If a heavier vehicle crashes into the "i" from the rear, the car will be pushed forwards before the fuel tank and passenger compartment are crushed because of this engine and fuel tank layout. The car has thus substantially enhanced self-protection ability against rear collisions.

#### (2) Evolution of occupant restraint system

The following are all essential in protecting vehicle occupants in a collision: quickly restraining occupants with seatbelts; reducing loads on the occupants through the load control provided by both deceleration resulting from deformation of the vehicles front (ridedown) and deceleration resulting from restriction by the seatbelts; further decelerating occupant movements by airbags and other supplemental restraint systems (SRS); and cushioning the impact from the instrument panel and other dashboard components. Thanks to the enhancement of occupant restraint technologies in recent years, the number of fatalities from crash-caused head injuries has declined sharply (Fig. 15). Compared to fatalities

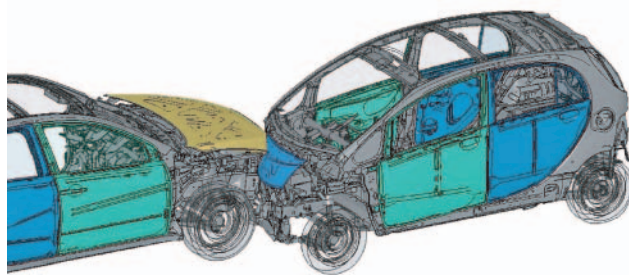


Fig. 14 Self protection design of Mitsubishi "i"

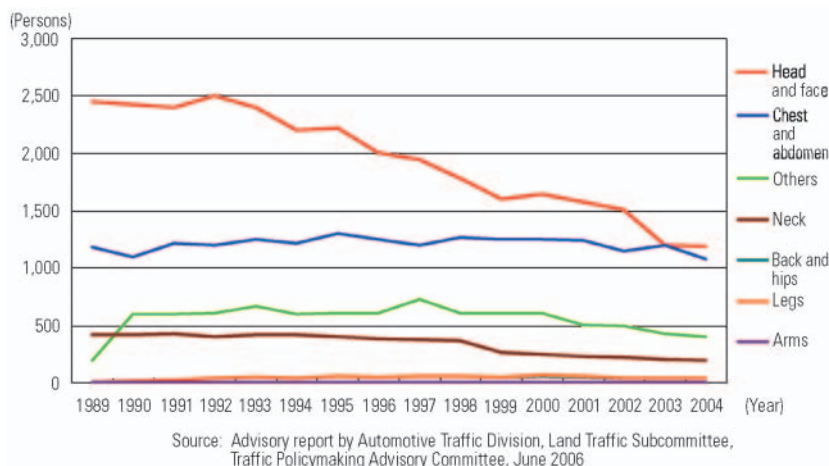


Fig. 15 Fatalities vs. major body parts injured<sup>(19)</sup>

due to head injuries, crash fatalities due to chest injuries show rather less reduction. Aged people especially are vulnerable to chest injuries and the death rate from both head and chest injuries is about equal<sup>(20)</sup>. In order to reduce chest injuries, minimizing chest flexure is considered most promising. One of the ways to reduce chest flexure is to increase the lap restraining force of the seatbelt while reducing its pressure on the wearer's chest.

On this point, MMC has set its own target pressure against injury from chest flexure, which is much lower than the legislation required critical pressure and the lowest in the industry. To increase the lap restraining force, the OUTLANDER is fitted with a lap pre-tensioner and the new DELICA and LANCER are fitted with knee airbags (see "Development of Driver Side SRS Knee Airbag" in this issue of Mitsubishi Motors Technical Review). Furthermore, the company adopted dual stage airbags that adapts the restraining force most appropriate to the severity of the impact by adjusting their output pressure.

### (3) Improving occupant retention in rollover accidents

In the USA, the rapid growth in popularity of vehicles with a high center of gravity such as SUVs and pickup trucks constitutes a cause of an increase in the probability of fatal rollover crashes, together with the lack of guard rails and other characteristic road forms as shown earlier (Fig. 3). Vehicle rollover is the top cause of fatalities in the accidents involving SUVs<sup>(4)</sup>. As men-

tioned earlier, electronic stability control (ESC) is effective to reduce rollover crashes. In addition to increasing vehicle's active safety performance using ESC or other safety devices, offering good protection in the event of a rollover is a known measure that has a positive effect on decreasing fatalities. When a vehicle rolls over, occupants are most likely to be ejected from the vehicle if they were not restrained by seatbelts. It is for this reason that, in order to promote the use of seatbelts, MMC introduced the seatbelt reminder system for the driver's seat beginning with the 2003 model year vehicles and, in addition, all new models after the GALANT are also equipped with a front passenger seatbelt reminder system.

Even occupants wearing seatbelts may be killed if their heads are ejected from the vehicle in a rollover crash. In order to tackle this, MMC has installed curtain airbags to prevent head injuries during rolling over on its products for the North American market, beginning with the 2007 ENDEAVOR, the American version of the OUTLANDER. In addition to the function of regular curtain airbags deploying in the event of a side collision, the MMC's system has a capability of sensing the vehicle's rollover behavior and causing the seatbelt pretensioners to operate simultaneously with deployment of the curtain airbags before the vehicle body hits against the ground. The system also has a function of elongating the time of retaining occupants' head inside the cabin by maintaining the curtain airbags inflated for a cer-

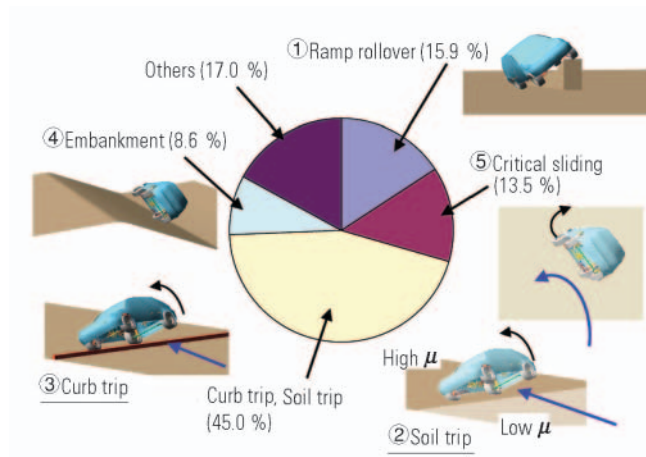


Fig. 16 Percentage of rollover accidents by type

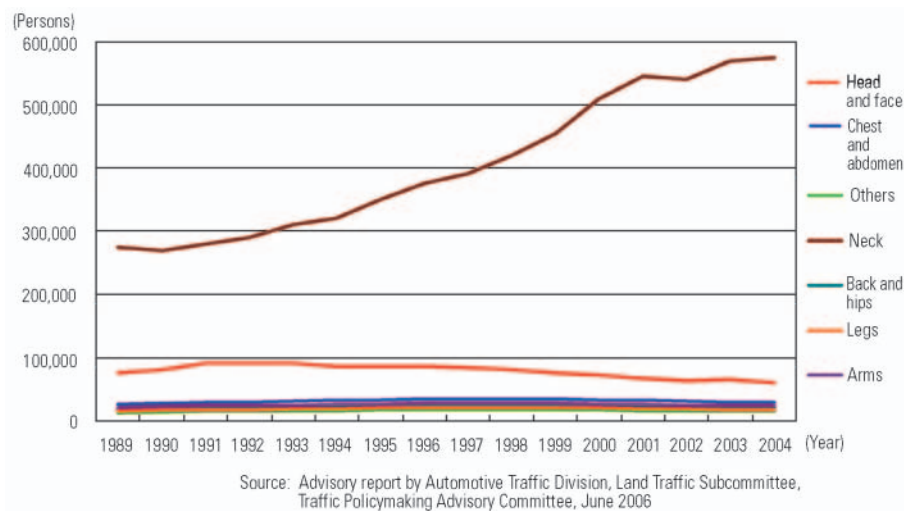


Fig. 17 Major body parts injured by accident<sup>(19)</sup>

tain period of time after deployment. Actual rollover crashes occurring in markets include many complicated phenomenal factors and there are no officially established test procedures. At MMC, the rollover crashes are classified into the following five categories: ① Ramp rollover; ② Soil trip; ③ Curb trip; ④ Embankment; and ⑤ Critical sliding (Fig. 16). For each of these categories, a test method is set up and the deployment and occupant retaining performance of the airbag system is evaluated.

#### (4) Enhancement in protection against whiplash

As mentioned above, fatal accidents in Japan are decreasing. However, the number of non-fatal accidents remains high with neck injuries on the rise (Fig. 17). Neck injuries are mostly caused by whiplash in low speed collisions, the main cause of which is thought to come from the S-shaped deformation of the cervical vertebrae which originates from the difference in movement between the upper body and the head in a rear-end collision<sup>(21)</sup>. An effective measure to reduce whiplash should be, therefore, to minimize the S-shaped deformation by appropriately restraining an

occupant with the seat and headrest. MMC has set the industry highest benchmark for S-shaped deformation reducing performance for seats and installed whiplash reduction seats on the Mitsubishi OUTLANDER, "i", eK WAGON and other recent MMC models that are designed to reduce the relative movement between the upper body and head more effectively than with the conventional seats (Fig. 18).

The USA is taking the initiative in forming a global technical regulation (gtr) for headrests and the work concerned is now in progress. Japan also made a proposal based on the results of researches including those carried out by MMC, and talks about its reflection into the regulation are under way.

## 5.2 Pedestrian protection

As shown above in the comparison of the number of fatalities by accident type in six countries (Fig. 3), the number of pedestrian fatalities in Japan and the UK are extremely high, showing that pedestrian protection is one of the major safety concerns for Japan. In the USA, the proportion of accidents causing pedestrian fatalities



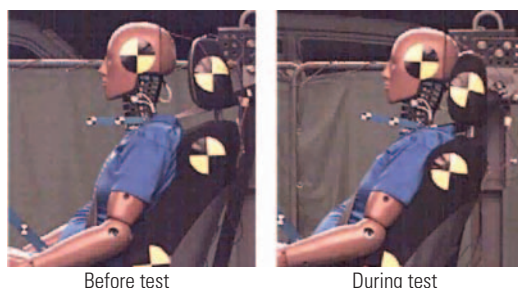


Fig. 18 New whiplash reduction seats of OUTLANDER

is small but has been on an increasing trend in recent years. Accidents involving pedestrians has now become a global problem. The majority of pedestrian fatalities are caused from head injuries, accounting for almost 60 %<sup>(18)</sup>. In Japan, legislation requiring all new vehicles to have an engine hood with certain level of performance to lessen the shock to pedestrian's heads on impact has come into force from September 2005. On the other hand, as high as 45 % of serious injuries are to the legs and, from October 2005, European legislation concerned has been applied to leg injuries. Japan is now presiding over the development of a gtr for leg injury prevention technologies by combining the relevant standards from various countries.

At MMC, the vehicle body design adopted for all its products after the OUTLANDER embodies further raised level of head impact damping performance. Especially with the OUTLANDER, a technology to reduce leg injuries is also incorporated in the vehicle design (Fig. 19).

### 5.3 Event data recorder (EDR)

In order to create effective vehicle safety measures, full analysis of an accident is necessary to provide enough fundamental data for the purpose. It is generally believed that use of data from an on-vehicle event data recorder (EDR) is of great effect for efficient accident investigation in addition to findings from traditional crash site examinations. In August 2006, the USA enforced the legislation that specifies among others the items to be recorded by an on-vehicle EDR and the format in which these items should be recorded<sup>(22)</sup>. Similar movements have begun in Europe and Japan to create the standards concerned<sup>(6) (23)</sup>.

At MMC, the OUTLANDER, new DELICA and LANCER are all fitted with EDRs that conform to the company standard for EDR, which was created using the US legislation as a guide. In a collision accident of a severity at which the airbag is caused to deploy, the airbag electronic control unit that functions also as EDR is capable of recording the vehicle speed, brake operations, acceleration of the vehicle body deformation and other data for the period just prior to and just after the crash. These data, being able to be retrieved as necessary using a special tool after the accident, greatly increase the accuracy and usefulness of the crash investigation. Also, in consideration of protecting customer privacy, the user's manual includes notes requesting

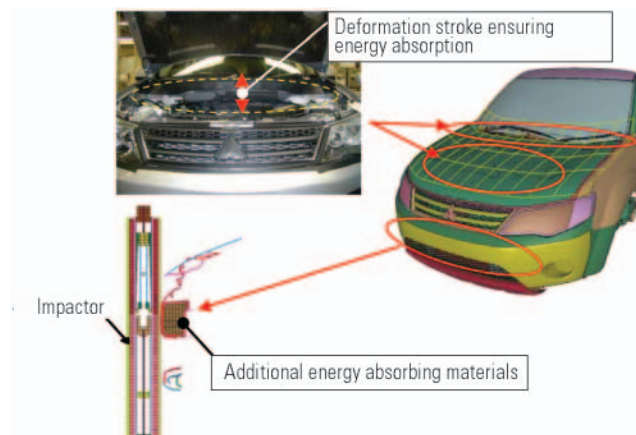


Fig. 19 Pedestrian protection design

customer's agreement about handling of the retrieved data.

## 6. Other efforts

### 6.1 Reaction to important social problems

Japan of tomorrow is expected to encounter various types of traffic-related problems, among which the biggest two that require special consideration are the sudden increase of elderly drivers and the growing number of elderly accident victims. Elderly drivers account for 25 % of all drivers who died in accidents while they are behind the wheel, and the number of accidental fatalities of elderly drivers will increase as the number of elderly license holders increases<sup>(23)</sup>. Decline in physical functions such as failing eyesight and slowing of reactions that come with aging constitutes important causal factors of an accident for both the party having caused an accident and the party having been involved in the accident. An approach from vehicle technology is as important as a socio-cultural approach to deal with this issue.

Recently, big accidents caused by driving under influence of alcohol have become a social issue, and the Japanese government is putting a lot of effort into its "Eradication of Drink Driving" policy<sup>(24)</sup>. As well as an intensified education and guidance against drink driving on the part of controlling party, an effective drink driving prevention means incorporated in vehicles is desired and it is a challenge the automotive industry should face.

### 6.2 Accurate accident analysis for proper evaluation of safety technologies

In recent years, the use of image storing "drive recorders" has been expanding in taxi and carrier companies. Images of an accident are effective for reducing accidents when used in safe driving education and facilitate post-accident handling when used for analyses<sup>(25)</sup>. Recorded images are also useful to know the actions of the driver during an accident, which in turn is beneficial for development of safety technologies. MMC will



Fig. 20 Safety promoting information (MMC homepage)

actively work on analysis of the mechanisms that lead to an accident in further details using drive recorders as well as on conventional accident analysis based on post-accident records.

Capability evaluation and effectiveness prediction of passive safety technologies is partially possible at present using collision test routines or their transposition into computer aided engineering (CAE) means. To develop active safety technologies, however, it is necessary to apply a different approach using such means as driving simulators and traffic flow simulation.

### 6.3 Education and activities for promoting road safety

In light of the notion that MMC should be active in contributing to those road safety education and promotion activity areas that are only appropriate for vehicle manufacturers to take care of, the company is making stronger efforts in the following activities for their enhancement.

#### (1) "Car School" MMC's safe driving program

The "Car School" is the education program aimed towards beginners and has had over 2,000 participants join since its beginnings in 1995. In 2006 the program included a "sporty driving course", in which MMC engineers of the vehicle development department served as instructors and the course participants could experience vehicle's marginal behaviors (see "Car School" – Sporty Driving Course in this issue of Mitsubishi Motors Technical Review).

#### (2) Donation of safety promoting information

In order to drive safely, drivers need knowledge of actual crash conditions on the marketplace and the correct usage of safety equipment. MMC has been making safety information available on the Internet and in pamphlet form (Fig. 20).

## 7. Conclusions

Cost, weight and space are the factors that must be spared for a new safety technology when incorporating it in a vehicle. The price of ABS was as high as 300,000 Yen when it was first introduced, although it is now standard equipment in most vehicles. MMC understands that continuing challenges to various approaches while keeping dreams alive is the way the company should select when endeavoring after the development of a new technology that will certainly lessen casualties

and damages from accidents and will form a safety device that will become standard equipment for all vehicles including mini-sized cars in the future, even if it is costly at first.

### References

- (1) [http://www.who.int/world-health-day/2004/infomaterials/world\\_report/en/summary\\_en\\_rev.pdf](http://www.who.int/world-health-day/2004/infomaterials/world_report/en/summary_en_rev.pdf), April 2004
- (2) Country Reports on Road Safety Performance, September 2006  
<http://www.cemt.org/JTRC/WorkingGroups/RoadSafety/Performance/TS3-report.pdf>
- (3) CARE (EU road accident database) or national publications, July 2006
- (4) National Highway Traffic Safety Administration (NHTSA): Traffic Safety Fact 2004
- (5) Cabinet Office, Government of Japan: "White Paper on Traffic Safety in Japan 2006"
- (6) European Communities: European Road Safety Action Programme, 2003
- (7) NHTSA: Safety Rulemaking and Supporting Research Priorities – January 2005
- (8) Cabinet Office, Government of Japan: The Eighth Fundamental Traffic Safety Program, March 2006
- (9) Global Automotive Industry Meeting  
[http://www.acea.be/ASB20/axidownloads20s.nsf/Category2ACEA/13620770D52DCCF2C1257125002C5EEE/\\$File/20060439att01.pdf](http://www.acea.be/ASB20/axidownloads20s.nsf/Category2ACEA/13620770D52DCCF2C1257125002C5EEE/$File/20060439att01.pdf), April 2006
- (10) Institute for Traffic Accident Research and Analysis: The Eighth Road Traffic Accident Investigation and Analysis 2005
- (11) Institute for Traffic Accident Research and Analysis: Road Traffic Accident Data (accidents involving Mitsubishi vehicles), 1995 – 2004
- (12) National Agency for Automotive Safety & Victims' Aid (NASVA): "Results of Examination on the Effect of Stability Control System", press information, February 18, 2005
- (13) [http://www.euroncap.com/content/safety\\_ratings/recommendation.php](http://www.euroncap.com/content/safety_ratings/recommendation.php)
- (14) <http://www.thatcham.org/safety/>
- (15) Mitsubishi Motors Technical Review No.14, 2002
- (16) Mitsubishi Motors Technical Review No.18, 2006
- (17) <http://www.mitsubishi-motors.co.jp/corporate/technology/safety/it-grandis.html>
- (18) Road Transport Bureau, Ministry of Land, Infrastructure and Transport: "The Current Status of Vehicle Safety Measures", November 2005
- (19) Automotive Traffic Division, Land Traffic Subcommittee, Traffic Policymaking Advisory Committee of the Ministry of Land, Infrastructure and Transport: "Desirable Vehicle Safety Measures of Tomorrow towards a Road Traffic Accidents Free Society", advisory report, June 2006
- (20) Institute for Traffic Accident Research and Analysis: ITAR-DA Information, No. 41, 2003
- (21) K. Ono, S. Inami, K. Kaneoka, T. Gotou, Y. Kisanuki, S. Sakuma and K. Miki, Relationship between Localized Spine Deformation and Cervical Vertebral Motions for Low Speed Rear Impacts Using Human Volunteers, 1999 IRCOB Conference, p.149 – 164, 1999
- (22) NHTSA: Event Data Recorders, NHTSA-2004-18029, RIN



2127-A172

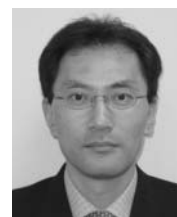
- (23) Traffic Bureau, National Police Agency: Characteristics of Fatal Road Traffic Accidents in 2005 and Policing Activities for Traffic Violation, January 26, 2006
- (24) Task Force on Transportation, Central Committee on Traffic Safety Measures: "Eradication of Drunk Driving", September 15, 2006
- (25) Road Transport Bureau, Ministry of Land, Infrastructure and Transport: "FY 2005 Report on Survey of Effectiveness of Installing Image Recording Drive Recorders on Vehicles"



Hiroyuki ASADA



Tetsushi MIMURO



Toshiaki FUJINO

# Valve Jump Prediction Using Dynamic Simulation on Direct Acting Valve Train

Akihiro FUJIMOTO\* Hirofumi HIGASHI\* Noritsugu OSAWA\*  
Hideo NAKAI\* Tokiichi MIZUKAMI\*

## Abstract

With regard to the direct acting valve train that has high stiffness in nature, it is generally believed that the valve spring surge is the sole and primary cause that induces valve jump. As Mitsubishi Motors Corporation (MMC) employs direct acting valve trains for its new model engines, clarifying the valve jump generating mechanism is essential for future improvement in product performance. In the study described in this paper, an analysis of the valve jump generating mechanism and prediction of the valve jump occurrence engine speed were conducted by calculating surge-induced valve spring load fluctuation, a difficult parameter to actually measure, through simulation using the commercially available software ADAMS/Engine valve train. It was confirmed that the valve jump occurrence engine speed predicted using the valve spring models created for this study agreed well with the results of actual tests.

**Key words:** Direct Acting, Valve Jump, Valve Spring, Surging, ADAMS

## 1. Introduction

Under the present circumstances of increasingly stringent regulations on fuel consumption and emission control, one conceivable solution for assuring continuation of MMC's "sports car line" is to increase the power output of naturally aspirated engines by increasing the speed.

However, one of the problems with high-speed engine operation is a phenomenon called "valve jump", in which intake and exhaust valves unexpectedly lift up and lose contact with the cam surface. Valve jump causes such problems as valve-to-piston interference and breakage of parts due to the shock when valves are resealed.

MMC's new model engines 4B1, 4A9 and 3B2 employ a direct-acting, double-overhead camshaft (DOHC) design advantageous for high-speed operation. However, it is conceivable that the direct-acting valve train is likely to induce valve jump due to load fluctuation of the valve spring resulting from spring surge although it offers such merits as higher stiffness, quicker opening and closing valve motions, and smaller valve spring load compared to the roller-type rocker arm valve train that MMC has thus far employed.

This paper presents the results of a study conducted by means of dynamic simulation of valve springs to clarify the mechanism that induces valve jump.

## 2. Valve jump

Under normal conditions, the valve train components including the valve, tappet, spring retainer and cotter are pressed against the cam surface by the valve

spring (Fig. 1) and move up and down while maintaining contact with the cam lobe as the camshaft rotates.

The force pressing these components against the cam surface is given as the difference between the valve train inertial force and the valve spring force. When the inertial force increases as the engine speed increases, the pressing force decreases in the region that has a negative inertial force. When the pressing force further decreases to zero, the set of valve train components loses contact with the cam lobe surface and valve jump occurs (Fig. 2).

When predicted based on the static spring load that varies with the amount of valve lift as shown in Fig. 2, valve jump should occur at a speed of  $9,300 \text{ min}^{-1}$  in the model used in this study.

However, because a resonance phenomenon called surge occurs in the valve spring and the valve spring load fluctuates during high-speed engine operation, jump occurs actually at a speed lower than the speed predicted based on static valve spring load. For this reason, prediction should be based on dynamic valve spring load derived from simulation or other appropriate methods.

## 3. Dynamic simulation of valve train

"ADAMS/Engine valve train" was used for dynamic simulation of the valve train.

This software is capable of including the stiffness of rocker arms and other valve train components as parameters. However, assuming that the valve, tappet, retainer and cotter are sufficiently stiff to prevent the generation of vibration that might affect valve jump, the simulations were conducted in this study with only the

\* Advanced Powertrain Development Dept., Development Engineering Office

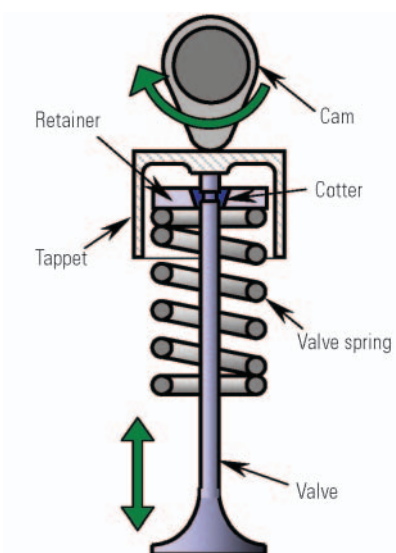


Fig. 1 Components of valve train

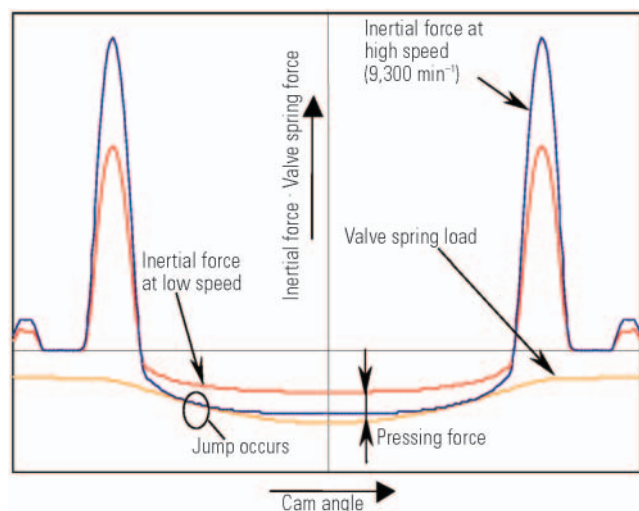


Fig. 2 Inertial force of valve train and valve spring load

valve spring regarded as an elastic body and all other components as rigid bodies. The valve spring was modeled by dividing the spring coil into four sections, each being formed by rigid-body spring model elements, i.e., the mass point, spring and dashpot as shown in Fig. 3.

### 3.1 Evaluated spring models

Two-stage, variable-pitch coil springs generally used as valve springs provide the effect of damping the resonance generated in them when the spring wire turns of the close-coiled section come into contact with each other.

Two types of springs were used as the simulation models, each having a different close-coiling ratio (given by dividing the number of close-coiled turns by the number of active coils) as shown in Table 1. The two springs were the same in static load characteristics and

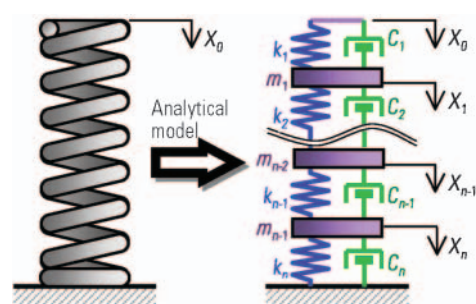


Fig. 3 Analytical model of valve spring

Table 1 Valve spring specifications for analysis

		Spring A with small close-coiling ratio	Spring B with large close-coiling ratio
Set load	(N)	180	180
Load at maximum load	(N)	470	470
Close-coiling ratio (number of close-coiled turns/ number of active coils)		0.18	0.39
Number of active coils		6.73	7.35
Number of open-coiled turns		5.49	4.46
Number of close-coiled turns		1.24	2.89
Natural frequency	(Hz)	543	644

installed dimension but differed in close-coiling ratio and dynamic characteristics of natural frequency. Due to these differences, the two springs were assumed to differ in resonance conditions and thus cause valve jump at different engine speeds.

Fig. 4 shows images of these two springs as installed in the cylinder head. It is clear that their close-coiling to open-coiling ratios differ and that the close-coiled turns come into contact with each other.

### 3.2 Valve spring characteristics

First, the behavior of each valve spring in the non-installed state was simulated to confirm how the software reproduced the spring's dynamic characteristics.

Fig. 5 shows chronologically arranged images of a surging spring thus simulated. The series of images shows satisfactory reproduction of spring resonance in which compression wave move vertically and repeatedly. Fig. 6 compares two springs to show the effect of close-coiled turns. It shows the spring load amplitudes that result in Spring A and in the model created from Spring A by removing the close-coiled section when extremely small amplitude of displacement is applied to both models. The spring without close-coiled section shows a quick rise in load fluctuation at a frequency nearly the same as its design natural frequency, which indicates the generation of resonance. The spring with close-coiled section, on the other hand, shows as much as 75 % reduction in load fluctuation compared with the other spring, indicating the significant surge damping effect of the close-coiled turns. Fig. 7 compares Spring A and Spring B on which the same simulation as the above was conducted. The close-coiling ratio of Spring

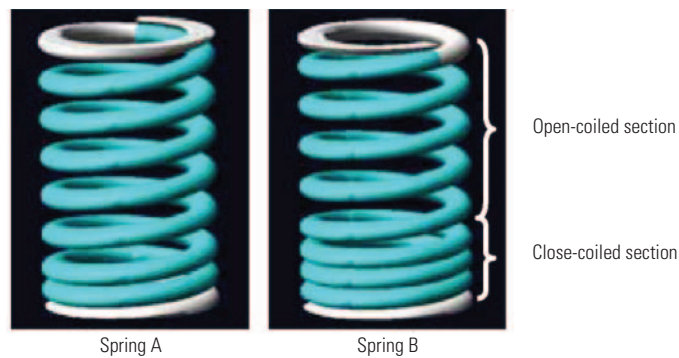


Fig. 4 Image of valve springs

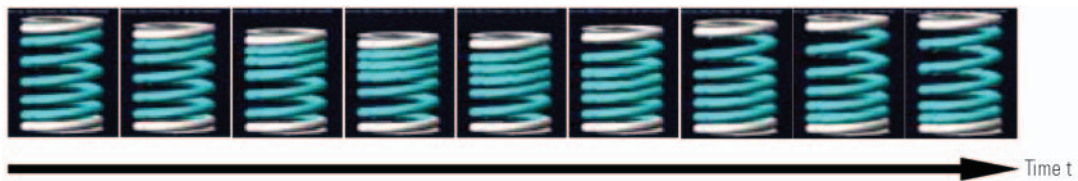


Fig. 5 Images of valve spring surge

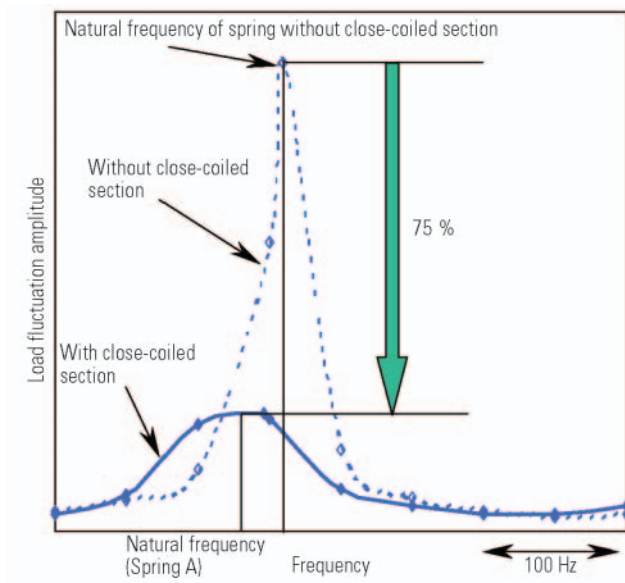


Fig. 6 Surge damping effect of close-coiled section

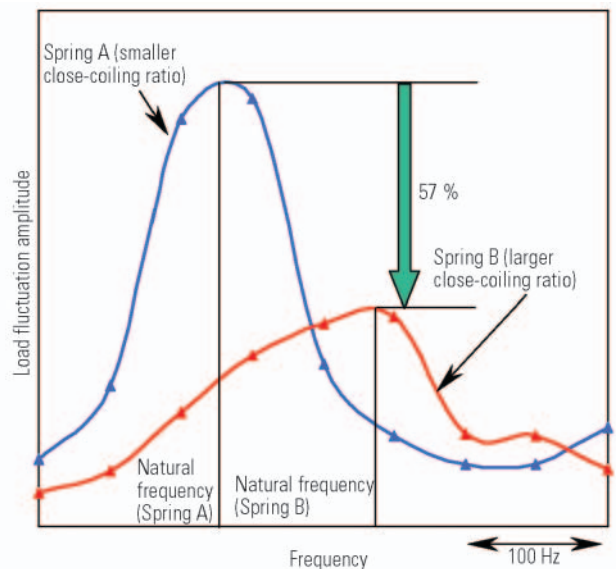


Fig. 7 Resonance characteristic of valve springs

B is more than twice that of Spring A and this provided Spring B with the effect of lowering the peak load amplitude by approximately 60 % compared with Spring A. Since the installed dimension of Spring B is the same as that of Spring A but Spring B has an increased number of close-coiled turns and a reduced number of open-coiled turns, the consequent higher natural frequency caused the peak load fluctuation point to shift toward the high-frequency side when compared with that of Spring A. This suggests that the difference in valve spring characteristics causes a difference in the jump occurrence engine speed.

### 3.3 Valve jump prediction

With actual engine operating conditions imitated, valve jump was predicted by calculating the above-mentioned spring load fluctuations.

Assuming all valve train components other than the valve spring as forming a rigid body, their mass was applied to the top of the spring and the valve lift was given in accordance with the cam lobe profile.

Fig. 8 shows the inertial force of an acting valve train at  $8,000 \text{ min}^{-1}$  and fluctuation in valve spring load when Spring A is used for the valve.

The simulation-predicted dynamic spring load fluctuation

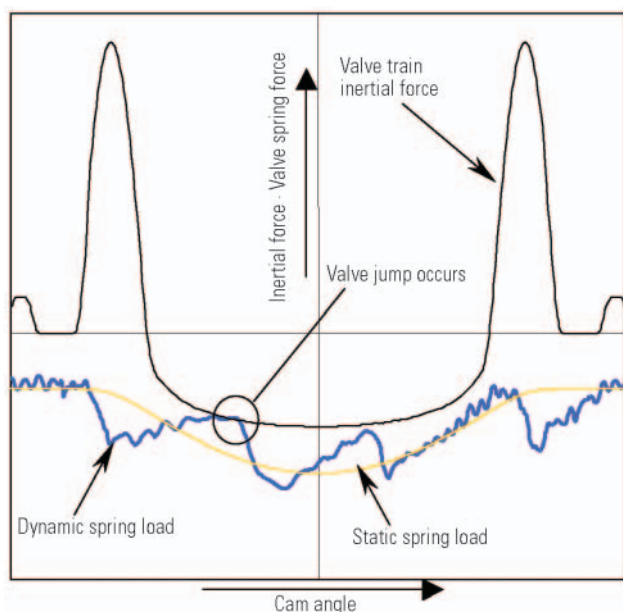


Fig. 8 Spring A's load fluctuation at 8,000 min<sup>-1</sup>

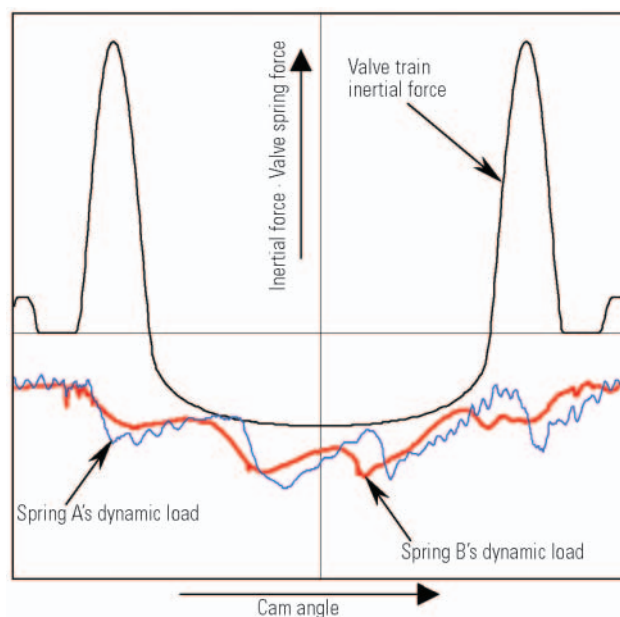


Fig. 9 Load fluctuation vs. spring characteristics at 8,000 min<sup>-1</sup>

tuates significantly and its curve has a section crossing the inertial force curve, which can be interpreted as the engine speeds at which valve jump occurs due to dynamic fluctuation of spring load.

The valve jump occurrence engine speed predicted based on static spring load is 9,300 min<sup>-1</sup> as shown in Fig. 2, which is lower than the actual valve jump occurring engine speed by as much as 1,300 min<sup>-1</sup>. Fig. 9 compares the simulation results for Spring A and Spring B. Being smaller in load fluctuation than Spring A, Spring B has no occurrence of valve jump, which indicates that the valve jump occurrence engine speed differs depending on the spring's dynamic characteristics. When the simulated engine speed was raised, valve jump occurred with Spring B at 8,500 min<sup>-1</sup> (Fig. 10).

#### 4. Results of tests on actual engine

The most desirable method for confirming the above simulation results using an actual engine is to directly measure the spring load or determine valve jump occurrence by measuring the load acting between the cam and tappet. However, since measuring these loads on an actually operating engine is extremely difficult, indirect measurement was applied to the actual engine tests, in which the valve jump occurrence engine speed was detected by measuring the valve lift, while the surge level was determined by measuring the distortion of the valve spring.

##### 4.1 Detection of valve jump occurrence

Under the same conditions as those for the simulations, valve lifts were measured using an engine motorizing tester.

In the test with Spring A installed, a sign of valve jump was detected at speeds beginning with 8,000 min<sup>-1</sup>

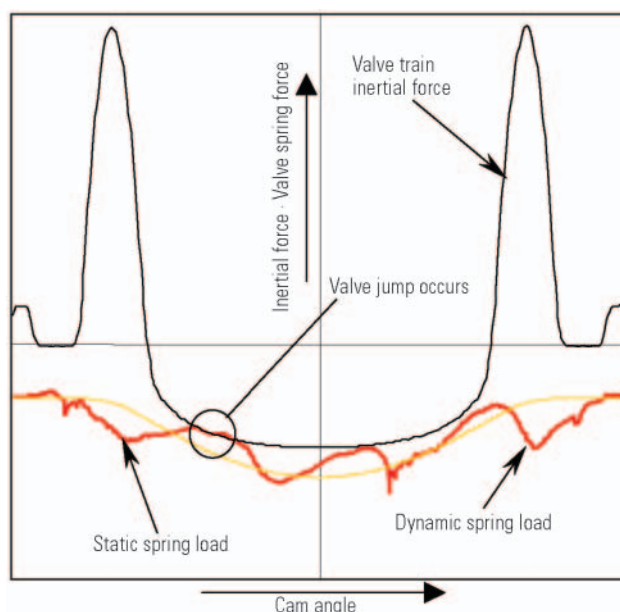


Fig. 10 Spring B's load fluctuation at 8,500 min<sup>-1</sup>

(the simulation-predicted jump occurrence speed for the spring) and jumps were evident at 8,500 min<sup>-1</sup>. Fig. 11 shows the valve lift curve obtained from the measurement at 8,500 min<sup>-1</sup>.

In the test conducted with Spring B installed, a sign of valve jump appeared at 8,500 min<sup>-1</sup> (the simulation-predicted jump occurrence speed for the spring) and became evident at 9,000 min<sup>-1</sup>. The curve shown in Fig. 12 represents the valve lift measurements at 9,000 min<sup>-1</sup>.

It should be said that the test measurements satisfactorily proved that the valve jump occurrence engine speed varies depending on the difference in characteristics of the valve springs.



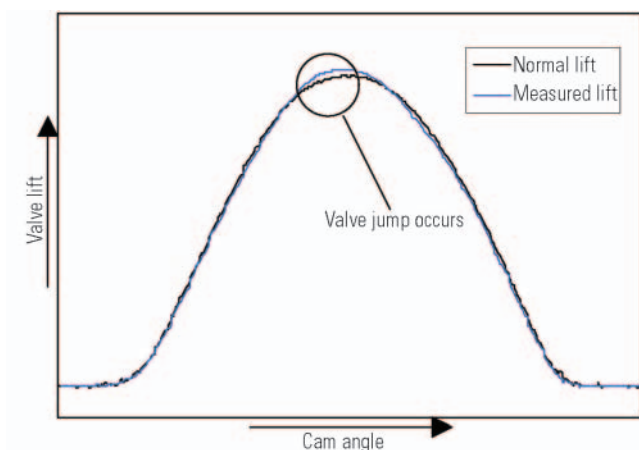
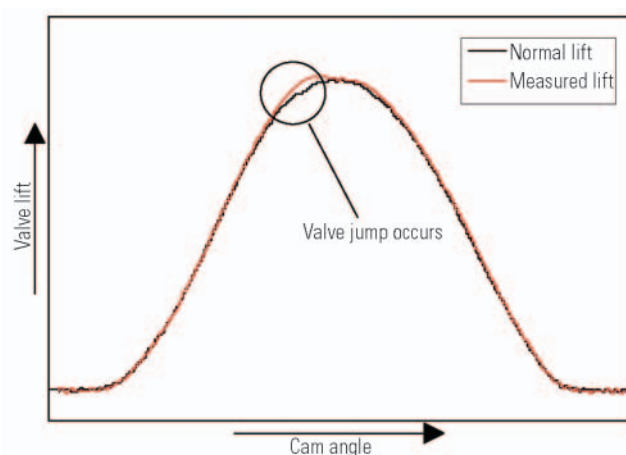
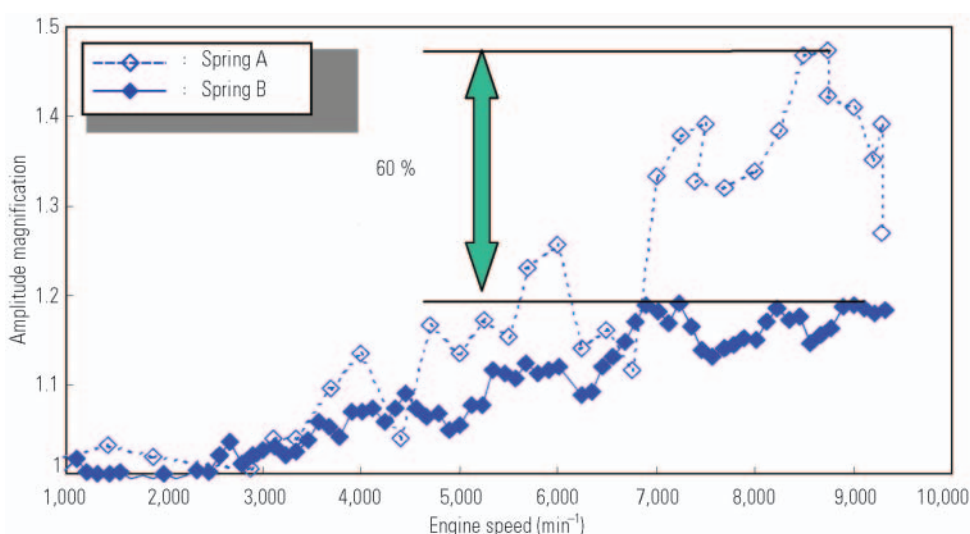
Fig. 11 Valve jump at 8,500 min<sup>-1</sup> with Spring AFig. 12 Valve jump at 9,000 min<sup>-1</sup> with Spring B

Fig. 13 Amplitude magnification of valve springs

#### 4.2 Measurement of amplitude magnification

Fig. 13 shows the amplitude magnification of the two valve springs. The amplitude magnification refers to the ratio between the distortion of a valve spring caused by static displacement given to the spring and the distortion of the spring measured on an actual engine, and indicates the surge level of the spring. It also indirectly indicates the load fluctuation of the spring.

The amplitude magnification of Spring A is relatively high with the peak reaching a ratio close to 1.5, while that of Spring B is low with a peak approximately 60 % lower than that of Spring A. This proves that the simulated difference in dynamic characteristics of the springs also holds true on an actual engine.

In addition, the difference in amplitude magnification between the springs shows values quite similar to the difference in resonance level of the non-installed springs shown in Fig. 7, which means that the simulation models closely imitate the conditions existing in the actual engine.

#### 5. Summary

Dynamic simulation of the direct-acting valve train using the commercially available software ADAMS/Engine valve train and valve jump and other measurements on an actual engine revealed the following:

- During high-speed operation, the spring load significantly fluctuates due to valve spring surges.
- Spring load fluctuation varies with spring characteristics such as the close-coiling ratio and natural frequency.

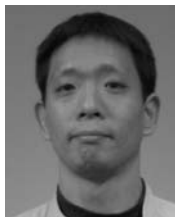
For the above reasons, predicting the valve jump occurrence speed on a direct-acting valve train requires prediction of dynamic load fluctuation of valve springs and ADAMS/Engine valve train is useful software for this purpose.

## 6. Postscript

Because the software used for the described simulation requires several hours to create the model of a spring, it would be indispensable to devise, for example, a method to minimize variations using a simpler analytical technique in order to handle a number of spring types. The authors intend to continue their efforts to develop such a technique.

### References

- (1) Ishikawa, Kitahara and Kato: Study on Surging of Valve Springs in High-speed Internal Combustion Engines, JSAE, Proceedings of Symposium 936, October 1993
- (2) Kurusu, Hatamura, Omori and Nomura: Discussion about Jumps and Bounce of Valve Train Mechanism, Mazda Technical Review, No. 9, p. 138, 1991



Akihiro FUJIMOTO



Hirofumi HIGASHI



Noritsugu OSAWA



Hideo NAKAI



Tokiichi MIZUKAMI

# Modeling and Control of Catalytic Reactions

Katsunori UEDA\* Toshiyuki MIYATA\*  
Koji KAWAKITA\* Junya KITADA\*

## Abstract

The authors have developed a control technique to maximize the performance of the three-way catalytic converter, which is a key to reducing gasoline engine emissions. This paper describes this control technique which mainly consists of two control methods: oxygen storage control based on knowledge obtained from simulating catalytic reactions, and catalytic temperature estimation control including onboard calculation of the reaction heat quantity using the above simulation model. This paper also describes software used to improve the efficiency of development.

**Key words:** Gasoline Engine, Combustion, Modeling, Electronic Control

## 1. Introduction

Since the late 1990s, prevailing themes for gasoline engine control have featured "catalytic control" to comply with ever-intensifying emissions regulations and "integrated control" to meet higher fuel efficiency demand. In 2000 and some subsequent years, emissions regulations have become even more stringent with the introduction of Japan's 2000 regulation, Euro 4, LEV II and the SULEV standards in the U.S., making it all the more important to improve and develop the control techniques for three-way catalytic converters, taking into consideration cost reduction as well.

We have been conducting analysis on how to control the three-way catalytic converter while also developing various related software. This report briefly describes the results.

## 2. Modeling of three-way catalytic converters for emissions reduction

### 2.1 Emissions reduction efforts

#### 2.1.1 Approach to cold-start HC emissions

In consideration of the stringency of emissions regulations, efforts for emissions control should focus mainly on the reduction of tailpipe HC (hydrocarbon) emission, especially that occurring immediately after the cold start, which account for the bulk of total emissions. On this point, Mitsubishi Motors Corporation (MMC) offers early activation of the catalyst with high-temperature exhaust gas by retarding the after-start ignition timing to help reduce emissions.

In this phase, the focus should not be on the catalytic reaction but on stable engine combustion and optimization of the raw emission before entering the catalyst. When the fuel injection quantity has been set to suppress the rich A/F (air-fuel ratio) after the start to decrease HC emissions, if the fuel used is low in volatility, the quantity of fuel transferred to the cylinder will be short<sup>(1)</sup>, resulting in an over-lean mixture and caus-

ing the engine to stall or hesitate. To ensure practical utility, a feedback correction has been applied to increase the fuel injection quantity upon the detection of partial misfiring (Fig. 1).

This feedback correction technique was developed from the lean limit control of the Mitsubishi Vertical Vortex (MVV™) lean-burn engines<sup>(2)</sup> marketed in 1991, which uses a combustion index highly correlated to the indicated mean effective pressure (IMEP) calculated from the crankshaft angular velocity at every 10° crankshaft angle during the expansion stroke.

Generally, the linear A/F sensor (LAFS) is effective in detecting the over-lean condition, but it is not applicable immediately after the cold start as it is still inactive. Detection of partial misfiring using the ion current has been put into practical use<sup>(3)</sup>; however, the feedback correction technique mentioned above achieves the same effect with a standard crank angle sensor<sup>(4)</sup> and a 32-bit microprocessor and therefore is more cost efficient and versatile.

#### 2.1.2 Approach to NOx after warm-up

Another hurdle is the tailpipe NOx (nitrogen oxides), which, unlike HC, is still emitted in considerable amounts after activation of the catalyst. It has been proposed that, in order to efficiently use a catalyst with an average emissions reduction efficiency of 99 % or more, the oxygen storage amount of the catalyst must be appropriately controlled<sup>(5)</sup>. However, the catalytic reaction cannot be regarded as equivalent to the oxygen storage, and quantification is required for optimum control. For these reasons, we developed a physical model for identifying the characteristics of the catalytic reaction and oxygen storage. Using the model, catalytic reactions were simulated and calculated and the parameters were identified.

## 2.2 Simulation of catalytic reactions

### 2.2.1 Model structure and simulation results

The simulation model consists of two types of sections: ① Ceria, which stores and releases oxygen; and

\* Powertrain Control Engineering Dept., Development Engineering Office

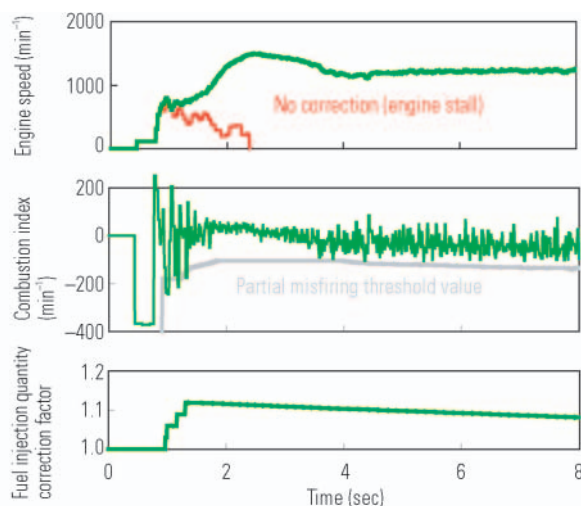


Fig. 1 Cold start with less volatile fuel

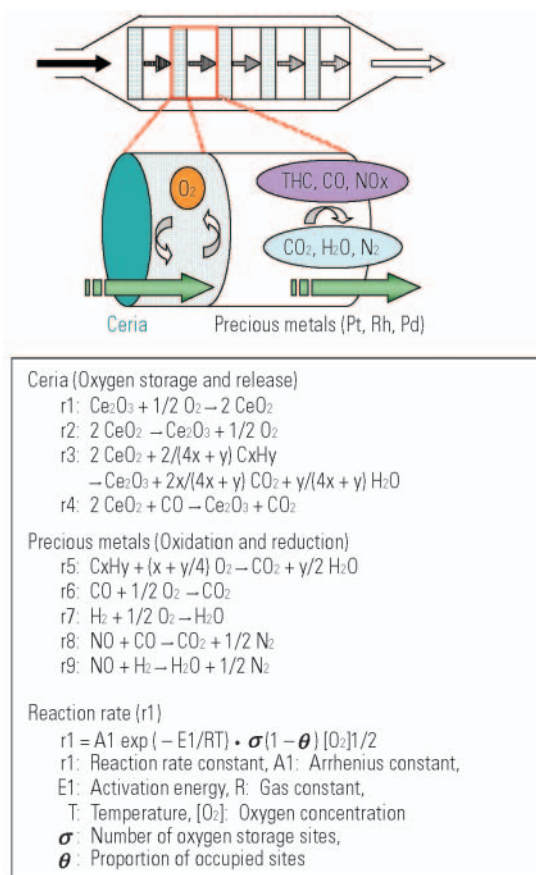


Fig. 2 Simulation concept of the three-way catalyst

② Precious metals for oxidation and reduction. The entire structure was approximated by constructing it with several dozen O<sub>2</sub> layers (Fig. 2). The reaction rates were calculated based on the assumption that all reactions occur as per Langmuir-Hinshelwood or Eley-Rideal mechanisms<sup>(6)–(12)</sup>. As for the parameters, the reaction rate constant was identified by the emissions levels upstream and downstream of the catalyst during actual steady-state operation and the number of oxy-

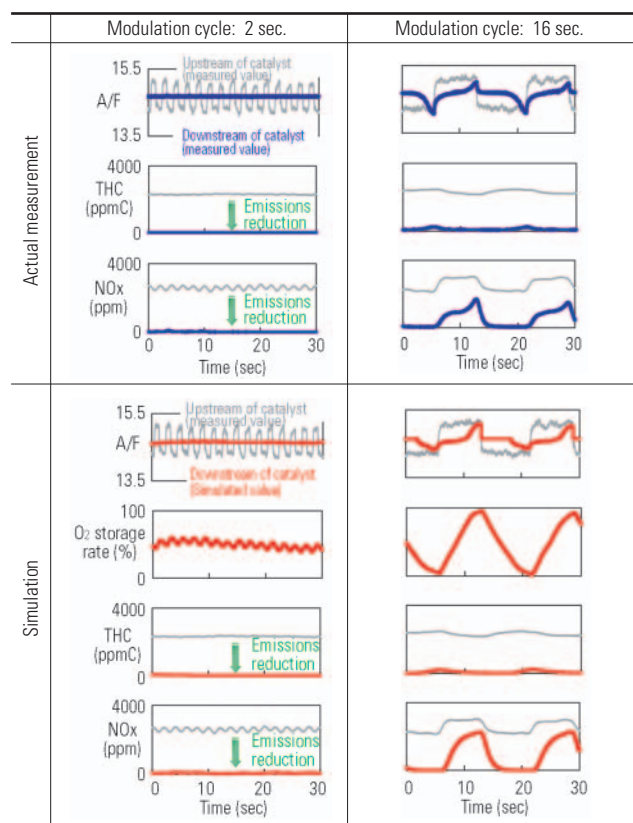
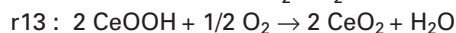
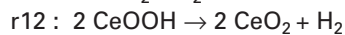
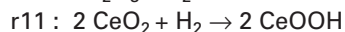
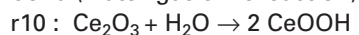


Fig. 3 Example of the catalytic reaction simulation

gen storage sites (equivalent to storage capacity) was identified by the variance in concentration in response to a step change of A/F.

Fig. 3 shows the variance in emissions levels downstream of the catalyst in response to rich-lean shifts of A/F in the exhaust gas entering the catalyst. Overall, the model achieved a fairly good approximation. During the transient state in rich-to-lean shift, however, the calculated NO<sub>x</sub> was greater than the measured NO<sub>x</sub>. This appears to be because the model did not accommodate the water-gas shift reaction and the reductive reaction by NO<sub>x</sub> and H<sub>2</sub> was estimated to be smaller than the actual level.

Ceria (water-gas shift reaction)



## 2.2.2 Findings and comments

The simulation quantitatively confirmed the widely held theory that ceria's oxygen storage and release function plays a role in sustaining the precious metals reaction against fluctuations in the incoming exhaust gas flow. It was also found that the percentage of occupied sites among the oxygen storage sites (storage rate) serves as a valid parameter.

Moreover, it was found that as the state of cells is not uniform from the upstream end to the downstream end of the catalyst, its internal conditions should not be

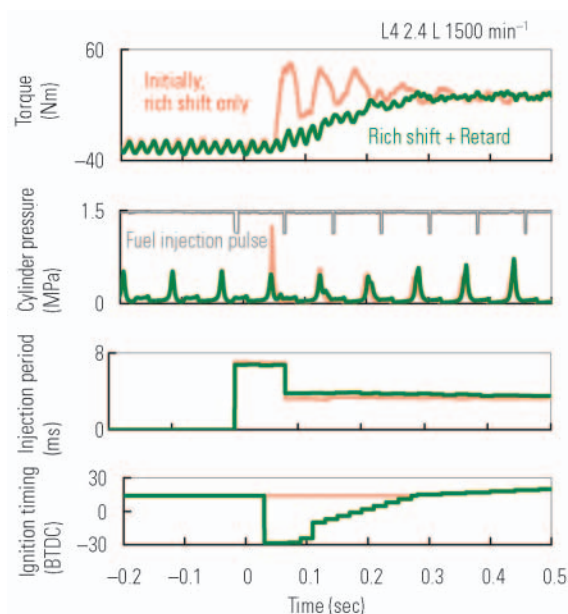


Fig. 4 Engine torque behavior after injection restart

treated uniquely but instead the control sequence which handles the condition of each layer independently is required to control the catalyst.

## 2.3 Oxygen storage control

### 2.3.1 Required features for injection restart

The bulk of the considerable amount of NO<sub>x</sub> emissions after warm-up as mentioned in 2.1.2 is from the temporary spike in emissions at injection restart after the fuel cut on deceleration and from the slip during subsequent acceleration. This is because the catalyst's oxygen storage sites become saturated with oxygen from the exhaust during the fuel cut, and the reducing agents (CO and HC) in the exhaust at the next injection restart react selectively with the oxygen, thus allowing NO<sub>x</sub> to be emitted in the atmosphere without reduction.

To curb the NO<sub>x</sub> emission, it is effective to temporarily shift the A/F to rich at the injection restart to supply a large volume of reducing agents to achieve early reaction and purging of the stored oxygen. At the same time, it is necessary to curb the sharp increase in torque and the shock caused by the rich shift at the injection restart by retarding the ignition timing or by other means. A control method that performs integrated control of the above items has been established.

### 2.3.2 Curbing the shock and NO<sub>x</sub> emission on injection restart

The key to simultaneously achieving a rich air-fuel mixture, reduced NO<sub>x</sub> emission through oxygen purging and less torque shock at injection restart, which apparently are conflicting demands, lies in MMC's engine performance simulator<sup>(13)</sup> and the findings in 2.2 (Figs. 4 and 5).

At an injection restart, the first combustion cycle is free of the burned gas that would normally exist. In steady-state operation, under a light load in particular, the percentage of burned gas reaches almost 50 %.

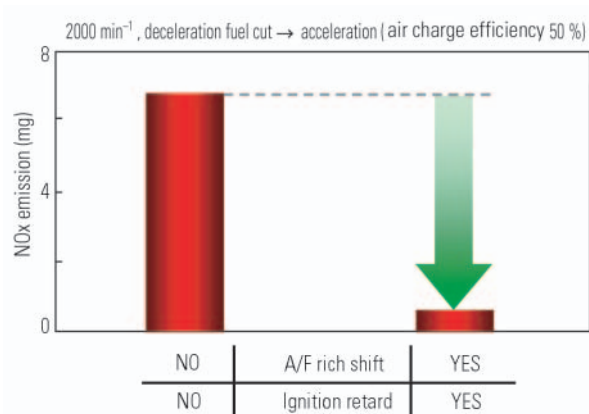


Fig. 5 NO<sub>x</sub> reduction after injection restart

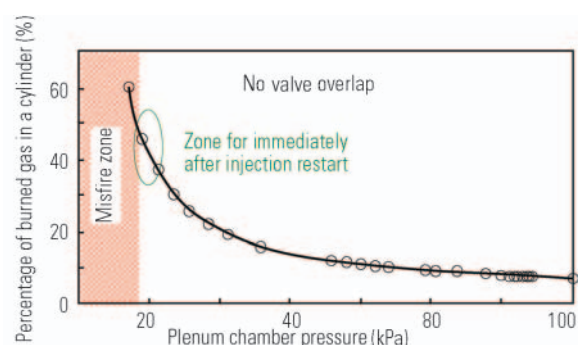


Fig. 6 In-cylinder residual burned gas ratio under steady condition

Immediately after an injection restart, there is nearly twice as much fresh air as in steady-state operation (Fig. 6). At this point, in the first cycle of each cylinder, the injection quantity is doubled to burn in the rich A/F. Because there is no burned gas, this sharply increases the combustion speed and torque. To handle this, the ignition timing is substantially retarded, to the point at which misfire or partial burn would normally result. Because there is no burned gas, retarding to that extent does not hamper stable combustion and only the torque drops substantially.

From the second cycle onward, with burned gas now remaining in the cylinders, the ignition retard will be lessened to the normal flammability limits while the injection quantity will be set to a level appropriate for the normal level of fresh air volume. The ignition timing will soon return to the standard value while the air-fuel ratio will be maintained on the rich side.

Subsequently, the A/F will gradually return to the stoichiometric ratio. At that time, little oxygen is stored in the upstream portion of the catalyst, while an appropriate volume of oxygen remains in the downstream portion. Namely, the overall oxygen storage rate has been reset to a level slightly below medium to enable the catalyst to comfortably purify HC, CO and NO<sub>x</sub> upon subsequent acceleration and deceleration (Fig. 7).

This reset concept is effective even when the catalyst is not completely activated. Even when the oxygen



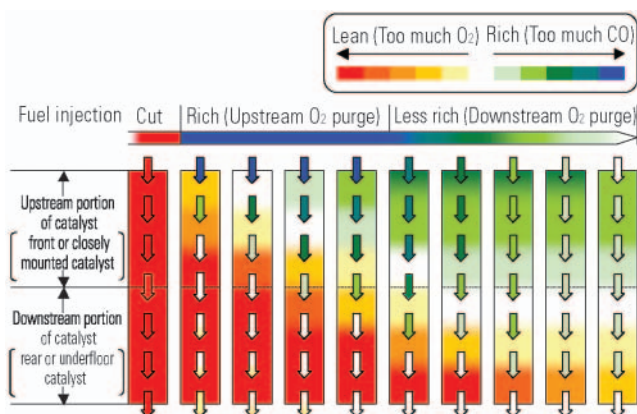


Fig. 7 Concept of O<sub>2</sub> purge in catalytic converters

storage capacity is still low with only part of the upstream portion having been activated, the catalyst is already saturated with oxygen if the engine was running on a slightly lean air-fuel mixture. If the oxygen is purged by generating a rich spike before the start of oxygen feedback, this enhances the emissions reduction efficiency of the catalyst that is not completely activated and, at the same time, contributes, although slightly, to catalyst warm-up through reaction heat.

Another effective method for initiating the dampening of a rich shift is to install an oxygen sensor in the middle of a range of catalysts connected in series, through which sensor voltage build-up following injection restart triggers a judgment that upstream purging is complete. Even when the oxygen storage capacity of the upstream portion of the catalyst has dropped, or degraded, this system is still capable of performing early rich-shift dampening corresponding to the capacity of the catalyst, enabling a constant level of oxygen purge appropriate for the state of the catalyst. At the same time, the system can also be used to monitor the upstream portion of the catalyst for deterioration.

Shifting the air-fuel ratio to rich appears to go against torque reduction. However, the range of flammability limits is greatest at around the air-fuel ratio for the maximum output in an ignition retard operation, and substantial ignition retard results in the greatest torque drop and lowers the level of raw NO<sub>x</sub> emitted from the engine proper. Therefore, this can be regarded as a good combination for the ignition retard requirements (Fig. 8).

### 2.3.3 Application to HC trap catalysts and degradation monitoring

The new HC trap catalyst that was introduced to comply with SULEV standards has three-way catalytic features, trapping HC under cold conditions and oxidizing them at desorption<sup>(14)</sup>. To promote oxidation in V6 engines, the fuel supply to one of the banks is cut during deceleration to supply oxygen to the underfloor catalyst to trap HC. In this case, the catalyst closely mounted on the bank to which fuel supply has been cut has already been activated and its oxygen storage sites saturated. This oxygen is then purged by generating a rich

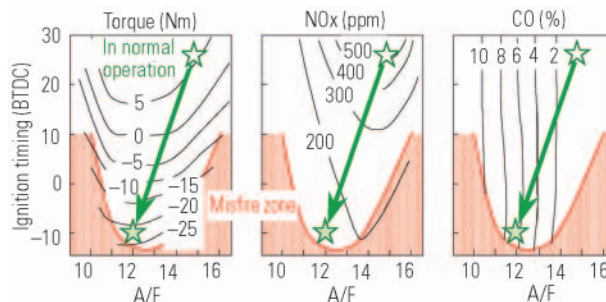


Fig. 8 Features of rich A/F and ignition retard

spike, as described earlier, to prevent NO<sub>x</sub> slip at the subsequent injection restart.

OBD regulations require that this catalyst be equipped with an on-board deterioration monitoring feature. Performance deterioration is typically indicated by a drop in oxygen storage capacity.

To meet this requirement, a technique similar to the one described earlier has been adopted. Namely, oxygen sensors are installed upstream and downstream of the catalyst, and monitoring for lack of oxygen storage capacity (deterioration) is performed based on the output from these sensors. This makes it possible to perform emissions reduction and deterioration monitoring at the same time in normal operations, eliminating the need to add a special dedicated monitoring mode while ensuring a reasonable rate of detection during actual driving.

## 2.4 Catalyst temperature estimation model with consideration to reaction heats

### 2.4.1 Catalyst protection and application model

To ensure efficiency of a catalyst, it is important to prevent the thermal deterioration that reduces the catalyst's durability.

Because of the importance of early activation of catalysts in a cold start as described in 2.1, an increasing number are being mounted ever closer to the exhaust port. This raises the need to control the fuel injection so that catalysts do not overheat and exceed the permissible temperature limit, including the three-way catalysts that are highly heat resistant. Shifting the air-fuel ratio to rich causes the exhaust temperature to drop, which then leads to a drop in the catalyst temperature. However, this also increases CO and HC emissions and should be limited to the minimum. Therefore, temperature control should be performed while monitoring the catalyst temperature. In terms of cost and response, it is more reasonable to adopt ECU-controlled on-board estimation than to use sensors.

So far, we have only examined simple ECU-controlled sequential processing and have not needed on-board calculation of the catalyst state. For the estimation of catalyst temperature, a control model was adopted for on-board simulation of the temperature at the center of the catalyst near the exhaust port.

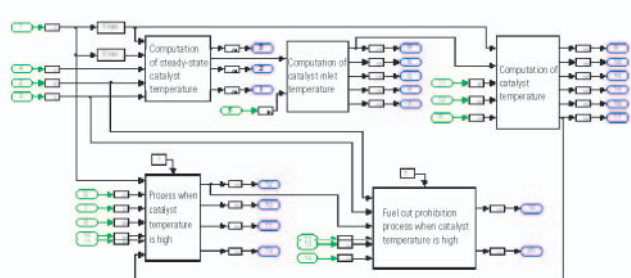


Fig. 9 Catalyst temperature estimation model

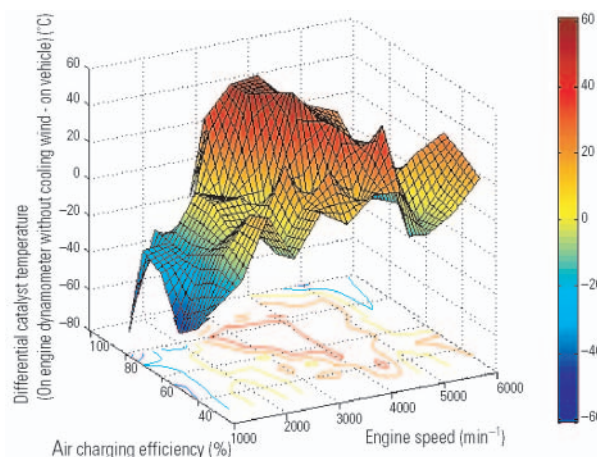


Fig. 10 Difference in catalyst temperature between that on engine dynamometer and on vehicle

#### 2.4.2 Accuracy of catalyst temperature estimation and influence of reaction heat

The operational expression of the catalyst temperature is represented by heat transfer equations that approximate the process in which heat from the exhaust gas is absorbed by the exhaust pipe as it travels to the catalyst where the exhaust gas gives off heat to the cells (or heat from the exhaust gas is absorbed by the cells) as it flows downstream. The distribution of temperature in the catalyst is represented by a multi-phased first-order delay system (Fig. 9). Specifically, the catalyst temperature in steady-state operation is mapped and stored, and then, after adding the heat release and transfer delay terms, the temperature behavior is simulated.

Initially, the catalyst temperature was estimated using the values measured on the engine dynamometer as the mapping values in the steady state and subtracting the heat radiation dependent on the vehicle speed and the flow rate of the exhaust gas. As for closely mounted catalysts, which were located under the hood making it difficult to clarify the relationship between cooling efficiency and vehicle speed, the values measured on actual vehicles in steady-state operation were used. Knowing the difference in catalyst temperature between that on an engine dynamometer and that on an actual vehicle and reflecting it on the target temperatures for engine dynamometer test sessions will be effective in improving the quality of final speci-

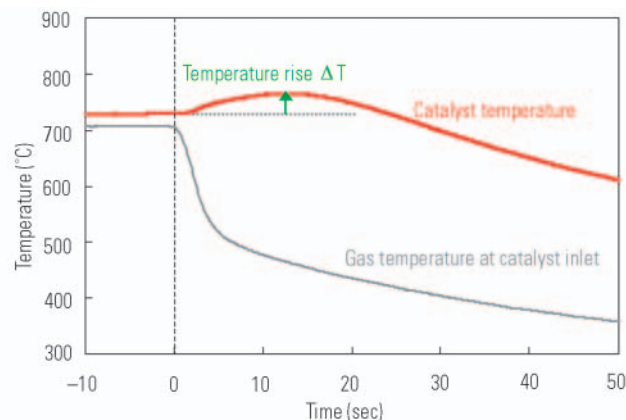


Fig. 11 Catalyst temperature rise after fuel cut

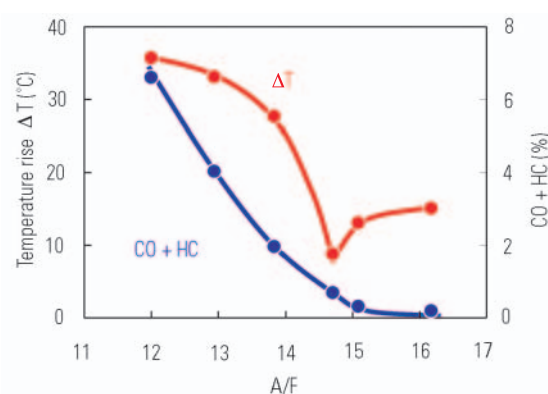


Fig. 12 A/F and catalyst temperature rise

cations (Fig. 10).

Through the measures described above, the accuracy of the catalyst temperature estimation neared the temporary target: within  $\pm 30^\circ\text{C}$ . However, the simple heat transfer model was not capable of sufficiently estimating the temperature rise<sup>(15)</sup> following the fuel cut during deceleration, thus generating a substantial error.

A more serious problem was catalyst oxidation deterioration under high-temperature lean conditions. This occurred when the catalyst temperature rose several dozen degrees Celsius due to the fuel cut and exceeded its permissible limit (overheat). In an extreme case, when the accelerator pedal was depressed and released repeatedly and therefore the fuel cut and injection restart were repeated, the catalyst temperature rose by more than  $100^\circ\text{C}$ . To prevent this, the model was modified to take into account the reaction heat during fuel cut as described in the following section, and a function was added to prohibit fuel cut when overheating was expected.

#### 2.4.3 Temperature rise features and modeling

Fig. 11 shows a rise pattern of catalyst temperature after a fuel cut on an engine in steady-state operation on a dynamometer. A richer A/F ratio leads to higher and longer-lasting temperature rise during a fuel cut. Too rich an A/F ratio, however, tends to lead to saturation (Fig. 12).

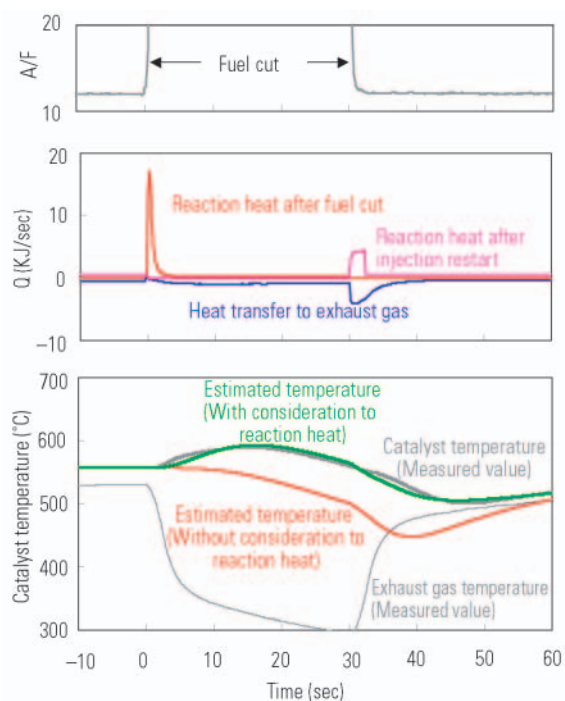


**Fig. 13** Heat release and temperature after fuel cut and injection restart

Based on the catalytic reaction simulation described in 2.2.1, further simulation was conducted by additionally incorporating the following concepts. The simulation reproduced fairly accurately the temperature behavior during a fuel cut and injection restart (Fig. 13).

We were also successful in approximating to some extent the rise in catalyst temperature during the repeated fuel cut and injection restart (Fig. 14).

- (1) Heat generation after a fuel cut is caused by the reducing agents (CO, HC, H<sub>2</sub>, etc.) that had been stored in the catalyst during steady-state operation, by reacting with the O<sub>2</sub> that flows in. The total amount of heat is determined by the total amount of heat radiating to the flowing air.
- (2) Richer A/F ratio leads to a higher percentage of reducing agents stored in the catalyst. Reducing agents can be stored until the storage sites are saturated.
- (3) Reaction volume (rate) per unit of time is calculated using the Arrhenius equation. The reaction speed constant is identified based on the actual testing results.

#### 2.4.4 Analysis of catalytic heat behavior

One characteristic of the catalytic heat behavior mentioned above is that the heat generation is slower to take place at the fuel injection restart than at the fuel cut. This means that the reacting volume differs between the cases when reducing agents (CO, HC, H<sub>2</sub>, etc.) flow into the catalyst that has become saturated with O<sub>2</sub> at a fuel cut and when O<sub>2</sub> flows into the catalyst that has become saturated with reducing agents during rich A/F operation. The reasons for this include the generation of H<sub>2</sub> in the catalyst in the water-gas shift reaction during rich A/F operation and the difference in the

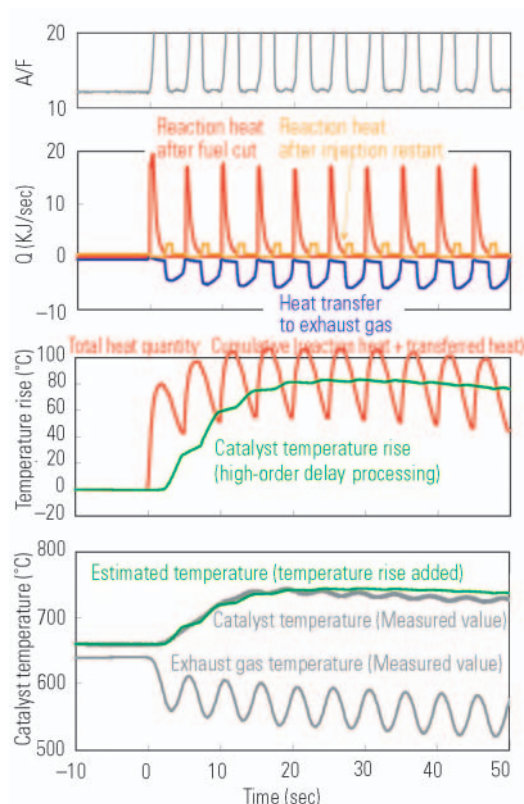


**Fig. 14** Heat release and temperature of catalytic converter under repeated fuel cut and injection restart

number of reacting moles between the storage state and the inflow state. This indicates that the method, mentioned in 2.3.2, of making the A/F ratio rich and supplying reducing agents in great volume at injection restart will not sufficiently accelerate the desired reaction so that the transient NO<sub>x</sub> emissions cannot be completely suppressed.

From the above, it was found that it would be extremely effective for minimizing catalyst temperature rise to consider not only the temperature at the center of the catalyst but also the entire catalytic heat behavior as control variables when studying ways to equip the target system on-board. This is because the catalyst has high heat capacity so that overheating cannot be predicted just by monitoring temperature change and, once the catalyst has become too hot, it is not possible to quickly stop further temperature rise by only correcting the injection quantity.

Through the activities mentioned above, namely modeling and quantifying not only O<sub>2</sub> storage but also the absorption and reaction of the reducing agents to calculate the heat balance of catalysts, we built confidence in the commercialization of a system that will effectively protect catalysts from heat deterioration.

#### 2.4.5 Improved on-board model

An improved version of the on-board catalyst temperature estimation model incorporating a computing block for storage and heat balance was implemented on the ECU. The result was a constantly high level of estimation accuracy (Fig. 15). With the improved version,



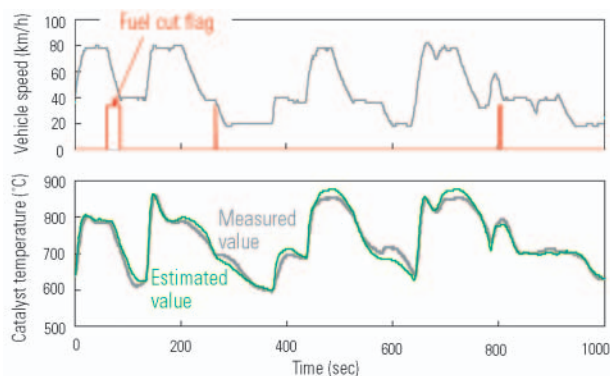


Fig. 15 Example of catalyst temperature estimation

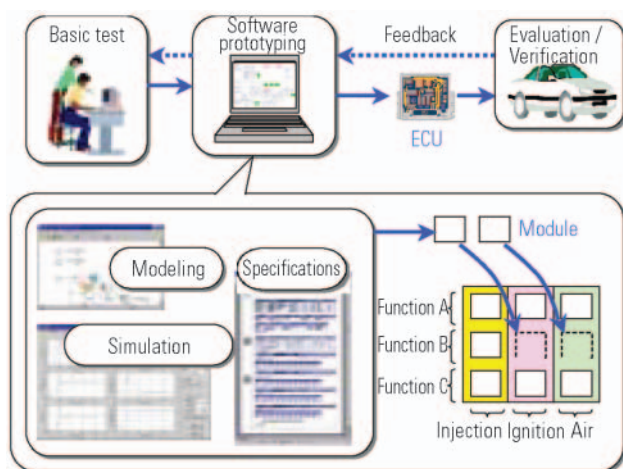


Fig. 16 Concept of software modules and autocoding

the catalyst temperature never exceeded the permissible upper limit under any acceleration and deceleration conditions, effectively minimizing heat deterioration.

In the on-board system conforming process, parameters such as reaction rate constant that were difficult to establish were simplified. To ensure versatility, the system obtains the A/F ratio at the catalyst inlet not by the linear A/F sensor but by the calculated estimation. The model was perfected into a production software module deployable on a wide range of vehicle models by adding processing capability in the event of sensor failure and temperature-based fuel injection control.

### 3. Control software and development tool

#### 3.1 Overall software configuration

Below is a brief description of the control models and ECU software.

A processing program consists of an operation system layer and an application layer. In recent years, the application layer has been reconfigured into an aggregation of many independent modules (parts).

Many of these modules are generic software that is versatile, does not often require specification change and has been programmed in C code. Some of the

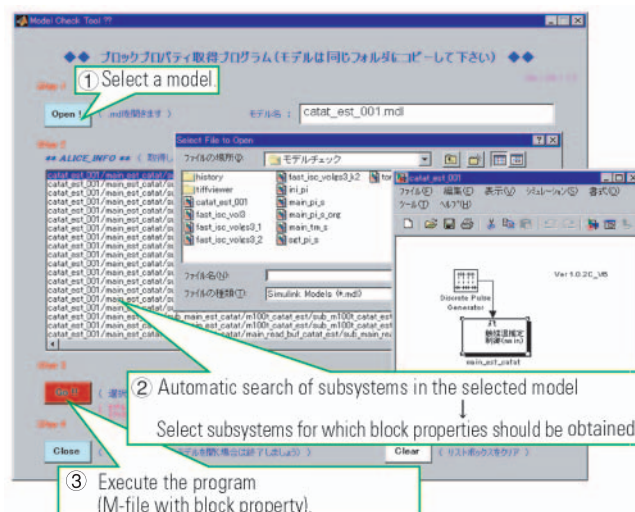


Fig. 17 Example of model check tool

strategic software, with new or improved technology for higher product competitiveness, uses C code automatically generated by MATLAB/Simulink<sup>(16)</sup> (Fig. 16).

#### 3.2 Simulink model and autocoding

Autocoding, which has become increasingly popular over the last several years, is a system that automatically converts the control algorithm (calculation) written as a Simulink block diagram into C code. For predetermined areas of the program, even a person who cannot edit the C source code directly can add or modify the control software on Simulink, and the autocoding system immediately converts it into an executable program for verification in an actual system. Because the final versions can lead directly to production programs, the time required for development is shortened and the quality is improved.

At MMC, this technique has been employed since the introduction of COLT in 2002 for EGR and idle speed control. Simulink describes the conditions using physical transfer systems such as gas dynamics and torque balance. This is ideal for software development and verification in actual use processes including simulations. It took only a few months from concept development to confidence in commercialization, enabling us to devote the remaining available time for optimization and improvement of reliability of the system. Because of its redundancy, autocoding requires ROM capacity approximately 1.2 times that required for manual coding. In the new system development process, however, the advantages of autocoding far outweigh its shortcomings.

The car manufacturer, as the developer, shares more than a small part of the responsibility for the quality of software models. At MMC, efforts are being made to increase reliability through mutual verification among our engineers and development of the tools to automatically sample and check the definitions of the model parameters (Fig. 17).



## 4. Results

Based on the quantification of three-way catalyst reaction behavior through simulation, a control algorithm for O<sub>2</sub> storage and catalyst temperature estimation was developed for practical use.

Considering the following achievements among other things, this should serve as a foundation to further advance emissions control technology.

- (1) The control algorithm treats the catalyst to be controlled as multi-layered cells.
- (2) The modeling covers not only O<sub>2</sub> storage but also the absorption and reaction of reducing agents.

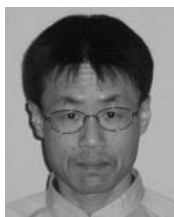
## 5. Conclusion

Through these technologies, MMC has successfully developed the super ultra-low emission vehicle (SULEV) 3L sports utility vehicle primarily relying on catalyst and related control technologies, without using additional devices such as a flow control valve, linear A/F sensor or secondary air injection. In future, we will use these technologies to develop multiple fuel vehicles and higher fuel economy models.

Finally, we would like to thank everyone in Electric Control Modules Department A of Himeji Works, Mitsubishi Electric Corporation for their valuable support with the ECU software and development tools.

### References

- (1) Katsunori Ueda: Automotive engine control, Journal of JSME, No. 990 (May 2001)
- (2) Shigetsugu Inoue, Toshiaki Umemura and Shoji Tashiro: Lean-Burn MVV Engines Mounted on New Mini-Sized Motor Vehicles, Mitsubishi Motors Technical Review No. 11, 1999
- (3) Morito Asano, Katsuyuki Kajitani, Tetsuo Kuma, Manabu Takeuchi and Yoshiyuki Fukumura: Development of new combustion control system by ion current, <http://www.diaelec.co.jp/randd/pdf/t9604.pdf>
- (4) Katsunori Ueda, Masaya Okamoto and Shinichi Kuratani: Powertrain control sensors, JSAE Journal, Vol. 56, No. 4, 2002
- (5) Noriyuki Kishi, Shinichi Kikuchi, Norio Suzuki and Naoyoshi Hayashi: Study on ultra low emission gasoline engines, Proceedings of JSAE Symposium 9933051, 1999
- (6) Makoto Misonou and Yasukazu Saito: Catalytic chemistry, p.1 – 39, Maruzen, 1999
- (7) Pontikakis, G. and Stamatelos, A.: Mathematical modeling of catalytic exhaust systems for EURO-3 and EURO-4 emissions standards, Proc. Instn. Mech. Engrs., Journal of Automotive Engineering, Vol. 215 Part D 1005-1015, 2001
- (8) Auckenthaler, T.S., Onder, C.H. and Geering, H.P.: Online estimation of the oxygen storage level of a three-way catalyst, SAE Paper 2004-01-0525, 2004
- (9) Balenovic, M., Hoebink, J.H.B.J., Backx, A.C.P.M. and Nievergeld, A.J.L.: Modeling of an automotive exhaust gas converter at low temperatures aiming at control application, SAE Paper 1999-01-3623, 1999
- (10) Chow, A. and Wyszynski, M.L.: Modelling the monolithic exhaust converter/fuel reformer reactor – a zonal approach, Proc. Instn. Mech. Engrs., Journal of Automotive Engineering, Vol. 214 Part D 905-917, 2000
- (11) Braun, J., Hauber, T., Tobben, H., Zacke, P., Chatterjee, D., Deutschmann, O. and Warnatz, J.: Influence of physical and chemical parameters on the conversion rate of a catalytic converter: A numerical simulation study, SAE Paper 2000-01-0211, 2000
- (12) Shayler, P.J. and Hayden, D.J.: Exhaust system heat transfer and catalytic converter performance, SAE Paper 1999-01-0453, 1999
- (13) Taizo Kitada, Masato Kuchita and Tomohiro Ohashi: Development of New-Version Engine Simulation Code, Mitsubishi Motors Technical Review No. 11, 1999
- (14) Kazuhiko Watanabe et al.: Development of OUTLANDER's Emission Control System to Meet North American Super-Ultra-Low Emission Vehicle (SULEV) Standards, Mitsubishi Motors Technical Review No. 19, 2007
- (15) Brinkmeier, C., Schon C., Vent, G. and Enderle, C.: Catalyst temperature rise during deceleration with fuel cut, SAE Paper 2006-01-0411, 2006
- (16) Jiro Sumiya, Seiji Anzai and Yoshiomi Yamashita: Powertrain control system development aids, Mitsubishi Denki Giho, September issue, 2000



Katsunori UEDA



Toshiyuki MIYATA



Koji KAWAKITA



Junya KITADA

# Knowledge-Based Diagnosis

## – Failure Detection and Isolation by State Comparison with Model Behavior –

Kazuo KIDO\* Kazuhide TOGAI\* Hiroki YAMAURA\*\*

### Abstract

Powertrain diagnosis has advanced to meet the legal requirements of On-Board Diagnostics (OBD) and to improve serviceability. Legal requirements are expected to become even more stringent, and quicker fault detection and better deterioration compensation will be needed. As a result, it will be necessary to detect performance degradation (product to product variation and aged deterioration). One promising method that has long been proposed in this area is a comparison between real-time plant models and detected values, but progress has been hindered by limited computing power. Although this limitation has now disappeared, the model structures and sensor characteristics still impose limitations. In this study, we applied the residual resolution method to the mean value engine model in quasi-steady-state operation, and investigated the reliability of diagnosis by the redundant system, the response of fault isolation, and the minimum change required to detect deterioration against the sensor and actuator faults. These performances were found to depend on the structure of the mean value model and the characteristics of physical quantity detection.

**Key words:** *Model Based Diagnosis, Fault Detection*

## 1. Introduction

Passenger cars have a wide range of applications, but they have a common feature: they are all used in daily life. Because of this, it is necessary to minimize failures and deterioration. It is even better if faults and deterioration can be predicted. Fault diagnosis is often likened to the diagnosis of human illnesses. Illnesses are diagnosed when certain values are out of their normal range, or indicated by other characteristic symptoms including specific reactions that emerge when test agents are used. These phenomena are then reviewed by knowledgeable medical staff before a final diagnosis is made. This type of knowledge-based diagnosis is also known as an expert system, which became popular some years ago. An expert system typically consists of a long flow chart of YES/NO questions. While it takes a long time to produce such a chart, it can only be used for diagnosing the phenomena for which it was originally intended.

Confirming that the related sensor outputs are within a specific range to determine if a component is faulty or not, is a conventionally used method. Doing this while the system is in operation, however, requires normal dynamic behavior and this is where modeling comes in. Under this concept, the possibility of diagnosis by monitoring for and evaluating deviations from the generated normal model is reviewed.

## 2. The history of automotive diagnosis

As electronic control systems became popular, there emerged a need for diagnostics to facilitate inspection and repair. Later, emissions regulation (OBD) requirements made diagnostics crucial to automotive development.

### 2.1 Diagnostics for inspection and repair

The numbers of onboard vehicle sensors and actuators have increased with the introduction of electronically-controlled engines and transmissions. This has made it difficult to make diagnostic decisions by using only the five senses. To help overcome this difficulty, diagnostic tools that are designed to be connected to onboard electronic control systems for diagnosis have been made available to service shops. Along with this, to aid troubleshooting, some onboard engine computers can now store data from the period prior to error detection. From the viewpoint of quality compensation, important aspects include deterioration monitoring, troubleshooting, deterioration warning and if possible, compensation for functional deterioration.

### 2.2 Regulatory requirements (OBD)

The introduction of diagnostic systems to vehicles has not been facilitated by customers who do not consider the feature to be important when they purchase their cars. Instead, the mounting of onboard diagnostic systems has been promoted by regulatory requirements. By law, a vehicle must be capable of monitor-

\* Advanced Powertrain Development Dept., Development Engineering Office

\*\* Mitsubishi Automotive Engineering Co., Ltd.

**Table 1** OBD II requirements

Item	Requirements	Introduction
Catalyst monitoring	SULEV, NMOG > 2.5 times the standard, Conversion efficiency drops to 50 % or less	For NOx 2005
Misfire monitoring	Multiple cylinder misfire, Catalyst damage	
Evaporative system monitoring	Purge flow, Leak detection	
Secondary air system monitoring	Exceeds 1.5 times the standard	
Fuel system monitoring	Exceeds 1.5 times the standard	
Oxygen sensor monitoring	Exceeds 1.5 times the standard, Detection of a lack of circuit continuity	
EGR system monitoring	Increase or decrease from the manufacturer's specified EGR flow rate, causing emissions to exceed 1.5 times the standard	
PCV system monitoring	Monitors for disconnection of system tubing/hoses	
Engine cooling system monitoring	Thermostat, ECT (Engine Coolant Temperature) sensor	
Cold start emission monitoring	Key control or feedback parameters	2006
Air-conditioning system monitoring	Exceeds 1.5 times the standard	2006
VVT system monitoring	Exceeds 1.5 times the standard	2005

ing its emissions control systems for deterioration and issuing a warning (turning on MIL) when required. This has led to the development of systems that are resistant to deterioration and if these fail, they can be restored to original performance levels.

In 1970, the U.S. Congress passed the Clean Air Act as law, which is designed to curb the impact of automotive emissions on the atmosphere. At the same time, it became mandatory for car manufacturers to mount OBD features on their vehicles for detection of emissions control performance deterioration. Back then, the EPA (Environmental Protection Agency) and CARB (California Air Resources Board) were also established. In 1988, OBD standards were re-organized to align these with SAE standards. In 1996, OBD II, a new standard, was introduced. Items that need to be monitored and related criteria are shown in **Table 1**. New monitored items and requirements are phased in on an annual basis and are becoming increasingly stringent. New regulations are first introduced in California and then spread elsewhere. Similar regulations are in place in Europe and Japan. It is expected that some of the requirements in these countries will be unified under the Agreement Concerning the Establishing of Global Technical Regulations for Wheeled Vehicles, Equipment and Parts which Can Be Fitted and/or Be Used on Wheeled Vehicles (Global Agreement).

### 3. Development of knowledge-based diagnosis

A range of diagnostic methods were proposed in the past. In the 1970s, knowledge-based diagnostics were released, which analyze emerging phenomena according to the knowledge of experts in the field. This is a so-called expert system. High-quality knowledge can lead to very accurate diagnoses. However, it takes time to compile knowledge into a database. Additionally, data revision following any change in knowledge is not

easy and knowledge-based diagnosis is not suitable for analysis of dynamic phenomena. In the 1980s, model-based interference emerged, in which system structure is modeled to predict behavior and, based on that, comparisons are made with the measured values of real systems. Diagnoses are performed, based on deviations from the norm. Benefits of this include the possibility of modeling knowledge (system structure) in accordance with certain rules and of partial correction and repetitive utilization. From the 1990s onwards, there has been an improvement in modeling techniques, while neural network and other new diagnostics have been introduced<sup>(1) – (3)</sup>.

Diagnosis is done in three stages: fault detection in which a fault is recognized; fault isolation in which the fault is located; and fault identification in which the significance and behavior of the fault are determined<sup>(4)</sup>. Rizzoni et al. applied a state-space

engine model and a residuals generation method to the diagnoses of throttle angle, manifold pressure and engine speed<sup>(5) (6)</sup>.

### 4. Model-based diagnosis

Conventional diagnostics were simply designed to detect states that should not exist in normal operation, such as sensor outputs being out of range, a short circuit to ground, a short circuit to power source and an open circuit, or to detect obvious inactive states such as constant output of the front oxygen sensor (monitoring of frequency). Model-based diagnostics aim to construct a fault detection system based on a set procedure and achieve higher diagnostic accuracy through within-feasible signal range intermediate fault detection, detection of deterioration and compensation for production tolerance, all of which are difficult to achieve with conventional diagnostics.

A model is a set of mathematical expressions or a system that enables simulation of plant behavior, based on measurable inputs from the plant. Models primarily employed in the field of automotive electronic control are those that can be constructed using an engine computer. Outputs from a model are used for diagnosis. **Fig. 1** shows the general concept of model-based diagnosis. Outputs from the plant and those estimated on the model are compared and, based on this, fault detection, isolation and identification are performed. Model-based diagnosis is basically a multiple diagnosis with redundancy offered by the software. The simplest method compares the plant output to the same model output. A single output is not sufficient to determine whether or not the fault is sourced to the input, process or output. Therefore, multiple outputs are employed for mutual verification so that faults are isolated and identified, based on majority rule principles. The benefits of model-based diagnosis include the possibility of conducting diagnosis without the need to equip the plant

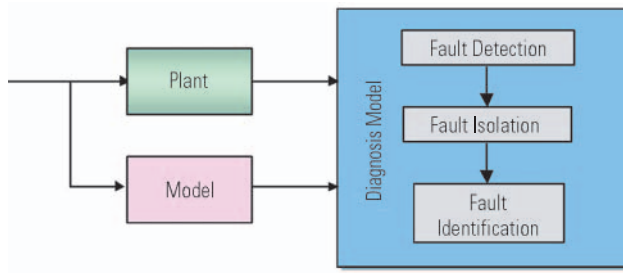


Fig. 1 Model-based diagnosis

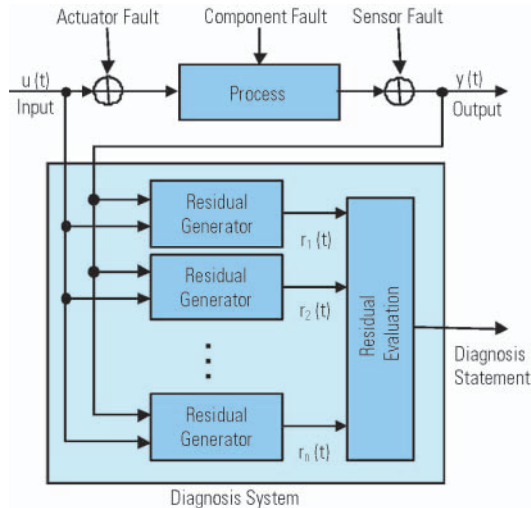


Fig. 2 Residual method

with additional devices and the ease of revising monitoring strategies.

#### 4.1 Residual Method

Model-based diagnosis includes residual method<sup>(7)</sup>, hypothesis testing, parameter identification and the extended Kalman filter. In our study, online parameter identification was initially attempted. However, this posed numerous problems for application to engines, in that sufficient excitation input was needed to ensure identification accuracy and that, if sufficient excitation input was not available, M-series noise signals needed to be added. With this aspect, the most common strategy, or residual method, was employed. As shown in Fig. 2, the diagnosis system is divided into two parts: residual generation and evaluation. There are three types of faults: a sensor fault, an actuator fault and a component fault, which consists of the two former faults. Inputs to the diagnosis system consist of plant process inputs and outputs. Residuals are differences between the model and the plant. Normally, residuals are set to zero as a normal state. Residuals deviate substantially from zero when a fault occurs. Multiple residuals must be used, with each being sensitive to a specific fault, in order to enable fault isolation and identification. Fig. 3 shows a simple example of fault identification. The "1" in the table means that residual  $r_i$  is sensitive to fault  $f_j$ . When residual  $r_1$  has emerged, this

	$f_1$	$f_2$	$f_3$	$f_4$
$r_1$	0	1	0	1
$r_2$	0	1	1	0
$r_3$	0	0	1	0
$r_4$	1	0	0	1

$r_i$ :  $i$ th residual between the plant and the model  
 $f_j$ :  $j$ th component fault

Fig. 3 Failure identification by multiple residuals

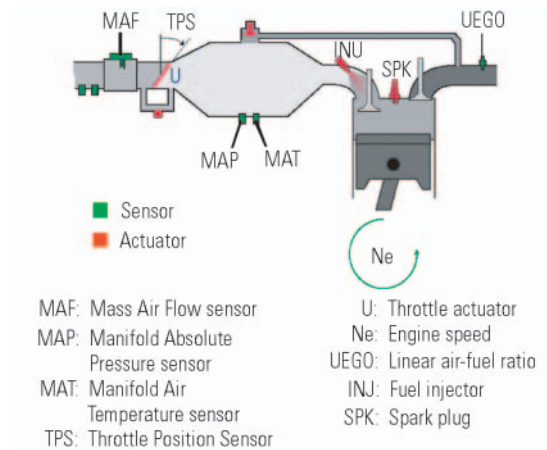


Fig. 4 Objects of diagnosis

means that either fault  $f_2$  or fault  $f_4$  has occurred. To know exactly which one has occurred, residual  $r_2$  needs to be examined: it is fault  $f_2$  if residual  $r_2$  has emerged and fault  $f_4$  if it has not.

#### 4.2 Monitored items

Fig. 4 shows the sensors and actuators that are to be monitored. The monitored sensors include: the mass air flow (MAF) sensor, the intake manifold absolute pressure (MAP) sensor, the intake manifold air temperature (MAT) sensor, the throttle position sensor (TPS) and the linear air-fuel ratio sensor (UEGO). The monitored actuators include: the fuel injector (INJ) for each cylinder and the throttle actuator (U). Engine speed (Ne) is also monitored.

#### 4.3 Selection of residuals

Table 2 shows the residuals examined in our study, the relevant monitored sensors and those sensors that were used to estimate the values of the relevant monitored sensors. Where direct estimation was not possible, observer-based estimates were used. Multiple residuals were used for the monitored sensors to achieve a comprehensive diagnosis. For the TPS, MAF and MAP sensors, it was possible to identify which sensor was faulty by using a duplicate check with multiple residuals. For the UEGO and MAT sensors, it was not possible to identify which of the monitored sensors



**Table 2 Selection of residuals**

Residual	Monitored sensor	Sensor used for estimation	Fault identification method
$r_1$	MAF	TPS, MAP	Duplicate check (cross-check)
$r_2$	MAF	MAP, Ne	
$r_3$	MAP	TPS, Ne with observer	
$r_4$	MAP	MAF, TPS, Ne with observer	
$r_5$	MAF	TPS, Ne with observer	
$r_6$	TPS	Im Duty	One of the two is faulty
$r_7$	UEGO	INJ, MAP, Ne, MAT	
$r_8$	MAT	TPS, MAP, Ne with observer	

MAF: Mass Air Flow

TPS: Throttle Position Sensor

UEGO: Linear air-fuel ratio

MAP: Manifold Absolute Pressure

Ne: Engine speed

Im Duty: Target duty current

MAT: Manifold Air Temperature

INJ: Fuel injector

 $r_i$ : Residual between sensor value and estimated value**Table 3 Construction of residuals**

Residual	TPS	MAF	MAP	Ne	MAT	U	INJ
$r_1$	1	1	X	0	0	0	0
$r_2$	0	1	1	1	0	0	0
$r_3$	1	0	1	1	0	0	0
$r_4$	1	1	1	1	0	0	0
$r_5$	1	1	0	1	0	0	0
$r_6$	1	0	0	0	0	1	0
$r_7$	0	0	1	X	1	0	1
$r_8$	1	0	1	1	1	0	0

**Table 4 Generation of residuals**

Residual	Description
$r_1$	MAF sensor value (Estimated air flow through the throttle valve)
$r_2$	MAF sensor value (Estimated air inflow to the cylinder based on a theoretical thermodynamic calculation)
$r_3$	MAP sensor value (Observer-based estimated intake manifold air pressure corrected by intake manifold pressure)
$r_4$	MAP sensor value (Observer-based estimated intake manifold air pressure corrected by intake air flow)
$r_5$	MAF sensor value (Observer-based estimated air flow corrected by intake air flow)
$r_6$	Throttle angle based on the TPS sensor (Throttle angle based on engine computer-controlled target driving current)
$r_7$	Estimated air-fuel ratio for each cylinder based on fuel injection volume (Estimated air-fuel ratio for each cylinder based on the linear air-fuel ratio sensor)
$r_8$	MAT sensor value (Observer-based estimated intake manifold temperature corrected by intake manifold temperature)

used for estimation was faulty, or if both of these were faulty.

#### 4.4 Examination of residuals

**Table 3** shows the relationship between residuals  $r_1$  to  $r_8$  in **Table 2** and the sensors and actuators used for fault identification. The “1” in the table indicates that the residual is related to the fault. The “0” in the table indicates that the residual is unrelated to fault. The “X” means that it is not known whether the residual is related to fault or not. For example, the MAF sensor is determined to be faulty when residuals  $r_1$ ,  $r_2$ ,  $r_4$  and  $r_5$  are all 1 and residuals  $r_3$ ,  $r_6$ ,  $r_7$  and  $r_8$  are all 0.

With the injector (INJ), only residual  $r_7$  is related to the fault. Residual  $r_7$  is generated when either the linear air-fuel ratio sensor, fuel injector actuator, MAP sensor, Ne or MAT sensor is faulty, as shown in **Table 3**. This makes it difficult to locate the cause. In other words, the fault is identified by applying majority rule to multiple residuals that are linked to faults.

**Table 4** shows the contents of residuals that were generated. Residuals  $r_1$  and  $r_2$  are residuals between a sensor value and an estimated value that was theoretically calculated. Residuals  $r_3$ ,  $r_4$ ,  $r_5$  and  $r_8$  are all residuals between a sensor value and an observer-based estimated value. Residual  $r_6$  is a residual between throttle angle based on the TPS sensor and throttle angle based on the target driving current of the engine computer. Small deviations of the throttle angle are corrected immediately by feedback control and therefore cannot be detected. Residual  $r_7$  is a residual between an air-fuel ratio for each cylinder, estimated from the engine computer-controlled fuel injection volume and that estimated from an air-fuel ratio sensor located in the exhaust manifold.

Some faults are temporal and recover within a short time. Therefore, diagnosis was conducted using the integrated values of residuals. Residuals were processed through a low-pass filter because they contained high-frequency noise and disturbances. The effects of these will be discussed later in this paper. To compare residuals of different units, these were normalized using the standard deviations during normal operation.

#### 4.5 Example of diagnosis

##### 4.5.1 Diagnosis of the MAF sensor

The MAF sensor characteristics were approximated by gain (slope) (output to input ratio) and offset. A typical fault was assumed in which deterioration led to a 10 % change in MAF sensor gain. The relevant simulation calculations are shown in **Fig. 5**.

The horizontal axis represents time while the vertical axis represents the residuals' behaviors. When a fault occurs with the MAF sensor at around the 20 seconds mark, residuals  $r_1$ ,  $r_2$ ,  $r_4$  and  $r_5$  increase as indicated in **Table 3** and upon exceeding the thresholds, these reach 1, which causes a fault diagnosis for the sensor. Other sensors are diagnosed in a similar manner.

##### 4.5.2 Diagnosis of fuel injectors

The diagnosis of fuel injectors was conducted in a slightly different manner. As shown in **Fig. 6**, the diagnosis was conducted by comparing the air-fuel ratio for each cylinder, estimated from the intake air volume and the engine computer-controlled fuel injection volume,

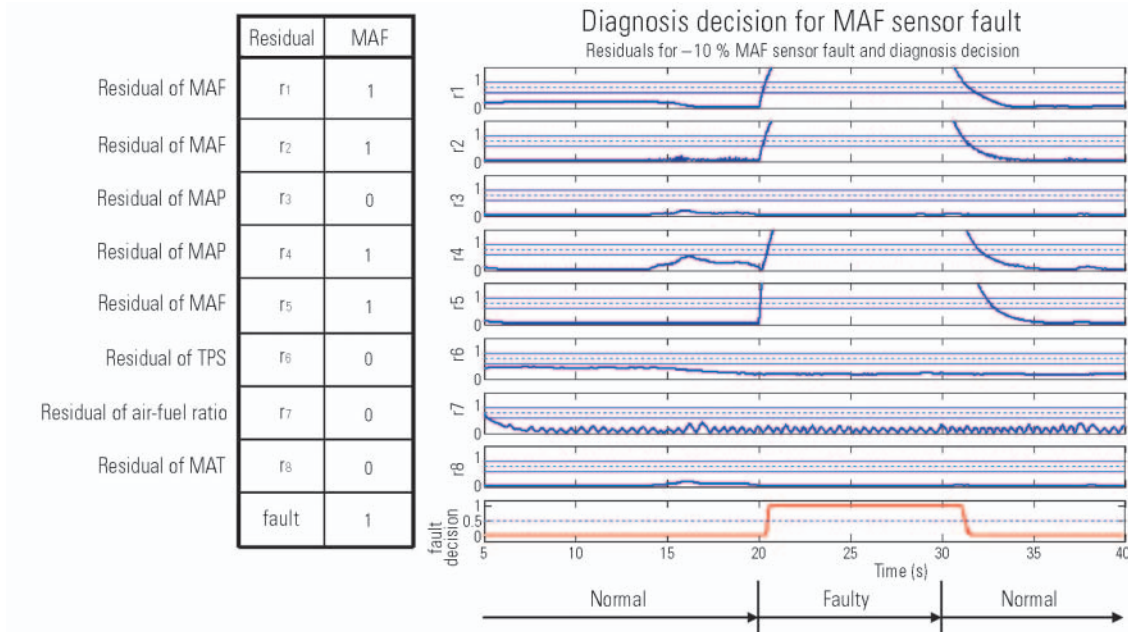


Fig. 5 Example of residual calculations

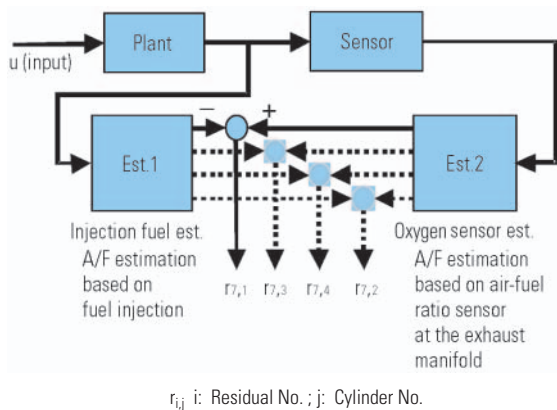


Fig. 6 Residual model of air-fuel ratio

with the air-fuel ratio for each cylinder estimated from the air-fuel ratio sensor located in the exhaust manifold. It was assumed that, after the expansion and exhaust strokes, exhaust gas with the estimated air-fuel ratio would be pushed out by subsequently expelled gas through the exhaust pipe until it reached the air-fuel ratio sensor without mixing with exhaust gas from other cylinders. For the air-fuel ratio for each cylinder, these are estimated from the air-fuel ratio sensor value for which compensation was made by inverse calculation of the first-order lag in exhaust gas transport, dead time and first-order lag in the air-fuel ratio sensor detection<sup>(8)</sup>.

Fig. 7 shows the estimated air-fuel ratios of both methods. "T" indicates the responsiveness of the air-fuel ratio sensor (first-order lag time constant). It has been shown that poor responsiveness significantly affects the estimation of the cylinder-specific air-fuel ratio. Therefore, when the air-fuel ratio for each cylinder is estimated with an oxygen sensor, the sensor

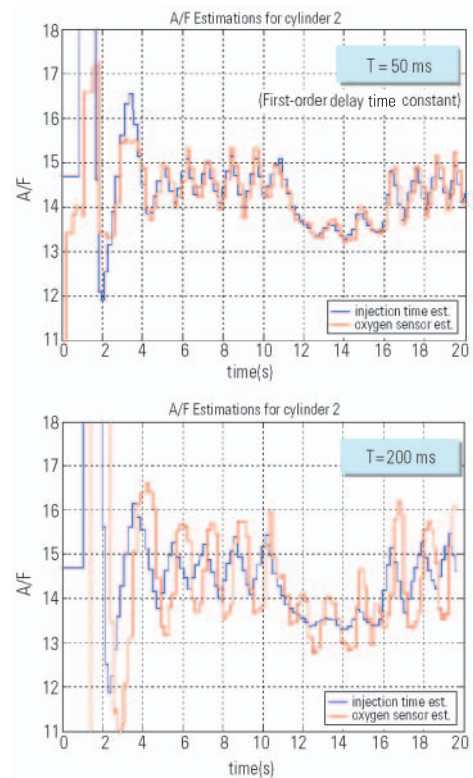


Fig. 7 Comparison of estimated air-fuel ratios for the No. 2 cylinder based on fuel injection time and air-fuel ratio sensor

needs to be very responsive.

Fig. 8 shows fluctuations of the residual related to air-fuel ratio when the No. 1 fuel injector became faulty. When the air-fuel ratio sensor had poor responsiveness, this affected the estimation of the air-fuel ratio for the No. 2 and No. 3 cylinders, which occur immediately

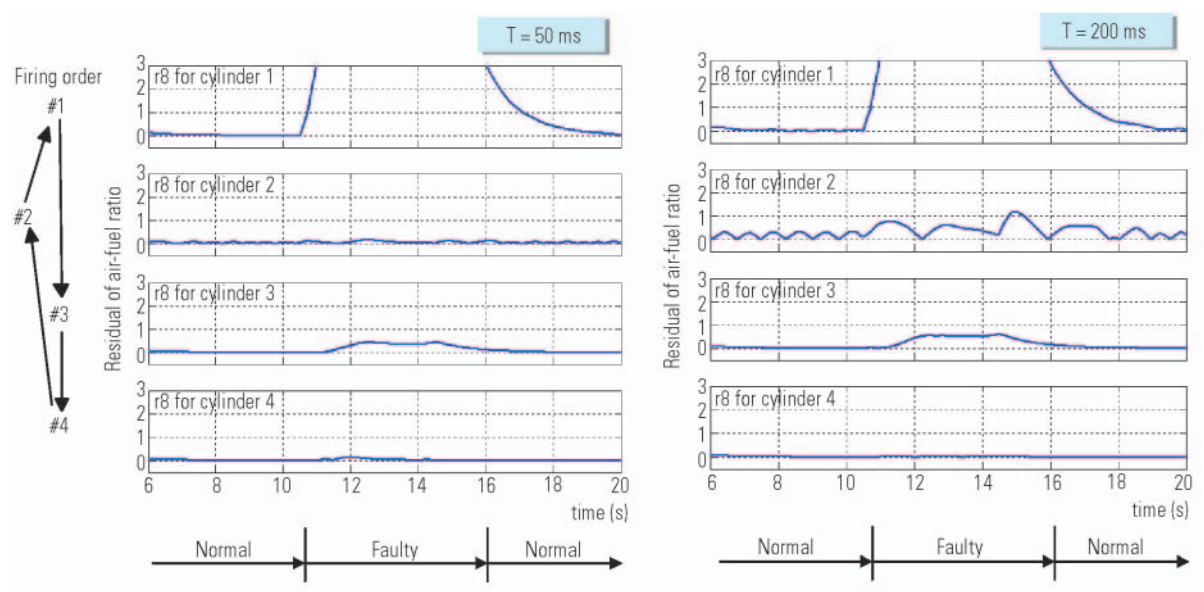


Fig. 8 Effect of air-fuel ratio sensor response to A/F residual of each cylinder

Table 5 Response of diagnosis

Residual	Sensor	Cause of delay in residual generation	Time required for fault detection
r <sub>1</sub>	MAF	Low Pass Filter	
r <sub>2</sub>	MAF	Low Pass Filter	
r <sub>3</sub>	MAP	Observer/Low Pass Filter	
r <sub>4</sub>	MAP	Observer/Low Pass Filter	
r <sub>5</sub>	MAF	Observer/Low Pass Filter	
r <sub>6</sub>	TPS	Low Pass Filter	
r <sub>7</sub>	UEGO	Low Pass Filter	
r <sub>8</sub>	MAT	Observer/Low Pass Filter	

MAF: Mass Air Flow  
MAP: Manifold Absolute Pressure  
MAT: Manifold Air Temperature  
r<sub>i</sub>: Residual between sensor value and estimated value  
Low Pass Filter: First-order delay low pass filter  
TPS: Throttle Position Sensor  
UEGO: Linear air-fuel ratio

before and after the No. 1 cylinder in terms of firing order. As a result, residuals were generated for the No. 2 and No. 3 cylinders despite the fact that these were in good condition. This then, makes it difficult to distinguish between normal and faulty cylinders.

4.6 Responsiveness of diagnosis

Generation of residuals can be delayed by low-pass filters that are used to block high-frequency noise by observer feedback being used for estimation. It is necessary to determine the maximum frequency at which faults can occur and whether or not the diagnostic system is capable of detecting them.

Table 5 shows the responsiveness of the residuals (diagnostic system) examined in our study. It takes approximately one second for a fault to arise and approximately another two seconds for it to disappear: approximately three seconds in total. The system, therefore, cannot detect faults that have a cycle of less than approximately three seconds.

4.7 Effect of mean-value engine model on diagnosis

The engine model examined in our study was a mean-value engine model. Table 6 shows the possible impact of the model on diagnosis. The MAF and MAP sensors would have no impact as their values are averaged over a stroke. Engine speed and torque would have no impact either, because these are also averaged over a stroke. The MAT and TPS sensors would have only a small impact because fluctuation in their values is small. Fuel injection signals, despite being averaged over a stroke, would still be affected by a delay in fuel delivery. The air-fuel ratio will fluctuate and also be affected by sensor delay.

5. Conclusion

The concept of a comparison between real-time behavior of a plant and that of a model of the plant that has the standard behavior of the plant and subsequent diagnosis based on the residuals between the two exceeding the predetermined limits, is both easy to

**Table 6 Effect of mean value engine model on FDI**

Sensor	Plant behavior	Sensor output	Impact on FDI
MAF	Small fluctuation	Stroke average	None
MAP	Pulsation	Stroke average	
MAT	Small fluctuation	Sampling every 10 ms + Sensor responsiveness	
TPS	Small fluctuation	Sampling every 5 ms	
INJ	Fluctuation	Stroke average + Delay in fuel delivery	May effect
UEGO	Fluctuation	Sampling every 10 ms + Sensor responsiveness	(Alternative misfire)
NE, Te	Pulsation	Stroke average	None

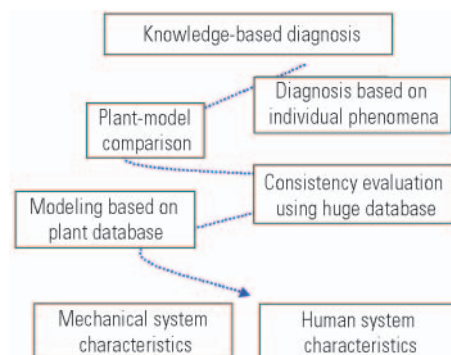
MAF: Mass Air Flow      TPS: Throttle Position Sensor      INJ: Fuel injector  
 MAP: Manifold Absolute Pressure      Ne: Engine speed      UEGO: Linear air-fuel ratio  
 MAT: Manifold Air Temperature      Te: Engine torque  
 FDI: Fault Detection and Isolation

understand intuitively and attractive. How such a system is composed and its performance evaluated, however, cannot be perceived intuitively. In this paper, we discussed methods for designing a diagnosis algorithm that is capable of identifying phenomena based on multiple information sources and, by providing examples, explored its fault detection potential and responsiveness through to fault identification. We also examined how design and responsiveness of the monitored components would affect the monitoring performance.

Currently, development is under way concurrently and separately in the field of legally-mandated deterioration monitoring and fault warning and that of deterioration monitoring and compensation for quality control. In the future, all of these will be restructured under a common methodology for fault detection and cause identification. However, as discussed in this paper, there remain limitations in responsiveness and resolution while detection characteristics depend on model selection. The highly sensitive single-characteristic extracting methods, therefore, cannot be ignored. Within the framework of legal requirements including those for deterioration monitoring, diagnostics is supposed to advance between the two major options, modeling and sampling (**Fig. 9**).

## 6. Acknowledgments

In this paper, we discussed model-based engine diagnosis algorithm, the result of our joint research with MB SIM Technology Co., Ltd., presenting it as an example of knowledge-based diagnosis. We would like to thank everyone concerned, especially Dr. Wang and Mr. Xia, for extending their cooperation to our study.

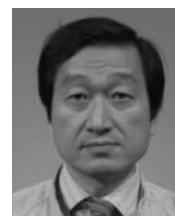
**Fig. 9 Future of diagnosis**

## References

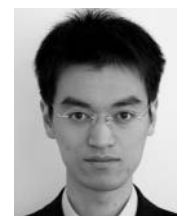
- (1) D. Cho and P. Paoletta.: Model-based failure detection and isolation of automotive powertrain systems. Proc. of ACC, pages 2898 – 2905, 1990.
- (2) J. Gertler and M. Costin.: Model-based diagnosis of automotive engines. IFAC Fault Detection, Supervision and Safety for Technical Processes, pages 393 – 402, Espoo, Finland, 1994.
- (3) Nyberg, M., Model-Based Diagnosis of an Automotive Engine Using Several Types of Fault Models, IEEE Trans. on Control Systems Technology, Vol.10, No.5, 2002
- (4) R. Isermann and P. Balle. Trends in the application of model-based fault detection and diagnosis of technical processes. Control Eng. Practice, 5(5): 707-719, 1997
- (5) G. Rizzoni and P.S. Min.: Detection of sensor failures in automotive engines. IEEE Trans. on Vehicular Technology, 40(2):487-500, 1991.
- (6) G. Rizzoni, P.M. Azzoni, and G. Minelli. On-board diagnosis of emission control system malfunctions in electronically controlled spark ignition engines. Proc. of the American Control Conference, pages 1790 – 1795, 1993.
- (7) W.B. Ribbens A Mathematical Model Based Method for Diagnosing Failures in Automotive Electronic System, SAE910069, 1991
- (8) Y. Hasegawa, et al., "Individual Cylinder Air-Fuel Ratio Feedback Control Using an Observer", SAE 940376



Kazuo KIDO



Kazuhide TOGAI



Hiroki YAMAURA



# A Method for Analyzing Car Driver's Sensitivity to Stress and Comfort

Makoto KATANIWA\* Sae KUMAKURA\*

## Abstract

The various factors that make car drivers feel "stress" and "comfort" from the cars they are driving were analyzed.

From the answers to the free-answer questionnaire used for the survey, sensitivity-related words were selected. Also, "stress" and "comfort" were subdivided into multiple categories to be able to map the positioning of the sensitivity-related words in relation to these categories. Through this process, a method for predicting the tendency of drivers to be sensitive or susceptible to certain factors has been established.

**Key words:** Human Engineering, Psychology/Kansei Engineering, Stress, Comfort, Hierarchy Structure Analysis

## 1. Foreword

People are subject to stress caused by different environmental factors in their daily lives. Stress induces mental and physical burdens, distortion and pressure. Under a situation involving continued tension, stress animates the sympathetic nerves. This upsets the balance between the sympathetic nerves and the parasympathetic nerves, the latter of which work to keep the bodily functions stable. It is widely known that this is a factor that causes various physiological disorders, such as psychosomatic and psychoneurotic disorders.<sup>(1)</sup>

Driver stress in the car is caused by various factors that can be broadly classified into two categories: short-term factors and long-term factors. One example of short-term stress is sudden emotional one that may be reflected in the driver's driving behavior. Such type of stress typically appears as anger and irritation. Also one example of long-term stress is one that accumulates over time, the typical of which is the stress induced by long-term inconvenience with car use. This type of factors may influence a customer's decision when purchasing next car.

It is important for automakers to gain an understanding of this driver stress and improve the brand strength of the car by eliminating these factors.

In this study, a free-answer questionnaire was distributed on the Web to extract stress factors. Also studied and analyzed in the study was comfort,<sup>(2)</sup> which was known to have a strong correlation to stress. The purpose was to identify the relation in characteristics between the driver's susceptibility to stress and to comfort.

## 2. Survey content

### 2.1 Survey method

A questionnaire was conducted over the Web with 2,819 people in Japan. This method was employed because it enabled the survey to be conducted relatively easily over a broad area with respondents from all age groups and also because it was a well-established method generally used to research market trends by quickly obtaining many responses.

Also, this survey method was matched to this study, which required sufficiently numerous answer samples to analyze the complex and diverse characteristics of drivers' susceptibility to stress and comfort.

### 2.2 Questions used for the survey

To extract answers that reflect the candid psychology of drivers, the questions used in the survey were designed in a free-answer format as shown below.

The psychological scale used for measuring the answers to the depth category questions was established utilizing the literature<sup>(3)(4)</sup> indicated at the end of this paper.

- (1) The questions asking about the stress felt by the driver regarding the car
  - ① What (object) do you feel stress about?
  - ② Why do you feel the stress?
  - ③ In what situation does the stress occur?
  - ④ How deeply do you feel the stress?
- (2) The questions asking about the comfort felt by the driver regarding the car
  - ① What (object) makes you feel comfortable?
  - ② How must a car be to feel comfortable for you?
  - ③ How deeply do you feel the comfort?

\* Advanced Vehicle Engineering Dept., Development Engineering Office

### 3. Classification of elements included in freely written answer

#### 3.1 Stress elements

The first thing necessary to realize is the nature of driver stress. The approach selected for this purpose was the classification of stress elements, in which the stress-related pieces of content that could be extracted from the freely written answer were integrated into superordinate concepts using the repertory grid method<sup>(5)(6)</sup>.

Through this process, the stress elements could be classified into the following five categories:

- (1) Trouble (failure, something wrong, bad condition)
- (2) Performance (acceleration, fuel efficiency, driving stability, braking, traction)
- (3) Usage (operation, function, storage ability, loading capacity, livability, easy access, easy drive)
- (4) Sense (somatic sensation, visual sensation, auditory sensation, olfactory sensation, cognitive judgment)
- (5) Domain of Kansei

Of these five categories, the "sense" and "domain of kansei" categories are conceptual. Their definitions are as follows, based on the literature<sup>(7)(8)</sup> indicated at the end of this paper.

The "sense" category corresponds in general to the five senses, and indicates the human function of feeling a stimulus from the outside world. The "sense" as defined in this study, however, includes an addition of "cognitive judgment" for understanding and judging the information obtained through the senses. Cognitive judgment is, for example, familiarity with driving or perceptions of the distance between vehicles.

The "domain of kansei" is defined as a cognitive judgment added to "evaluation". For example, the answer, "The car's interior looks cheap for the price," expresses the results of "evaluation" of the interior that looks cheap for the driver. Answers such as these with the added element of evaluation are classified into the "domain of kansei" category.

#### 3.2 Comfort elements

The same process as for the stress elements was applied to the classification of the comfort elements.

The comfort elements were classified into the following seven categories:

- (1) Trouble (failures, something wrong, bad condition)
- (2) Performance (acceleration, fuel efficiency, driving stability, braking, traction)
- (3) Usage (operation, function, storage ability, loading capacity, livability, easy access, ease drive)
- (4) Sense (somatic sensation, visual sensation, auditory sensation, olfactory sensation, cognitive judgment)
- (5) Driving support (automated driving, safety/peace of mind)
- (6) Stress-free
- (7) Domain of Kansei

#### 3.3 Kansei words extracted from the freely written answer

The kansei words were extracted from the freely written answer to analyze the characteristics of driver's susceptibility to the stress elements categorized in the above sections.

The contents extracted from the answers to a free-answer type questionnaire like that employed for this study are sentences, not words that are difficult to directly extract. Text mining was used as a method to extract kansei words necessary for this study<sup>(9)(10)</sup>.

The text mining process applied to this study consisted of splitting up a sentence in the freely written answers into individual words and then classifying them into kansei words by identifying the part-of-speech information. The following is an example.

Example of sentence: "Driving makes me tired because the shape of the seat is inappropriate to hold my body."

Breakdown into words: Driving / makes / me / tired / because / the / shape / of / the / seat / is / inappropriate / to / hold / my / body

The following five parts of speech are selected as significant kansei words as a result of the part-of-speech information analysis conducted on these separated words.

- (1) Adjectives (Examples: happy, tired)
- (2) Verbs (Examples: to move, to fatigue)
- (3) Adverbs (Examples: much, leisurely)
- (4) Nouns derived from adjectives (Examples: safety, quietness)
- (5) Nouns expressing the state of things or of mind (Examples: lack, peace)

Of the separated words indicated in the example above, the adjective "tired" corresponds to a kansei word.

Further, the kansei words with a low frequency of appearance are replaced by more frequently appearing synonyms or quasi-synonyms for consolidation.

#### 3.4 Selection method of multiple kansei words in the same sentence

Because of the employment of the free-answer format for the questionnaire, there were instances where two or more kansei words appeared in the text of one answer. Therefore, hierarchy structure analysis was applied to this case to select the single word subject to the analysis. This method could choose kansei word which was the most dominant concept. The following is an example.

Example of sentence: "The trunk is small and inconvenient."

Breakdown into words: The / trunk / is / small / and / inconvenient

Dominant conception: Inconvenient (adjective having a noun as derivative)

Subordinate conception: Small (adjective)

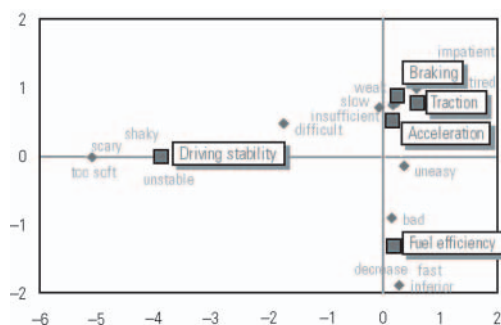


Fig. 1 Stress: Vehicle dynamics and text words  
[Cumulative contribution rate: 0.690]

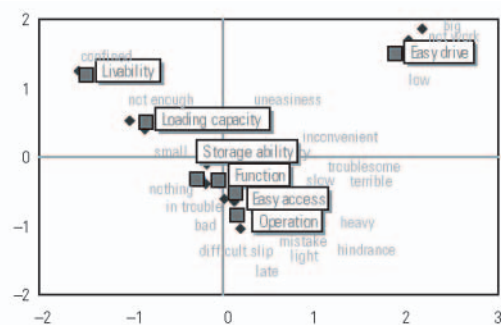


Fig. 2 Stress: Vehicle usage and text words  
[Cumulative contribution rate: 0.576]

## 4. Classification method

The correspondence analysis<sup>(11)</sup> was applied to both the stress elements as categorized above and the kansei words extracted from the answer texts in order to identify correlations between them.

A correspondence analysis represents the correlation between multiple data using a scatter diagram. The strength of the relationship is expressed by the relative distance of the plotted points; the closer the points, the stronger the relative relationship.

As the kansei word analysis uses sentences as the data source, the frequency of appearance of such words is an important factor. Another factor to which this study placed importance was the stress depth. The correspondence analysis conducted was therefore so designed that the depth factor would be reflected in the result.

The same analytical method was also applied to the comfort analysis and the results were correlated with those of the stress analysis to identify the difference in characteristics of driver's susceptibility between comfort and stress.

## 5. Analytical results

### 5.1 Stress analysis

The samples containing text pieces about the "kansei domain" stress elements had vast variety of expressions because this category depended on a subjective evaluation, making it difficult to apply the above-mentioned analytical method to this category. For this reason, an analysis of the "kansei domain" has been omitted from this paper.

#### 5.1.1 Trouble

Most of the answers regarding trouble indicated the fact of trouble occurrence and few contained any kansei or sensitivity-related words. This made the employed analytical method unfit to the answers of this category. The occurrence of trouble, however, is thought to have a direct influence on driver stress.

#### 5.1.2 Performance (Fig. 1)

For the performance category, the stress elements can be generally classified into three groups according to their positioning on the distribution map: the first

group consists of "acceleration", "traction", and "braking"; the second group consists of "fuel efficiency"; and the third group consists of "driving stability". As to the "fuel efficiency" element, drivers anonymously showed tendencies of being susceptible to the vehicle's functionality, which was expressed by such words as "bad", "fast", and "inferior". Also with the "driving stability" element, which was the farthest away from the map origin (0,0), words were used to express functionality in regard to stability, including "unstable", "shaky", and "soft". Meanwhile, a diversity of words were used for expression with the "acceleration", "traction", and "braking" elements, which were clustered the closest to the origin (0,0), making it difficult to identify the tendency of driver's susceptibility to these stress elements.

#### 5.1.3 Usage (Fig. 2)

In the category of usage, the "livability", "loading capacity", and "easy drive" elements showed a tendency of taking different mapping positions from the other elements. With the "livability" and "loading capacity" elements, such words as "confined" and "not enough" were used to express functionality. Sensitivity words that were also observed for the "easy drive" element expressed such functionality related concepts as "not work (at tight turns)".

Like with the analytic results for the performance category, there was a wide range of susceptibility characteristics indications for the "storage ability", "function", "easy access", and "operation" elements, all of which were located the closest to the origin (0,0).

#### 5.1.4 Sense (Fig. 3)

For the sense category, it was found that the individual stress elements are scattered away from the origin (0,0), showing that each element has its own tendency. This peculiarity is thought to be attributable to different recipients for different sensations, resulting in that they each exhibit distinctive susceptibility characteristics. Of these, "auditory" and "olfactory" sensations are mapped at the similar positions, while visual sensation and "cognitive judgment" also take other similar positions. What is characteristic of the "auditory" and "olfactory" sensation elements is that the very presence of odor or sound is the source of stress, as shown by the words "terrible" and "noisy". The characteristics of driver's susceptibility to stress for the "visual sensa-



**Fig. 3 Stress: Sense and text words**  
[Cumulative contribution rate: 0.604]

tion" and "cognitive judgment" elements, on the other hand, related to the perception of conditions, as expressed by such words as "unidentifiable" and "impossible".

### 5.1.5 Results of stress analysis

The map positioning analysis that provided positional relationship between stress elements revealed the following two major characteristics about all elements except those of the sense category.

#### (1) Function-related characteristics of susceptibility

Drivers anonymously share the same tendency in susceptibility to those stress elements that take positions away from the origin (0,0). This is advantageous to car engineers in focusing on specific points for improvement. The elements that showed these characteristics were most often modified by kansei words representing the performance of the car.

#### (2) Psychology-related characteristics of susceptibility

Those stress elements that cluster around the origin (0,0) of the map have stress cause modifiers expressed by a variety of words, therefore, it is difficult to converge driver's susceptibility to stress into certain tendencies. The answers had a variety of words expressing psychological states, and this is believed to be a factor that caused the diversity.

## 5.2 Comfort analysis

Comfort analysis was conducted for the same categories of elements as the stress analysis in order to clarify the difference in the characteristics between the driver's susceptibility to stress and that to comfort. Therefore, the comfort element categories "stress-free", "driving support", and "domain of kansei" were omitted from the analysis described in this paper.

### 5.2.1 Trouble

As with stress, most of the answers indicated "non-occurrence (of trouble)". This indicates that the absence of trouble is the minimum functional requirement and is remotely related with comfort.

### 5.2.2 Performance (Fig. 4)

In regard to the performance category, the "braking" and "driving stability" elements are differently mapped from those for stress, showing that the characteristics of the driver's susceptibility to comfort is differ-

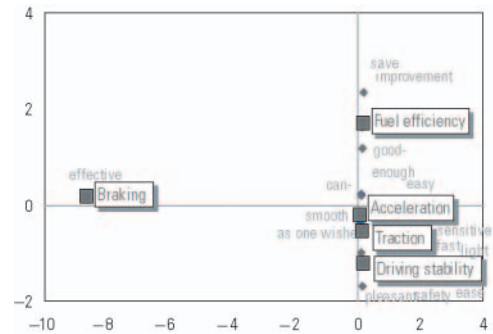


**Fig. 4 Comfort: Vehicle dynamics and text words**  
[Cumulative contribution rate: 0.747]

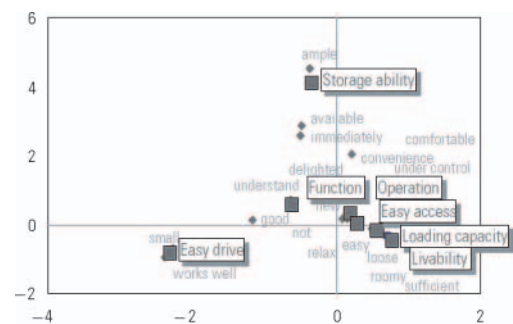


**Fig. 5 Comfort: Vehicle usage and text words**  
[Cumulative contribution rate: 0.500]

ent from those to stress. The "braking" element is mapped at a position different from the others, because its modifier in the samples was "effective", the word expressing a purely functional characteristic. In contrast, "driving stability performance" is positioned close to the origin (0,0). This can be explained by that the driver's susceptibility to comfort is characterized by modifiers expressing rather vague feeling such as "smooth" and "as one wishes", not by modifiers expressing functional characteristics regarding stability as observed with stress.

### 5.2.3 Usage (Fig. 5)

The map for the comfort elements of the usage category shows "storage ability" taking a position different from the other elements of the same category. This is because drivers are most susceptible to comfort when they are impressed by the storage's functionality characteristics as indicated by such words as "ample" and "(storage is) available". Like with "storage ability", words that indicate functional characteristics were observed for "livability" and "maneuverability", such as "roomy" and "sufficient" for the "livability" element and "good (at tight turns)" for the "easy drive" element. These functionality characteristics are thought to be highly dependent on the equipment setting and basic specifications.



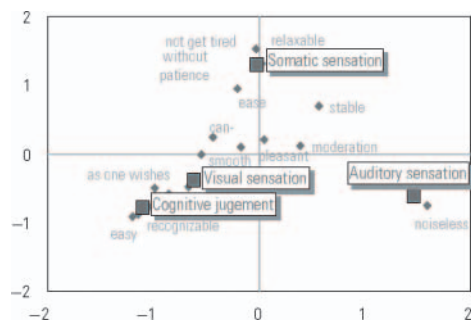


Fig. 6 Comfort: Sense and text words  
[Cumulative contribution rate: 0.714]

#### 5.2.4 Sense (Fig. 6)

Regarding susceptibility to comfort, what is characteristic to the sense category is that there are no indications related to olfactory sensation in the samples. A possible reason for this is that olfactory sensation is an element for which it is difficult to cause drivers to feel comfort. Another characteristic is that, as with stress, "visual sensation" and "cognitive judgment" are closely mapped with each other, suggesting that "visual sensation" has the greatest influence on the driver in the process of making a cognitive judgment.

#### 5.2.5 Results of the analysis for difference in characteristics of the driver's susceptibility between stress and comfort

The following results were obtained for the difference in characteristics in the driver's susceptibility tendencies between stress and comfort.

- (1) Elements showing functional characteristics that cause susceptibility to stress or comfort  
((1), (2) and (3) in Fig. 7)

It was observed that the elements of this type cause drivers anonymously to show a uniform level of susceptibility to stress or comfort. Since the relevant answer samples include indications about functionality of vehicle, it is possible that the result of this analysis can be directly incorporated into the policy for improvement.

- (2) Elements showing psychological characteristics that cause susceptibility to stress and comfort  
((4) in Fig. 7)

The samples containing the elements of this type were represented by words of abstract nature, therefore, it would be difficult to incorporate the result of this analysis directly into the measure for improvement. Before the analysis result on these elements can be used for future improvement, it is necessary to conduct another analysis for the association between these psychological characteristics and replace them with functional characteristics. For example, to make drivers feel that acceleration is smooth, it will be necessary to develop driver's "psychological concept" into a "functional concept" and then examine specific measures.

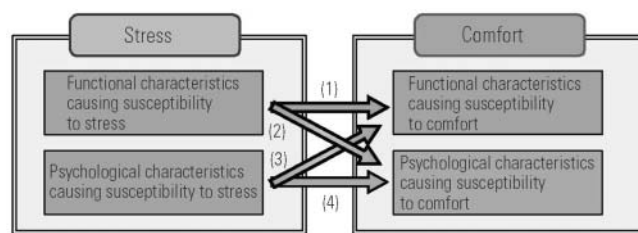


Fig. 7 Relationship between "stress" and "comfort"

## 6. Summary

This paper identifies the characteristics of susceptibility to the stress and comfort the driver receives from vehicle using kansei words as mediums and by deducting them from the positional relationship of the stress- and comfort-causing elements plotted on maps using a positioning analysis technique. The study could not identify tendencies regarding psychological susceptibility characteristics. For the analysis of the psychological area, it is necessary to identify the concept formation with a structural analysis of the driver's psychology using the repertory grid method and other interview-dependent methods. A task for the future will be providing feedback to integrate the research results in the cognitive science and psychology fields into text mining.

### References

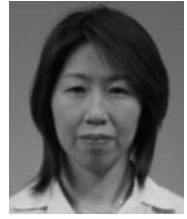
- (1) Masaki Yamaguchi, Junichiro Arai: Biometric Engineering, 2004
- (2) Hideo Nakane: Biochemical Analysis of Stress and Comfort, Toyota Central R&D Labs. R&D Review, Vol. 32, No. 3, 1997
- (3) Hiromichi Hori, Mariko Yamamoto: A Collection of Psychological Scales I, 2003
- (4) Hiromichi Hori, Mariko Yamamoto: A Collection of Psychological Scales II, 2003
- (5) Junichiro Sanui, Masao Inui: Extraction of Residential Environment Evaluation Structures Using Repertory Grid Development Technique – A Study on Residential Environment Evaluation Based on Cognitive Psychology –, Journal of Architecture and Planning No. 367, Architectural Institute of Japan, 1986
- (6) Mari Ogi: Fundamental Research on Parent and Child Dwelling Places and Their Evaluation Structure, 2003
- (7) Fumitoshi Mori, Mie Sato, Masao Kasuga: Study on Content Processing and Display Environment for Raised Entertainment Characteristics, KANSEI Engineering, Vol. 5, No. 3, pp. 57 – 60, 2005
- (8) Akichika Mikami, Shin Nakagawa, Madoka Yatsuiwa, Takashi Moreda, Toru Endo: Playing with Five Senses, 2000
- (9) Shinobu Ogi: Word-derived Kansei and Movies – Extraction of Kansei by Text Mining –, KANSEI Engineering, Vol. 5, No. 3, pp. 43 – 47, 2005
- (10) Hiromi Ban, Hidetaka Nanbo, Takashi Oyabu: Quantitative-Linguistics-Based Characteristics Extraction

from Modern American Movies, KANSEI Engineering,  
Vol. 5, No. 3, pp. 49 – 55, 2005

- (11) Takaho Ueda, Shota Kuroiwa, Keiko Toya, Hirotaka  
Toyota: Market Research Utilizing Text Mining, 2005



Makoto KATANIWA



Sae KUMAKURA

# Development of Inter-Vehicle Communication Type Driving Support System in the ASV-3 Project

Masayoshi ITO\*

## Abstract

As measures to reduce traffic accidents are being promoted using the technologies of second-stage Intelligent Transport Systems (ITS), the development of cooperative driving support systems using wireless communication technologies has been gaining momentum in Japan and abroad. Mitsubishi Motors Corporation (MMC) participated in the 3rd phase Advanced Safety Vehicle (ASV-3) project, which was led by the Ministry of Land, Infrastructure and Transport (MLIT) with the objective of "Developing new technologies"; we took part in the verification test of the inter-vehicle communication (IVC) type driving support system for preventing collisions through vehicle-to-vehicle communication. The test revealed issues to be addressed concerning the technology for recognizing surrounding vehicles by obtaining their location information via wireless communication.

**Key words:** Preventive Safety, Intelligent Transport Systems (ITS)

## 1. Introduction

Each day, the media reports another string of traffic accidents. Fatalities are on the decline, but road accidents continue to occur at the same rate and with the same devastating effect. In response, accident prevention efforts are being made in conventional areas such as road design, traffic regulations, driver education and vehicle safety, and moreover, progress is being made in promoting measures that utilize second-stage ITS. The New IT Reform Strategy<sup>(1)</sup>, formulated in January 2006 by the IT Strategic Headquarters of the Japanese government, sets forth a policy to promote the practical application of vehicle-to-infrastructure cooperative driving safety support systems which use IT to help reduce traffic accidents. Data from roadside sensors and position information from surrounding vehicles is used to supplement the recognition function of the driving support system, which is not possible with the conventional autonomous-detection type system. In this paper, we attempt to classify the existing driving support systems and describe the history of related R&D in Japan and abroad. We also outline a verification test, part of the MLIT-led Phase 3 ASV Project in which we participated, of the inter-vehicle communication type driving support system utilizing wireless communication technology. MMC is also developing autonomous-detection type driving support systems. An example of such efforts is presented in the article "GRANDIS ASV-3 – Unlikely to Strike, or Be Struck by, Another Vehicle –" in this issue of Mitsubishi Motors Technical Review.

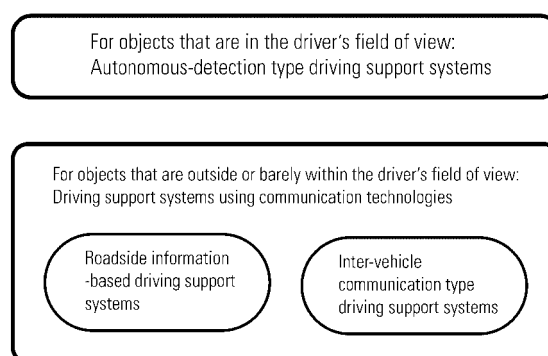


Fig. 1 Positioning of the systems developed in the ASV project

## 2. Classification of driving support systems

Drivers drive their vehicles in the three sequential steps of "recognition", "decision" and "action". Driving support systems are designed to help reduce the work load by taking over some of the driver's tasks while assisting in driving performance. "Recognition" refers to the detecting step of the situation around the vehicle, so the system must be capable of detecting conditions around the vehicle. For this purpose, two types of systems are required: one that is designed to cover those areas that the driver can see, namely, a system using onboard sensors; the other designed to cover those areas that the driver cannot see or can hardly see. In the ASV project, these systems are positioned as shown in Fig. 1<sup>(2)</sup>.

\* Advanced Vehicle Engineering Dept., Development Engineering Office

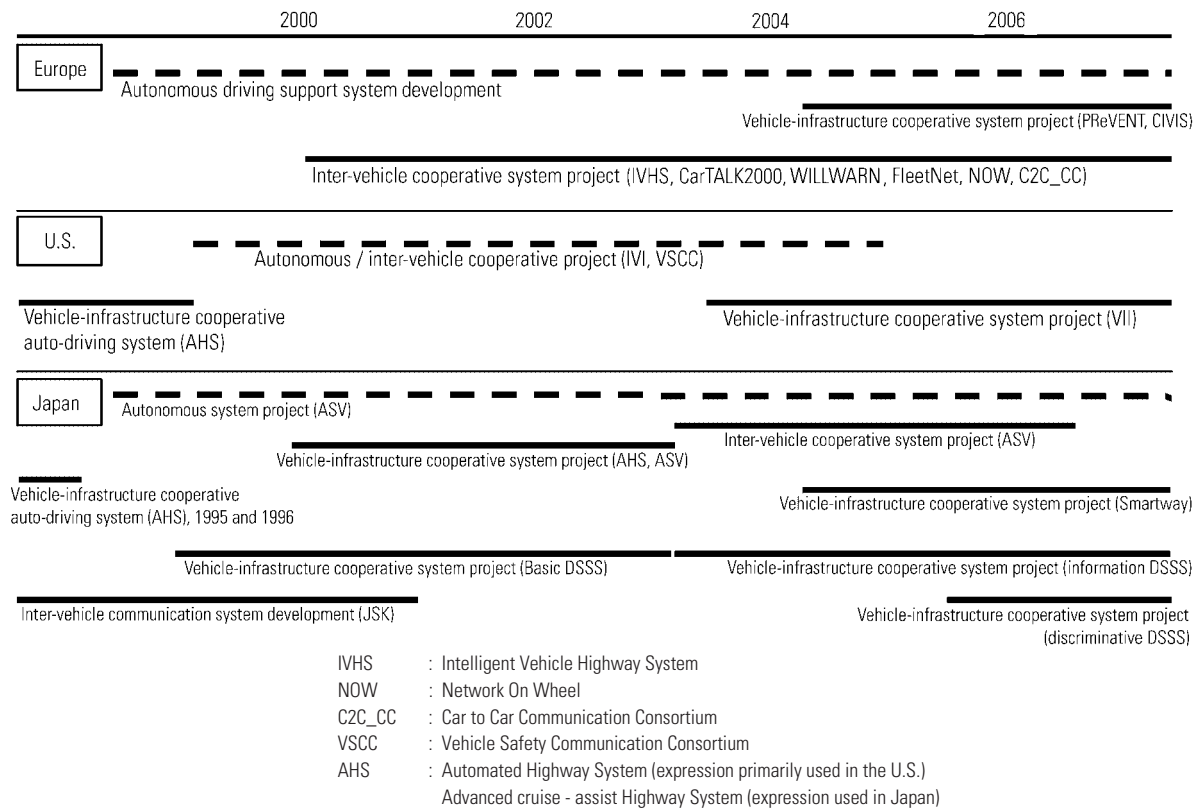


Fig. 2 Research and development history of cooperative type driving support systems

### 3. History of R&D on cooperative driving support systems

Many years of research and development efforts in autonomous-detection type driving support systems have led to commercial products with good performance. On the other hand, the development of communication technology-based vehicle-to-infrastructure cooperative driving support systems has made significant progress but such systems have only recently entered the commercialization stage due to reasons related to cost-effectiveness of road infrastructure installation, user acceptance and limited applications. Similarly, vehicle-to-vehicle cooperative systems have not yet entered practical use in spite of years of studies and experiments. The history of R&D on communication technology-based cooperative driving support systems is outlined below<sup>(3) - (5)</sup> (Fig. 2).

In Europe, early R&D efforts targeted vehicle-to-vehicle support systems. In recent years, vehicle-infrastructure cooperative system projects, PReVENT (Preventive and Active Safety Applications) and CIVIS (Cooperative Vehicle-Infrastructure Systems), were developed to reduce traffic accidents at intersections, etc and they are still in action. In the United States, the cooperative vehicle-infrastructure auto-driving system was the focus of development in the 1990s. In 1998, the spotlight shifted to the Intelligent Vehicle Initiative (IVI) system, particularly onboard equipment. In recent years, as in Europe, vehicle-infrastructure cooperative systems regained attention for reducing traffic acci-

dents at intersections, and the Vehicle Infrastructure Integration (VII) system project has been in progress since 2004.

In Japan, verification tests on the vehicle-infrastructure support system were conducted (on test and actual roads in 2000 and 2002) jointly in the autonomous type driving support system development project (ASV) and the cooperative vehicle-infrastructure system development project – Advanced cruise-assist highway system (AHS). Since then, there has been active development of practical AHS systems and pilot programs conducted primarily on highways under the Smartway project<sup>(4)</sup>. In addition, another vehicle-infrastructure cooperative driving support system project to prevent traffic accidents at intersections on ordinary (non-highway) roads, etc. – the Driving Safety Support System (DSSS) – conducted basic experiments and verification experiments for information supply, and was successfully introduced as an information system in limited regions in 2005. Currently, DSSS is promoting the development of discriminative information service whereby the onboard system judges the danger of the present situation based on information about the vehicle's behavior and the surrounding conditions from the roadside devices, and supplies the necessary information to the driver<sup>(5)</sup>.

### 4. ASV-3 project – inter-vehicle communication type driving support system

The MLIT-led ASV project has been developing automotive safety technologies for over 15 years. Since



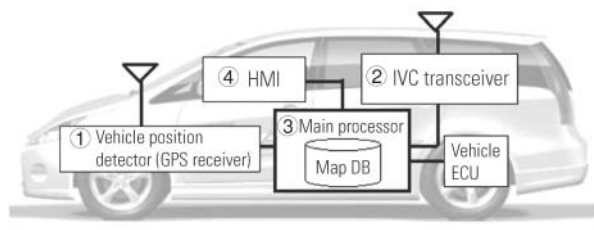


Fig. 3 Configuration of the Mitsubishi ASV-3

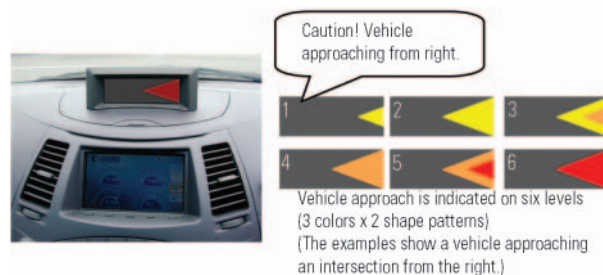


Fig. 4 Examples of HMI image

2001, when the third phase of the project was launched, efforts have been made to promote the technologies already developed under the project while at the same time developing new technologies. As part of the new technology development theme, verification tests of roadside information-based driving support systems were conducted jointly with AHS, using wireless communication technologies as a means of vehicle-infra-structure communication.

Roadside information-based driving support systems using roadside sensors did not function in regions not equipped with such systems. Therefore, efforts were made to develop driving support systems that function in any region. Inter-vehicle communication type systems were developed that allow vehicles to exchange information on their position and behavior using the latest wireless communication technologies to keep drivers informed of their own vehicle's separation from surrounding vehicles. In 2005, verification tests were conducted on test roads, for which Japanese car manufacturers provided large-, medium-, compact- and mini cars, motorcycles and pedestrian-simulating mannequins.

#### 4.1 Test vehicle system configuration

Fig. 3 shows the system configuration of the test vehicle, GRANDIS ASV-3, which MMC contributed to the verification test on inter-vehicle communication type driving support systems.

The IVC driving support system basically consists of an IVC transceiver, a vehicle position detector and a human-machine interface (HMI). The experiment was primarily aimed at clarifying the feasibility and acceptability of the system's wireless inter-vehicle communication-based driving safety support functions. The wireless communication means available at the time (2005), namely the 5.8-GHz DSRC (dedicated short-range communication), was used for the test. The actual method of applying the system would be based on the most appropriate wireless communication technologies available at the time.

In the test, the position of the test vehicle was measured using a commercially available GPS receiver. The measurement was then projected onto a previously prepared shared map of the test course (hereafter "the map database (DB)") stored in the main processor in order to determine the test vehicle's position. The positions

of surrounding vehicles were then measured and the measurements were sent via the IVC transceivers to the main processor of the test vehicle. The position data was then projected onto the map DB of the test vehicle. The determined relative positions of the test vehicle and surrounding vehicles were then converted into separations using the map DB scale, based on which decisions were made regarding the timing of driver notification.

Driver notification was made via an on-dash HMI unit, using different colors and shape patterns as well as voice messages to alert the driver to approaching vehicles. Fig. 4 shows examples of the HMI display.

#### 4.2 Verification test

One of the test items was collision prevention at intersection corners. To create poor visibility conditions, walls were erected at an intersection of the test course (Fig. 5). The GRANDIS ASV-3 was equipped with nose-view cameras. Images of an approaching vehicle on the crossing road of the intersection that were sent from the camera, combined with corresponding driver notification messages based on inter-vehicle communication, proved effective in making the driver aware of the approaching danger.

#### 4.3 Issues identified in the verification test

In the autonomous-type driving support system, the surrounding vehicle position detection sensor mounted on the vehicle directly measures the separation (relative positions) between the vehicle and the surrounding vehicles. The accuracy of measurements, therefore, depends on the accuracy of the vehicle's sensor. On the other hand, with the IVC-type system, the tests revealed various issues that must be resolved in order to achieve accurate vehicle positions (Fig. 6). These include: measurement error by vehicle position detectors of own vehicle and surrounding vehicles; asynchronous measurement timing among vehicles; and the fact that vehicles will be at different positions by the time the measured positions are communicated between the vehicles.

The levels of driving support offered (caution, warning, control) depend heavily on position accuracy. For practical implementation, it is important to remember that the levels of driving support offered should be set in accordance with the position accuracy that can be achieved by the technologies employed.

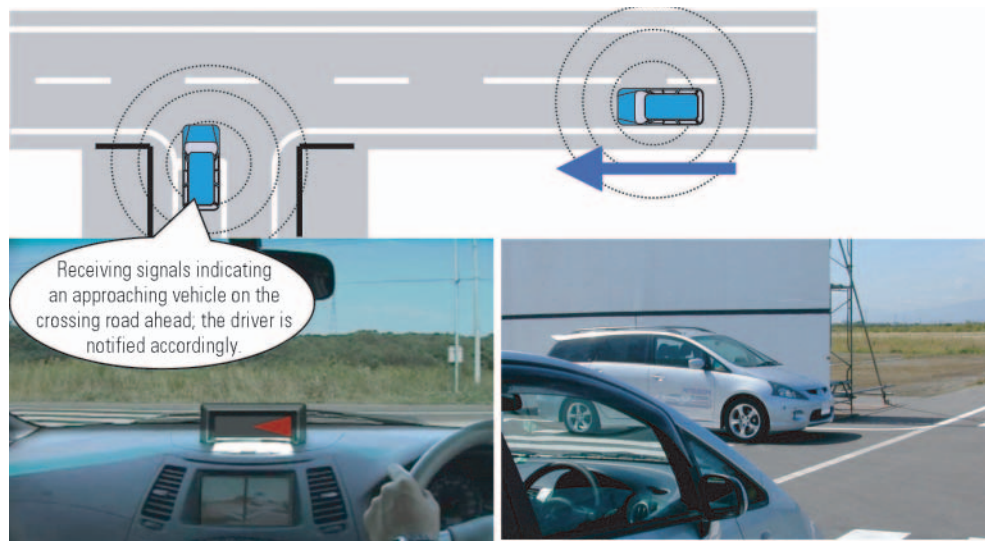


Fig. 5 Verification test on collision prevention at intersections

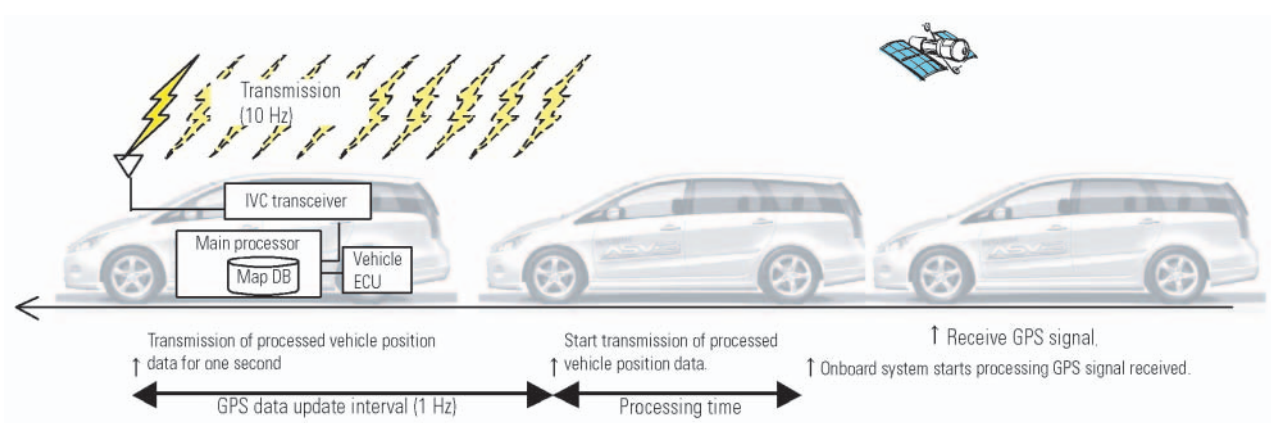


Fig. 6 Consideration of delay in positional information processing

## 5. New IT Reform Strategy and the future of cooperative-type driving support systems

The New IT Reform Strategy sets targets and policies to achieve the "World's safest road traffic environment.". One of the targets aims to "Reduce the number of traffic fatalities and serious injuries by deploying Cooperative Driving Safety Support Systems that cooperate with traffic infrastructure.". To achieve the target, a joint public-private sectors' project road map has been set up, as outlined in **Fig. 7**. In line with the scenario, related activities have been started, such as the establishment of specifications and basic experiments across the country. In other words, approximately 10 years after the Vehicle Information Communication System (VICS) was launched in 1996, the route to practical implementation of next-generation cooperative driving support systems is now clear.

To prevent traffic accidents, it is important not only to ensure cooperation between vehicles and roadside systems, but also to maintain vehicle-pedestrian and inter-vehicle cooperation. Expectations are high for wireless communication technology to further improve vehicles' capability to recognize surrounding circum-

stances, for onboard sensors to ensure such vehicle recognition capability, and for cooperative driving support systems based on the integration of the two to emerge.

## 6. Conclusion

In this paper, we presented an overview of the existing cooperative driving support system development projects, and described the issues identified in a verification test on an IVC-type driving support system that we developed.

In an attempt to help eventually eliminate road traffic accidents by means of cooperative vehicle-infrastructure driving support systems that will be deployed in 2010 and onwards, we will continue with technological development and commercialization efforts for integrated autonomous, vehicle-infrastructure and inter-vehicle driving support systems, by collaborating with other concerned bodies.

In conclusion, we thank all those involved in the ASV verification test for their cooperation, including those from the ASV coordination office and from the companies that participated in the test.

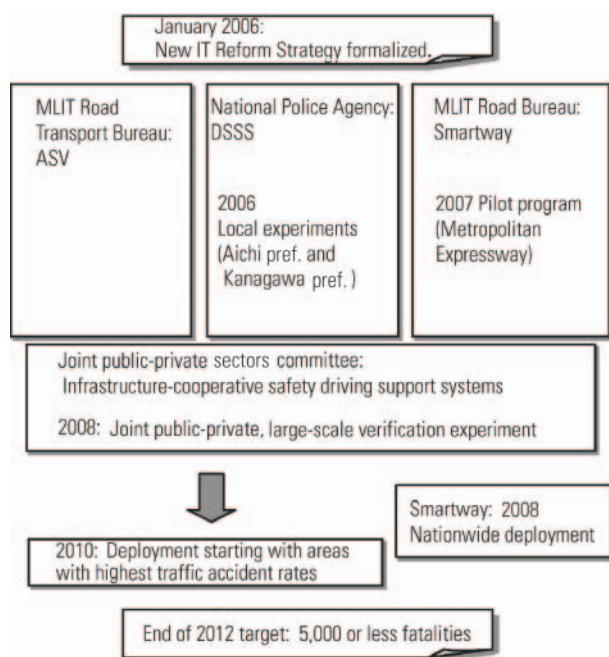
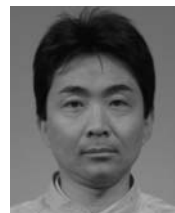


**Fig. 7 Road map for the development of cooperative driving support system**

## References

- (1) Strategic Headquarters for the Promotion of an Advanced Information and Telecommunications Network Society (IT Strategic Headquarters)  
<http://www.kantei.go.jp/jp/singi/it2/index.html>
- (2) ASV Promotion Committee of the Ministry of Land, Infrastructure and Transport; Advanced Safety Vehicle (ASV): Inter-Vehicle Communication (IVC)-type Driving Support System Pamphlet; 2005
- (3) ASV Promotion Committee of the Ministry of Land, Infrastructure and Transport; Update Meeting of the 3rd Phase of the Advanced Safety Vehicle (ASV) Project; 2006
- (4) 2006 AHS Symposium Report; June 2006
- (5) The 3rd Universal Traffic Management System (UTMS) Meeting; July 2006  
<http://www.npa.go.jp/koutsuu/kisei29/20060727.pdf>
- (6) The 7th Smartway Project Advisory Committee Working Groups; November 2006  
[http://www.its.go.jp/ITS/j-html/topindex/topindex\\_smartway\\_bukai.html](http://www.its.go.jp/ITS/j-html/topindex/topindex_smartway_bukai.html)



Masayoshi ITO

# GRANDIS ASV-3

## – Unlikely to Strike, or Be Struck by, Another Vehicle –

Susumu MASUDA\*

### Abstract

Rear-end collisions are the most frequent cause of road traffic accidents. To reduce accidents of this type, Mitsubishi Motors Corporation (MMC) has been engaged in safe vehicle development under the ASV-3 \*1 project with the theme “Unlikely to strike, or be struck by, another vehicle”. The GRANDIS ASV-3 (Fig. 1) is an experimental advanced safety vehicle incorporating active and passive safety technologies such as a display system employing a new type of control, an emergency stop signal system and a pre-crash safety system. MMC is now working to commercialize these systems.

\*1: Phase 3 Experimental Advanced Safety Vehicle Project (Advanced Safety Vehicle-3) under the auspices of the Ministry of Land, Infrastructure and Transport of Japan.

**Key words:** Safety, Preventive Safety

## 1. Introduction

In recent years, fatalities from road traffic accidents have been on a gradual decline thanks to a range of safety measures implemented. On the other hand, the annual total number of road traffic accidents stays high, amounting to approximately 950,000. This has led to active safety measures being increasingly regarded as important<sup>(1)</sup>. Among the causes of accidents, rear-end collisions are the most frequent cause, accounting for nearly 30 % of all accidents<sup>(2)</sup> (Fig. 2). In recent years, around 360,000 people per year are suffering from neck injuries, or whiplash, caused by rear-end collisions, making it a potential immediate risk for everybody<sup>(3)</sup> (Fig. 3). Against this background, MMC has developed the GRANDIS ASV-3 by placing focus on prevention of rear-end collisions, the most frequently occurring type of accident, with the theme “Unlikely to strike, or be struck by, another vehicle”.

## 2. GRANDIS ASV-3's onboard systems

The GRANDIS ASV-3's onboard systems will be described below under the subsection titles of “Strategies to avoid striking another vehicle”, “Strategies to avoid being struck by another vehicle”, “Strategies for safety when vehicle is about to strike or strikes another vehicle” and “Strategies for safety when vehicle is about to be struck or is struck by another vehicle”, which represent the stages of active and passive safety strategies adopted against rear-end collisions.

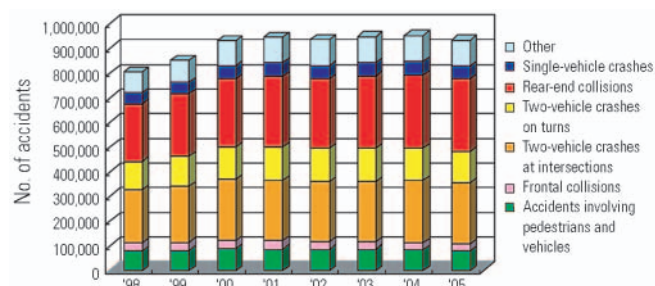
### 2.1 Strategies to avoid striking another vehicle

#### 2.1.1 New display system

To avoid distracting a driver's attention during driving, the meter and information display system of the



Fig. 1 GRANDIS ASV-3



Source: Institute for Traffic Accident Research and Data Analysis

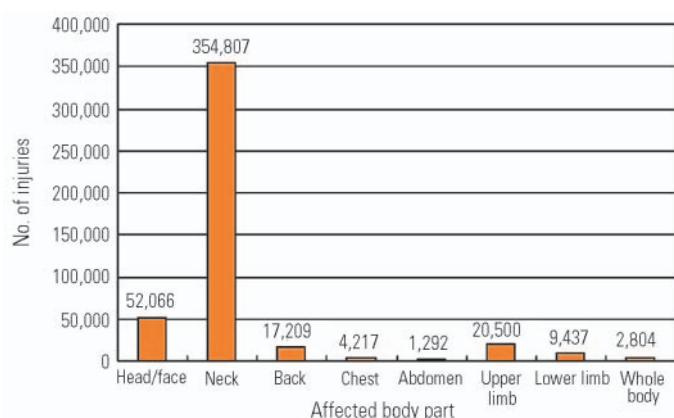
Fig. 2 Types of traffic accidents and their share in totals of accidents

GRANDIS ASV-3 is formed of a multiplex display and an easy-to-use touchpad control. An illuminated area on the display indicates the position of the driver's finger on the touchpad, which allows the driver to operate the system without looking at the control and thus minimizes the driver's eye movements.

The LCD meter integrates multiple displays, being

\* Advanced Vehicle Engineering Dept., Development Engineering Office





Source: The General Insurance Association of Japan

Fig. 3 Number of rear-end-collision injuries by affected body parts

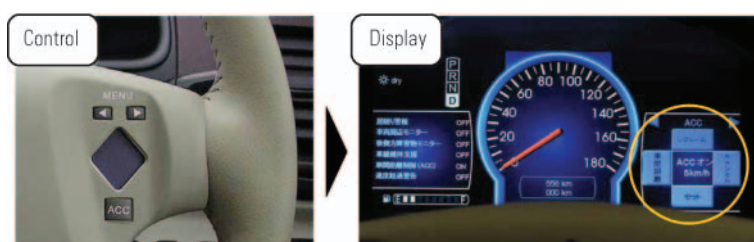


Fig. 4 Touchpad on steering wheel and LCD meter

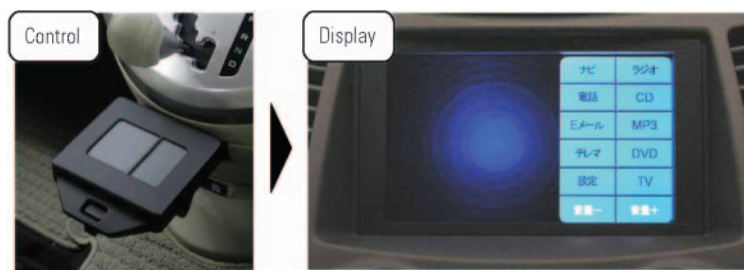


Fig. 5 Center touchpad and center display



Fig. 6 Emergency stop signal system

able to show information on the adaptive cruise control and other driving support systems on a single display. For easy operation and reduced driver load, the touch-

pad control is located on the steering wheel (Fig. 4).

Another touchpad control is used for the center display that is provided for car navigation and audio systems. The driver can easily reach the touchpad and operate it without compromising his/her driving posture and with minimum eye movements (Fig. 5).

### 2.1.2 RADAR brake prefill system

When the RADAR senses that the distance from the preceding vehicle is too short, the system slightly increases the brake line pressure for quicker brake system response to the driver's pedal action.

### 2.1.3 Brake assist system

When the system senses an emergency braking from an unusually quick brake pedal motion, the brake assist system produces a force so as to increase the pedal pressure and to boost the braking force.

### 2.1.4 Adaptive cruise control

The adaptive cruise control system monitors the distance from the preceding vehicle using signals from the RADAR to maintain an appropriate distance from the vehicle ahead. The system gives warning to the driver when the distance has become too short.

## 2.2 Strategies to avoid being struck by another vehicle

### 2.2.1 Emergency stop signal system

When the system's control unit senses an emergency braking based on inputs from the vehicle speed sensor, brake switch and ABS unit, the control unit causes the rear stop lamps to flash rapidly (4 Hz). This actively signals the sudden braking to the drivers behind, encouraging them to take braking and other appropriate actions for preventing rear-end collisions and mitigating damages (Fig. 6). When the vehicle comes to a stop, the system then automatically activates the hazard lamps to prevent secondary accidents.

## 2.3 Strategies for safety when vehicle is about to strike or strikes another vehicle

### 2.3.1 Pre-crash safety system

The pre-crash safety system consists of the following components: a forward-monitoring millimeter-wave RADAR; sensors that sense the speed, behavior and other relevant conditions of the vehicle; a control unit that determines likelihood of collision; a buzzer that alarms the driver to the danger of collision; seat belts and cushions to restrain the occupants in preparation for imminent collision; and an automatic brake unit (Fig. 7).

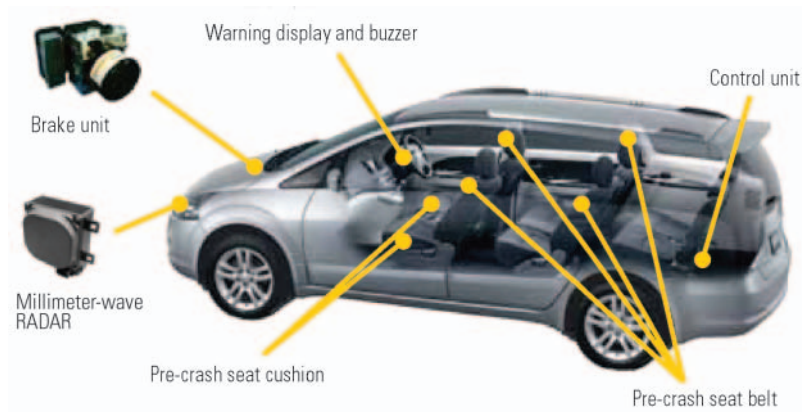
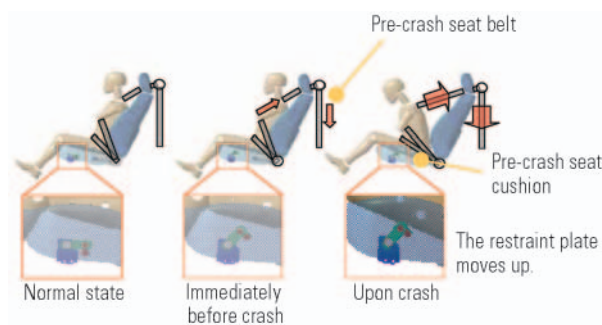


**Fig. 7 Components of pre-crash safety system**



- Pre-crash seatbelt  
Prior to a crash, the seatbelt is retracted to produce an additional force to restrain the occupant in a posture in which maximal protection by the airbag and other safety systems is provided.
- Pre-crash seat cushion  
Prior to a crash, the restraint plate at the occupant's lower back moves up to offer a firmer grip of the body region, thus preventing the occupant from sliding under the belt upon impact.

**Fig. 8 Restraining force intensification process**

### 2.3.2 Operation of the pre-crash safety system

- (1) When the control unit determines that the vehicle is potentially in danger of colliding with an object (such as a preceding vehicle) detected by the RADAR installed behind the front grille, the system alarms the driver to the danger by sounding the buzzer.
- (2) If the object ahead gets nearer and the risk of crash increases, the pre-crash seatbelts and cushions activate to restrain the occupants in their seats in preparation for the impact of a possible crash (**Fig. 8**).
- (3) If the control unit determines that a crash is unavoidable, the system activates the automatic braking unit rapidly to slow down the vehicle, thus mitigating the impact from the crash.

## 2.4 Strategies for safety when vehicle is about to be struck or is struck by another vehicle

### 2.4.1 Whiplash reducing seat

The whiplash reducing seat has a frame located further rearward than standard seats, which allows the back of the occupant to sink more easily upon impact in the event of a rear-end collision. Quicker sinking of the occupant's upper body into the seat enables his/her

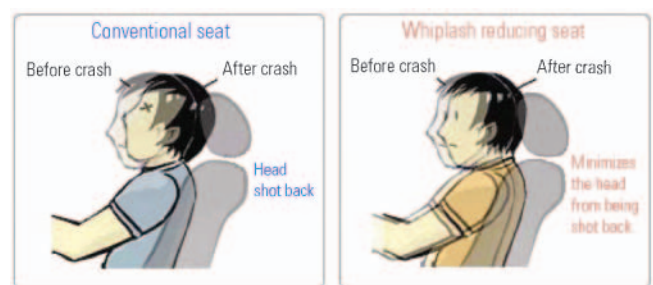


**Fig. 9 Whiplash reducing seat**

head and back to be simultaneously supported by the headrest and seatback. This minimizes the occupant's head being shot back, thus reducing load on the neck (**Fig. 9**).

## 3. Conclusion

The GRANDIS ASV-3 was put on display at the "ITS Special Expo." within the Nagoya Motor Show (November 2005) and the JSAE Automotive Engineering Exposition (May 2006) (**Fig. 10**). At these shows, visitors were invited to experience some of the vehicle's features. Although not in a moving vehicle, visitors were able to operate the touchpad controls while seated in the vehicle and experience the retraction and tensioning of the pre-crash seatbelt that was activated immediately before a simulated crash. These shows provided MMC with an opportunity to receive customer feedback as well as to publicize the technologies that it offers to the public. MMC's ASV development projects will be continued while listening to "the voice of the customer".



Fig. 10 JSAE Automotive Engineering Exposition

#### References

- (1) Study Group for Promotion of ASV, Ministry of Land, Infrastructure and Transport: The Report Meeting of Phase 3 of the Advanced Safety Vehicle (ASV) Project, 2006
- (2) Institute for Traffic Accident Research and Data Analysis: Traffic Accidents Data, Road Traffic Statistics (2005), 2006
- (3) The General Insurance Association of Japan: Facts about road traffic accidents based on automobile insurance data – April 2004 through March 2005, p. 21, 2006



Susumu MASUDA

# Multi-around Monitor System

Keiji UEMINAMI\* Kenji HAYASE\* Eiji SATO\*

## Abstract

This paper discusses a driver view assist system that has been developed to provide the driver with views around the vehicle and of blind spots on both sides at confined intersections using three onboard cameras. The system features Multi-view display that shows a composite of the images from two cameras to allow the driver to see blind spots around the vehicle at a glance. In addition, the system offers an auto display mode in which the image from the necessary camera is displayed automatically once the selected gear and vehicle speed conditions are met without having to push the switch of the camera, thus relieving the driver of the burden of operating the camera switch while enhancing safety.

**Key words:** *Intelligent Vehicle, Safety, Electric Equipment, Comfort, Human-Machine-Interface, Intelligent Transport Systems (ITS)*

## 1. Introduction

Mitsubishi Motors Corporation (MMC) has thus far offered the following onboard systems that assist drivers in checking safety around the vehicle: the first system was the Corner Sensor that warns the driver of detected obstacles by means of ultrasonic waves and was installed on the 1999 DELICA model as a factory-installed option. The Around Monitor on the CHARIOT GRANDIS released in 2000 featured corner sensor inputs superimposed on images from a rear-view camera to help eliminate blind spots behind the vehicle. The 2003 model GRANDIS was equipped with the Dual-around Monitor that consisted of a nose-view camera, a rear-view camera and corner sensors for enhanced left and right side fields of view at intersections and under road conditions with restricted views. With the growing popularity of car navigation systems, there are more systems that assist the driver's view by using multiple cameras available, also in vehicles from other manufacturers.

The results of a recent survey show that drivers desire easy visibility of their vehicle's surroundings more than any other attribute of automotive comfort. This suggests that there is a potential demand for devices that provide a view of blind spots around the vehicle. In Japan, it is mandatory to install a mirror that provides views of the immediate front left side (the side opposite to the driver) of the vehicle on all new models sold during and after January 2005. This fact clearly indicates that offering a system that provides the driver with views of the front and side blind spots, contributes not only to comfort, but also to safety.

The Multi-around Monitor on the new DELICA D:5, launched in January 2007, was developed to meet this demand for better visibility. It employs nose-, rear- and side-view cameras to provide views of blind spots, including those in the areas just below the front of and on the left side of the vehicle.

## 2. System configuration

Fig. 1 shows the configuration of the Multi-around Monitor system. All components are controlled by the camera control unit. Images from the three cameras are sent to the control unit, which then outputs them to the display unit. According to signals from the camera switch on the instrument panel, as well as from Controller Area Network (CAN) derived data, such as vehicle speed and gear position data, the control unit selects appropriate camera(s) and sends their images to the display through the CAN.

## 3. Camera specifications and coverage

To compensate for blind spots that are likely to occur at intersections with restricted views, those in the front and rear areas of the vehicle and those on the side opposite to the driver, camera coverage requirements have been determined for each of these areas. Assuming these requirements as prerequisites, the camera specifications and mounting locations have been examined, while also considering cost implications and the feasibility of camera installation at each location. From the examination, it was decided to install three cameras, one at the front, another at the rear and the third in the door mirror. Fig. 2 shows the locations and the coverage of these cameras. The specifications and coverage requirements for each camera are described below.

- Nose-view camera (also covering the area just below the front of the vehicle)

Mounted in the center of the front grille, the nose-view camera incorporates a combination of a prism and wide-angle lens and covers the fields of view in three directions. The use of a prism enables this single nose-view camera to offer the same viewing coverage of blind spots on both sides (shown in yellow in Fig. 2) at

\* Electronics Engineering Dept., Development Engineering Office



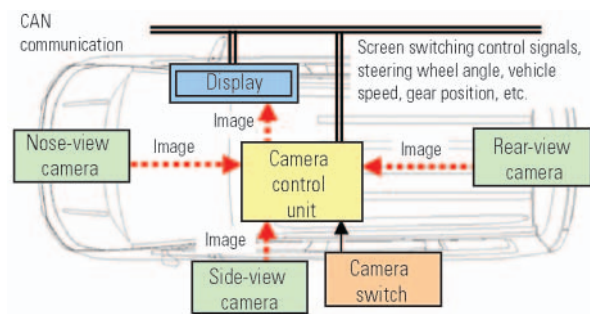


Fig. 1 System configuration

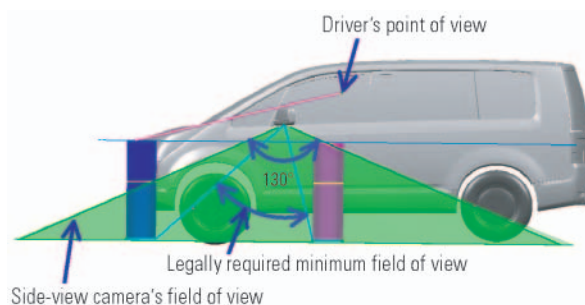


Fig. 3 Side-view camera's field of coverage

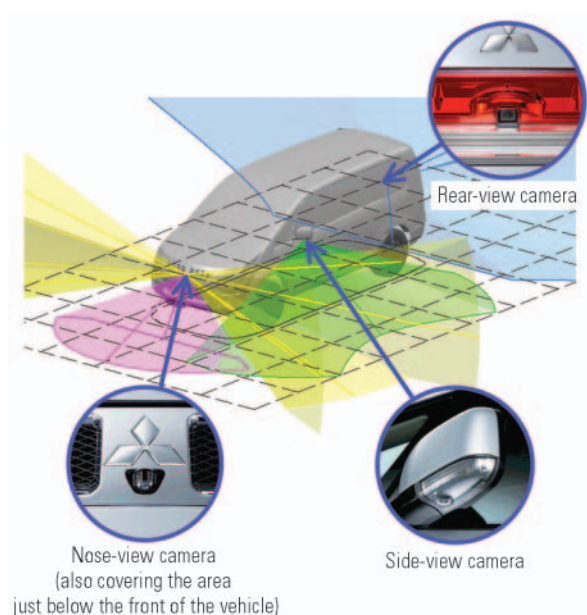


Fig. 2 Mounting locations of cameras and fields covered by them

confined intersections, as that provided by two nose-view cameras (one for the right side view and the other for the left side view) of the Dual-around Monitor system. The angles of the prism have been so determined that the camera coverage angle on each side is  $30 - 45^\circ$ , because too small an angle is not sufficient to cover the full width of the intersecting road, whereas too large an angle causes the image of an approaching vehicle to appear too small to give the driver a proper sense of distance.

The strategy employed for enabling this single nose-view camera to also cover the blind spots present in the area just below the front of the vehicle (shown in pink in Fig. 2), is to form a camera with a combination of a prism and a special wide-angle lens. The selected maximum lateral angle of coverage for the wide-angle lens is  $130^\circ$ , which is necessary to cover the full width of the vehicle.

- Side-view camera

The side-view camera is a wide-angle lens camera that is incorporated in the left door mirror and is directed nearly straight down so as to cover an area wide

enough to include blind spots on the left side of the vehicle. The factors considered in determining camera coverage are the fields of view required for installing the immediate front and left confirmation mirror by the relevant Japanese regulation and also the practical benefits that the camera offers in actual use (Fig. 3). The regulation stipulates that the driver shall be able to recognize a column measuring  $\phi 300 \times 1,000$  mm in the mirror, which is placed at a location defined by the driver's viewing point and the shape of the vehicle (the area between the light blue lines in Fig. 3). The side-view camera of the Multi-around Monitor system satisfies the above requirements and furthermore, its coverage is set to provide a view of a point on the ground 200 mm in front of the vehicle's front end. The rearward coverage of the side-view camera is so determined that the camera provides a view of the left rear tire rotating in contact with the ground so that the driver can check any contact between the tire and an obstacle during a left turn. To meet the above coverage requirements, a camera capable of covering a front-rear angle of  $130^\circ$  (shown in green in Figs. 2 and 3) has been employed.

- Rear-view camera

The rear-view camera is a wide-angle lens camera with a lateral coverage angle of  $130^\circ$ , which is nearly equal to that of the Dual-around Monitor system. The camera is mounted in the rear garnish and covers an area wide enough to include the blind spots at the rear of the vehicle (shown in blue in Fig. 2).

#### 4. Display specifications

The most characteristic feature of the Multi-around Monitor system is its specification of the display screens. While some competing brands use three cameras, all of their displays are only capable of displaying an image from just one camera at any given time, which requires the driver to switch cameras in order to see, for instance, blind spots in the area just below the front end of the vehicle while viewing those on the side of the vehicle. The Multi-around Monitor's display system can show composite images from more than one camera on a single screen, which eliminates the need for the driver to switch cameras and enables him/her to view all blind spots simultaneously. The processing necessary for this effect, including cutting out required portions, enlarging/shrinking/rotating, and combining images

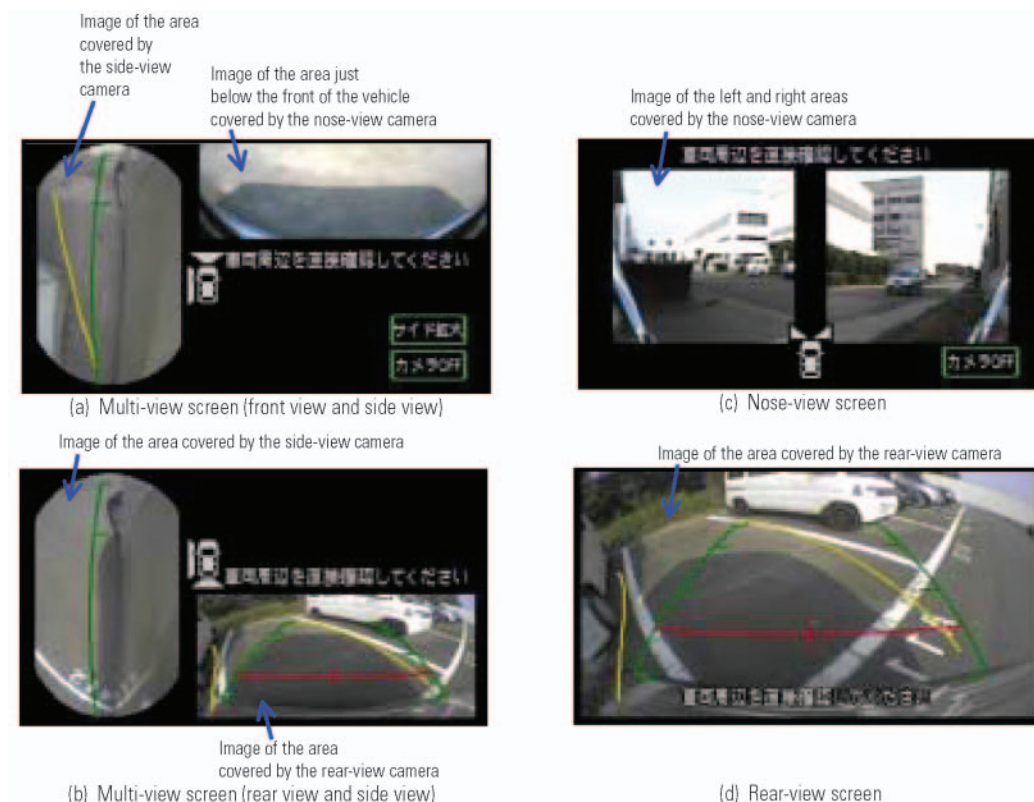


Fig. 4 Display specifications for images from the cameras

from the cameras, is performed by the camera control unit. To be able to perform these tasks almost in real time, the control unit has a dedicated image-processing LSI chip.

The specifications of the display screens are described below.

- Multi-view screen (front view and side view)

To enable the driver to see blind spots on a single screen simultaneously while moving the vehicle forward, images of the area just below the front of the vehicle from the nose-view camera (shown in pink in Fig. 2) and of the area from the side-view camera (shown in green in Fig. 2) are combined for displaying on the same screen (Fig. 4 (a)). To match the driver's instinct for realizing the positional relationship, the image from the side-view camera is displayed on the left portion of the screen with the front being at the top and the image of the area just below the front of the vehicle being displayed on the upper portion of the screen. A symbol representing the vehicle, accompanied by guide marks, is also shown to help the driver recognize the location of the displayed areas at a glance. On the side-view image, the expected path that will be followed by the vehicle during a left turn, as predicted from the steering wheel angle, is superimposed to help the driver remain aware of the inner rear wheel's tracking.

- Multi-view screen (rear view and side view)

Similarly to forward movement, when reversing the vehicle the screen shows both images of the area shown by the rear-view camera (shown in blue in Fig.

2) and of the area shown by the side-view camera (shown in green in Fig. 2) simultaneously (Fig. 4 (b)). This multi-view screen appears when the driver presses the camera switch, although a full-size single image from the rear-view camera is displayed automatically upon moving the gearshift lever to the R range. To prevent the driver from perceiving inconsistency when switching from the full-size, single-view screen to the multi-view screen, the same rear view image as that on the full-size, rear-view screen (described below) is also displayed on the bottom of the multi-view screen by reducing it in size.

- Nose-view screen

The image from the nose-view camera is displayed after splitting it into images corresponding to the left and right fields of view (shown in yellow in Fig. 2). The left and right images are arranged laterally on the screen (Fig. 4 (c)).

- Rear-view screen

A full-size image of the area within the coverage of the rear-view camera (shown in blue in Fig. 2) is displayed on the screen (Fig. 4 (d)). The path of the vehicle, predicted from the steering wheel angle, is superimposed on the display to help the driver back up smoothly.

## 5. Displaying scheme of camera-provided images

Keeping a close watch on the multi-view screen (front view and side view) and nose-view screen while

Option A	Individual screens for front, side and rear views: any one of these is selectable with a switch. The switch is installed in the centralized control area of the instrument panel. Inputs from the camera switch are accepted with the gearshift lever in P. Auto-display mode is selected on a camera-provided image screen.
Option B	Multi-view screens (front + side and rear + side) are provided. The switch is situated near the navigation screen. Inputs from the camera switch are not accepted with the gearshift lever in P. Auto-display mode is selected on the navigation set-up screen.

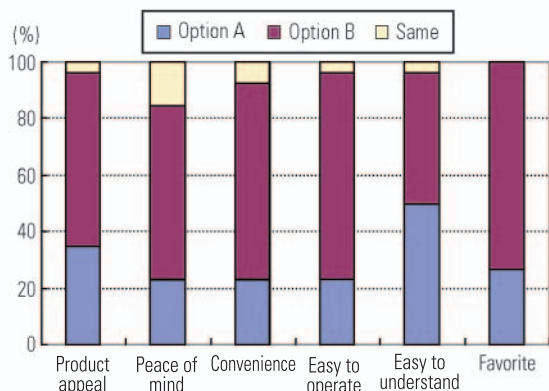


Fig.5 Usability evaluation results

driving forward can affect safety, because this can distract the driver's attention. To prevent this, the display system is programmed to accept the driver's switch inputs only when the vehicle's speed is lower than approximately 10 km/h and it turns the display off when the vehicle exceeds approximately 12 km/h. In addition, when the gearshift lever is moved (N or D  $\leftrightarrow$  R) while a multi-view screen being displayed, the system continues to display the multi-view screen. Drivers most frequently want a multi-view display when they need to pay attention to blind spots on the opposite side of the vehicle, typically when edging towards the side of the road. Because this situation involves repeated shifts between forward and reverse gears by the driver, the system is programmed so that the side-view screen is displayed continuously, so that the driver does not have to press the camera switch each time of changing direction.

## 6. Auto-display modes

The system offers the user a selectable auto-display mode that automatically turns the display on to show an appropriate screen when specific conditions have been met, without requiring the driver to press the camera switch, in order to enable the driver to pay attention to the surroundings in a safer manner.

- Automatic nose-view screen during deceleration

In this mode, the nose-view display comes on automatically when the vehicle slows down to a speed lower than approximately 10 km/h while moving forward. This mode relieves the driver of having to press the switch every time the vehicle comes to an intersection in a dense residential area or other similar environment.

- Automatic multi-view screen at start up

In this mode, a multi-view display comes on automatically upon the first gearshift lever movement from P to N, D or R after starting the engine. This mode ensures safety checking around the vehicle before starting off.

## 7. Usability evaluation

During the development of the system, usability evaluations were conducted to verify the specifications and improve the system. Fig. 5 shows the evaluation results, in which two options were examined. Although option B gained higher marks than option A in the overall evaluation, the final specifications of the system were determined by which option gained higher marks on each specification item, such as the combined two-view display, location of the switch and acceptance of switching inputs in gearshift lever position P.

## 8. Summary and acknowledgement

- (1) A new camera system has been developed by employing a combination of three cameras. The camera system is capable of covering almost all blind spots at the front, rear and left side of a vehicle.
- (2) The system is capable of displaying images of the areas covered by two cameras on a single screen, which enables the driver to see blind spots around the vehicle simultaneously.
- (3) The image displaying scheme, including the auto-display mode, was determined by taking into consideration both practicality and safety.

In conclusion, we sincerely thank Clarion Co., Ltd., Sumitomo Electric Industries, Ltd. and Sumitomo Wiring Systems, Ltd., and everyone inside and outside MMC who extended their valuable cooperation during the development of the Multi-around Monitor system.



Keiji UEMINAMI



Kenji HAYASE



Eiji SATO



# Development of Active Cornering Light System

Kazunari KOBAYASHI\* Satoshi SHINOHARA\*\*

## Abstract

The new standard for cornering light system allows not only the conventionally approved ON-OFF control mode interlocked with the operation of the turn signal switch but also an automatic ON-OFF control according to the steering wheel angle. The active cornering light system (ACL system) (Fig. 1) on the new DELICA D:5 has a dedicated ECU to control the operation of the lamps. In addition, the light distribution of the ACL system is coordinated with that of the high-intensity discharge headlights to offer higher nighttime visibility of road shoulders at intersections.

In recent years, global harmonization of automotive regulations has led to changes in Japanese vehicle equipment and design. This paper also introduces change in regulatory requirements regarding lighting equipment and the accommodation of such changes by the vehicle design.

**Key words:** Lighting, Lamp, Electronic Control, Regulation

## 1. Introduction

While every country has its own regulatory requirements concerning the installation of automotive lighting equipment, there has been a growing trend in recent years towards global harmonization of related regulations. Under such legislative circumstances, cornering lights of higher luminous intensity than before and those with an automatic ON-OFF control according to the steering angle have become accepted in Japan. Installing such cornering lights enhances safety by providing the driver with better visibility at intersections and curves. This paper describes the ACL system which Mitsubishi Motors Corporation (MMC) has developed for its production vehicles as the first of its kind in Japan, focusing on the objective of development and the control algorithm. The paper also describes regulatory requirements regarding automotive lighting equipment that have been introduced recently in Japan.

## 2. Design and features of the ACL system

### 2.1 Changes in regulatory requirements

There have been the following three major changes to the regulatory requirements concerning cornering lights:

- (1) Downward luminous intensity of up to 10,000 cd is now accepted, and the use of halogen bulbs is permitted.
- (2) Automatic ON-OFF control in accordance with the steering wheel angle is permitted.
- (3) Illumination of cornering lights with the headlights off and at speeds of 40 km/h or higher is not permitted.

The new cornering light system (or the ACL system) developed by MMC in compliance with the above requirements offers a luminous intensity 1.9 times as high as that of the conventional system.

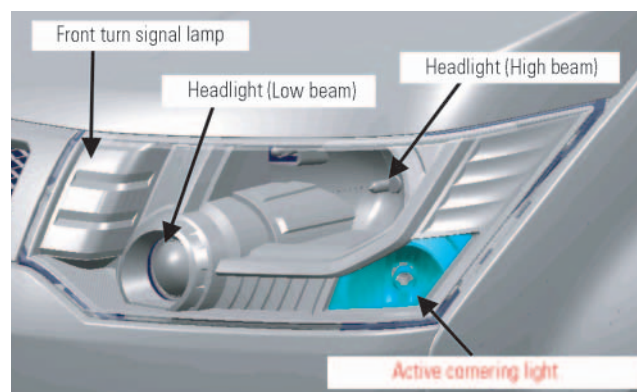


Fig. 1 ACL installed on vehicle (new DELICA D:5)

### 2.2 Light distribution of the ACL system

35 W halogen lamps are used in the new ACL system instead of the conventional 21 W incandescent lamps. The luminous intensity has been raised because otherwise the system would lose its effect when combined with high-intensity discharge headlights. In addition, the reflector has been specially designed by optical simulation to ensure that the ACL, in spite of its small size, can distribute light of intensity as high as that from fog lights (Fig. 2).

Headlights illuminate a wide area brightly but their beam coverage is limited. The ACL system has been designed to provide the areas outside the headlight beams with illumination wide enough in coverage and intense enough in luminosity to allow the driver to have a sufficiently good view ahead to be able to recognize pedestrians and road shoulders on both sides.

The major consideration when designing the light distribution of the ACL was to avoid a dark stripe that would appear on the road surface if there were a luminous gap between headlight and cornering light beams.

\* Body Design Dept., Development Engineering Office

\*\* Electronics Engineering Dept., Development Engineering Office



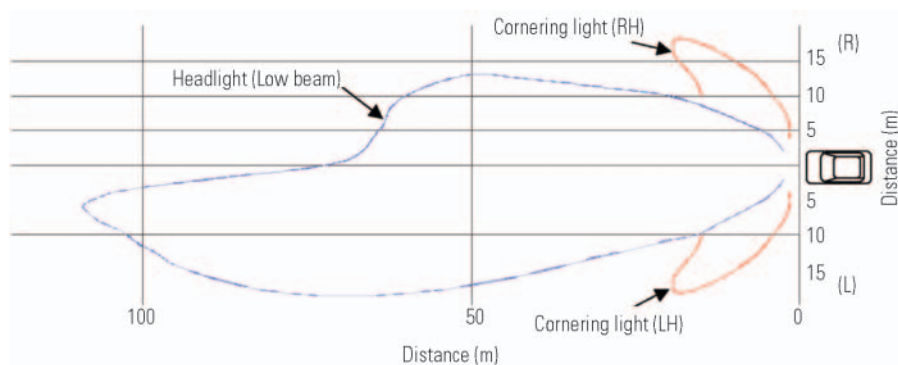


Fig. 2 Isolux area (5 lx line)

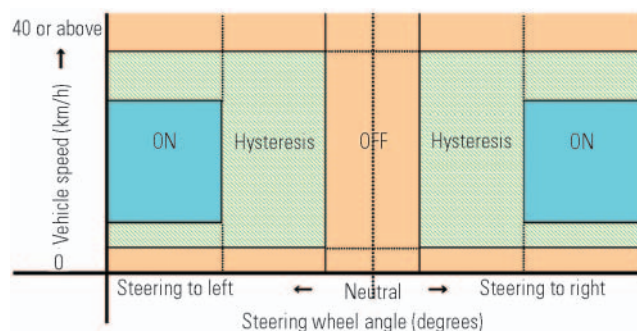


Fig. 3 ACL ON-OFF control linked with steering wheel angle and vehicle speed

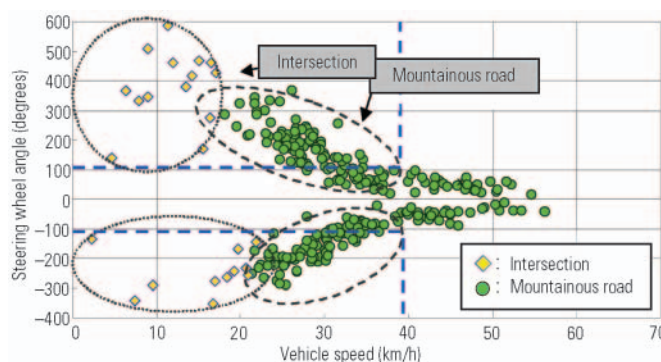


Fig. 4 Relationship between vehicle speed and maximum steering angle

This stripe would move during cornering and might be annoying to the driver.

### 2.3 Control of the ACL system

With regard to ON-OFF control, the ACL system differs most significantly from the conventional cornering light system in that the control is not only interlocked with the turn signal switch but also illuminates the inner cornering light automatically when the driver steers the vehicle to a direction. This enables the driver to have a better view ahead and thus helps increase safety even when the driver makes a sharp turn without operating the turn signal switch.

As the conventional circuit design is insufficient to enable this control, the system is provided with a dedicated ECU.

The ECU has been designed with the following four considerations.

- (1) The steering wheel angles at which the cornering light turns on or off should be selected so as not to annoy the driver (Fig. 3).

The optimum steering wheel angles have been determined based on the results of driving tests in which maximum steering angles were measured under various road conditions (Fig. 4), and in consideration of the following.

- Early illumination.
- OFF timing with a reasonable hysteresis lag from ON timing. This is necessary to prevent repeated ON-OFF of the light caused by holding the

steering wheel at angles around the ON-OFF boundary, which would be annoying to the driver.

- (2) The cornering lights should not be illuminated when the vehicle is reversing or moving forward at 40 km/h or faster.
- (3) The ECU should be compatible with controller area network (CAN) based communications systems, thus enabling it to use such data as steering wheel angle, vehicle speed and switch position as control parameters (Fig. 5).
- (4) The ECU should be made usable on multiple vehicle models by applying model-specific coding techniques.

This ACL ECU is also applicable to the additional-light-source type Adaptive Front-lighting System (AFS), which is similar in function to the ACL. The ECU can be modified relatively easily for application to both ACL and AFS when combined with the coding technique.

## 3. Recent changes and trends in requirements in automotive lighting equipment regulations

The year 2006 saw significant changes in the Japanese regulations on automotive lighting equipment (Table 1). One of these changes is the mandatory installation of a headlamp leveling system that keeps the headlight beam axis at a constant angle even when the vehicle angle changes to prevent pedestrians and

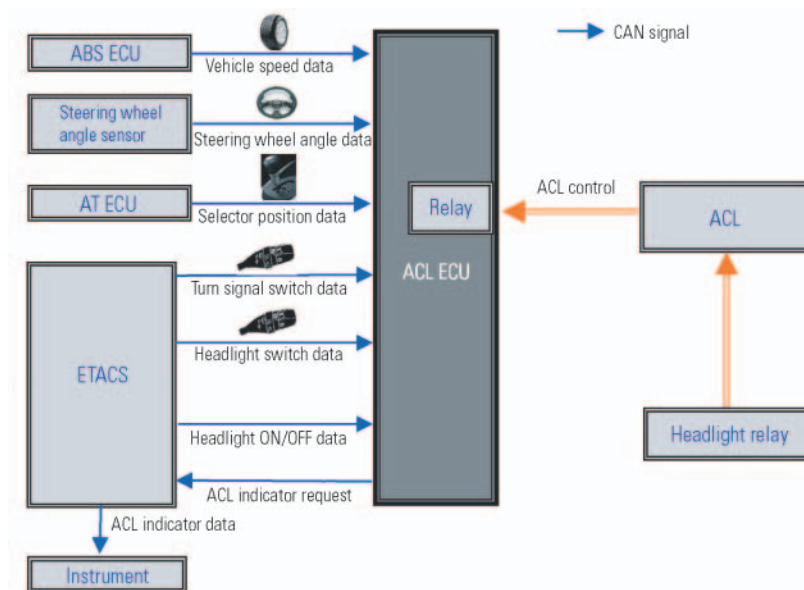


Fig. 5 System configuration

Table 1 Revised requirements in 2006 lighting equipment standard (examples)

Requirement	Purpose
Mandatory installation of automatic leveling system for low-beam headlights (manual leveling system is permitted for light beams not exceeding 2,000 lm)	Glare prevention for pedestrians and oncoming drivers
Modification of requirements in terms of the number of lamps and the definition of the number	Harmonization with relevant European requirements
Establishment of requirements for visibility of lights in terms of geometrical angles	Improved visibility

oncoming drivers from being dazzled. Another change concerns the visibility of lights, requiring that automotive lights are visible from any point within the specified area in terms of the angle and intensity, making it necessary, for example, to install a rear-mounted spare tire typically found on SUVs at a location where it does not hinder visibility of the lights. The regulations were also reviewed with respect to the number of lamps required and definition of the number of lamps. For example, installing such lamps as stop lamps on the trunk lid had been permitted to date, but under the relevant new regulation, installation of any lamps away from those installed on an unmovable component is not legally permitted. Following enforcement of this regulation, fewer Japanese passenger cars recently are equipped with tail/stop lamps of the conventional four-lamp design. All of the new requirements mentioned above are originally European legislation requirements that were introduced into Japan. For this reason, Japanese and European passenger cars will increasingly share the same design of lighting equipment.

#### 4. Future MMC activities in the lighting equipment field

In addition to compliance with future regulatory requirements, MMC will continue to develop lighting equipment that offers higher safety. Such equipment may include a full AFS which is capable of controlling the headlights and fog lights for optimum light distribution based on an overall judgment of weather, traffic conditions and road environment.



Kazunari KOBAYASHI



Satoshi SHINOHARA

# Development of Driver Side SRS Knee Airbag

Kazuyuki KATO\* Yukihiro FUKAYA\*  
Mutsuo MURAMATSU\* Hideki FUJIMOTO\*\*

## Abstract

Interest in crashworthiness has been increasing in recent years and now almost all passenger cars are equipped with seatbelts and Supplemental Restraint System (SRS) airbags that improve occupant protection in the event of a collision. For even better occupant protection performance, Mitsubishi Motors Corporation (MMC) developed a driver side SRS knee airbag as an added feature to the SRS system on the new LANCER for the North American market, the first MMC model to be fitted with this type of equipment. This paper discusses how the system works, its effect on occupant protection performance, and provides an actual installation example for the new LANCER.

**Key words:** Crashworthiness, Airbag

## 1. Concept of occupant protection afforded by driver side knee airbag

In the event of a frontal collision, a conventional occupant restraint system suppresses forward driver movement by restraining the chest and pelvic regions with a seatbelt and the head and chest regions with a deployment of a driver side SRS airbag.

In unbelted impact testing conducted according to US regulatory requirements, the driver side dummy moves forward due to inertial forces and its knees come into contact with the instrument panel. The energy from the dummy's lower extremities is then absorbed by the knee protector installed inside the instrument panel. Subsequent deployment of the driver side SRS airbag restrains the dummy at the head and chest and retraction of the steering column helps absorb the energy from the driver's upper extremities.

Earlier restraint initiation during a frontal collision generally increases energy absorption efficiency of ride-down (absorption of the kinetic energy conferred on the driver by deformation of the vehicle body) and helps the kinetic energy of the occupant to be more efficiently absorbed. One potential strategy for earlier restraint initiation is to deploy an airbag between the driver's knees and the instrument panel. The driver side SRS knee airbag is just such a strategy.

The driver side SRS knee airbag is installed in front of the driver's knees, at the bottom of the steering column under the instrument panel. In the event of a frontal collision, it deploys simultaneously with the driver side SRS airbag and fills the space between the instrument panel and driver's knees as shown in Fig. 1. The deployed SRS knee airbag restrains the driver's lower limbs at the very beginning of the collision, and this allows efficient use of the ride-down effect, which is the primary purpose of its installation.



Fig. 1 Driver side SRS knee airbag

## 2. Effectiveness from installation of driver side SRS knee airbag

The driver side SRS knee airbag is particularly effective in reducing the risk of chest injury. Rib displacement (referred to as chest deflection hereafter) and chest deceleration expressed in terms of G force (referred to as chest G hereafter) are the two indices used for measuring the severity of chest injury. The following sections illustrate how the knee airbag effectively reduces chest deflection and chest G levels.

### 2.1 SRS knee airbag effectiveness in reducing chest deflection for belted drivers

Fig. 2 illustrates the difference in driver movement for cases with and without a driver side SRS knee airbag installed. Fig. 2(a) corresponds to the with case and Fig. 2(b) corresponds to the without case. The series of pictures for the latter case shows the driver's chest and pelvis restrained by the seatbelt and the head and chest restrained by the driver side SRS airbag early in the collision, but the driver's lower extremities are not restrained at collision initiation.

\* Interior Design Dept., Development Engineering Office

\*\* Safety Testing Dept., Development Engineering Office

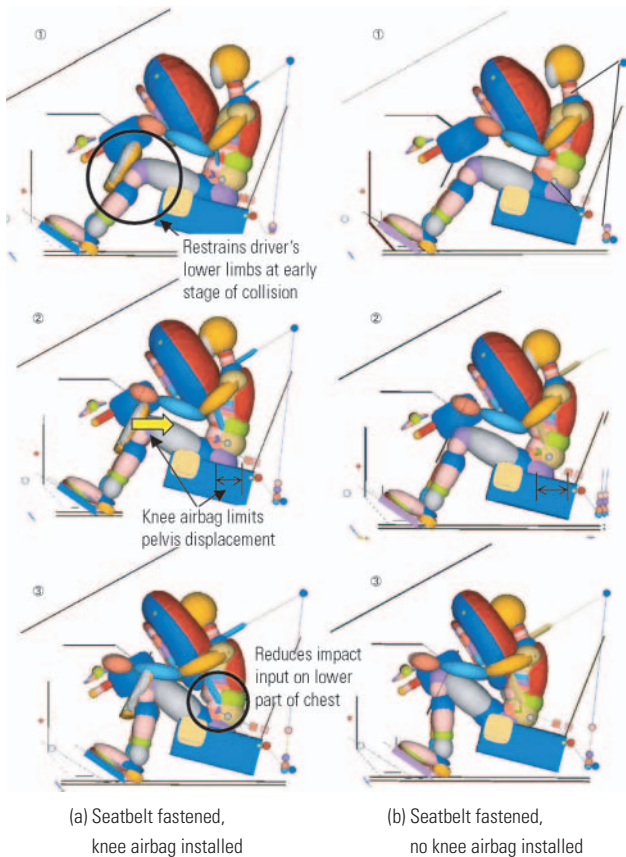


**Fig. 2 Difference in behavior between drivers with and without knee airbag**

By contrast, the with case shows how deployment between the instrument panel and the driver's knees directly restrains the lower extremities at an earlier stage in the collision (See **Fig. 2(a)①**).

Early and direct restraint of the driver's limbs by the SRS knee airbag, coupled with upper body restraint by the seatbelt and SRS airbag, improves the efficiency with which the ride-down effect contributes to absorption of the driver's kinetic energy, which limits the driver's pelvis displacement to a distance smaller than that when there is no SRS knee airbag installed (**Fig. 2 (a)②**). Smaller pelvis displacement reduces the load on the lap belt, and this in turn reduces the load input by the seatbelt to the lower part of the chest, consequently reducing chest deflection.

## 2.2 Effect of SRS knee airbag in reducing chest G for belted driver

As in the case with the chest deflection, if pelvis displacement is limited by early restraining of the driver provided by the SRS knee airbag, the driver's upper extremities turns forward about the pelvis as shown in **Fig. 3 (a)**, making the driver face toward the steering wheel at a more direct angle than when there is no SRS knee airbag installed. This prevents the input steering wheel impact from concentrating in a small area of the driver's chest, and thus reduces chest G.

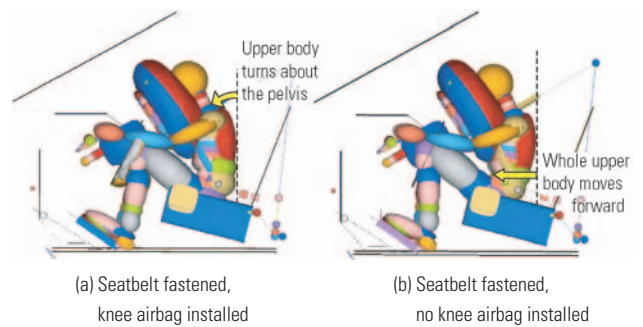


**Fig. 3 Difference in upper body behavior between drivers with and without knee airbag**

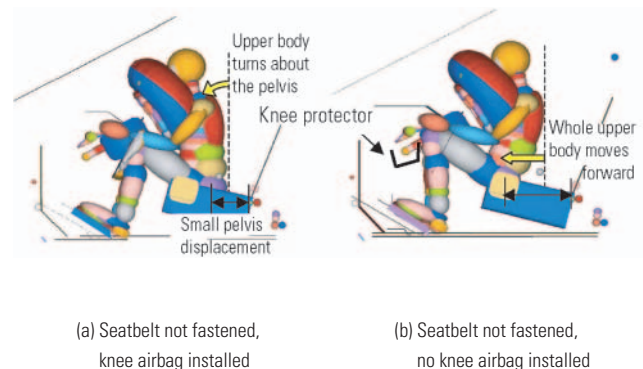


**Fig. 4 Difference in behavior of seatbelt unrestrained drivers with and without knee airbag**

## 2.3 Effect of SRS knee airbag for unbelted driver

If a collision occurs when the driver is unbelted in a vehicle without any SRS knee airbag installed, there is nothing that restrains the driver at the initial stage of the collision. The driver's knees then hit the instrument panel and the driver is moved forward until the knee protector starts restraining the driver's lower limbs (**Fig. 4 (b)**). If the SRS knee airbag is provided, it can restrain the driver's knees beginning at the initial stage of a collision as shown in **Fig. 4 (a)**, and this increases the efficiency of the ride-down effect. Also, since this provides the effect of making the driver's upper extremities face the steering wheel at almost a direct angle, similar to when the driver is belted, reduction in both chest deflection and chest G is possible.

## 3. SRS knee airbag on new LANCER for North American market

**Fig. 5** shows an SRS knee airbag installed in the new LANCER for the North American market. The SRS knee airbag system installed on this new model consists of a sheet-metal panel, which serves as a base for fitting the system to the vehicle body and a strength component for receiving reactive force resulting from airbag deployment (**Fig. 5 (2)①**), a reaction can (**Fig. 5 (2)②**), an inflator (**Fig. 5 (2)③**), an airbag (**Fig. 5 (2)④**) and an airbag lid (**Fig. 5 (2)⑤**).



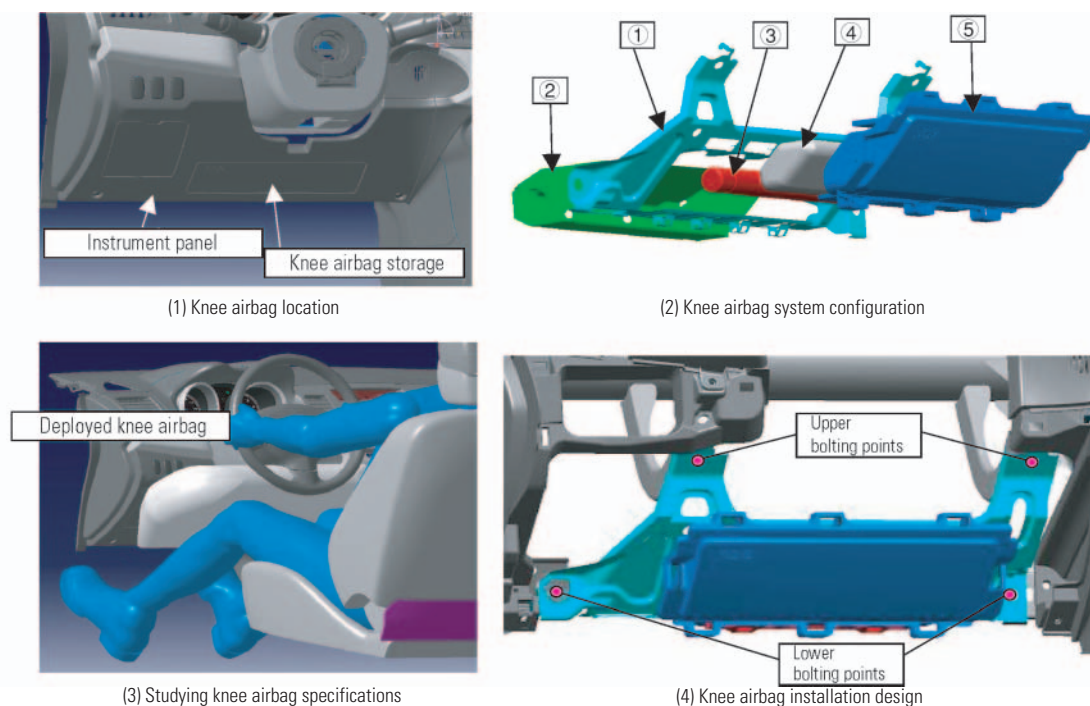


**Fig. 5 SRS knee airbag installed in new LANCER for North American market**

The airbag is designed to a shape that fits a variety of knee positions and to a capacity of 20 liters that is large enough to accommodate the knees of a large driver (**Fig. 5 (3)**). The design process also involves tuning that is indispensable for the strategy of enabling the airbag to deploy in the confined space between the instrument panel and driver's knees in a fraction of a second to protect and restrain the driver's lower limbs. The tuning applied to the new LANCER for the North American market is based on the airbag motion sequence consisting of initial small rearward deployment followed by quick obliquely upward deployment (so that it can deploy along the surface of the instrument panel).

The knee airbag is installed on the vehicle body by bolting its sheet-metal panel to the body side brackets at four points (**Fig. 5 (4)**).

The shape, angles and bolting points of the sheet-metal panel are determined so that the panel can properly bear the airbag's reactive force that is generated during a collision by the forward movement of the driver while assuring the airbag's full restraining performance, and it is also taken into account that the knee airbag is appropriately laid out relative to the neighboring components and driver's knee position. The bolting angles of the knee airbag are so determined that the lower two bolts are fastened in the horizontal direction, whereas the upper two bolts are fastened at 43° downward, also considering ready installation with minimum change of working posture during the production process.

**Fig. 6** shows the results of the crash tests conducted

during the development of the new LANCER for the North American market, indicating the difference in efficiency of the ride-down effect between the cases with and without the SRS knee airbag. In this figure, the improvements in ride-down efficiency are indicated under the assumption of 100 % efficiency for the case without the SRS knee airbag. As seen from the graphs, the SRS knee airbag improved the ride-down efficiency by about 5 % for the upper extremities and about 40 % for the lower extremities when the driver was restrained by a seatbelt, whereas it improved the efficiency by about 30 % for the upper extremities and about 120 % for the lower extremities when the driver was not restrained by the seatbelt.

**Fig. 7** shows another crash test result, which indicates the difference in severity of chest injury and pelvis displacement between the cases with and without the SRS knee airbag installed. In this figure, the reduction in severity of injury and pelvis displacement is indicated under the assumption of 100 % severity of injury and pelvis displacement for the case without the SRS knee airbag. Installation of an SRS knee airbag contributed to a reduction of about 10 % in chest G and about 40 % in chest deflection when the driver was restrained by a seatbelt and about 30 % in both chest G and chest deflection when the driver was not restrained by the seatbelt.

These results give proof of the effectiveness of the SRS knee airbag in improving driver protection performance of the vehicle in a crash.

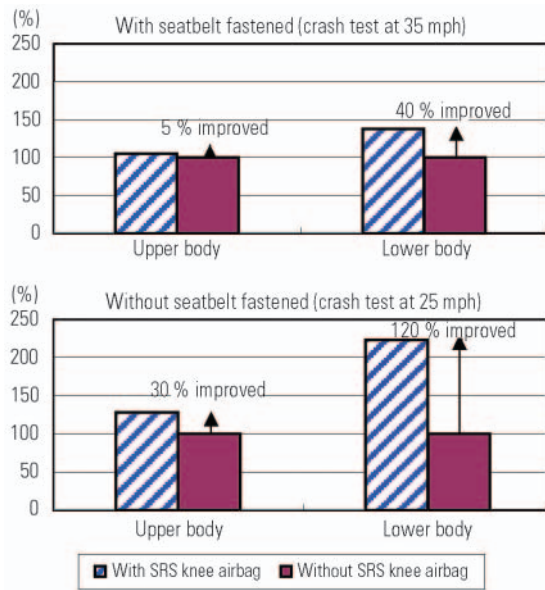


Fig. 6 Effect of knee airbag (in terms of ride-down efficiency)

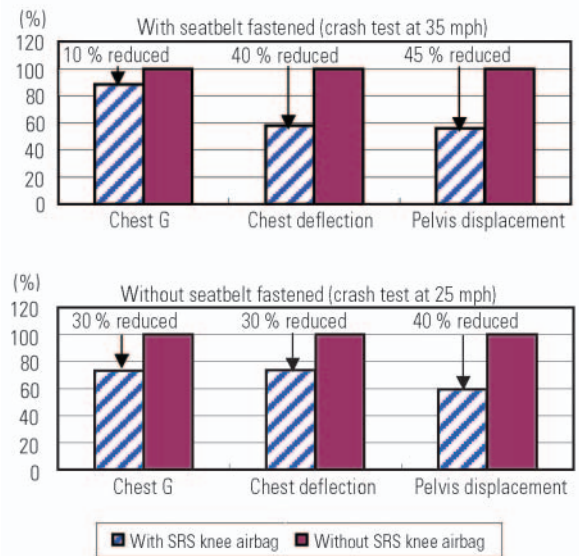


Fig. 7 Effect of knee airbag (in terms of reduction in occupant injury)

#### 4. Conclusion

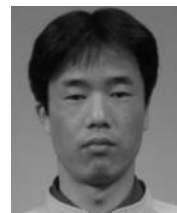
The driver side SRS knee airbag developed for installation on the new LANCER for the North American market proved successful in reducing the severity of chest injury and improving driver protection performance in a frontal collision. Since there are several constraints that affect design layout of a driver side SRS knee airbag including pedal operational performance and the space required in front of the driver's knees, detailed study of the layout for each vehicle model is necessary. MMC would like to increase its number of driver side SRS knee airbag applications to more models after further study of overall driver protection performance for each model. Lastly, we wish to express our gratitude to Sankyo Trading Corporation, Toyoda Gosei Company Limited, and all others concerned both in and outside the company for their cooperation in developing this driver side SRS knee airbag.



Kazuyuki KATO



Yukihiro FUKAYA



Mutsuo MURAMATSU



Hideki FUJIMOTO

# Development of Next-Generation Electric Vehicle “i-MiEV”

Kazunori HANDA\* Hiroaki YOSHIDA\*

## Abstract

We have developed a new electric vehicle “i-MiEV” based on the minicar “i”. Electric vehicles are considered the ultimate eco-car, emitting no exhaust emissions. To address problems encountered by the existing electric vehicles, i-MiEV employs innovative components such as high-capacity lithium-ion batteries and a compact high-performance motor. We will perform joint researches with electric power companies and fleet monitoring tests to survey the market acceptability prior to commercial application.

**Key words:** Electric Vehicle (EV), Environment

## 1. MMC history of electric vehicle development

Electric vehicle (EV) development by Mitsubishi Motors Corporation (MMC) dates back as early as 1971, the year when Japan established its first agency governing environmental affairs, the then Environment Agency of Japan, to address air pollution and photochemical smog that were major social issues at the time. At the height of Japan’s rapid economic growth, EV was expected to be the trump card in addressing air pollution and automakers competed to develop EVs. MMC’s EV activities began with the development of the MINICA VAN EV and the MINICAB EV under commission by an electric power company and 108 units were delivered. MMC continued to develop EVs, producing the DELICA EV in 1979 and the MINICA ECONO EV in 1983 in response to the oil crises and air pollution.

In the 1990s, demand grew for protecting the ozone layer and reducing CO<sub>2</sub> emissions to address global warming. The EVs that MMC developed in this period were the LANCER EV and the LIBERO EV, which were delivered to an electric power company. This period also saw a boom in EV development by major automakers seeking to meet the requirements of the California Zero Emission Vehicle (ZEV) Program. Although MMC was not included among the automakers designated by the Program and thus had a relatively relaxed timeframe for developing products conforming to the ZEV requirement, the company actively evolved its EV technologies, developing in 1998 the FTO-EV that was powered by a large-capacity lithium-ion battery that could cover a much longer distance per charge, and in 2001 the ECLIPSE EV (Fig. 1).

An EV depends on electricity for 100 % of its power, so such vehicles make the greatest contribution to preventing air pollution and reducing CO<sub>2</sub> in the air. However, using electricity as the energy source introduces various problems that have prevented the electric vehicles developed so far by automakers from being marketed widely. The three major problems are: 1)

vehicle performance, including too short driving distance per charge and too long charge time; 2) component technologies, such as the batteries and motors being too heavy, bulky and costly; and 3) battery charging infrastructure.

Due to the difficulty of overcoming these challenges, automakers have switched the focus of their research and development from EVs to fuel cell vehicles (FCVs) that do not emit pollutants while having relatively long driving ranges and hybrid electric vehicles (HEVs) that offer substantially improved fuel economy. Especially, with FCVs that can run on hydrogen, the driving range can be extended by enlarging the capacity of the hydrogen tank and the refill time can be shortened. FCVs are expected to be the ultimate eco-car because the exhaust gas contains only water vapor. However, it will take a while before FCVs become widely used for reasons of component technologies such as the fuel cell, and infrastructure such as the hydrogen filling stations.

HEVs, which are regarded as a stopgap before full-fledged commercialization of FCVs, are now becoming increasingly popular. HEVs combine electric vehicle technologies (such as motor and battery technologies) with internal combustion engine technologies to achieve a substantial reduction in fuel consumption over the conventional internal combustion engine vehicles (ICEVs). HEVs also offer higher power performance than ICEVs, proving that hybrid technology can concurrently achieve both superior fuel economy and high power performance. For this reason, automakers are keen to develop a hybrid electric powerplant as the next-generation powertrain component. The hybrid electric powerplant successfully resolves the component problems of EVs by permitting smaller motors and batteries to be used through the concomitant use of an internal combustion engine, while also resolving the infrastructure problems as gasoline can be used as the energy source. However, HEVs are perhaps best described as the ultimate ICEV, because they still run on fossil fuel and still produce significant emissions.

\* MIEV Promotion Dept., Development Engineering Office

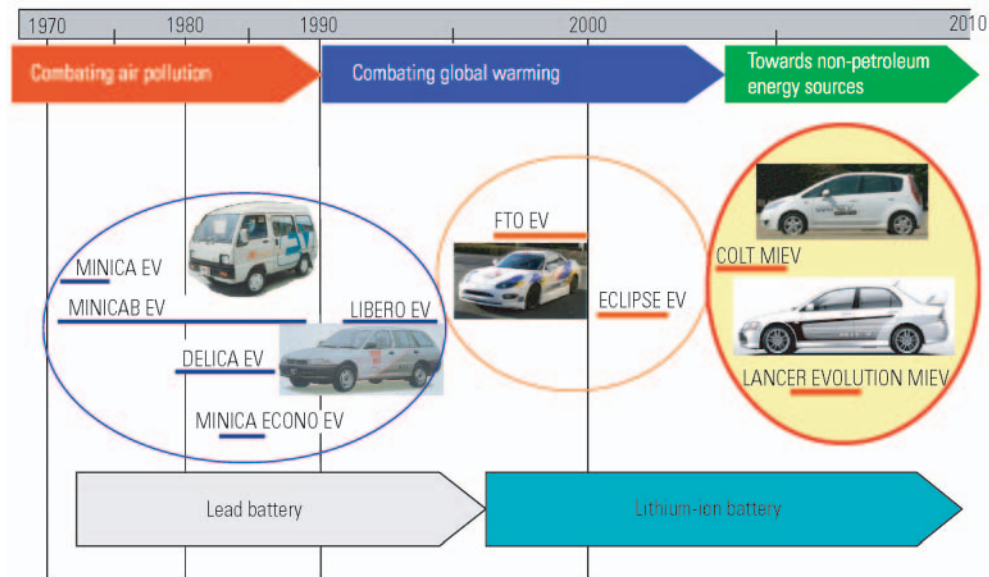


Fig. 1 History of electric vehicle development

Table 1 Total energy efficiency

Vehicle type	Well to Wheel		
	Well to Tank	Tank to Wheel	(Total energy efficiency)
EV	Refining, power generation, electricity transmission 43 %*	On-the-vehicle efficiency 67 % (including charging efficiency of 83 %)	29 %
Diesel engine vehicle	Refining, transportation 88 %	On-the-vehicle efficiency 18 %	16 %
Gasoline HEV	Refining, transportation 82 %	On-the-vehicle efficiency 30 %	25 %
Gasoline engine vehicle		On-the-vehicle efficiency 15 %	12 %

\*: The above figures are based on Japan's average composition of energy sources for power generation.

## 2. Potential benefits of EVs

EVs score highly on environmental performance as they produce no air pollution and provide a means of moving away from fossil fuels. In terms of total energy efficiency, CO<sub>2</sub> emissions and energy economy, EVs rank above any other powered vehicles in all of these respects.

The total energy efficiency<sup>(1)</sup> data shown in **Table 1** are based on “Well to Wheel” analysis (covering the total energy path from fuel production and supply to consumption on the vehicle). Here, efficiencies of a vehicle's energy sources are compared in terms of the “Well to Tank” (from fuel production and supply to tank filling) and “Tank to Wheel” (from tank filling to driving) analyses, the two analytic segments of the “Well to Wheel” analysis. In terms of the “Well to Tank” segment, the oil refining efficiency is generally estimated to be 82 % for gasoline and 88 % for diesel fuel. As for electricity, the refining efficiency is generally rated at 43 % when based on the average energy source composition in Japan (the refining efficiency varies with the composition of the energy sources used for power gen-

eration). Comparing the on-the-vehicle efficiency of the same energy sources in terms of the “Tank to Wheel” analysis assuming that vehicles are operated in 10·15 mode, the efficiency of gasoline engine vehicles is rated at approximately 15 % and that of gasoline HEVs at 30 %. Diesel engine vehicles show a better on-vehicle energy efficiency than gasoline engine vehicles but are still around only 18 %. In contrast, the on-the-vehicle energy efficiency of EVs is 67 % even when counting the loss during charging; this value is far higher than the other two energy sources. When compared in terms of the overall “Well to Wheel” analysis, the energy efficiency is rated at 25 % for gasoline HEVs, 16 % for diesel engine vehicles, and 29 % for electric vehicles. The results indicate that EVs are the highest in total energy efficiency. MMC is now striving to develop EVs that can achieve a total energy efficiency of 32 % by improving their on-the-vehicle energy efficiency.

**Fig. 2** compares total CO<sub>2</sub> emission values of the vehicles of three different energy source types in terms of “Well to Wheel” analysis<sup>(1)</sup>. The EV (i-MiEV) produces 72 % less CO<sub>2</sub> than the base gasoline engine vehicle (“i”), and 47 % less CO<sub>2</sub> than the gasoline HEV now



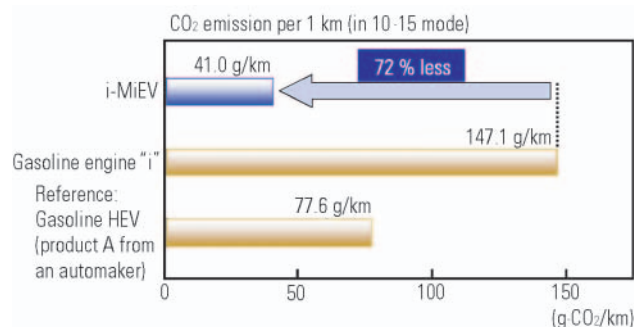
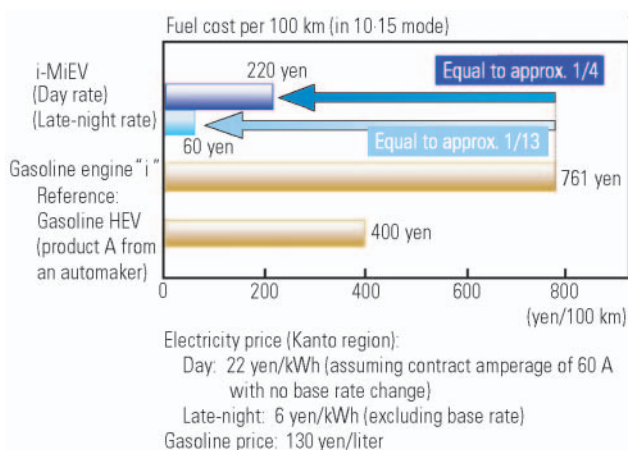
Fig. 2 CO<sub>2</sub> emission

Fig. 3 Energy economy

available from an automaker. Furthermore, EVs emit CO<sub>2</sub> only during electricity generation in the power plant and not while driving.

The EV (i-MiEV) outperforms other vehicles also in energy economy and fuel cost (Fig. 3). To cover a distance of 100 km, the EV costs just 220 Yen, which is approximately one quarter that of "i" gasoline engine vehicle. Furthermore, using the late-night electricity billing rate in Japan, the cost falls to only 60 Yen, or 1/13th that of the gasoline engine vehicle. Even though the late-night billing plan varies between electric power companies, the EV is still by far the most economical.

The comparisons described above demonstrate the high environmental and economic potential of EVs. However, it is essential to overcome the three barriers described earlier for their widespread use. The i-MiEV newly developed by MMC incorporates innovative technologies including lithium-ion batteries and a compact high-performance motor to clear these hurdles. In ongoing joint research with electric power companies, the i-MiEV will be fleet-tested to verify its marketability.

### 3. Technical features of the i-MiEV

The i-MiEV (Fig. 4) directly inherits the advantages of its base model "i", which means that the modifications required to turn the base vehicle into an EV were kept to a minimum. When starting out on the design of



Fig. 4 i-MiEV

Table 2 Specifications

Overall dimensions (L x W x H)		3,395 x 1,475 x 1,600 mm
Vehicle weight		1,080 kg
Seating capacity		4
Maximum speed		130 km/h
Per-charge distance (10-15 mode)		130 km/160 km*
Motor	Type	Permanent magnet synchronous motor
	Maximum output	47 kW
	Maximum torque	180 N·m
Drive system		Rear wheel drive
Batteries	Type	Lithium-ion
	Total voltage	330 V
	Total wattage	16 kWh/20 kWh*

\*: MY2006 joint research vehicle / MY2007 fleet test vehicle

the i-MiEV, the intention was to make it an EV capable of covering a sufficient per-charge distance for daily use while offering sufficient power performance for sports driving. The major specifications of the i-MiEV are listed in Table 2.

#### 3.1 Packaging

In MMC's past experience of EV development, converting a base model into an EV involved substantial modification to accommodate the motor, batteries and other electric vehicle specific components, but converting the "i" into the "i-MiEV" was different. Taking full advantage of the rear-midship engine design specific to the "i", all EV components were efficiently packaged by only adding a rear chassis cross member for supporting the motor and controller.

In the i-MiEV, the motor and inverter are mounted in the same space as the engine compartment of the "i". Also, the driving power battery system is installed under the floor in the same place as that occupied by the fuel tank in the "i"; this enabled enough cabin space for four adult occupants, as on the "i", and ample rear cargo space (Fig. 5).

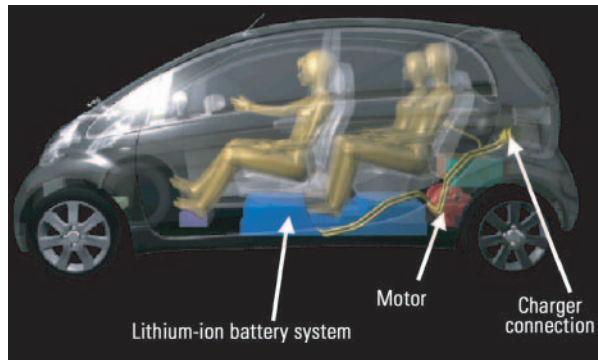


Fig. 5 Packaging of i-MiEV

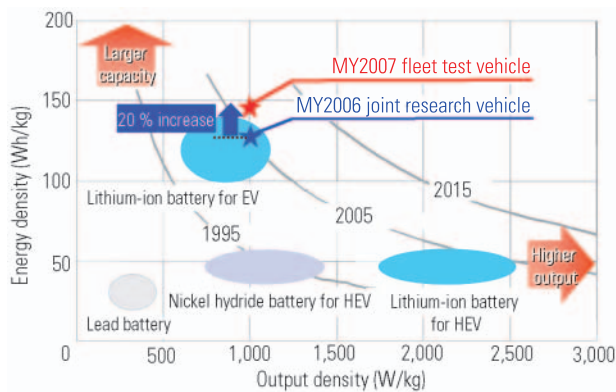


Fig. 6 Performance profile of lithium-ion battery

### 3.2 Extended driving range per charge

The i-MiEV uses lithium-ion batteries as the driving power source. These compact, high-performance batteries have a per-weight energy density of at least four times that of conventional lead-acid batteries. Lithium-ion batteries offer excellent output performance because of their internal resistance that stays low irrespective of the level of discharge, thus ensuring stable power performance right down to the discharge limit (Fig. 6).

The current battery system enables the i-MiEV to travel 130 km in 10-15 mode. In preparation for the MY2007 fleet test, MMC will continue aiming at a 20 % increase in energy density and per-charge distance of 160 km.

### 3.3 Higher power performance than the base model

The i-MiEV uses a compact, high-performance, permanent magnet synchronous motor in place of an engine. This motor can deliver the maximum torque even from 0 rpm and, unlike internal combustion engines, can cover the entire driving speed range without any transmission system. A motor with maximum output of 47 kW and maximum torque of 180 N·m combined with a speed reducer of fixed total reduction ratio at 6.066 can cover entirely the same traction performance zone as the base model (Fig. 7).

The powertrain of the i-MiEV has been proved to

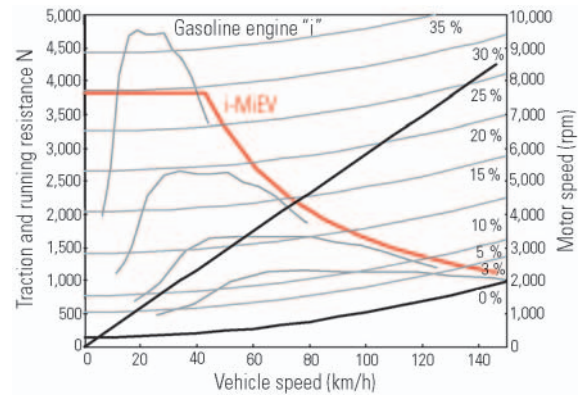


Fig. 7 Automobile performance diagram

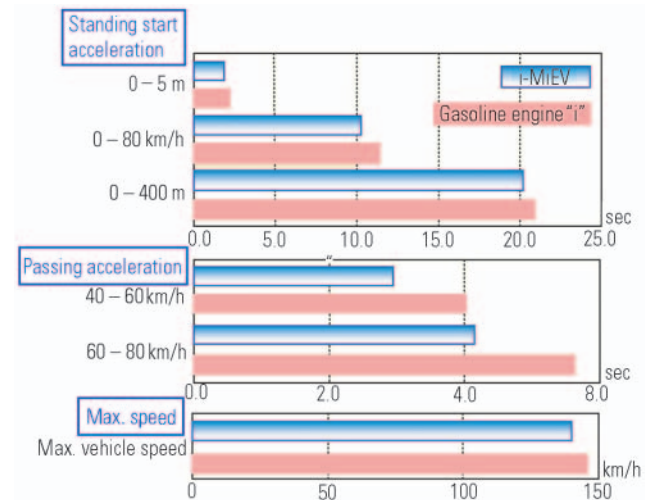


Fig. 8 Test results (power performance)

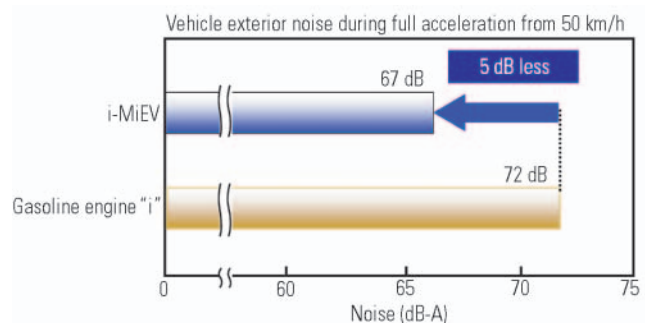


Fig. 9 Exterior noise level

offer better power performance than the base model in both standing start acceleration and passing acceleration (Fig. 8). Upon stepping on the accelerator pedal, the i-MiEV increases speed powerfully without transmission kickdown, which is a cause of engine speed surge in ICEVs.

The i-MiEV is also less noisy: its exterior noise during full acceleration from 50 km/h is lower by as much as 5 dB than the base model (Fig. 9). Furthermore, the i-MiEV does not generate any noise when at a standstill

**Table 3 Quick charge and home charge**

Charge time (to 80 % SOC)		
Type	Power source	Charge time
Quick charge	3-phase 50 kW/200V	20 – 25 minutes*
Home charge	200 V (15 A)	5 – 7 hours*
	100 V (15 A)	11 – 13 hours*

\*: MY2006 joint research vehicle / MY2007 fleet test vehicle

unlike an ICEV that is stopped with the engine idling. In fact, it is so quiet that there is some concern that pedestrians may be unaware of it, especially when the i-MiEV starts. It will be a new challenge for EVs that they must emit an appropriate sound to make people aware of their movements.

### 3.4 Quick charge and normal charge from household 100 V/200 V outlets

The battery system can be charged by either quick charge or normal charge from a household 100 V/200 V outlet for enhanced convenience (Table 3).

The quick charger is a stand-alone type (Fig. 10) using a 3-phase 200 V/50 kW power supply, and can charge the battery system to 80 % state of charge (SOC) in just 20 minutes, which will be useful for quick charging when away from home.

The home charger is an onboard equipment and compatible with both 100 V and 200 V outlets. It automatically distinguishes between 100 V and 200 V sources upon connection to an outlet, and charges the battery system to 80 % SOC in 11 hours when using a 100 V/15 A power source, and in five hours when using a 200 V/15 A power source. This is expected to be used for overnight charging at cheaper late-night electricity rates in a household garage.

Battery charge time hinders the widespread use of EVs. There is a trade-off between charge time and per-charge distance; if the battery capacity is increased to extend the per-charge distance, the charge time becomes longer. This is why infrastructure with a sufficient number of quick chargers needs to be addressed urgently to adequately shorten the charge time. For MMC, as an EV manufacturer, it will be essential to select the most appropriate battery capacity considering the per-charge distance and charge time based on the requirement for the vehicle class and the state of the infrastructure rather than increasing the battery capacity without such consideration.

## 4. Joint research with electric power companies

As mentioned in the preceding section, not only development of EVs but also building and implementing the battery-charging infrastructure is one of the prerequisites for the widespread use of EVs. MMC has started an advanced joint research with multiple elec-

**Fig. 10 Quick charger**

tric power companies. The first phase of the research started in November 2006 and will verify the adaptability of i-MiEV to the intended work of the partner electric power company and its compatibility with the already-constructed quick charger infrastructure. From the fall of 2007, MMC will begin fleet-testing in order to collect and analyze field data, based on which it will evaluate initial market acceptance towards the ultimate goal of commercialization.

## 5. Conclusion

Despite the expectations placed on them as the ultimate eco-car, EVs have not become popular due to various hurdles. However, the last decade has seen significant advances in related technologies and changes in social circumstances. Many things that were not possible 10 years ago are now possible using today's technologies. It is also especially noteworthy that people are now more aware of the environment, and this has created a favorable trend for EVs. MMC will further refine the i-MiEV to clear the remaining three obstacles to its widespread use in daily life.

### Reference

- (1) Japan Hydrogen & Fuel Cell (JHFC) Total Energy Efficiency Study Group (Japan Automobile Research Institute): JHFC Total Efficiency Study Report, March 2006



Kazunori HANDA



Hiroaki YOSHIDA

# Newly Developed V6 MIVEC Gasoline Engine

Setsuo NISHIHARA\* Takehiro NISHIDONO\*

## Abstract

This paper describes the new V6 engine developed for the new OUTLANDER sport utility vehicle (SUV) for the North American market.

Since 2004, Mitsubishi Motors Corporation (MMC) has been refining gasoline engines for passenger vehicles under the common themes of achieving higher performance, better fuel economy, lower emissions, and weight and size reductions. MMC has thus far launched the 4A9 4-cylinder engines (1.3 L and 1.5 L) for the COLT for Europe in May 2004, the 4B1 4-cylinder engines (2.4 L) for the OUTLANDER for Japan in October 2005, and the 3B2 3-cylinder engines (0.66 L) for the "i" in January 2006. The introduction of the fourth engine, the 6B3 V6 engine (3.0 L), now completes the lineup of these new-generation engines.

Like the other new engines, the new V6 engine offers class-leading performance in maximum output and torque, etc., by employing such technologies as a variable valve timing mechanism, an aluminum cylinder block, and a resin-made variable intake manifold. Furthermore, the new engine weighs approximately 25 kg less and offers approximately 5 % better fuel economy than our conventional 6G7 V6 engine (3.0 L). In addition, through the use of high-performance catalysts, etc., the new OUTLANDER has acquired Super Ultra Low Emission Vehicle (SULEV) certification stipulated in the California Low Emission Vehicle Regulations. Furthermore, by conforming to the zero evaporative emissions regulations, the new OUTLANDER has earned the title of the first qualified Partial Zero Emission Vehicle (P-ZEV) among the compact SUV category models with 3.0 L-class engines.

**Key words:** V6, MIVEC, Gasoline Engine, P-ZEV

## 1. Targets

The 6B3 engine was designed to excel in quietness and low-vibration which are suitable for 3.0L V6 class engines.

In addition, this engine achieves better fuel economy, lower emissions and weight and size reductions, which are common to all engines in the new engine lineup developed under the engine renovation program since 2004.

State-of-the-art technologies and MMC's know-how are applied throughout the 6B3 engine's design to achieve all these targets.

## 2. Features

This section describes the technologies employed for achieving the above-mentioned targets for the 6B3 engine. Since many of these technologies (including the components that embody them) relate to achievement of more than one target, they are indicated in **Table 1** to show how the technologies and components correspond to the targets.

### 2.1 High output and low fuel consumption

This engine achieved class-leading output and fuel economy while achieving the abundant low- and mid-speed torque requested as an SUV.

The first of the main strategies used to achieve this is to improve air intake efficiency by applying the MIVEC™ (Mitsubishi Innovative Valve-timing Electronic Control) system (valve timing & lift switching-type), and also optimizing the intake/exhaust-ports in the cylinder head, and employing a variable intake manifold.

The second strategy is to reduce mechanical friction by using an offset crankshaft and other technologies.

The third strategy is to improve anti-knocking performance by more efficient cooling of the cylinder head/combustion chambers.

The fourth strategy is to adopt twin knock sensors (for sensing & control in each bank) to optimize combustion.

**Fig. 1** shows the engine performance curves with wide-open throttle, **Fig. 2** shows the structure and benefits of the MIVEC system, and **Fig. 3** shows the benefits provided by combining the MIVEC system with variable intake manifold.

### 2.2 Low emissions

The emissions of the 6B3 engine were reduced by the following means: optimization of intake/exhaust port design in the cylinder head; improvement in mixture charging efficiency and combustion stability by using the effect of the low-speed cams of MIVEC; improvement in combustion by ultra-fine atomization injectors; and the upstream heat capacity of the catalyst

\* Engine Designing Dept., Development Engineering Office



**Table 1 Applied technologies and their objectives**

Technology/component \ Target	High performance and fuel economy	Weight and size reductions	Low emissions	Low vibration and noise	High reliability
Aluminum die-casting cylinder block		○		○	
Offset crankshaft layout	○				
Resin-made rocker cover		○			
Variable valve timing system (MIVEC) (valve timing & lift switching type)		○		○	○
Cogged belt-driven camshaft		○		○	○
Auto tensioner for the accessories drive belt				○	○
Guideless oil level gauge		○			
Resin-made two-stage variable intake manifold	○	○			
Catalyst integrated in exhaust manifold			○		
Water-cooled EGR					○
Twin knock sensor system	○			○	○
Directly mounted crank angle sensor (stick type)		○			○

was reduced by adoption of the clamshell type exhaust manifold which has a built-in catalyst to make catalyst activation earlier.

Another low-emission strategy is reducing the emissions of untreated exhaust gases directly discharged from the engine (or gases upstream of the catalyst) by the following measure: the setting of compression ratio at a rather low ratio of 9.5:1 to optimize the balance between performance and emission level; the reduction of unburned hydrocarbons in exhaust gases by the reduction of the volume of gaps in combustion-chambers where flame cannot propagate.

Moreover, the OUTLANDER with the 6B3 engine sold in California in the US has been certified as a partial zero emission vehicle (P-ZEV), the first vehicle in the 3.0L-class SUV segment in the world.

This is thanks to measures such as a new high-performance hydrocarbon-trap catalyst and a direct ozone reduction (DOR) catalytic radiator\*.

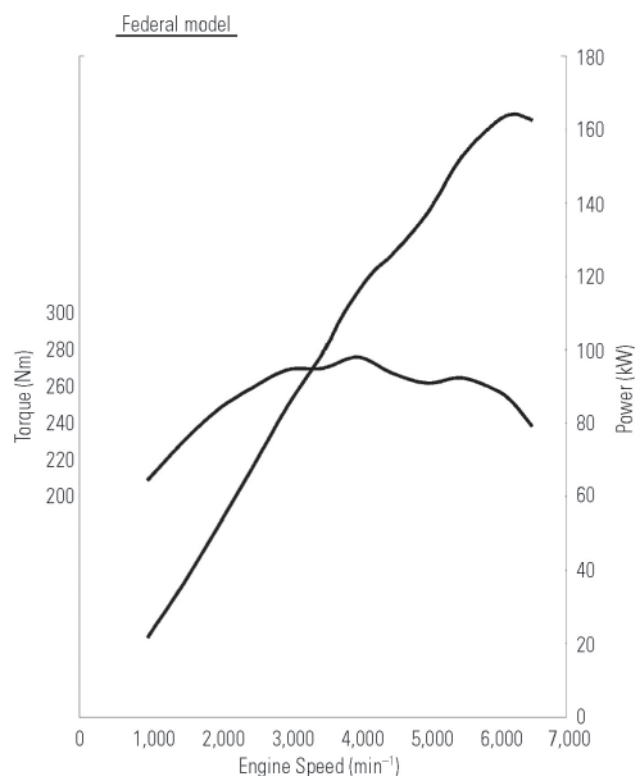
\*: Radiator with ozone reduction catalyst (Prem-Air®) (catalyst capable of directly resolving ozone)

### 2.3 Light weight and compact design

The weight of the engine has been reduced by using aluminum die-casting for the cylinder block and resin materials for the rocker cover and variable intake manifold.

Other parts of the engine have also been made lighter, such as the use of a guideless oil level gauge, direct mounting of accessories to the engine block and shape optimization by CAE analysis. In all, these strategies have reduced the weight of the engine by approximately 25 kg compared with the conventional 6G7 3.0L engine in spite of the adoption of MIVEC system.

Compact design strategies include a single overhead camshaft (SOHC) design to reduce the size of the cylinder head, thus minimizing the overall size of the base engine. In addition, the layout of the accessories as well as their mountings onto the engine was reviewed for optimization and reducing the overall

**Fig. 1 Engine Performance**

width. As a result, the overall width of the 6B3 engine is 60 mm less than that of the 6G7 SOHC 3.0L engine, which enables the crashable zone to be increased and collision safety to be enhanced.

### 2.4 Low vibration and noise

Low vibration and low noise are achieved by substantial improvement of the flexural rigidity of the powertrain (by higher stiffness of the cylinder block and oil pan), and adoption of auto-tensioner for the accessory-drive-belt, and the MIVEC system for stable combustion.

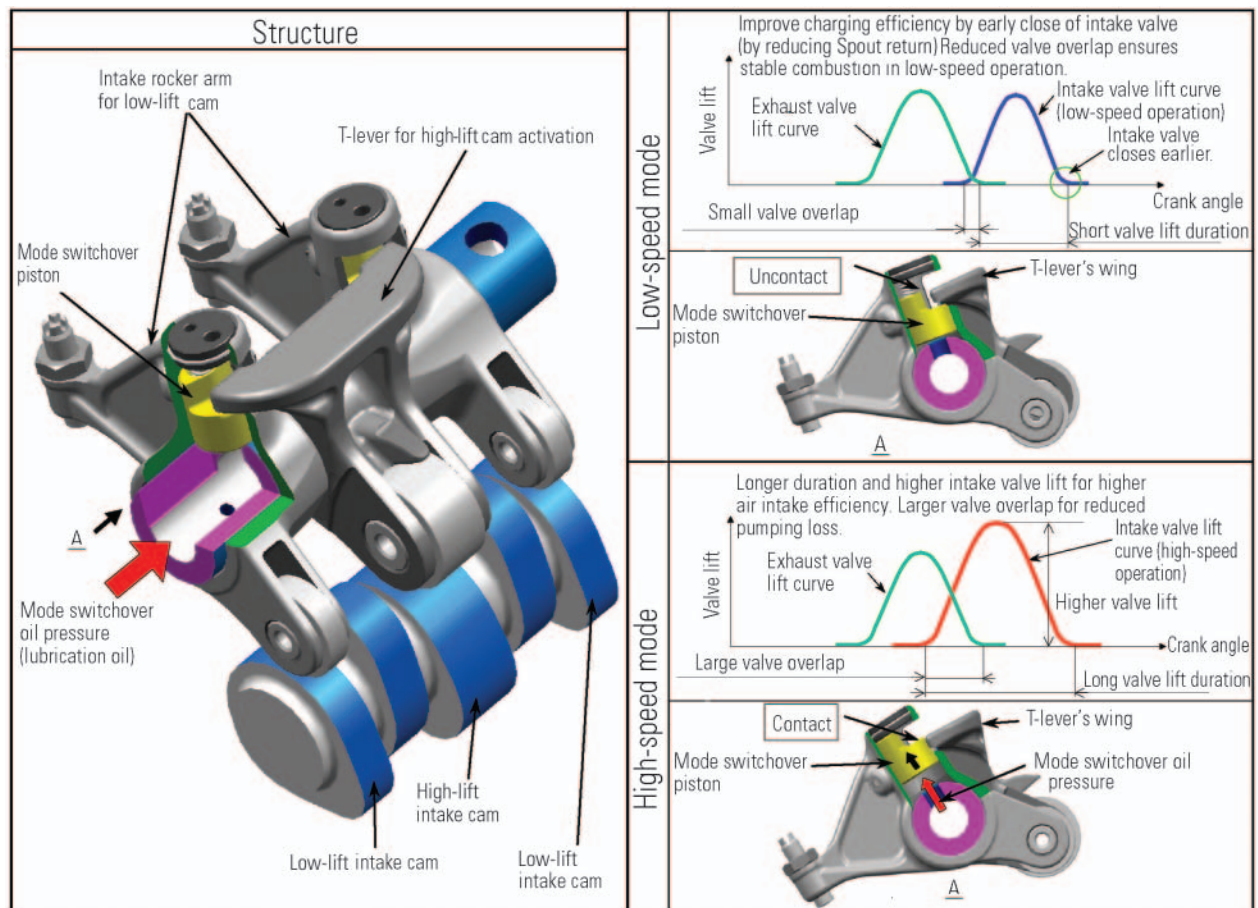


Fig. 2 Operation of MIVEC system

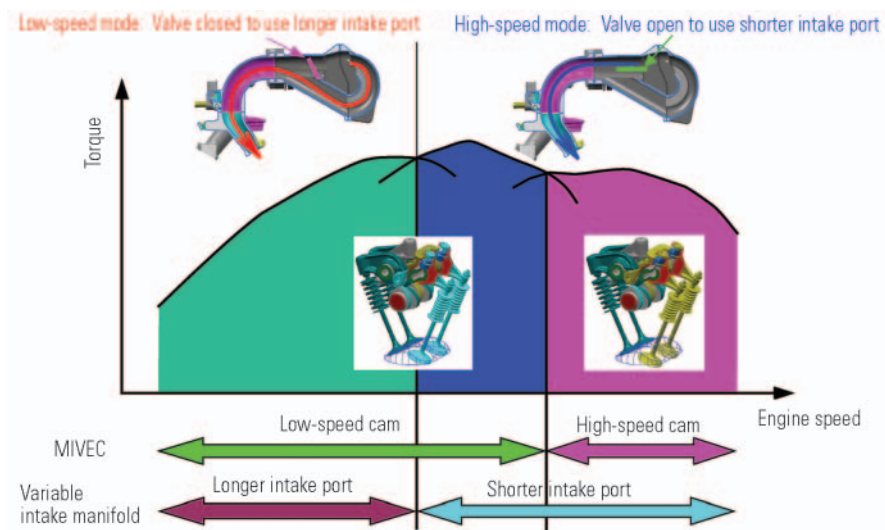


Fig. 3 Combined effects of MIVEC and variable intake system

Table 2 Major specifications

Engine Item	6B31 (3.0 L)		4G69 (2.4 L) <reference>		6G72 (3.0 L) <reference>
Vehicle model	New OUTLANDER		Current OUTLANDER		05MY ECLYPS
Market	FED	CALF+*2	FED	CALF+*2	FED (50S)
Conforming emission control standard	Tier2-Bin5	LEV2-SULEV*3	LEV1-LEV	LEV1-ULEV	LEV1-LEV
Displacement (cc)	2,998		2,378		2,972
Bore (mm)	87.6		87.0		91.1
Stroke (mm)	82.9		100.0		76.0
Stroke/bore ratio	0.95		1.15		0.83
Cylinder bore pitch (mm)	98		93		108
Big to small end distance of connecting rod (mm)	145		150		154
Compression ratio	9.5				10.0
Cylinder block material	Aluminum die-casting		Cast iron		
Valve mechanism	Roller rocker arm, SOHC, 24 valves MIVEC (valve timing & lift switching type), auto lash adjuster (exhaust only)		Roller rocker arms, SOHC, 16 valves MIVEC (valve timing & lift switching type)		Roller rocker arms, SOHC, 24 valves, auto lash adjusters
Variable intake manifold	Equipped		Not equipped		Equipped
Recommended fuel	Regular gasoline				Premium gasoline
Maximum torque (N·m/min <sup>-1</sup> )	276/4,000	276/4,000	220/4,000		278/3,750
Maximum output (kW/min <sup>-1</sup> )	164/6,250	159/6,250	120/5,750		157/5,750
Weight*1 (kg)	155		149		180

\*1: Base engine only (excluding mountings for installation on vehicle)  
\*2: California and other US states that adopt LEV2 emission standard  
\*3: P-ZEV certified

3. Specifications

The specifications of the 6B3 engine are indicated in Table 2.



Setsuo NISHIHARA



Takehiro NISHIDONO

# Development of OUTLANDER's Emission Control System to Meet North American Super-Ultra-Low Emission Vehicle (SULEV) Standards

Kazuhiko WATANABE\* Kazuma SANADA\* Yuji SATO\*  
Katsuhiko MIYAMOTO\*\* Masayuki YAMASHITA\*\* Hiroshi TANADA\*\*  
Setsuo NISHIHARA\*\*\* Katsunori UEDA\*\*\* Hitoshi KAMURA\*\*\*

## Abstract

The North American Specification OUTLANDER has been developed to meet the Californian Super-Ultra-Low Emission Vehicle (SULEV) standard, some of today's most stringent emission standards in the world. As, based on the corporate emission strategy, vehicles with a relatively small displacement had been offered as SULEVs, it was a new challenge to meet the same standards with SUV (Sport Utility Vehicle) powered by a 3.0-liter V6. The major technological difficulties were reduction of hydrocarbon (HC) and nitrogen oxides (NOx), emitted mainly during cold operation after engine start and during hot operation with high temperature combustion, respectively. The secondary-air system employed by some competitors was found detrimental for this vehicle in terms of weight and system complexity. The OUTLANDER utilizes an HC trap catalyst, instead, combined with relevant control strategies, thus realizing the world's first 3.0-liter V6 SUV without a secondary-air system.

**Key words:** HC Trap Catalyst, SULEV

## 1. Introduction

The 2007 Mitsubishi OUTLANDER is a high-performance SUV that embodies Mitsubishi Motors Corporation's (MMC's) sporty DNA. Since it is expected to deliver high power, it needs an emission control system whose impact on engine performance is minimal. Some competitors comply with the SULEV standards by using secondary air systems to significantly cut exhaust emissions. With a V6 engine, however, the engine layout means that any secondary air system is detrimental in terms of weight, system complexity and cost. An attractive alternative that has recently become viable is a system employing an HC trap catalyst, which offers similar benefits in terms of emission reductions but does not significantly affect engine performance and does not add much weight. With the 2007 OUTLANDER, MMC adopted an HC trap catalyst and various other new technologies to realize an emission system for compliance with the SULEV standards. This paper gives an overview of the system's development.

## 2. California's SULEV standards

The State of California is one of the most densely car-populated parts of the world, and it suffers resultant air quality problems, which is particularly severe in the Los Angeles area. Consequently, the California Air Resources Board (ARB) strictly regulates automotive

exhaust emissions using standards that it establishes independently of those set by the US federal government. The ARB regulations apply to the average emissions of all vehicles sold by each automaker, so the 2007 Mitsubishi OUTLANDER must comply with the LEV-II SULEV standards, which are some of the most stringent regulations in the world.

North American emission standards are shown in **Fig. 1**. California's SULEV regulations are far stricter than the federal Tier2 Bin5 fleet-average NOx-emission standards that must be satisfied in states other than California. Further, the SULEV standards apply to vehicles that have reached 150,000 miles, meaning that system durability is crucial. Under the SULEV regulations, each automaker must conduct surveys to verify the regulatory compliance of sold vehicles and must report the results of the surveys to the state department.

The SULEV standards are to regulate non-methane organic gases (NMOG) as part of the unburned hydrocarbon emissions, carbon monoxide (CO) resultant from incomplete combustion of gasoline, and NOx (formed by thermal reaction of nitrogen under high-temperature combustion conditions). In particular, they apply most stringently to NMOG emissions, which are greatest when a vehicle's engine and catalysts are cold; their NMOG requirements are extremely difficult to satisfy. Systems for compliance with the SULEV standards demand major development efforts mainly to minimize NMOG emissions.

\* Performance Testing Dept., Development Engineering Office

\*\* Advanced Powertrain Development Dept., Development Engineering Office

\*\*\* Engine Designing Dept., Development Engineering Office

\*\*\* Powertrain Control Engineering Dept., Development Engineering Office



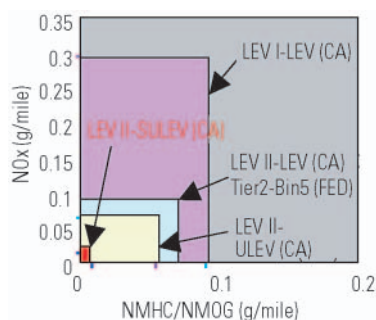


Fig. 1 Emission standards in North America

### 3. Selection of emission system

The 2007 OUTLANDER's engine is the newly developed 6B31 3.0 L V6 model. For the SULEV-compliant emission system, a basic layout consisting of manifold catalytic converters (MCCs) and an underfloor catalytic converter (UCC) was selected. In addition, the technologies listed below were considered, and the resulting effects of emission reduction were studied.

- (1) High-density-cell MCC
- (2) Mitsubishi Innovative Valve timing Electronic Control (MIVEC™) system
- (3) Secondary air system
- (4) HC trap catalyst
- (5) Injectors with improved atomization
- (6) Compression-ratio optimization (reduction)
- (7) Engine control

#### 3.1 High-density-cell MCC (Fig. 2)

The most effective way to achieve quick catalyst activation is to position the catalyst immediately downstream of the exhaust manifold. And for activation at low temperatures, high-density cells, which give a high monolith geometric surface area, are effective. With regard to catalyst technology, the MCC must have enough durability against high exhaust gas temperatures to maintain its low-temperature activation capability. To satisfy these requirements, a monolith with 900 cells per square inch (cpsi) was adopted. For the precious metals, a trimetal (Pt/Pd/Rh) system consisting of palladium (Pd), platinum (Pt), and rhodium (Rh) was selected. Pd was selected in light of its good thermal durability and its good ignition performance with respect to HCs. The platinum and rhodium were selected for the advantages they offer in terms of reducing NOx over a wider air/fuel ratio window.

#### 3.2 HC trap catalyst

The HC trap catalyst has an HC trap layer that adsorbs and holds HCs emitted by the engine while the engine and exhaust system are cold, and it has a function of a three-way catalyst that converts the HCs as they separate from the HC trap layer during engine warmup. It must effectively adsorb HCs and facilitate their oxidation. These attributes depend on the amount

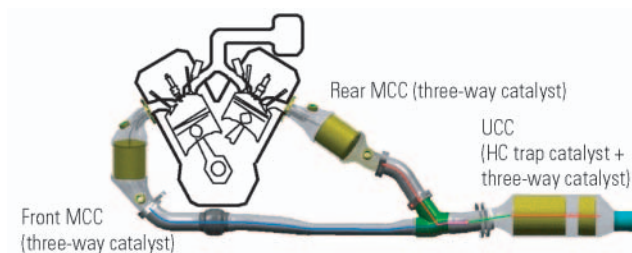


Fig. 2 Catalyst system of 6B31 engine

of the HC-trapping substance and the catalyst's heatup speed, which have a trade-off relationship. For good performance, therefore, it's essential to achieve a balance between the amount of the HC-trapping substance and the catalyst's heatup speed. Further, increasing the HC-trapping layer thickness is advantageous to facilitate oxidation. To satisfy these requirements and ensure the necessary balance of catalyst performance and engine performance, an HC trap catalyst with a 400 cpsi substrate was adopted.

#### 3.3 MIVEC™ system

At the beginning of the development program, application of the MIVEC™ system to the intake and exhaust valves was planned. In light of cost/performance considerations, however, it was applied only to the intake valves.

#### 3.4 Secondary air system

A secondary air system introduces fresh air into the engine's exhaust ports as a way to add oxygen to the exhaust gases, thereby speeding up catalyst activation and increasing conversion efficiency. European automakers typically use secondary air systems for emission control. It can fit easily on inline engines. When it was tried with the V6 engine of the OUTLANDER, however, the plumbing used to supply secondary air was complex; the system was difficult to lay out, and it added considerable weight.

#### 3.5 Injectors with improved atomization

Injectors optimized of their nozzle geometry were adopted for better fuel atomization to promote its vaporization even under cold operation. Their mounting angle was also optimized since it affects the manner in which fuel flows into the intake ports in the cylinder head and thus affects the exhaust emissions.

#### 3.6 Compression-ratio optimization

For the development of 6B31 engine, its compression ratio was initially planned to be 10.3. However, lower compression ratios were later studied for SULEV-regulation compliance and improved low-speed torque. Lowering the compression ratio reduces engine-out HC emissions, so a compression ratio of 9.5 was selected.

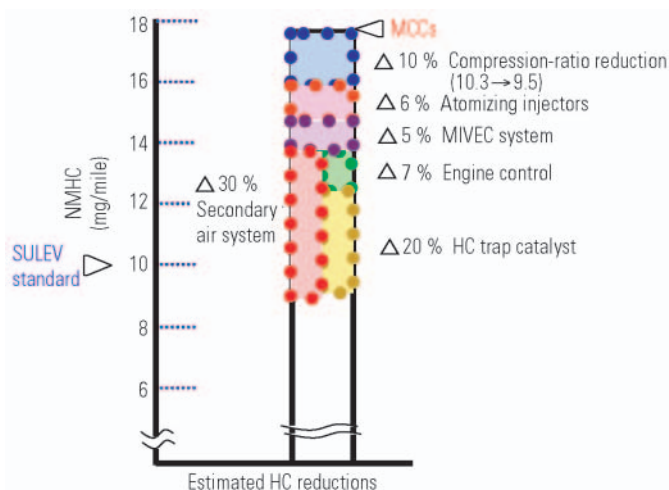


Fig. 3 Estimated HC reductions

### 3.7 Engine control strategies

Two forms of engine control strategies were adopted to reduce exhaust emissions. One is catalyst warmup control, which promotes rapid catalyst activation when the engine and exhaust system are cold. The other is HC trap catalyst temperature control, which improves the efficiency of emission reduction.

## 4. Secondary air system and HC trap catalyst

Fig. 3 shows estimation of the HC reductions possible with the technologies listed earlier in this paper. Table 1 shows the respective pros and cons of a secondary air system and an HC trap catalyst.

In light of the aforementioned factors, the secondary air system was not used for SULEV-regulation compliance with the OUTLANDER. The technologies adopted were MCCs, MIVEC system, improved atomization injectors, compression-ratio reduction, the HC trap catalyst though it provides somewhat lower HC conversion efficiency than the secondary air system.

## 5. Verification of catalyst-system durability

The SULEV standards apply to exhaust emissions over 150,000 miles of vehicle mileage, so catalyst-system durability is vital. Driving 150,000 miles in an actual vehicle would take about a year, so durability tests are typically conducted by means of bench tests in which catalyst deterioration is simulated. Thermal histories are determined from catalyst temperatures measured during actual vehicle operation, and thermal loading equivalent to that experienced during 150,000 miles of vehicle operation is then applied to the catalysts. Emission control performance is then tested with the aged catalysts.

Table 1 System comparison

	Secondary air system	HC trap catalyst
Weight	High	Low
Complexity	High	Low
Cost	High	Moderate
Installation	Difficult	Easy
HC reduction	ca. 30 %	ca. 20 %

## 6. Engine control for higher catalyst efficiency

Most HC emissions occur when the engine and exhaust system are still cold immediately after engine startup, i.e., before the catalysts have warmed up sufficiently to yield highly efficient conversion. Consequently, a key requirement of engine control immediately after engine startup is achieving rapid catalyst warmup with HC emissions at a low level. It is possible to hasten catalyst warmup by increasing the flow rate of exhaust gases, but the mass of exhaust emissions increases as a result. On the other hand, limiting the exhaust-gas flow rate results in slower catalyst warmup, also resulting in an increased mass of exhaust emissions during warmup. An adequate engine control strategy that efficiently raises the catalyst temperature and limits HC emissions is thus required.

### 6.1 Catalyst warmup control

Ratarding the engine's ignition timing from its thermally optimum point raises the temperature of the exhaust gases and at the same time lowers the emissions of HCs and NOx. Reduced combustion efficiency means reduced torque. The engine, however, can run under post-startup idle. This catalyst warmup control employing these characteristics was therefore adopted. Fig. 4 shows catalyst temperature increase with and without the catalyst warmup control. It can be seen that increase in catalyst temperature is accompanied by reduction in HC emissions and that total HC emissions are accordingly reduced.

### 6.2 Application of HC trap catalyst

Increasing the flow volume of exhaust gas immediately after engine startup to promote catalyst warmup causes an increase in the mass of HC emissions. However, the HC trap catalyst adsorbs the HCs. As the HC catalyst warms up, it releases the HCs, and the three-way catalyst, which is now active, converts the released HCs. In this way, the mass of HCs when the engine and exhaust system are cold can be reduced. Fig. 5 shows how HC emissions are reduced by use of the HC trap catalyst. From this figure, the pattern of post-startup adsorption and subsequent release of HCs by the HC trap catalyst can be inferred. When HCs are released from the HC trap catalyst, oxygen is needed for their conversion. Making the air/fuel mixture lean as a way to increase the oxygen concentration in the exhaust emissions has limitations from the viewpoint

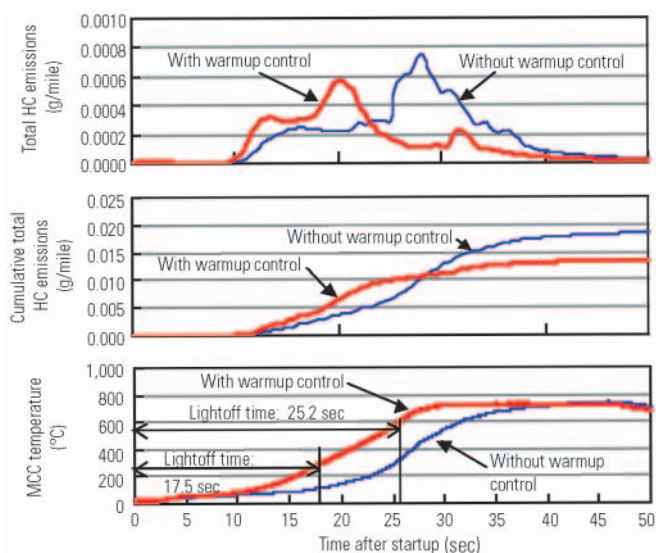


Fig. 4 Emission behavior with and without catalyst warmup control

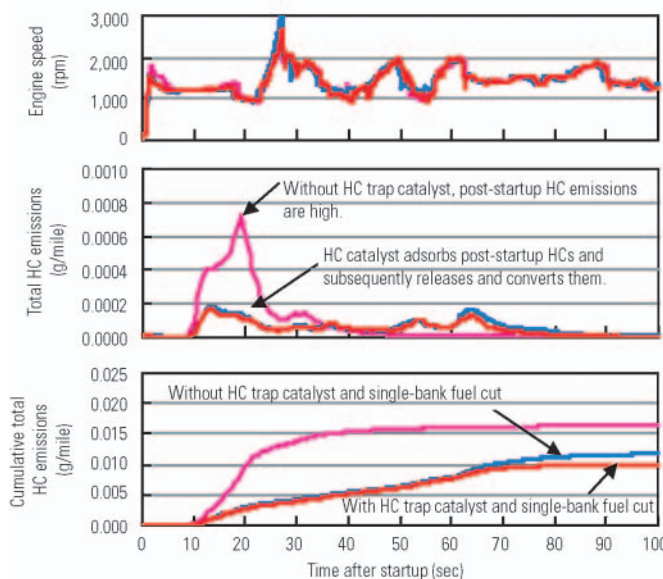


Fig. 5 Effect of HC trap catalyst

of ensuring combustion stability and suppressing NO<sub>x</sub> emissions, so a fuel-cut control, which has no impact on combustion, was adopted. Applying the fuel cut to all the cylinders immediately after startup would have caused a sharp drop in engine speed, thereby deteriorating the idle quality. Consequently, the fuel cut was applied to only one bank of the V6 engine such that the engine speed is kept stable while oxygen is supplied to the HC trap catalyst. With this combination of the engine control and HC trap catalyst, the mass of HC emissions when the engine and exhaust system were cold was reduced by about 20 %. The resulting level of HC emissions was compliant with the SULEV regulations, but there was not a sufficient margin with respect to the emission standard.

## 7. Direct ozone reduction (DOR) radiator

Although exhaust emissions were successfully reduced through the development of an emission system and application of engine control strategies, there was still not a sufficient margin with respect to the NMOG emission standard. Consequently, application of a DOR radiator was studied.

A DOR radiator is a radiator whose surfaces are coated with catalytic substances. It converts the ozone in the air that passes through it while the vehicle is moving. The California ARB allows NMOG credits for DOR-radiator-equipped vehicles, so a DOR radiator was used in a SULEV-compliant version of the 2004 North America-specification Mitsubishi GALANT. It was apparent that a DOR radiator could be used to secure NMOG credits for the OUTLANDER, too. Addition of devices to prevent the conversion functionality from being lost as a result of aftermarket radiator replacement secured a credit of 5 mg/mile (one half of the emission standard), resulting in an ample margin with

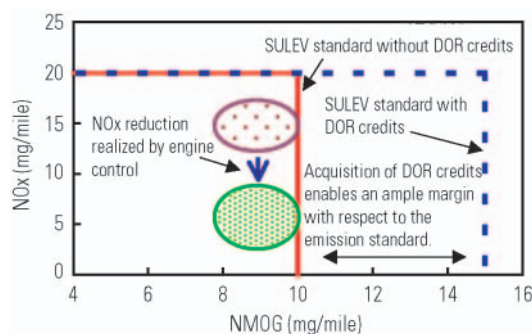


Fig. 6 Emission standards and benefits of DOR NMOG credits

respect to the NMOG standard (Fig. 6).

## 8. Handling of non-NMOG exhaust-emission components

The SULEV standards define extremely stringent limits not only for NMOG emissions but also for NO<sub>x</sub> emissions. NO<sub>x</sub> is generated under conditions in which the engine's combustion chambers are at high temperatures and contain excess oxygen, so they are typically not generated in significant quantities under cold conditions immediately after startup. If the air/fuel mixture is made lean as a post-startup NMOG countermeasure, however, excessive oxygen in the combustion chambers may generate NO<sub>x</sub>. Therefore, optimization of the air/fuel ratio is essential. Also, when the catalyst temperature has risen sufficiently, the catalyst's conversion efficiency is high such that most of the NO<sub>x</sub> is converted. However, immediately after the end of a fuel cut, when a large amount of oxygen has been adsorbed by the catalyst, the reductant is insufficient, meaning that NO<sub>x</sub> is inadequately converted and thus emitted. To

deal with this problem, it is necessary to supply fuel in slightly increased quantities for consumption of the oxygen in the catalyst after the end of a fuel cut. Through optimization of the fuel-injection amount in accordance with the duration of the fuel cut, it is possible to suppress post-fuel-cut NOx.

With regard to CO emissions, rapid catalyst activation and air/fuel-ratio control realize an ample margin with respect to the emission standard.

## 9. Summary

Through the adoption of various new technologies and engine control strategies, an emission system that enables an SUV with a 3.0 L V6 engine to comply with the SULEV standards was developed. The vehicle is the first in its class to comply with the regulations without a secondary air system.

The catalysts and DOR radiator of the current system are costly, so there's a need to continue making improvements in pursuit of a low-cost system. There's also a need to keep close track of the exhaust emissions of vehicles that have been sold and to keep pursuing further emission reductions.



Kazuhiko WATANABE



Kazuma SANADA



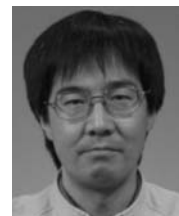
Yuji SATO



Katsuhiko MIYAMOTO



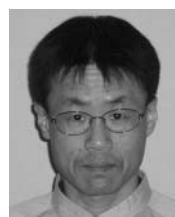
Masayuki YAMASHITA



Hiroshi TANADA



Setsuo NISHIHARA



Katsunori UEDA



Hitoshi KAMURA



# Newly Developed Six-Speed Automatic Transmission

Yoshihiro OHASHI\* Kenichi TAKAHASHI\* Tadashi HIRAOKA\*  
Akira MINO\*\* Toshiki OHARA\*\* Akihiro TONE\*\*

## Abstract

This paper describes the six-speed automatic transmission (6A/T) used in the North America-specification OUTLANDER.

The 6A/T was newly developed by Mitsubishi Motors Corporation (MMC) and is the first to be used by the company. It has a wide gear range, close gear ratios, low friction, and a wide torque-converter lockup range for high performance and low fuel consumption. Despite having six speeds, it has the same number of planetary gears as a previously used five-speed automatic transmission (5A/T) and fewer clutches and brakes than the 5A/T, meaning that it is light, compact, and inexpensive. It has become one of MMC's mainline A/Ts for future front-engine, front-wheel-drive passenger cars.

**Key words:** Automatic Transmission, Power train, Torque Converter, Hydraulic System

## 1. Development targets

The 6A/T was developed in pursuit of the attributes listed below. Target values for each attribute were established in accordance with the needs of the vehicle in which the 6A/T was going to be used and in accordance with benchmarks.

- (1) Wide gear range and close gear ratios (for superior power performance and shift performance)
- (2) Low friction (for superior fuel economy)
- (3) Wide lockup range (for superior fuel economy and power performance)
- (4) Lightness and compactness (for easy packaging)

Optimal gear ratios were selected for proper exploitation of driving force in wide range and in consideration of driveability and fuel economy. With regard to environmental compatibility, minimal friction and a wide lockup range were pursued for fuel economy. At the same time, a high level of shift performance was targeted (Table 1).

## 2. Basic structure

The respective specifications of the 6A/T and previously used 5A/T are shown in Table 2. As shown, the 6A/T represents a reduction in overall length, a reduction in weight, and a reduction in the distance between the first and third shafts, meaning that it is easier to be packaged. It can also be seen that the 6A/T has a wider gear range and closer ratios between gears, meaning that it permits better power performance and fuel economy.

Table 1 Applied technologies and their objectives

Item \ Purpose	Fuel economy	Vehicle's power performance	Shift performance	Compactness and lightness
New six-speed structure (wide gear range; close gear ratios)	○	○	○	○
Ultra-flat torque converter				○
High-load waved discs	○		○	
Optimized oil-pump capacity	○			
Optimized bearing capacity	○			
Optimized number of rollers in one-way clutch	○			
Use of linear solenoids for all pressure controls			○	
Variable line-pressure control	○			
Wider lockup range	○			

omy.

By allowing improved levels of power performance, fuel economy, and driveability, the 6A/T has enabled more attractive products to be offered.

A cross-sectional view of the 6A/T, which is based on the Lepelletier system, is shown in Fig. 1. A schematic is shown in Fig. 2.

The gear train consists of three planetary gear sets: a single-pinion-type front planetary gear set, a double-sun-gear-type rear planetary gear set and, at the very back, a double-pinion-type reduction planetary gear set.

The clutch and brake system consists of three clutches (a 3-5 reverse clutch (3-5R/C), a low clutch (L/C), and a high clutch (H/C)) and two brakes (a low and reverse brake (L&R/B) and a 2-6 brake (2-6/B)), which are arranged in this order as seen from the engine side.

The 6A/T has the same number of planetary gear sets as the 5A/T and fewer clutches and brakes (Table 3). The reduced number of components promotes light-

\* Drivetrain Engineering Dept., Development Engineering Office

\*\* Mitsubishi Automotive Engineering Co., Ltd.

\*\* JATCO Ltd.

Table 2 Major specifications

Specification		Type	New 6A/T	5A/T (reference)
Torque capacity			320 N·m	352 N·m
Gear ratio	1st		4.199	3.789
	2nd		2.405	2.162
	3rd		1.583	1.421
	4th		1.161	1
	5th		0.855	0.686
	6th		0.685	—
Rev			3.457	3.117
Gear range (1st to 6th/5th)			6.12	5.523
Final gear ratio			3.571	3.325
Hydraulic control	Shifting	Electronically controlled		
	Line pressure		Electronically controlled	Fixed
Overall length			396.8 mm	430 mm
Weight			101.4 kg	111 kg
Distance between first and third shafts			205 mm	215 mm

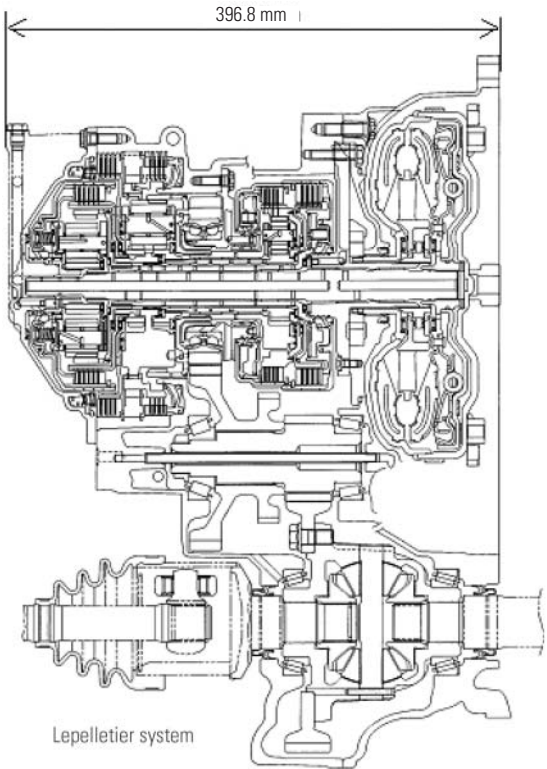


Fig. 1 Cross-sectional view

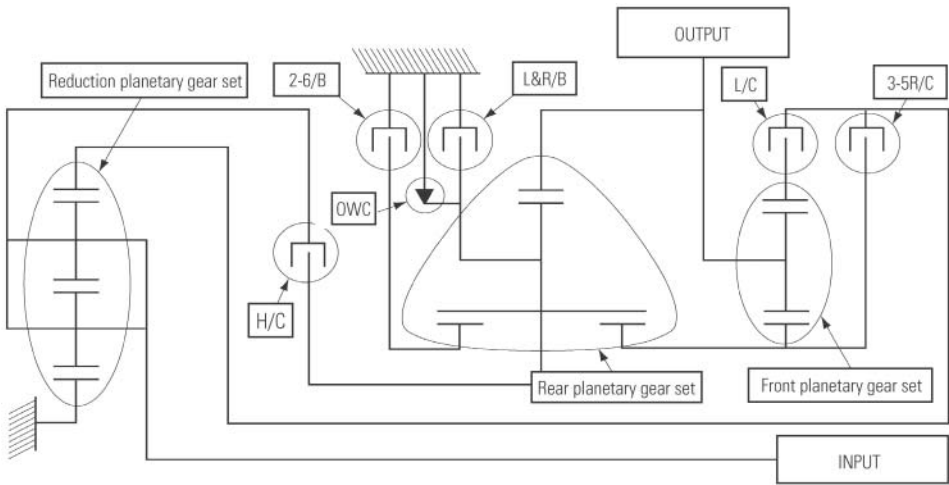


Fig. 2 Gear train schematic

Table 3 Number of components

	6A/T	5A/T
Planetary gear sets	3	3
Clutches and brakes	5	7
One-way clutches	1	2

ness and compactness but does not compromise the 6A/T's functionality.

Table 4 shows the operation of each of the clutches, brakes, and solenoids. The hydraulic pressure that activates each of the clutches and brakes is directly controlled by a linear solenoid, resulting in superior shift performance. Also, a one-way clutch (OWC), which is located at the outside of the rear planetary gear set, ensures good shift performance during 1st–2nd shifts, where there are significant differences in torque.

### 3. Hydraulic control system

The hydraulic control system is configured using three-way linear solenoids that directly control all clutch and brake pressures, thereby providing the precise hydraulic control that is essential for smooth shifting. Each of the linear solenoids is either of two types: normal-low or normal-high (Fig. 3). The linear solenoids of these two types are combined with hydraulic switches to form a compact control valve unit that does not need to include a fail-safe valve. The previously used 5A/T

Table 4 Operation of clutches, brakes and solenoids

Gear position	Clutch			Brake		OWC	Solenoid (SOL)						
	L/C	3-5R/C	H/C	2-6/B	L&R/B		Linear					ON-OFF	
	L/C SOL	2-6/B SOL	3-5R/C SOL	H/C SOL	L/U, L&R/B SOL		L/C SOL	2-6/B SOL	3-5R/C SOL	H/C SOL	L/U, L&R/B SOL	L/C SHIFT SOL	L&R/B SHIFT SOL
1st	○					○	○						○
2nd	○			○			○	○			○		
3rd	○	○					○		○		○		
4th	○		○				○			○	○		
5th		○	○						○	○	○	○	
6th			○	○				○		○	○	○	
1st engine brake	○				○		○				○		○
P													○
Rev		○			○				○		○		○
N													○

○: Operating

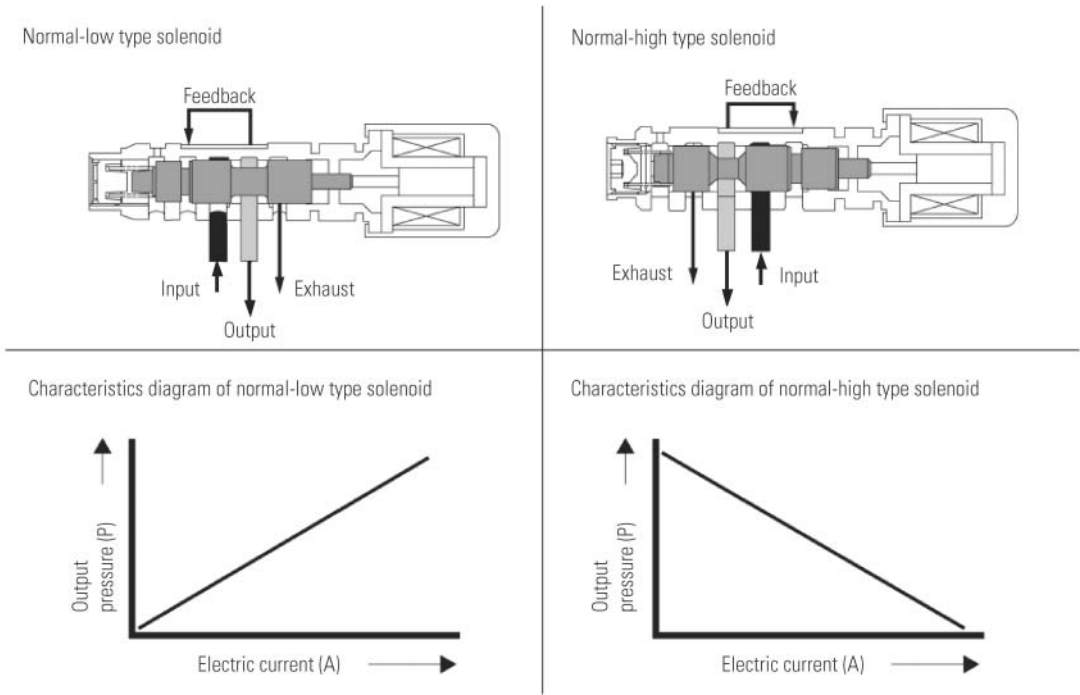


Fig. 3 Characteristic of three-way linear solenoid

contains a fail-safe valve.

4. Electronic control system

The electronic control system is outlined in Fig. 4. Information from the engine and other parts of the vehicle is transmitted to the A/T electronic control unit (A/T ECU) via a Controller Area Network (CAN), which is an internationally standardized local area network for in-car communication. The A/T ECU uses this information and data from the A/T unit to effect optimal control in accordance with the condition of the vehicle. The three clutches and two brakes are directly activated by the lin-

ear solenoids, realizing appropriate shifting and optimal driving performance.

5. High performance and fuel economy

(1) Wide gear range

Whereas the gear range of the 5A/T is 5.52, that of the new 6A/T is 10 % wider at 6.12. Combined with an optimal final gear ratio, the wide gear range yields benefits both in terms of superior standing-start and acceleration performance and in terms of superior fuel economy in high-speed gears thanks to reduced engine speeds in those gears. Although the gear range is wider

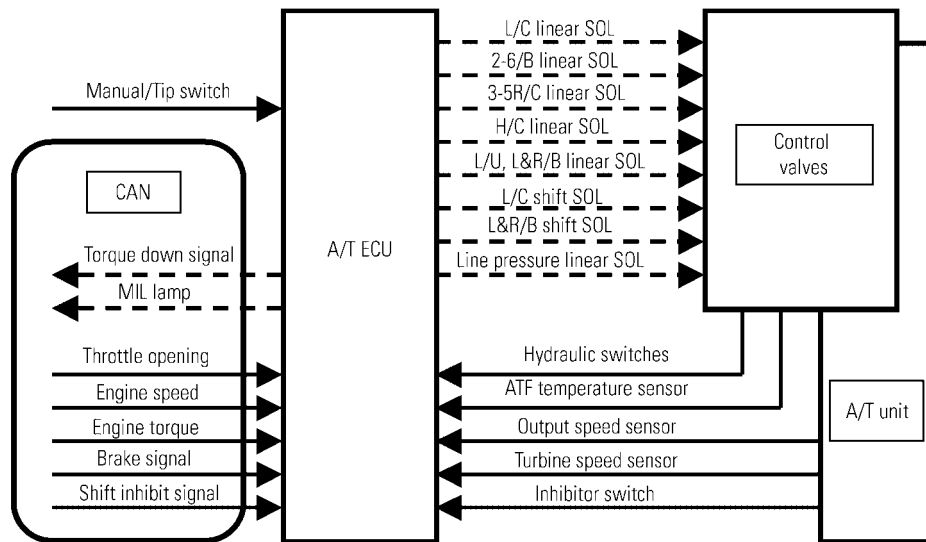


Fig. 4 Electronic control system diagram

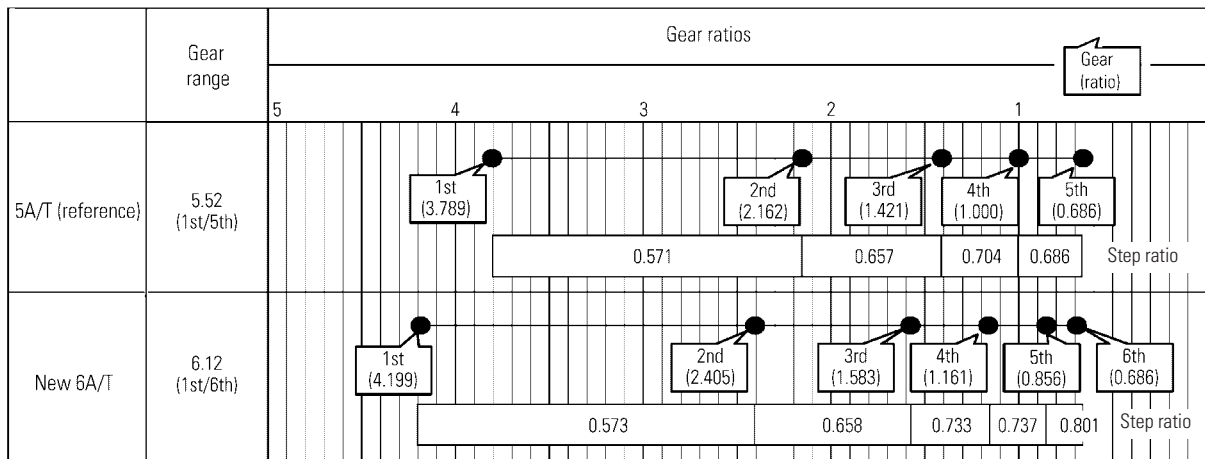


Fig. 5 Comparison of gear ratio

than that of the 5A/T, the ratios are closer, ensuring smooth gearshifts (Fig. 5).

## (2) Low friction

Even the smallest details of the new 6A/T's components reflect extensive friction-minimizing efforts. The main friction-minimizing measures are as follows:

### ① Reduction of oil pump driving torque by optimized oil-pump capacity

The use of three-way linear solenoids and a reduction in the number of valve spools yielded a reduced amount of leakage from the control valves. Consequently, it was possible to use an oil pump smaller than that used with the 5A/T. The torque needed to drive the oil pump was accordingly lowered (Fig. 6).

### ② Optimized bearing capacities

Adoption of a ball bearing to support the output gear, adoption of an optimal number of rollers in the taper bearings of the second and third shafts, and adoption of needle bearings for plain bearings realized lower

bearing friction.

### ③ Use of waved disks

Friction caused by the drag of disks that do not contribute to engagement was reduced by the use of waved disks in the two brakes and one clutch of each gear.

The principle of friction reduction by a waved disk is shown in Fig. 7. The flow of oil between the disk and plates causes pressure such that the disk is held in place by oil films between the plates. This arrangement reduces drag between the disk and plates. The magnitude of the pressure is determined by the angle ( $\theta$ ) shown in Fig. 7. Increasing this angle enables friction to be reduced but causes worse shift shock, so the angle was optimized for low friction without undue shift shock.

### ④ Optimal number of rollers in one-way clutch (OWC)

The number of rollers in OWC was changed in accordance with the applied engine torque to reduce friction.



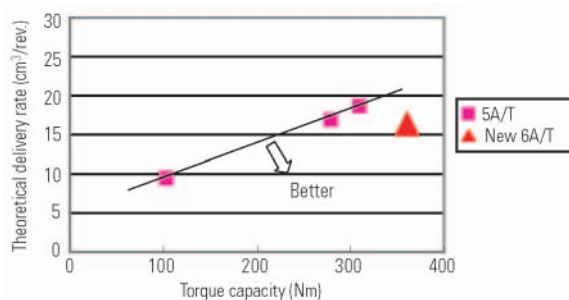


Fig. 6 Oil pump performance

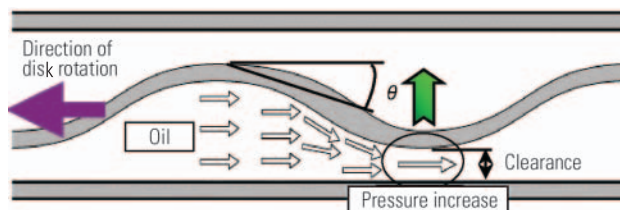


Fig. 7 Principle of frictional reduction by waved disk

### (3) Lockup

For fuel economy and quietness, lockup was adopted with the third to sixth gears. The lowest ATF temperature at which lockup is operational was lowered to make lockup operate immediately after startup for further improvements in fuel economy.

### (4) Slip lockup

In low-speed, high-torque ranges, where lockup control cannot be applied because of noise and vibration, slip lockup control is employed for superior noise, vibration, and harshness performance together with superior fuel economy. Even when the vehicle is coasting, lockup and slip lockup are made available for superior driveability and fuel economy.

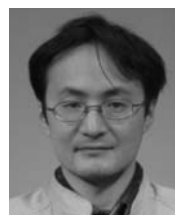
## 6. Conclusion and acknowledgement

In the development of the 6A/T, quality was heightened through analyses conducted using state-of-the-art simulation technologies, application of digital modeling technologies, joint development efforts with partner companies, careful production preparations, and introduction of state-of-the-art production facilities.

The authors would like to express their gratitude to everyone who cooperated with the development program.



Yoshihiro OHASHI



Kenichi TAKAHASHI



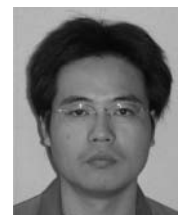
Tadashi HIRAOKA



Akira MINO



Toshiki OHARA



Akihiro TONE

# Development of Inner Rail Type Power Sliding Door

Masahiro KYOTO\* Toshiya SHIMPO\*\* Takehiro IWAMI\*\*  
Fumihiko KOBAYASHI\*\* Fumitoshi TAKENAKA\*\* Kouji KAMIO\*\*

## Abstract

This paper outlines the development of a power sliding rear door for the new eK WAGON. The door is the first of its kind applied to bonnet type minicars. With bonnet type minicars, the distance between the rear door and the rear end of the vehicle is short and thus, if the rear door is of a sliding type, the distance available for the sliding door center rail is too short to provide the necessary longitudinal length of the door opening. The method adopted to resolve this problem is the Mitsubishi Motors Corporation (MMC) original inner-rail-type sliding door mechanism with the center rail on the door. Employed along with this mechanism is a module design applied to the numerous functional components of the power sliding system, in which these components are subassembled on a module panel for their collective quality control during production.

**Key words:** Door, Design, Modularize

## 1. Introduction

Power sliding doors are commonly found on minivans whose popularity is now soaring in Japan. However, such doors are not common in the minicar segment; they are offered on only a limited number of one-box type models and on none of the bonnet type minicars. Nevertheless, there is a potential demand for power sliding doors among users of bonnet type minicars who typically own them as second family cars. They want power sliding doors for such reasons as preventing their children from bumping the door against a car parked nearby when opening/closing the door and the convenience of door opening/closing when carrying shopping bags. In response to such desires of customers, MMC has developed a power sliding rear door applying the company's original inner door rail mechanism for the new eK WAGON; this is the first of its kind for bonnet type minicars.

## 2. Packaging strategies

### 2.1 Inner rail mechanism

With bonnet type minicars, there is only a short distance available between the rear end of the rear door and the rear edge of the car body. This is the main reason why the conventional outer rail type sliding door system has not been used for bonnet type minicars to date; more particularly, it is impossible to install a sufficient length of center rail on the quarter panel. The MMC original inner-rail-type sliding door system with the center rail built into the door overcomes the problem. **Fig. 1** shows the difference between the outer-rail-type and inner-rail-type sliding door systems. Sliding doors generally use three rails, i.e. the upper, center and lower rails. With the inner-rail-type system, the center

rail is located inside the rear door, and this enables the car to have a larger door opening. In the system used on the new eK WAGON, the door opening is as wide as 530 mm when fully opened without the door protruding beyond the rear edge of the body. This width is sufficient for passengers to get in and out of the car easily.

The inner-rail-type design also eliminates the need for installing a garnish, which is necessary for aesthetically covering the center rail that is installed on the outer surface of the car body with an outer-rail-type system. The result is a clean and neat body appearance.

### 2.2 Head clearance

The new eK WAGON inherits an overall height of 1,550 mm from the previous versions to fit in multistory car parks. This height is rather too low for cars with a sliding door, making it difficult to secure sufficient head clearance for the front passenger and easy entry/exit. The measures employed to solve the problem are the following: a cover that is located below the upper rail to help reduce the height of the rail, and the upper rail layout was optimized to minimize the protrusion of the head lining into the cabin. These methods have successfully provided an adequate head space and ease of entry/exit (**Fig. 2**).

While developing the sliding door system for the new eK WAGON, the quality in terms of ease of entrance/exit and cabin comfort was evaluated and verified repeatedly using a dedicated mock-up, which was modified every time the design was changed in any detail.

\* Body Design Dept., Development Engineering Office

\*\* Function Testing Dept., Development Engineering Office

\*\* Electronics Engineering Dept., Development Engineering Office

\*\* Mitsubishi Automotive Engineering Co., Ltd.

### 3. Structure of the inner-rail-type power sliding door

#### 3.1 Components

**Fig. 3** shows the components of the inner-rail-type power sliding door system. The system includes the following basic components: the upper, center and lower rails; the upper, center and lower roller arms; and the rollers which roll inside the rails. It also includes the latching/locking components, most of which are arranged in the area above the center rail. These include the front and rear latches that retain the door in the fully closed position, and the locking mechanism that holds the door in the fully open position, which is subassembled on the upper roller arm and the lower guide. The system also has a release actuator that unlatches the door during power sliding operation of the door and a lock actuator that locks/unlocks the door. The inside and outside handles of the door are of a lever type for reduced effort and enhanced ease of operation by the following. The lever type handles allow the latching/locking device to be released to be selected by changing the turning direction, which enables the user to release the front and rear latches when opening the door and the upper and lower open locks when closing the door without difficulty. These locking mechanism operations are coordinately controlled via a link assembly.

Located in the lower portion of the door are the power sliding door unit, the control unit, and the power feeder unit that relays both battery power and signals. For added safety, a touch sensor is provided on the front edge of the door to prevent an obstacle or passenger from being trapped as the door closes.

#### 3.2 Power sliding door unit

**Fig. 4** is a schematic drawing showing the principle of operation of the power sliding door. The open and close cables, the ends of which are attached to the center arm, are routed via the front and rear pulleys respectively, and wound round the cable drum that is located at the center of the door and forms an integral part of the power sliding motor unit. The door is opened and closed as the drum takes up a cable and pays out the other cable.

As shown in **Fig. 5**, the door drive cables are linearly arranged between the center arm and front pulley and between the center arm and rear pulley. This eliminates the need to use cable outer casing and thus reduces frictional resistance and ensures smooth and stable movement of the door.

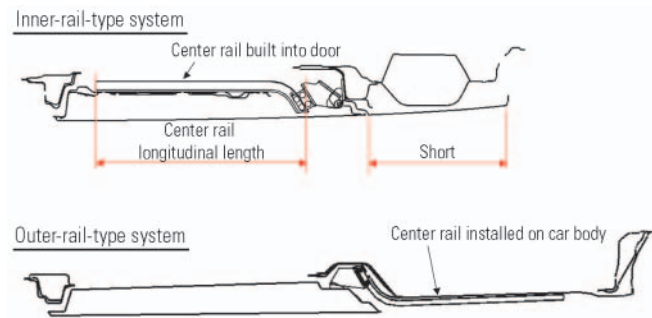


**Fig. 1 Inner-rail-type design vs. outer-rail-type design**

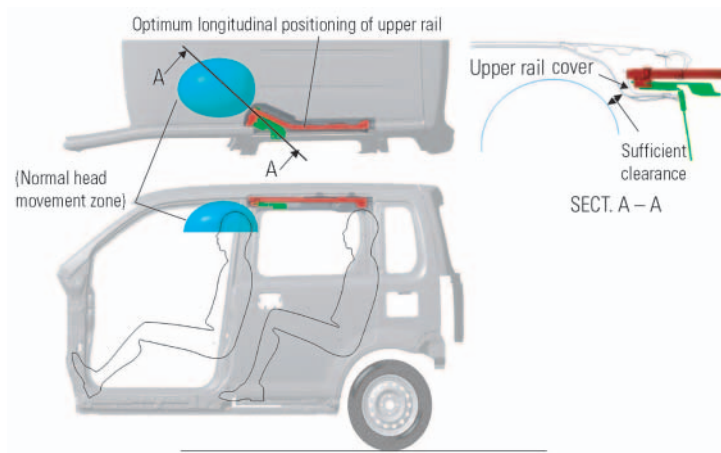


**Fig. 2 Upper rail layout**

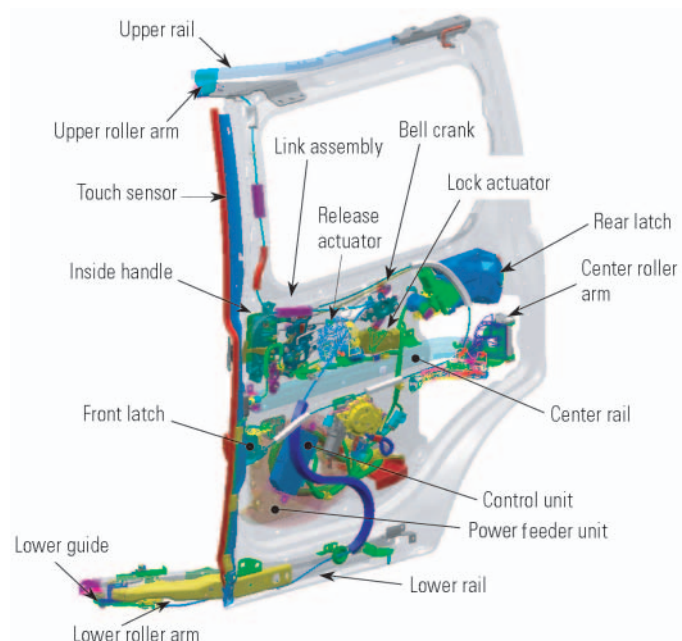


**Fig. 3 Components arrangement**

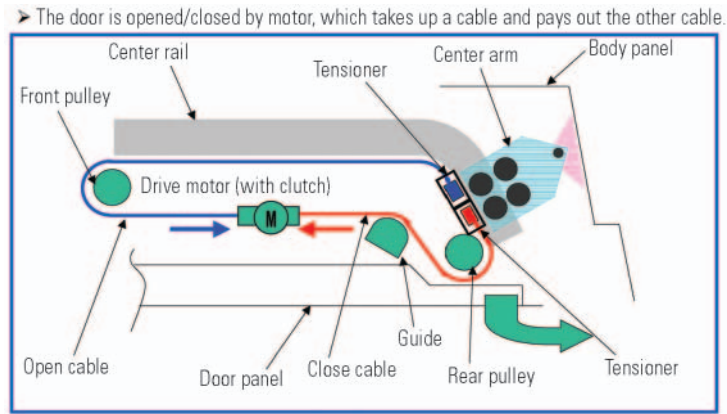


Fig. 4 Schematic of power sliding door operation

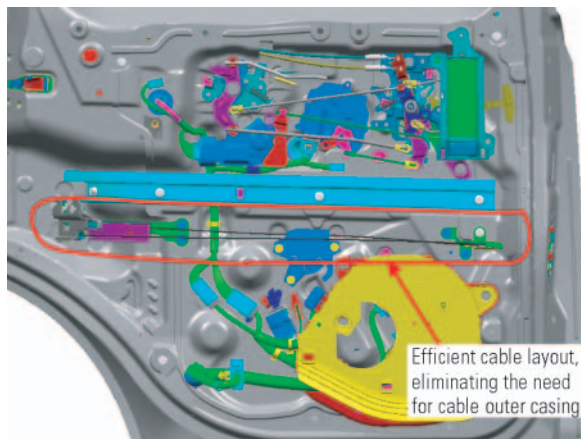


Fig. 5 Power sliding door cable layout

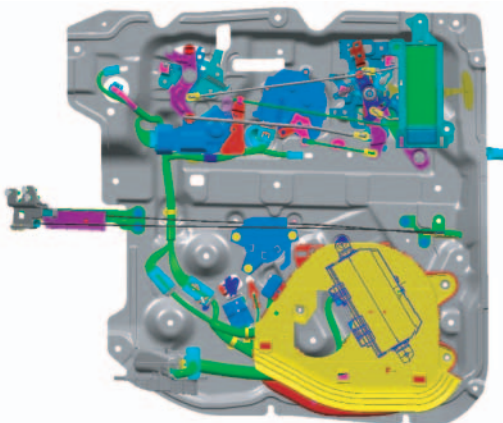


Fig. 6 Power sliding door module

### 3.3 Module design

The locking/latching components, power sliding door unit components and electric harness parts are modularized to integrate the complicated locking/latching mechanism and power sliding related components into a single module for collective quality control and improved assembling efficiency during production.

Fig. 6 shows the external appearance of the power sliding door module. The locking/latching mechanism parts and harnesses are subassembled on the upper portion of the module panel while the power sliding door unit parts are grouped on the lower portion of the panel.

## 4. Control of power sliding door

### 4.1 System configuration

Fig. 7 shows the configuration of the control system for the power sliding door.

The control unit, which governs opening and closing of the power sliding door, is installed inside the door. The unit receives power from the vehicle's power supply circuit via the power feeder unit, and also receives control switch inputs and vehicle status data via the power feeder unit. The control unit issues commands to the sliding door motor and rear latch motors based on these signals in addition to the signals from the locking/latching switches and the sensors within the door.

### 4.2 Control of door operation

The power sliding door is controllable using any of the driver's switch, rear switch, door handles, and key switch for remote control. The driver's power switch is used to switchover between power sliding and manual sliding of the door. Also, the control system has a function for prohibiting power sliding of the door during fuel refilling and driving.

Speed control of the sliding door motor at the stages just before fully closing and fully opening motions of the door is programmed so as to reduce the risk of injury and increase the impression of quality.

The speed-change sensing system, which consists of the pulse sensor in the sliding door motor and the touch sensor at the front end of the door, is designed to prevent becoming trapped by the closing door.



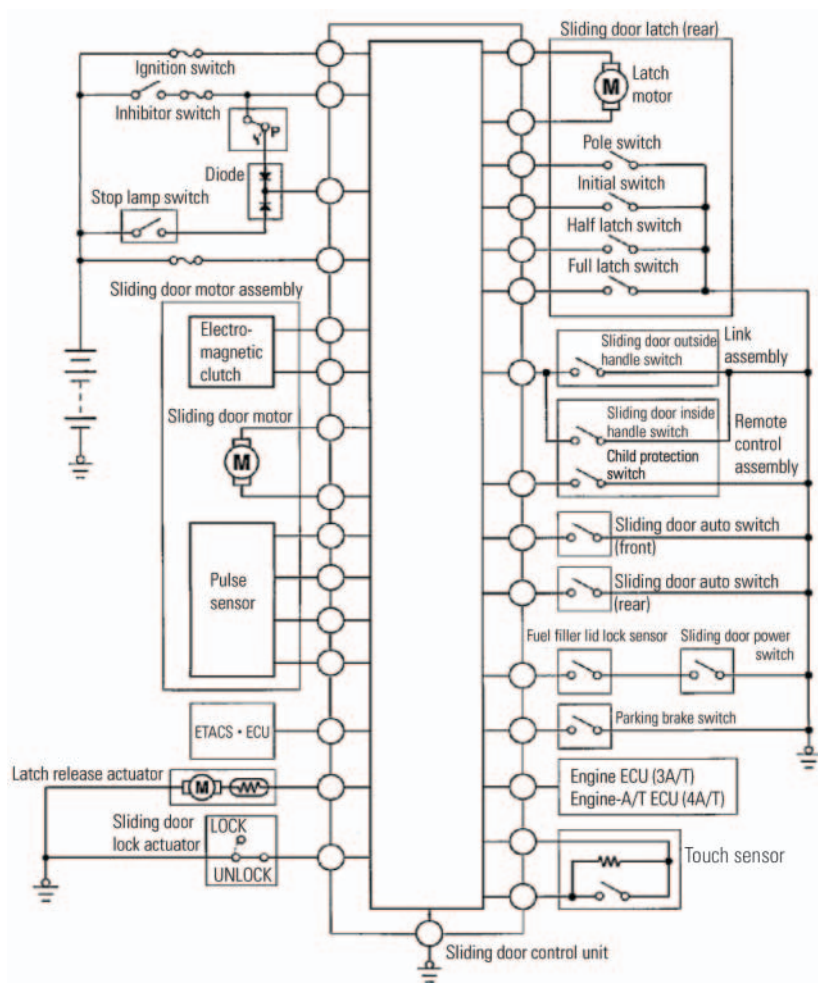
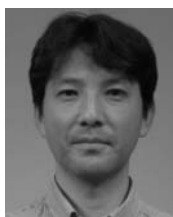


Fig. 7 System diagram

## 5. Summary

The power sliding door system that features MMC's original inner-rail-type sliding door technology has been successfully tailored for installation on the new eK WAGON. The system is the first of its kind not only in MMC but also in the entire bonnet-type minicar segment.

The power sliding door system will be developed by refining its components for even greater user comfort.



Masahiro KYOTO



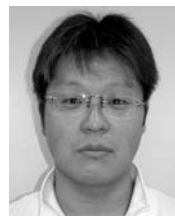
Toshiya SHIMPO



Takehiro IWAMI



Fumihiko KOBAYASHI



Fumitoshi TAKENAKA



Kouji KAMIO

# New Aluminum Hairline Finish Decoration Process

Kazuhiro YOSHIDA\* Kazuto YAMAUCHI\* Shinji KONDO\*\*  
Naoko KOBAYASHI\*\* Hiroshi SAKAGUCHI\*\* Toshikazu KANBE\*\*

## Abstract

Mitsubishi Motors Corporation (MMC) has been researching decoration materials and techniques for improving customer satisfaction.

MMC developed the Simultaneous In-Mold Decoration and Design Transfer Systems (IMD-TR), with part suppliers in order to decorate ornament panels. IMD-TR allows sophisticated designs using a gravure film, and actual metal is vaporized and adhered on the film to give the plastic panels a metallic appearance. Since this technique decorates the panels during the injection molding process, it reduces not only production costs but also chemical solvents discharged from the plant. This paper describes IMD-TR taking the aluminum hairline decorations in the new PAJERO as an example.

**Key words:** *Comfort, Surface Treatment, Quality*

## 1. Introduction

In the development process of the new PAJERO, we conducted extensive benchmark search involving not only automotive parts but also home appliances. Based on the results, we set the following target with the underlying concept of achieving a high-quality appearance:

Add table-knife-like metallic accents to the interior to create a sporty and muscular feel (Fig. 1).

## 2. Selection of decoration technique

Normally, an aluminum plate is assembled on a plastic molding. However, aluminum costs for its processing, and holds heat, which is disadvantageous as a material for automotive interiors. We therefore decided to decorate plastic moldings to create a realistic appearance of aluminum.

To select the best decoration technique, we examined some actual aluminum ornaments.

### 2.1 Attributes for realistic aluminum appearance

Attributes for a realistic aluminum appearance and their contributions to the effect are shown in Table 1.

### 2.2 Comparison of candidate techniques

Candidate techniques were selected and compared in terms of color, gloss and hairlines. The results are shown in Table 2.

### 2.3 Final selection of decoration technique

The studies concluded to choose IMD-TR. It offers realistic "brightness by metal deposition", "expression of the uneven metallic surface by film transfer process", and "fine hairlines by gravure printing".



Fig. 1 A table-knife selected as the target for realistic decoration

## 3. IMD-TR

With the IMD process, a film on which the design has been printed is inserted into the mold. The mold is then closed and molten resin is injected into the mold to perform the molding and decoration in one process.

Among various IMD techniques, IMD-TR is a unique technique that transfers the printed design from the film to the molded part.

### 3.1 Injection molding

The injection process of IMD-TR is shown in Fig. 2.

The design is transferred to the component during injection molding. During the process, the film, fed into the mold, is clamped as shown in Fig. 2. After injection of molten resin, the mold is opened and the film is rolled down from the filmroll mounted on the mold. In the meantime, position sensors installed on the injection molding machine control the film position. To prevent the film from moving during the molding process, it is clamped to the cavity block. It is then sucked onto

\* Interior Design Dept., Development Engineering Office

\*\* Design Promotion Dept., Design Office

\*\* Material Engineering Dept., Development Engineering Office

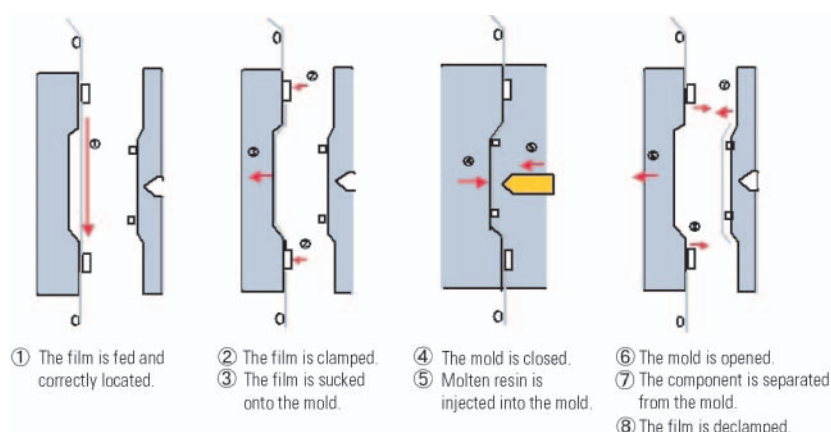
\*\* Nissha Printing Co., Ltd.

**Table 1 Attributes for realistic aluminum appearance**

		Contribution to the effect (on a scale of 100)
Visual	Hairline	15
	Radius	10
	Color and gloss	70
Touch	Hardness	± 0
	Coldness	5
	Smoothness	± 0

**Table 2 Comparison of candidate techniques**

Attribute Technique	Color		Gloss		Hairline	
	Brightness		Low gloss		Denseness	
IMD-TR (film transfer method)		Realistic surface design by vacuum metal deposition		Physical hairline available by film surface processing		Clear image due to low film stretching rate
Painting	○	Vivid expression	○	Adjustable gloss	×	Impossible
Hydraulic pressure transfer	△	Reproducible only by printing	○	Adjustable gloss by painting	△	Film dislocation during transfer, causing hairline to twist
IMD-P (film insertion method)	△	Reproducible only by printing	△	Low reproducibility due to limited number of film types	△	Film dislocation during molding, causing hairline to twist

**Fig. 2 IMD-TR molding process**

the mold by an applied vacuum to prevent air bubbles from the injecting resin.

When the film is set at the correct position, molten resin is injected into the mold. Due to the heat of the resin, the ink on the film transfers to the resin. When the component has cooled, the mold is opened. The film, which is still sucked onto the mold, separates from the component.

On the film, only the printed design where it came into contact with the component is peeled off (**Fig. 3** and **Fig. 4**).

### 3.2 Gravure printing

With IMD-TR, the design is printed on the film using gravure printing method. The printing plate has dents (cells) on its surface, into which ink is deposited, and the ink is then transferred to the film. The printing plate is normally a plated metal for long life. The ink layer on the film is thicker than that of relief or planographic printing, making the print more impressive. Moreover, gradation, or delicate expression, can be achieved by adjusting the cell depth of the printing plate.

The gravure printing press we employed is a rotary press for continuous printing. Cells are arranged on a cylindrical printing plate. Ink in the pan is picked up and

transported by the printing plate towards the film. Most of the ink is scraped off by a doctor, and the remaining ink in the cells is transferred onto the film, which is running between the printing plate and the impression cylinder. This process is repeated to print the film.

**Fig. 5** shows a schematic drawing of the unit.

### 3.3 Color adjustment

In gravure printing, the design is expressed with multi-color layers. Each layer is thicker than that of relief or planographic printing, but is only approximately 1 – 2  $\mu\text{m}$ . The surface color is the product of intricate concealing and mixing of the layers and therefore color matching is a complicate work. After adjusting one color, the color needs to be compared with its master sample. Also, it is necessary to make a correct choice from among multiple options to achieve an ideal adjustment. Wood grain printing, for example, consists of several layers. The adjustment and comparison take place for the same number of times as the number of the layers. In general, color consists of three aspects, i.e. hue, brightness and chroma, and color matching is normally made after visually checking the items. In practice, brightness and chroma can be adjusted by changing the density of ink (the concentration of pigment in the ink).



Fig. 3 Film after molding is completed



Fig. 4 Molded component

Gravure printing using a rotary press is suitable for this adjustment process.

## 4. Hairline

### 4.1 Considerations

On the new PAJERO, we aimed to achieve an interior accentuated with a high-quality aluminum texture by offering the “subdued gloss” exclusive to aluminum and “fine hairlines”.

The exquisite gloss of aluminum was produced by metal vapor deposition on a film. Since ink has only a limited expression of gloss and cannot deliver the gloss we desired. On the other hand, transfer of design with vacuum metal vapor deposition provides the component with a whitish gloss, making it closely resemble aluminum in texture.

Hairlines give matte finish, which is achieved by streaking thin hair-like lines in one direction on the surface of a metal. Special steel that has been processed into long threads thinner than human hair is normally used as an abrasive to achieve the finish on a metal sur-

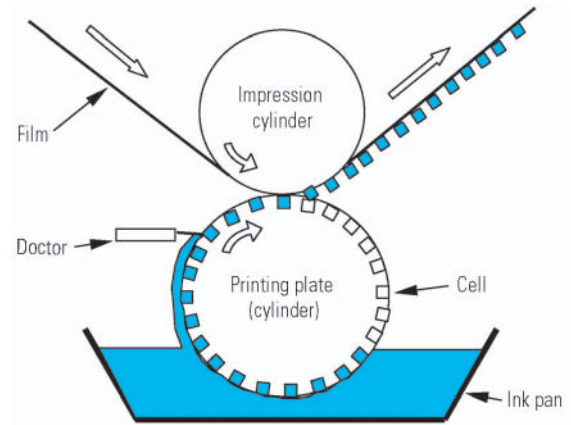


Fig. 5 Principle of gravure printing

face. A hairline effect can be achieved either by making the film surface scratchy or by printing. With the former method, the matte layer easily loses its effect due to processing, affecting the exquisite gloss of aluminum.

Based on the above considerations, we decided to express hairlines by printing to avoid affecting the matte layer. The hairline design is created on a computer by setting the line length, line width, blurring and pitch. The minimum width for stable expression of continuous lines is approximately  $150\text{ }\mu\text{m}$ , because the size of the cells (halftone dot) is  $120\text{ }\mu\text{m}$  square and they are arranged at a distance of  $25\text{ }\mu\text{m}$  apart. Hairlines are unnecessary to be visible as lines, and in many cases the hairline design consists of lines of various widths and lengths.

Our target hairline design for the new PAJERO was modeled on the surface of a table knife. As the pattern of the knife surface is unable to be scanned, photos were taken and the lines on the knife surface in those photos were used as the basis for our hairline pattern.

The hairline design, which we selected, has the finest random pattern thus far handled by the IMD-TR supplier, Nissha Printing Co., Ltd. (Nissha), which developed the IMD technology for automotive parts. The hairline is printed in normal by extremely low-density black while highly bright metallic ink on chrome deposit forms the base below the hairline. The brightness of the metallic ink and the glare of the base deposition combine to create the realistic appearance of the overall design. With these techniques, we succeeded in producing realistic aluminum panels that is unaffected by the sun, with “subdued gloss” and “fine hairline” while preserving the rich texture of aluminum (Fig. 6 and Fig. 7).

### 4.2 Pattern creation

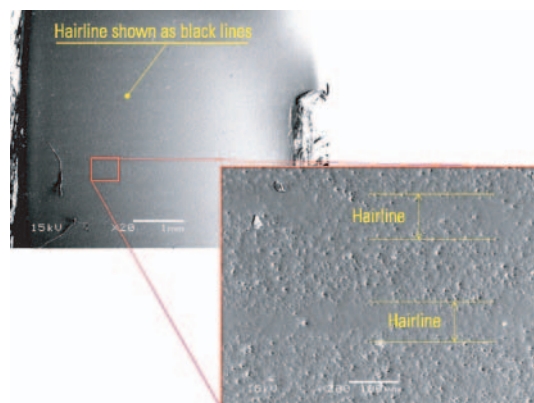
The first step is to obtain digital images of the material using cameras, scanners or other devices. Through RGB filter, the obtained images are decomposed into the four process colors of printing: C (cyan), M (magen-





(a) Real aluminum

(b) IMD-TR version

**Fig. 6 Comparison of microscope images****Fig. 7 Electron microphotograph of IMD-TR hairline**

ta), Y (yellow) and K (black). Basically, all colors can be created with these four colors (plates) except special colors such as gold, silver and pearl.

For more realistic hairline, however, we used three special colors (three printing plates) instead of the standard four-color process.

The material is a natural object, which normally has inappropriate elements such as distortions, unevenness and stains. Printing plates must be free of these elements, and this is achieved through image data processing on a computer.

## 5. Shape

### 5.1 Design requirements

The IMD-TR method has design limitations due to the flexibility of the film. The basic design requirements are as follows.

- Depth from the top of the component to the bottom in the direction of mold ejection
- A two-dimensional component shape (Inappropriateness to complex shapes)

### 5.2 Shape refining

We checked candidate component shapes in terms of the design requirements to identify possible problems. The most important requirement was the height of the component; for instance, corner radii, draft angles, and the parting line (hereafter "PL"). We collaborated with Nissha to refine the shapes. Nissha's advice from the manufacturing point of view was reflected on the component shapes, including the round shapes of the design surface, character lines, radii of the character lines, and PL profile. In the initial stage of trials, film breakage occurred, which was then resolved by changing the thickness of the film and other means. In the end, we succeeded in obtaining not only the desired shapes but also a paintless process.

<Example of reshaping>

Outer side of the instrument panel ornament (**Fig. 8**)

The PL may be visible to customers. The film is unable to cover the surface beyond the PL on the core

side; that is, the resin color is visible.

<Example of gate selection>

Shift indicator panel (**Fig. 9**)

While the molten resin should ideally be injected through a single central gate, a sink mark may then appear. Therefore, we initially tried various combinations of multiple gates, and finally settled on a single gate, which works well and makes weld lines inconspicuous.

By properly locating the gate, we successfully eliminated weld lines, overflow of ink and burns on the vacuum deposited design.

In the area shown with an arrow, a PL on a side runs perpendicularly to the other PL occurring at the corner of a component (**Fig. 10**). This makes the film three-dimensional (dome-like shape) and creates wrinkles.

This concern was solved by making the radius of the corner bigger. To prevent the surface from turning whitish due to metal foil deposited on the film, molding conditions were set properly and a hot pack was used.

A hot pack is an extra process to ensure that the film follows a relatively deep mold recess by heating and sucking the film. Heating makes the film stretch more easily, but may make it difficult to locate the film in the correct position. On the new PAJERO, this process is used for cup holders at which the precise film position is unnecessary (AT models) (**Fig. 11**). Heating may also cause extensive burns on the component. Although this actually occurred on the prototype of the manual transmission shift panel, the problem was solved by changing the molding conditions as advised by the molding contractor, Sakae Riken Kogyo Co., Ltd.

As a result of collaboration with manufacturers and designers, we obtained realistic decoration panels without problems at a mass production level.

## 6. Initial market acceptance

In March 2006, an initial survey for market acceptance, called "a marketing clinic", was conducted.

The survey provided interesting market comments.

Overall, the survey revealed the interior was

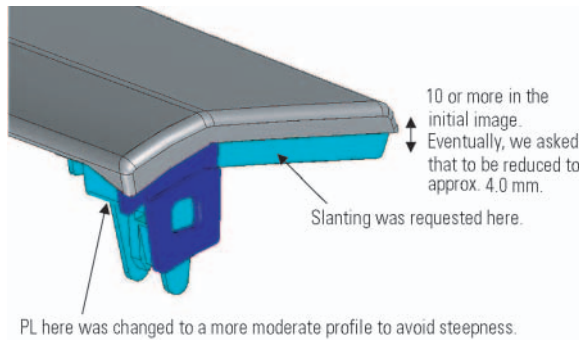
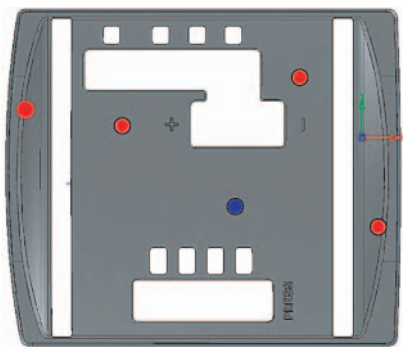


Fig. 8 Example of shape refining



Fig. 10 Example of component shape



Initially, five gates (circles) were planned. Eventually, a single-gate (blue circle) design was selected.

Fig. 9 Gate position examples

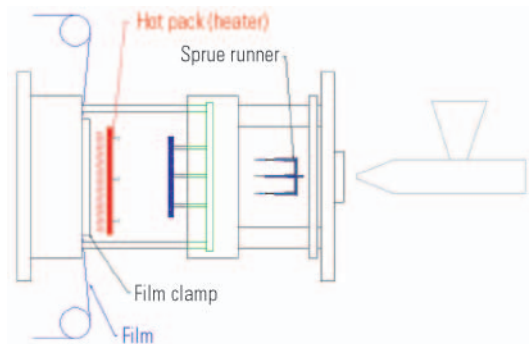


Fig. 11 Hot pack

“sophisticated and high-quality” (Fig. 12).

While there were no specific comments on the decoration panels, a meter featuring the specially-printed aluminum plate, the first of its kind at MMC, was evaluated as excellent texture. The market thus appeared to associate aluminum appearance with high quality and refinement. The wood grain pattern combined with metallic panels on the instrument panel seemed to provide a high-quality touch.

From these initial results, we concluded that our approach to create a high-quality appearance was correct and we decided to move ahead in that direction.

## 7. Physical properties

A clear layer sits on the top of the multi-layer structure of the film. This made us concerned about the resistances to scoring, wear, chemicals, light, etc. (Fig. 13). In addition, VOC-control measures needed to be taken as the New PAJERO was one of the voluntary restraint models in MMC.

After comparing various types of clear layers for the required resistances, an ink-based clear layer was selected (Table 3).

VOC measurements on the initial prototypes substantially exceeded the target levels in aldehyde A and

aromatic hydrocarbon A.

The original ink was replaced with low-VOC ink while the heating conditions were reviewed. As a result, VOC levels became lower than the targets, as shown in Fig. 14.

## 8. Market acceptance

In August 2006, after the start of commercial production, workshops were held at 20 locations across Japan, providing us with the market's initial reaction to our final design.

- The combination of wood grain and silver color around the console shift indicator is good.
- The instrument panel is of high quality and makes a good combination with the decoration panels.

Follow-up workshops were held among the development and sales departments and customers. Many of the participants agreed on the underlying concept of “higher quality appearance” for our decoration design project. We were especially encouraged that the participants found the aluminum panels to be high in quality and refined.

The new PAJERO went on sale on October 4, 2006, and initial evaluations by the market have started. There has been much praise for the high quality of the



Fig. 12 Interior of the new PAJERO

Table 3 Results of physical properties test

Item	Ink-based clear layer	Single liquid-type acrylic clear layer	Hard coat clear layer
Anti-scoring	○ (Slight scoring)	○ (Slight scoring)	No scoring
Anti-wear	○ (Slight scoring)	○ (Slight scoring)	No scoring
Anti-chemical	○ (No damage)	○ (No damage)	○ (No damage)
Anti-light	○ (No damage)	○ (No damage)	○ (No damage)
Cost		△	×

interior, especially the various aluminum-panel accents. We therefore believe that our commitment has been achieved.

## 9. Conclusion

IMD-TR, introduced to the new PAJERO, apparently contributes to raise the quality. We are encouraged with the initial results and continue to offer high quality to our customers through research and development.

IMD-TR has great potential such as: simultaneous component molding of different designs by means of position alignment, which offers substantial cost reduction; and application to interior lighting by means of transparent printing. We will continue to explore further possibilities of IMD-TR.

In conclusion, we sincerely thank Sakae Riken Kogyo Co., Ltd., Nissha Printing Co., Ltd. and others for assisting our IMD-TR project for the new PAJERO.

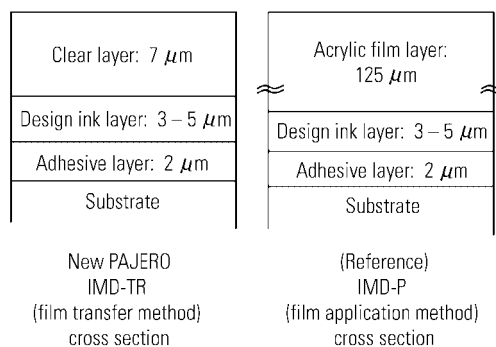


Fig. 13 Structure of printed layers

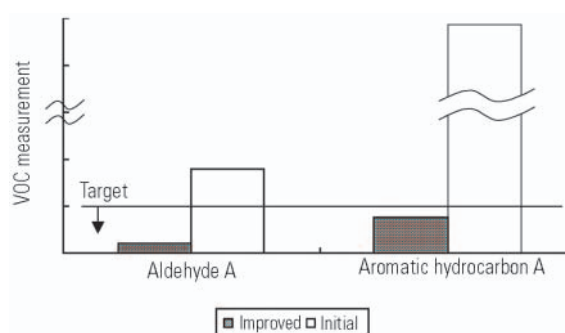


Fig. 14 VOC measurements



Kazuhiro YOSHIDA



Kazuto YAMAUCHI



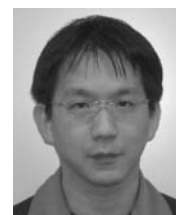
Shinji KONDO



Naoko KOBAYASHI



Hiroshi SAKAGUCHI



Toshikazu KANBE

# Development of Plastic Fender for New DELICA D:5

Shigeru ITO\* Yasuhide FUKUHARA\* Hiroshi HAMANE\*\*  
 Kosaku UCHIDA\*\* Yuichi HASEGAWA\*\*\* Kazuki BABA\*\*\*  
 Yuichi ISHIKAWA\*\*\*

## Abstract

On the new DELICA D:5, the use of on-line paintable, highly heat-resistant, electroconductive plastic enabled the integration of fender parts, thus reducing vehicle weight by approximately 4 kg and suppressing cost. Furthermore, the flexibility of plastic remarkably improved the product resistance to low-intensity collision damage. The new plastic fender is molded at the plastic parts factory in Mitsubishi Motors Corporation (MMC)'s Nagoya Plant, then installed to the vehicle body on the body welding and assembling line, painted through the paint process, and finally its fitting is adjusted in the trim fitting process in PAJERO Manufacturing Co., Ltd.

CAE analysis was performed for the thermal behavior of the fender in the painting process to optimize the locations of fixing points and the shapes of parts. Based on the results of actual line trials and laboratory experiments, optimal molding conditions were established, body dimensional precision control points were reviewed and corrected, temperature distribution in the coating drying oven was improved and new ideas were embodied for better ways of fitting trim parts, thereby raising the quality of the plastic fender.

**Key words:** Exterior, Plastics, Weight Reduction, Injection Molding

## 1. Introduction

MMC used plastic in the fenders for the first time on the new DELICA D:5, making the fender approximately 4 kg lighter than that of steel. As the plastic fender is installed on the front part of the vehicle, it achieves a better weight balance and increased resistance to low-intensity collision damage. The latter means that the new fender has higher resistance against, for example, a collision with a shopping cart, and so offers a feeling of security in case of an accident.

One of the features of this plastic fender is that it can be painted with the body for uniform appearance. MMC has overcome many challenges to apply this feature through full teamwork involving all departments concerned from development to production, such as carrying out part design taking thermal behavior into consideration, molding operation and quality control at the in-plant plastic part factory, assurance of dimensional precision at fitting-to-body points, oven temperature control and improvement of trim part fitting method, all to ensure that the product is of commercial quality. This paper describes the development process of the plastic fender.

## 2. Engineering plan

The plastic fender is molded at the plastic part factory, installed on the body in the body welding and

assembling line as is the case with the conventional steel fender, painted while on the line, and finally adjusted for proper installation in the trim parts fitting line (Fig. 1). Because of the heat resistance of the resins, adhesiveness of the paints used, etc., plastic parts such as bumpers and garnishes are usually coated separately from the body using dedicated paints after molding. In this case, however, since a different paint material such as urethane paint is used on the plastic parts, it is difficult to achieve color matching between the plastic parts and body. Especially when painting parts that continue on the same plane, uniform coating quality is crucial for a better appearance. In view of this, the application of the same paint simultaneous with the body to achieve a uniform appearance, as well as lower coating cost, was set as a precondition for developing the plastic fender.

To enable the plastic fender to be coated on the body coating line, its material has to be sufficiently heat resistant to withstand the temperature of electrodeposition or other coat drying oven, and must be electroconductive to enable electrodeposition. To meet these needs, nylon resin was selected as the base material, to which carbon was added to give sufficient electroconductivity to enable electrodeposition.

\* Material Engineering Dept., Development Engineering Office

\*\* Vehicle Testing 1 Dept., Development Engineering Office

\*\*\*Production Engineering Paint Dept., Production Engineering Office

\*\* Body Design Dept., Development Engineering Office

\*\* Stamping & Plastic Engineering Dept., Production Engineering Office



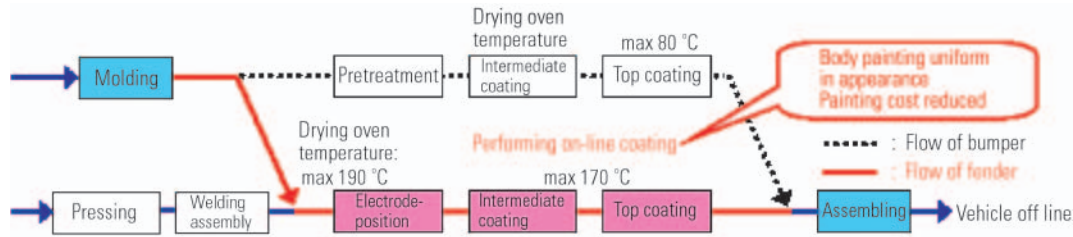


Fig. 1 Line flow

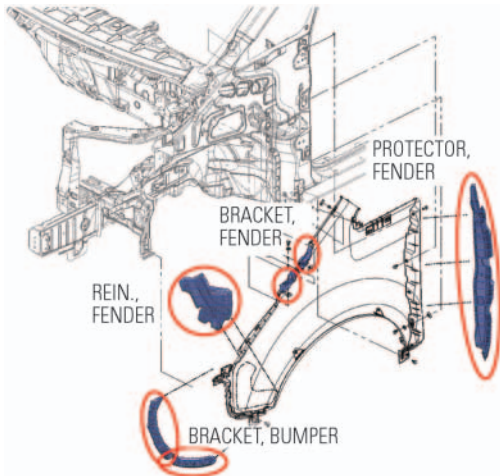


Fig. 2 Integration of fender-related parts

### 3. Design

The design engineering advantages of a plastic fender include structural rationalization owing to a high degree of shaping freedom of the material and functional improvement as a part, in addition to commercial attractiveness such as lighter weight and higher damage resistance. Specifically, the plastic fender can be readily integrated with associated fender parts, designed to be pedestrian protection-oriented and given optimal outside plate rigidity. However, challenges to be addressed in the future include maintaining dimensional accuracy under thermal load during on-line coating and elimination of distorted appearance.

#### 3.1 Structural study

When developing the plastic fender, the first consideration is to reduce the number of parts. As shown in Fig. 2, associated parts in separate pieces for a steel fender, such as bumper fitting brackets, reinforcements and anti-sound and snow partitions, were molded integrally with the fender panel. Also, as the panel thickness of the plastic fender can be freely selected, it was reinforced where absolutely necessary for rigidity, thus reducing weight by approximately 4 kg per vehicle.

Next, the energy absorption of the fender for head protection of pedestrians was improved. Normally, steel fenders require separate fitting brackets to be raised from the body framework to the hood line at the fender top to provide the necessary travel to absorb

impact energy. In the case of a plastic fender, the greater flexibility and shaping freedom of plastic than steel enable the fender to be molded in the form of a one-piece wall to serve as a shock-absorbing member.

In designing the plastic fender, one challenge was to create a structure capable of absorbing thermal expansion and contraction. Especially, since the fender is coated in the same coating line with the body, in-oven thermal behavior control was critical. Therefore, the fixing points were chosen so as not to hinder the fender's movement (see below). Also, as the fender has so many peripheral parts to fit, such as the doors, hood, headlamps and bumper, it must be adjusted easily for better fitting and satisfactory appearance. Gaps and flushness between the fender and door line, hood line and A-pillar line were so sensitive to the position of the fender fixing brackets and surface precision that the installing position pitch tolerance and bracket position were controlled taking the thermal behavior of the fender into account.

#### 3.2 Optimization of fixing points

The plastic fender is exposed to a high temperature near 200 °C in the drying oven. To avoid partial stress concentration in the fender due to thermal expansion and contraction, its fixing points and panel thickness were optimized using thermal behavior CAE (Fig. 3 and Fig. 4). The fender is constructed so that, when thermally expanded and contracted, its behavior is relaxed in the forward and downward direction with its reference point as a fulcrum. It was made horizontal all over in the engine hood line surface for easy forward movement, and was provided with fixing points on the same plane on the door line to make downward movement easy. Each fixing point is rectangular, and the fender is fastened to the body with collars and clips. To maintain rigidity during thermal expansion and contraction, the panel thickness of the fender was increased at the fastening points. For the fixing points along the door line, they were located as close to the design surface as possible to ensure the optimum fit. At the hood line, brackets are adjustable to facilitate adjustment of flushness during installation. At the A-pillar line, fixing points were provided on the windshield glass side to allow the gap and flushness to be adjusted during trim fitting process to ensure a good fit.

#### 3.3 Verification

The results of desktop studies using CAE, etc. were evaluated in the laboratory using actual parts with

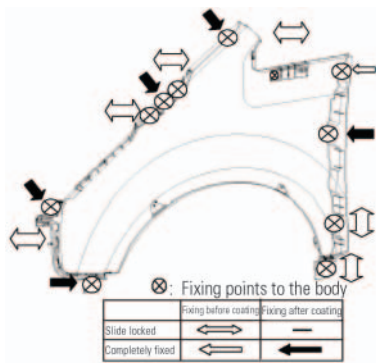


Fig. 3 Optimization of fixing points

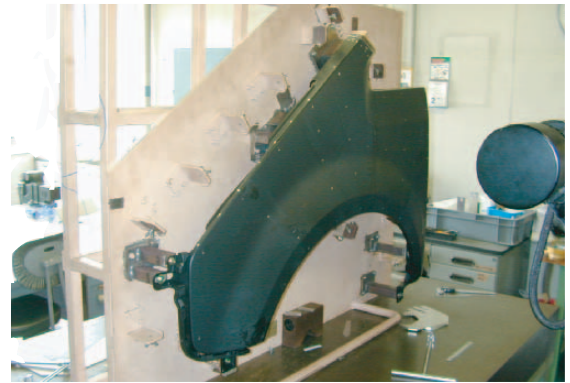


Fig. 5 Part evaluation

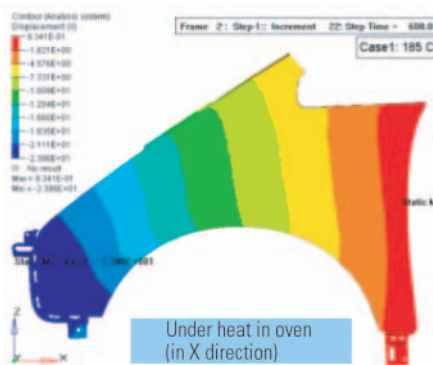


Fig. 4 Thermal behavior analysis



Fig. 6 Line trial using prototype body

emphasis on thermal behavior, and minute alterations were made (Fig. 5). Furthermore, actual adaptability of the fender to the coating line was verified by repeating tests using a prototype body for detailed evaluation (Fig. 6).

## 4. Production engineering

### 4.1 Molding

The molding die to be used to mold exterior parts made of the highly heat-resistant electroconductive resin was designed to work with sufficient accuracy in a high-temperature atmosphere. Also, actions different from those for general plastic molding were taken, such as taking the moisture absorption of the material into account when setting the molding conditions.

#### 4.1.1 Tooling design

To ensure dimensional precision of the molding, fluidity analysis was conducted to optimize ① the position of the molten material injection gate, ② the thickness of molding, ③ the layout of water ports, etc. (Fig. 7). Especially, the thickness of the molding was determined so as to minimize the increase in weight without sacrificing tensile rigidity and moldability (Fig. 8).

The parting line at the windshield section was located not exposed on the outer surface of the body in order to improve the appearance after coating. To form flanges, etc. in the engine compartment including

pedestrian protection structure, large two-piece inclined cores were employed. For the tubular A-pillar that characterizes this plastic fender, the mold is provided with a slide on the cavity side.

#### 4.1.2 Molding operation

The plastic fender is molded at the plastic part (bumper) factory in Okazaki Plant using molding machines with 2,200-ton mold clamping force and delivered to Pajero Manufacturing Co., Ltd. where vehicle assembly is performed. To mold the plastic fender at this bumper factory, material dryers and temperature controllers for high-temperature use were introduced. Furthermore, insulation was provided near the injection units of the molding machines to be able to handle the electroconductive material. Unlike bumpers molded of polypropylene, the plastic fender requires thermally unstable high-temperature, high-speed molding of nylon. For molding of actual parts, therefore, new work standards were established including drying conditions. As to the setting of the injection cylinder temperature and injection profile in particular, molding tests were repeatedly conducted to determine the conditions that minimize oxidation deterioration of the material by shearing heat-buildup and retention.

### 4.2 Coating

To run plastic exterior panels on the coating line originally designed for steel, particular attention was

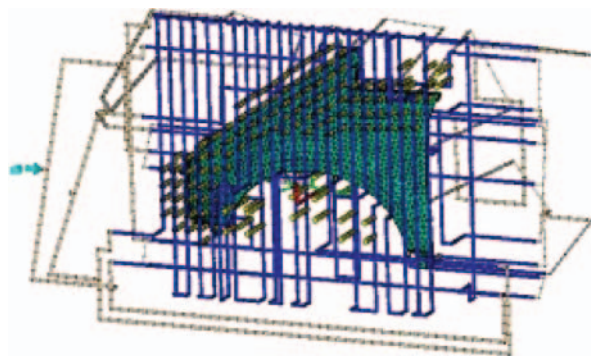


Fig. 7 Optimization study result on cooling water channel

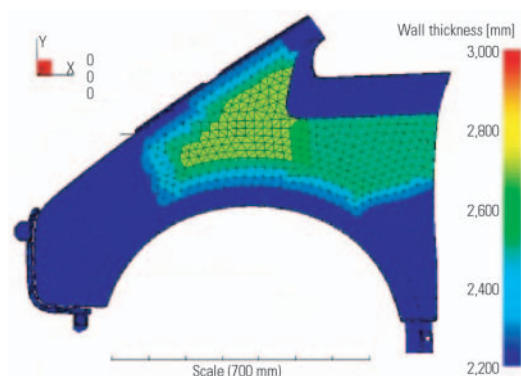


Fig. 8 Optimization study result on panel thickness

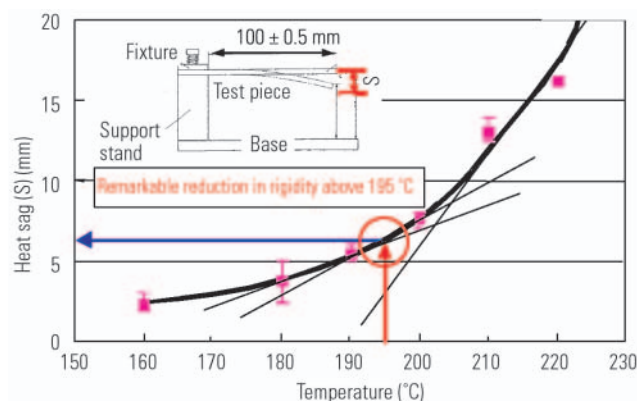


Fig. 9 Temperature vs. heat sag

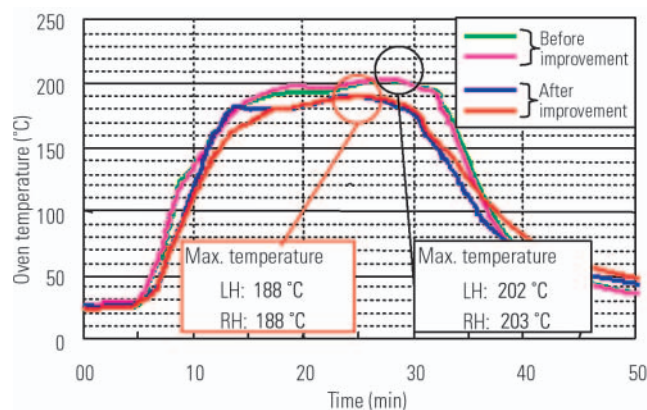


Fig. 10 Fender surface temperature in drying oven

paid to the oven temperature control and the coating finish.

#### 4.2.1 Oven temperature control

To minimize heat sag in the oven, oven temperature is controlled according to the thermal characteristics of the resin (Fig. 9). By improving the efficiency of heat transfer by increasing hot air circulation in the oven, the surface temperature of the fender can be kept below 190 °C without adversely affecting the drying parameters for steel parts of the body (Fig. 10).

#### 4.2.2 Finish

The finish of the plastic fender was compared with that of a steel part (door).

The result was satisfactory in respect to the waviness-induced "orange-peel" texture of the painted surface and M-WS value indicating grain and fade with some difference in short-wave value after intermediate coating but no difference after top coating. Also, comparative spectro-colorimetry revealed no noticeable color difference and the uniformity of the coating quality of the entire body appearance was confirmed (Fig. 11).

### 4.3 Assembling

#### 4.3.1 Body dimensional precision control

Various fixing points at given distances from the fender fitting reference point are set for controlling the dimensional precision of the body so that the thermal

behavior of the plastic fender in the electrodeposition oven is not impeded (Fig. 12).

The plastic fender expands and contracts in the forward and downward directions of the vehicle body from the reference fitting point in the electrodeposition oven. In order to obtain distortion-free appearance, these movements of the plastic fender under heat must take place steadily and smoothly. To make this possible, irregularities in the levelness of the fender supporting brackets, fixing point-to-point distance, etc. must be kept within constant limits.

#### 4.3.2 Fitting of trim parts

Fitting of the plastic fender in relation to the door, engine hood and other peripheral parts is adjusted on the body welding and assembling line when the fender is installed and on the trim fitting line after coating. On the body welding and assembling line, the fender is fastened to the body at body reference and fender weight support points using slidable collars and clips.

On the trim fitting line, mainly the points which affect appearance are fixed while adjusting the fitting to the body and peripheral parts.

Fitting on welding and assembling line (before coating) (Fig. 13)

- ① Fastened with body side pins with plastic clips
- ② Slide bolt installed
- ③ Bolt tightened while aligning the highlight line



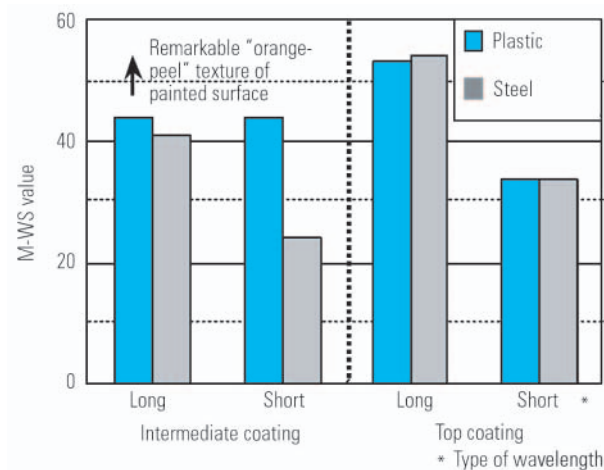


Fig. 11 Results of paint finish evaluation

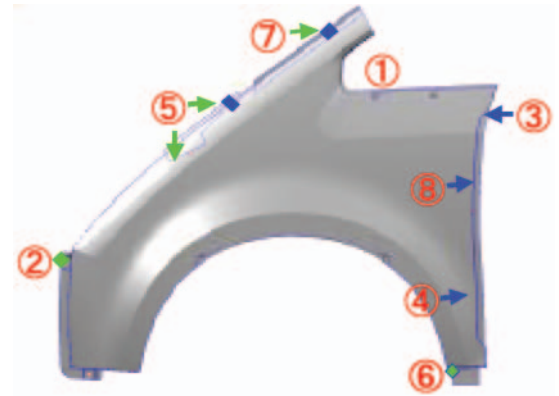


Fig. 13 Fitting points

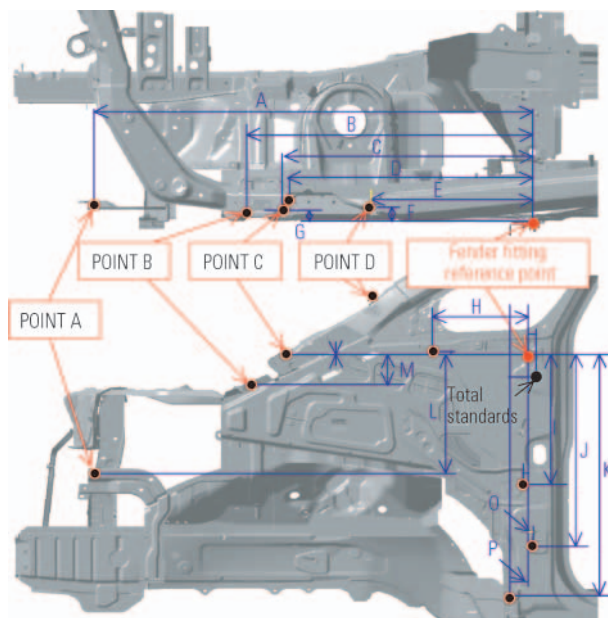


Fig. 12 Reference point for fixing point control

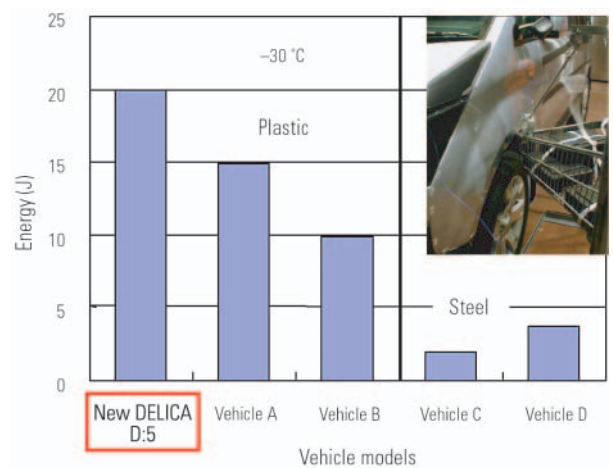


Fig. 14 Low-temperature collision impact test

- with that on the door
- ④ Fastened with slide collars while checking the door opening and closing movement
  - ⑤ Fastened with slide collars while adjusting the flushness with hood
  - ⑥ Slide bolt install
- Fitting on trim line (after coating) (Fig. 13)
- ⑦ Bolt tightened while adjusting the gap between the fender and A-pillar
  - ⑧ Bolt tightened while adjusting the flushness with door
  - ⑨ Slide bolt installed in step ⑥ tightened

## 5. On-vehicle practicality

### 5.1 Resistance to low-intensity collision damage

One of the aims in developing the plastic fender was to improve the resistance to low-intensity collision dam-

age. To verify that this had indeed been achieved, two collision impact tests were conducted by making a shopping cart collide with the fender and by running a test vehicle into an offset stationary wall.

#### 5.1.1 Shopping cart test

Simulating its frequent daily shopping use, a large shopping cart loaded with 50 kg to simulate purchases (60 kg in total), was run into the plastic fender while gradually increasing its speed until the fender was damaged. The test found that the plastic fender was damage-free at normal temperature. In addition, as plastics are generally fragile at very low temperatures, the same evaluation was performed at a very low temperature (-30 °C) (Fig.14). In this particular temperature range as well, the plastic fender was clearly superior to the conventional steel fender.

#### 5.1.2 Offset barrier impact test

The plastic fender was tested for damage in a low-speed offset frontal collision which is particularly common in actual traffic accidents (Fig. 15).

The plastic fender was heavily waved in the surface upon collision by the rearward impact input. Examination after stopping, however, found no damage



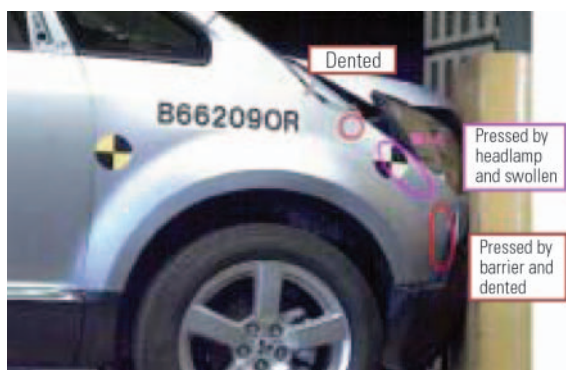


Fig. 15 15 km/h right offset rigid barrier test (offset frontal collision)



Fig. 17 Water impact test

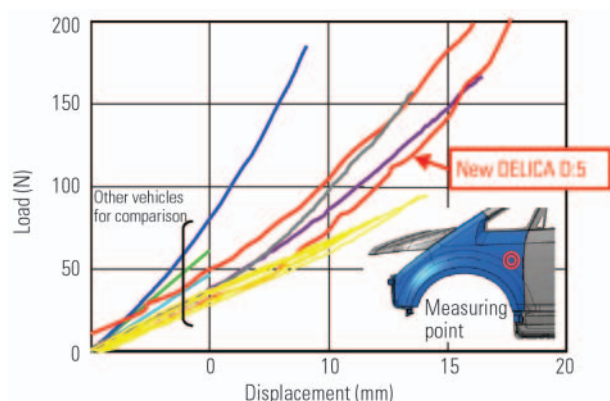


Fig. 16 Tensile rigidity test

to the fender in the installed condition and the deformation had been restored to some extent. From this, and considering its restorability if deformation is limited, repair cost is likely to be lower.

### 5.2 Tensile rigidity

The plate thickness of the plastic fender was partly optimized to effectively obtain the necessary rigidity as a body exterior part. The results of comparative rigidity tests performed with the plastic fender installed on a test vehicle are shown in Fig. 16. The optimization of panel thickness provided appropriate tensile rigidity to the plastic fender as a body part.

### 5.3 Durability

The plastic fender was road tested for looseness in fitting points caused by impact load from the road surface (Fig. 17), and the results were satisfactory. The plastic fender dispersed the impact input softly without any damage or deformation.

## 6. Conclusions

Many studies on the use of plastics in vehicle exterior panels have long been conducted. After many years of R&D, MMC has succeeded in using the plastic fenders on a mass-produced vehicle, the New DELICA D:5. Our affiliated companies and many people both within and outside the company collaborated enthusiastically in the development work to make this possible. MMC will continue this passion for improving customer satisfaction with new attractive components.

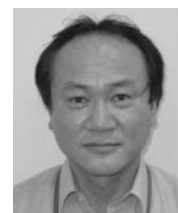
Finally, MMC sincerely thanks GE Plastics Japan Ltd., Kyowa Kogyo Co., Ltd., Pajero Manufacturing Co., Ltd. and many other people for their fruitful involvement and cooperation in the development of the new plastic fender.



Shigeru ITO



Yasuhide FUKUHARA



Hiroshi HAMANE



Kosaku UCHIDA



Yuichi HASEGAWA



Kazuki BABA



Yuichi IISHIKAWA

# Development of Aluminum Space-Frame Body with New Structure in Front

Hayami NAKAGAWA\* Takuo NAKAMURA\* Yoshinobu MATSUMURA\*  
Katsuhiko TAKASHINA\*\* Junichi YANASE\*\* Hisayuki ISHIZU\*\*  
Hiroaki KANO\*\*\* Hiroyuki SEINO\*\*\* Akinori YASUI\*\*\*  
Hideki ITO\*\*\* Koji FUJII\*\*\*

## Abstract

The aluminum space-frame body used on some mass production vehicles is one of the most sophisticated technologies for reducing the weight of the vehicle body.

In this development, a new construction for the front side members has been adopted to reduce minimum turning radius as well as a technology for manufacturing high-quality aluminum space-frame bodies at low cost.

In addition, good improvement of handling and stability has been confirmed by the increased rigidity at the local sections such as joints as well as the weight reduction.

**Key words:** Body, Structure, Aluminum, Lightweight, Spaceframe

## 1. Introduction

Weight reduction is a crucial issue not only for the needs for lower fuel consumption and better environmental-friendliness but also for the improvement of vehicle dynamics – a vehicle's basic performance.

Generally, current vehicle bodies are of a steel monocoque structure. Car manufacturers are making an effort for weight reduction by applying extra-high tensile steel and by optimizing the body structure. For a drastic weight reduction by more than tens of percent, however, extensive structural studies including the change of material from steel to lighter aluminum or plastics are necessary. In the future, it is expected that R&D efforts will be further accelerated for a lighter body structure with such materials.

In this study, we have established the manufacturing technology for a high quality aluminum space-frame light-weight body built of aluminum extrusions and aluminum die-castings laid out and combined for optimal effectiveness with a low cost. In addition, we have developed a new front side member construction which allows a large tire steer angle to reduce the minimum turning radius.

Furthermore, on the driving evaluation test using a prototype vehicle, it has been confirmed that both the weight reduction and the locally increased body rigidity highly improve the handling and stability. This paper will give an overview of this development mentioned above.

## 2. Developmental target

In applying the aluminum space-frame body in place of the existing body of a steel monocoque vehicle (hereinafter referred to as base vehicle), the target for vehicle weight reduction was established with (1) through (5) itemized below as preconditions.

- (1) The layout of the major parts such as the power train and suspension should not be changed from that of the base vehicle.
- (2) The following static and dynamic body rigidity should be equal to that of the base vehicle.
  - Body bending/torsional rigidity
  - Rigidity of suspension mounts
- (3) The crashworthiness should be equal to that of the base vehicle.
  - 55 km/h full overlap frontal impact (J-NCAP)
  - 64 km/h offset frontal impact (J-NCAP)
  - 55 km/h side impact (J-NCAP)
  - 15 km/h offset frontal low speed impact (R-CAR)
- (4) The body vibration characteristics should be equal to that of the base vehicle.
- (5) The durability should be equal to that of the base vehicle.

## 3. Outline of structure

### 3.1 Basic structure

The extrusions and the high-vacuum die-castings were combined and arranged in the right places to reduce the number of parts. The extrusions can be formed into closed-section, one-piece frame members

\* Advanced Vehicle Engineering Dept., Development Engineering Office  
\*\* Safety Testing Dept., Development Engineering Office  
\*\*\* Vehicle Testing 2 Dept., Development Engineering Office

\*\* Digital Engineering Dept., Development Engineering Office  
\*\* Vehicle Testing 1 Dept., Development Engineering Office  
\*\*\* Production Engineering Body Dept., Production Engineering Office

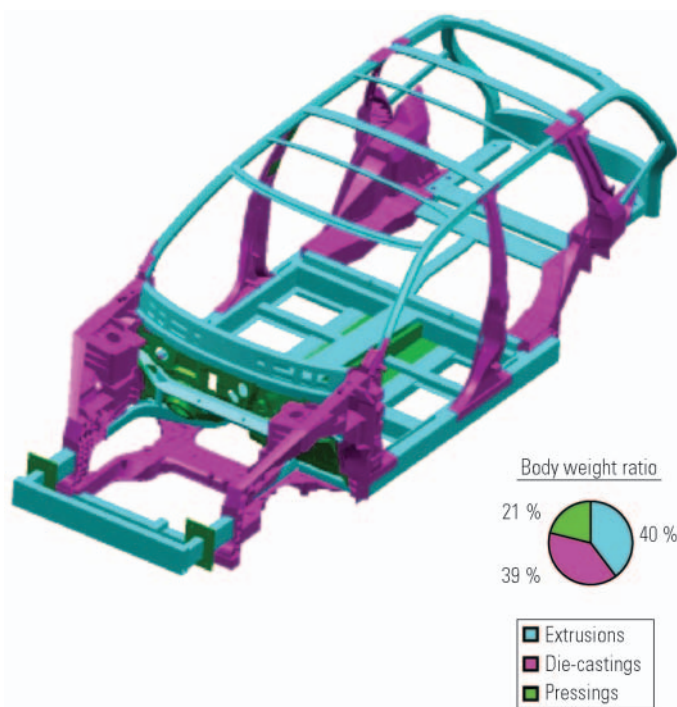


Fig. 1 Aluminum space-frame body

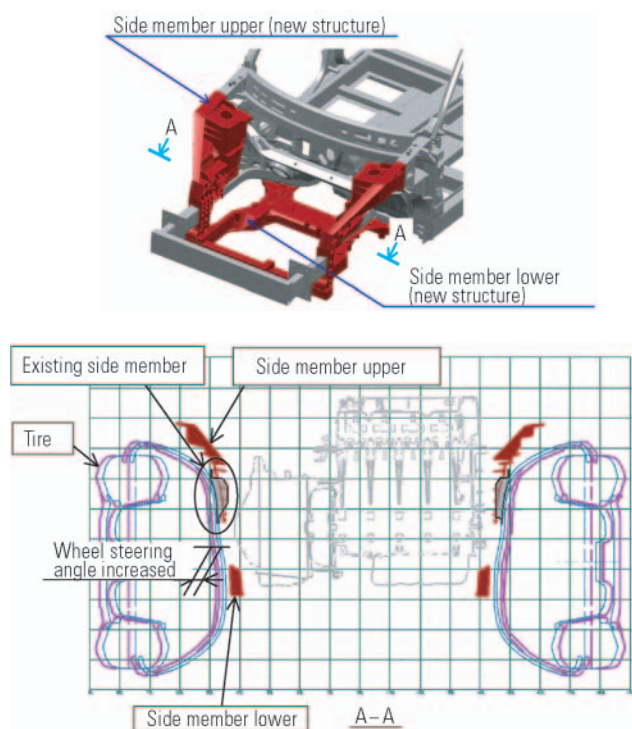


Fig. 2 New front side member arrangement

with relatively low tooling costs, and the high-vacuum die-castings permit the consolidation of multiple parts into single parts thanks to their form flexibility – a single part can be composed of a different thickness and rib form. Moreover, the machining areas were minimized. Thus the production cost was reduced (Fig. 1).

The number of parts was reduced to about a half of that of the steel monocoque body for the base vehicle. The number of welding operations was reduced almost by half as well, making it easier to stabilize the body dimensional precision, whereby production investments and costs could be curtailed.

As to the weight of an aluminum space-frame body, a 32 % reduction could be achieved from the weight of the steel monocoque body of the base vehicle.

### 3.2 New front side member arrangement

To reduce the minimum turning radius, which is mostly effective for sport utility vehicles with large tires, a new structure which separates the side members into the upper and lower side members at the front wheel position to increase the tire steer angle was applied (Fig. 2).

In this study, the minimum turning radius was reduced by 0.3 m with the increase of the tire steer angle.

## 4. Performance assessment

### 4.1 Body rigidity

At the initial stage of study, CAE analysis was conducted using a simplified model \*1 (Fig. 3) to assess the contribution of each frame and joint to the body rigidity

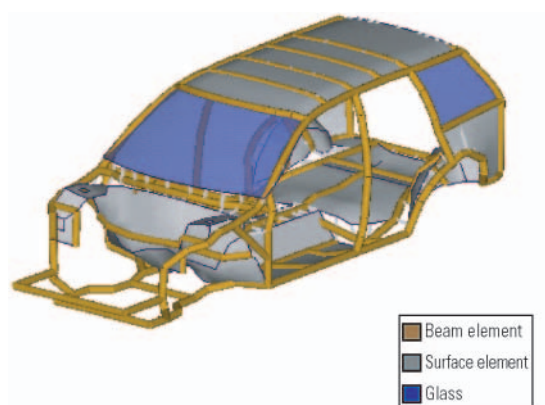


Fig. 3 Simplified model

and determine the rigidity distribution of the basic framework for optimal weight efficiency, thereby attaining the target level of body rigidity.

Also, at the suspension joints that affect steering stability, ribs are added and thickness is increased for the die-castings to ensure local rigidity.

\*1: Simplified model with framework members as beam elements and panel members as surface elements

### 4.2 Crashworthiness

In accessing its crashworthiness, the rupture property of aluminum is crucial. Therefore, the material characteristic of aluminum obtained from the element test was applied to CAE analysis for new structural research.

With the new structural side member arrangement,



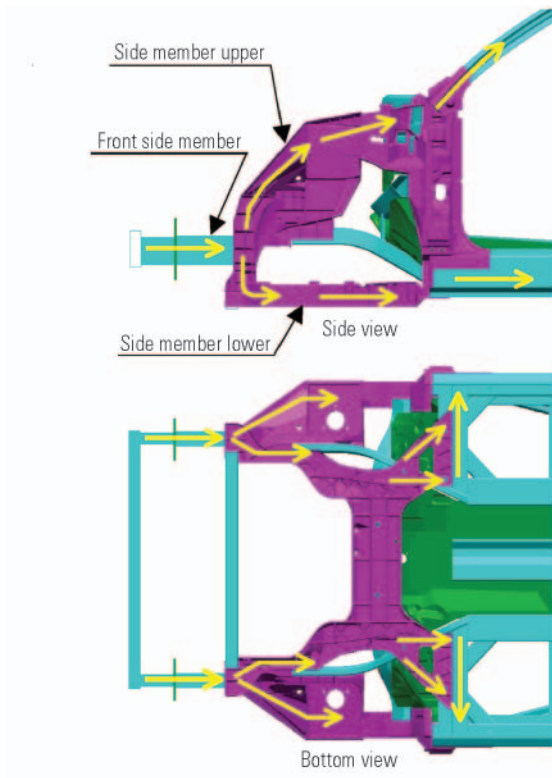


Fig. 4 Load distribution in full frontal impact

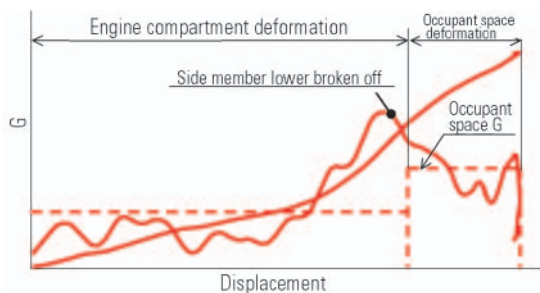


Fig. 5 Crashworthiness characteristics in full overlap frontal impact

the impact load is dispersed to the upper and lower side members in order to absorb energy sufficiently (Fig. 4).

In a full overlap frontal impact, input energy is absorbed enough by the front side members, and then the lower side members break off at the rear attached points to reduce the possibility of occupant injury (Fig. 5).

In an offset frontal impact, in order to reduce deformation of the passenger compartment, the impact load is dispersed to the side sills and backbone that are not deformed in the full overlap frontal impact in addition to the upper and lower side members (Fig. 6).

In a side impact, the center pillar bends at the waist level of the dummy without any die-casting parts being broken, thereby reducing the intrusion velocity at the chest level of the dummy to decrease the possibility of

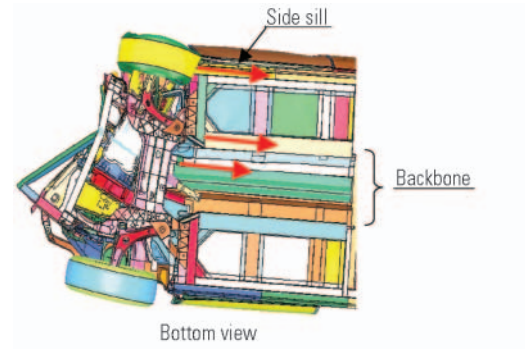


Fig. 6 Deformation mode in offset frontal impact

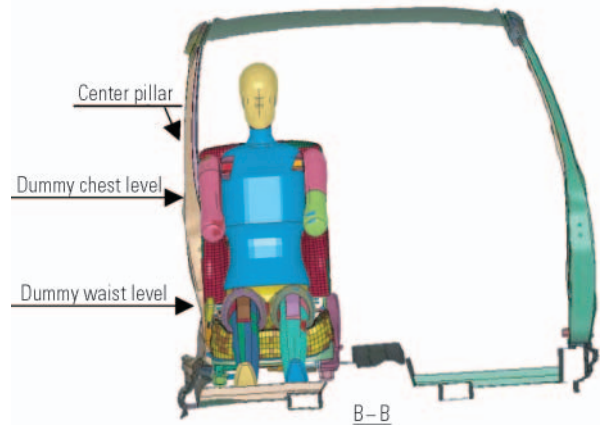
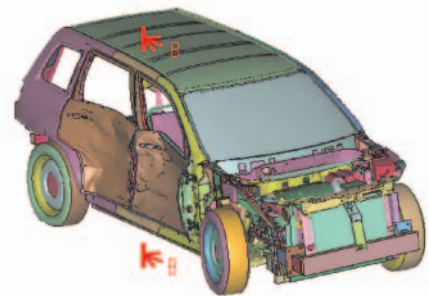


Fig. 7 Deformation mode in side impact

occupant injury (Fig. 7).

In a low speed impact, considering the difficulty of aluminum part repair in the market, it is so constructed that the plastic deformation does not propagate to a die-casting part (Fig. 8).

#### 4.3 Vibration characteristics

If the vehicle weight is reduced, apprehension arises about a peak-level increase in framework sympathetic vibration with the decrease of mass. By optimizing the balance of joint rigidity in the space-frame structure, a body vibration level lower than that of the base vehicle could be achieved. Fig.9 shows an example of an idling vibration level comparison with the base vehicle.



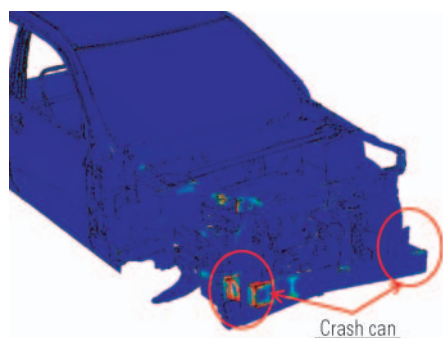


Fig. 8 Strain distribution in low-speed impact

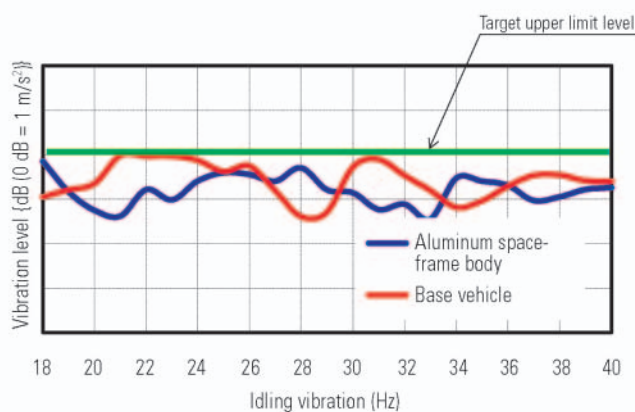


Fig. 9 Idling vibration level

#### 4.4 Handling and stability

As weight reduction in the peripheral portion of a vehicle body can effectively decrease the inertia moment, its contribution to an improvement in handling and stability, as well as in acceleration performance, is significant.

Furthermore, as the characteristic feature of the extrusions and die-castings applied in the space-frame structure, their contribution to the improvement not only in overall body rigidity but in local rigidity can be cited.

In a conventional monocoque structure, it is a general practice to join pressings by spot welding. However, spot-welding is an intermittent joining that allows very small openings to be locally made between joined points. For such local openings, they can be suppressed by adopting continuous welding such as laser welding. On the other hand, an extrusion, being a constant cross-section, continuous body, is equally or more effective than continuous welding in this respect.

In addition, by adding ribs and thickening the wall sections at the specified sections of the die-cast members used in the strut house, the local rigidity in suspension joints can be improved.

It could be confirmed that the increase of these local rigidities remarkably improves the feeling of handling and stability.

As a result of a feeling assessment by an on-vehicle

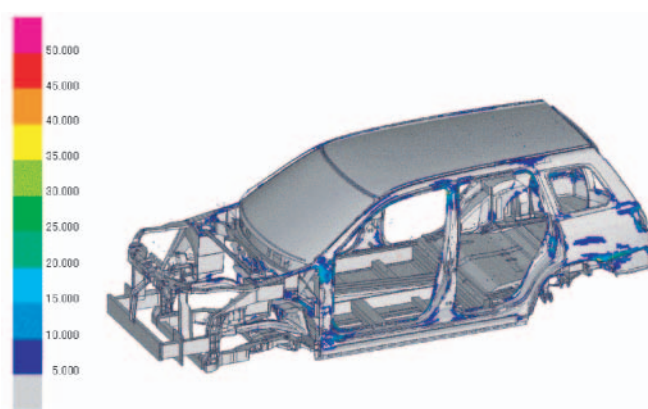


Fig. 10 Durability analysis with complete vehicle model

test, the improvement of the steering feel and flat riding feel by the increase of local body rigidity could be confirmed, in addition to the improvement in steering response by the decrease of the inertia moment.

#### 4.5 Durability

Aluminum is lower than steel in material strength. By reducing impact load input through weight reduction and increasing basic material thickness, however, generated stress could be made lower than the standard value and durability equal to or higher than that of the base vehicle could be obtained (Fig. 10).

### 5. Element technology

For higher accuracy of CAE analysis, test results with simple formed member samples were matched with CAE analysis. An example of it is given below.

#### 5.1 Die-castings dynamic bending crush test

A dynamic bending crush test was conducted using simple-formed member samples imitating center pillar (Fig. 11).

Matched with the deformation form, broken rib locations and load-displacement characteristics revealed by the test, CAE analysis using an actual vehicle model was performed applying the analytical know-how acquired here.

### 6. Production engineering

With the application to mass production vehicles as the premise, the joining method and process are introduced as a study guide for workmanship stabilization and manufacturing cost optimization.

#### 6.1 Joining method

To join aluminum extrusions with aluminum die-castings, fusion welding is adopted. This paper presents the results of verification tests conducted for application of MIG welding and laser welding to the space-frame structure as candidate means of joining in

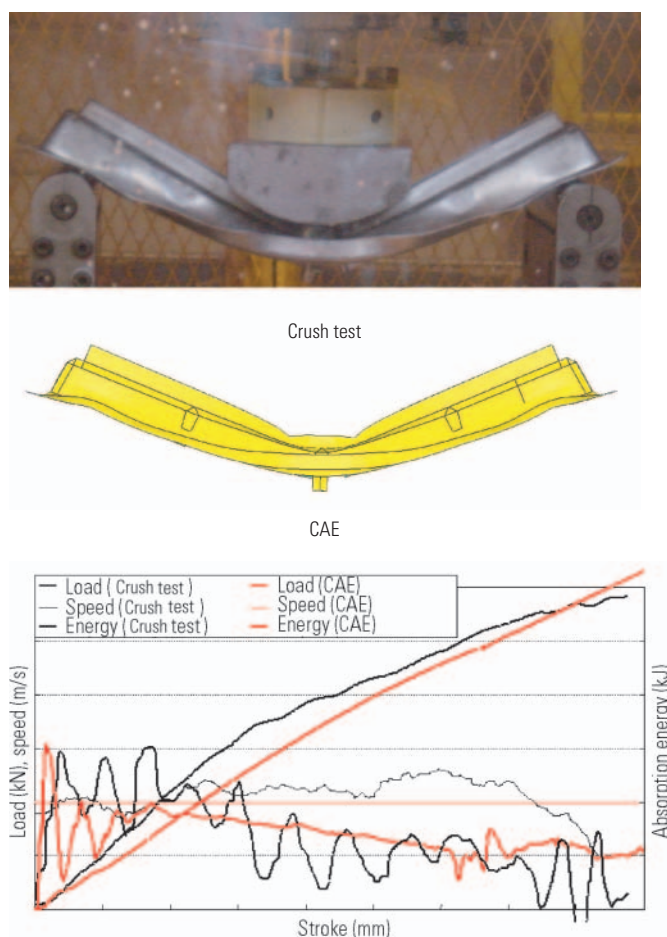


**Fig. 11 Results of dynamic bending crush test and CAE analysis using simplified member samples**

**Table 1.**

MIG welding is used for tack welding and repair, but thermal strain is large. For minimum thermal strain, it is necessary to take time to cool after welding and then release the jig.

Laser welding is a low heat input joining technique and develops little thermal strain. It is therefore used for additional welding on the production line to stabilize body dimensional precision after welding assembly.

## 6.2 Joining process


Line operation planning was done with the ease of parts setting and welding work and the dimensional precision stability taken into account (Fig. 12).

Compared with the steel monocoque structure, its aluminum space-frame counterpart requires a half number of operations to assemble owing to the smaller number of parts.

## 7. Conclusions

A mass production-oriented low-cost aluminum space-frame body structure that allows a 32 % body weight reduction as compared with the steel mono-

**Table 1 MIG and laser welding comparison**

Type of welding	MIG	Laser
Strength	<p><b>Shearing</b></p> <p>Ruptures in base material and from heat-affected zone were observed but strength was almost equal, indicating that sufficient strength can be obtained.</p> <p>Ruptured from base material      Ruptured from heat-affected zone</p>   <p><b>Bending</b></p> <p>Bent through 180 degrees without any resultant defect observed.</p> 	<p><b>Shearing</b></p> <p>Base material was ruptured and sufficient strength is possible to obtain. Since the weld was hair-cracked due to thermal shrinkage, however, filler was supplied.</p> <p>Ruptured from base material      Hair cracked</p>   <p><b>Bending</b></p> <p>The same as MIG.</p>
Gap allowance	<p><b>Up to 1.0 mm</b></p> <p>Pitting shown below occurred if gap exceeded 1 mm in some cases, and frequency of pitting increased as gap widened.</p> 	<p><b>Up to 0.7 mm</b></p> <p>With 0.9 mm gap, recess observed on weld bead</p> <p>Gap 0.7 mm      Gap 0.9 mm      Weld broken</p>  <p>Recess observed in weld</p>
Thermal strain	<p><b>Large</b></p> <p>3.2 – 3.8 mm Heat input reduced: 1.9 – 2.1 mm</p> 	<p><b>Small</b></p> <p>0 – 0.2 mm</p> 
Welding speed	<p><b>Slow</b></p> <p>0.5 m/min</p>	<p><b>Fast</b></p> <p>1.5 m/min (3.5 kw)</p>

coque body and a 0.3 m minimum turning radius reduction through the application of a new side member arrangement was developed.

It could be confirmed that the aluminum space-frame body contributes greatly not only to body weight reduction but to the improvement of body properties and vehicle dynamics.

In the future, we intend to work on further structural rationalization for still lighter vehicles and lower production costs and propose new structures with more commercial values based on this structure.

## 8. Acknowledgement

The authors wish to extend sincere appreciation to the staff of the Automotive Department of Mitsubishi Aluminum Co., Ltd. for their overall cooperation and assistance in the development of the new aluminum

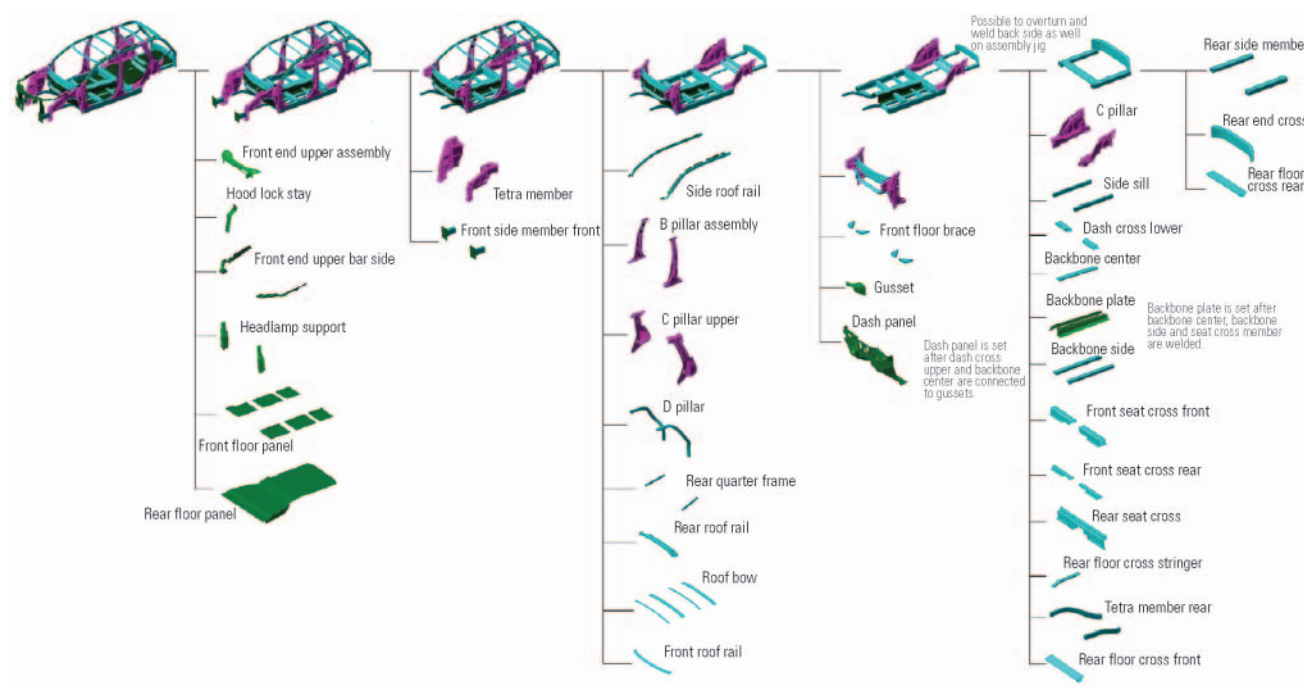


Fig. 12 Joining process flow chart

space-frame body structure. Our special thanks also go to all the development people at Ahresty Corporation and Ryobi Limited for their great cooperation in the development of diecast parts.



Hayami NAKAGAWA



Takuo NAKAMURA



Yoshinobu MATSUMURA



Katsuhiko TAKASHINA



Junichi YANASE



Hisayuki ISHIZU



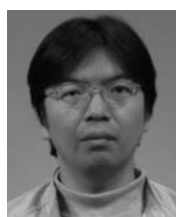
Hiroaki KANO



Hiroyuki SEINO



Akinori YASUI



Hideki ITO



Koji FUJII

# Development of High-Efficiency MAC System

Kazumi OKINAKA\* Akihisa YAMATANI\*\*  
Masaru KADOI\*\*\* Hideto NOYAMA\*\*\*

## Abstract

The fuel efficiency of vehicles needs to be improved further to help mitigate global warming and contribute to the protection of the environment. Consumers are interested in actual fuel consumption on the road, not on the chassis dynamometer in a controlled chamber. It is therefore necessary to reduce the power consumption of the mobile air-conditioning (MAC) system.

In order to improve actual fuel efficiency, Mitsubishi Motors Corporation (MMC) developed a high-efficiency MAC system which consumes at least 30 % less power than the conventional MAC system.

**Key words:** Air Conditioning, Fuel Economy, Control, MAC system

## 1. Introduction

Recently, gasoline prices have been soaring because of the rapidly increasing demand for gasoline driven by remarkable economic growth mainly in the BRIC countries (Brazil, Russia, India and China) and growing concerns over oil shortages due to political instability in oil-producing countries. In addition, global warming and the trend toward environment-friendly products have renewed interest in reducing fuel consumption in many countries including the United States and Japan.

The so-called "catalog value" for fuel consumption assumes driving on a series of roads of a specific pattern, and differs from the fuel consumption in diverse actual environments. Vehicle users must pay for the fuel their vehicles consume in real life (or the "actual vehicle fuel consumption") as a running cost, so users are more interested in the actual consumption than the catalog value. Air conditioning significantly affects the actual vehicle fuel consumption, and discussions on how to deal with fuel consumption when using air conditioning system have started in Japan, the US and Europe. This will likely become subject to regulatory controls in the near future, so MMC has started working with Mitsubishi Heavy Industries (MHI) on reducing the power consumed by a vehicle's air conditioning system.

## 2. Breakdown of power consumed by air conditioning system, and target for power consumption reduction

### 2.1 Power consumption analysis of system components

The first step to reducing the power consumed by the air conditioning system was to clarify which parts of the system should be improved, so the power consumed by individual components was analyzed. The air

conditioning system of the AIRTREK was used for the analysis. The power consumed by the compressor was measured, as well as the electric power consumed by electrically driven units such as the condenser cooling fan and blower motor. The electric power measurements were converted into alternator load equivalents in order to ensure equivalency of all power consumptions.

An air conditioner bench test system was used for the power measurements. Tests were conducted for various outside air conditions (temperature and humidity) and at different vehicle speeds. Each test condition was assigned an occurrence frequency in order to calculate and compare the power consumption for any season (Fig. 1).

These test conditions and occurrence frequencies were determined based on data such as weather conditions, daily air temperature changes, driving distances and traffic volume by time, for Japan.

Fig. 2 shows a breakdown of air conditioning power consumption. Among the system components, the compressor consumes the largest percentage at 85 % of the total. If the power consumed by the electromagnetic clutch is counted as part of the compressor load, the compressor alone accounts for as much as 90 % of total system power. As the cooling fan operates together with the compressor, its power consumption should automatically be lowered if the compressor's rate of operation is lowered.

The blower motor is the only component whose electric power consumption is independent of the compressor operation, suggesting that compressor power must be reduced in order to save power in vehicles using an air conditioning system.

### 2.2 Setting of targets

Based on the above power consumption analysis of system components, an examination was conducted

\* Mitsubishi Motors R&D of America

\*\* Interior Design Dept., Development Engineering Office

\*\* Function Testing Dept., Development Engineering Office

\*\*\* Mitsubishi Heavy Industries



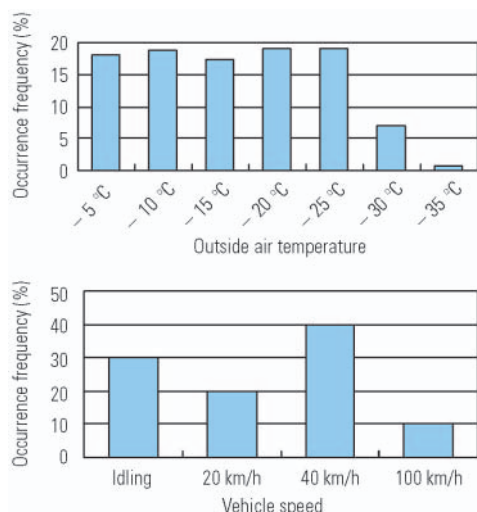


**Fig. 1 Occurrence frequencies of outside temperature and vehicle speed**

seeking for methods to reduce the power consumed by the compressor which accounts for the majority of the system power, using the OUTLANDER's air conditioning system. The development target was to reduce the power consumption of this system to 30 % lower than that of AIRTREK's system.

We focused on improving the efficiency of the compressor for reducing its power consumption and also reducing the rate of operation of the compressor (including the electromagnetic clutch and cooling fan).

### 3. Study for reducing compressor power consumption

#### 3.1 New scroll compressor

MHI has developed a new type of next-generation compressor for improved refrigerant compressing efficiency, so we decided to use this compressor. This new compressor features a three-dimensionally designed special scroll shape for higher compression efficiency. This compressor also has an oil separator function for improved heat exchange efficiency. This compact, lightweight compressor reduces the overall weight and thus saves fuel.

The new compressor has almost the same cooling capability as MHI's MSC105CA compressor, even though it is approximately 10 % shorter in overall length and 30 % lighter (Table 1).

#### 3.2 Study for power saving by improved control (reduction in compressor's rate of operation)

The compressor is controlled based on such parameters as the temperature of the air after passing through the evaporator to prevent water condensate in the evaporator from freezing. When the outside air temperature is so low that not much cooling is required, the air taken into the system does not need to be cooled to the limit, so the control temperature may be set above the freezing temperature and this reduces the compressor's rate of operation.

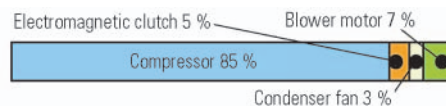


**Fig. 2 Breakdown of system power consumption**

**Table 1 Characteristics of new compressor**

	New compressor	Current MSC105CA
Overall length	174 mm ( $\Delta$ 18 mm)	192 mm
Weight	4.0 kg ( $\Delta$ 1.8 kg)	5.8 kg

The original control logic used in the OUTLANDER's system has the highest control temperature set taking odor and defogging performance into account. To review this temperature limit setting, an investigation was conducted to know occupants' feelings and defogging conditions when using actual vehicles.

The results showed that a temperature approximately 4 °C higher than the highest control temperature of the OUTLANDER's system did not affect the occupants' degree of comfort or defogging performance. The results also showed that raising the control temperature beyond this temperature caused occupants to become sensitive to the odor, which was likely attributable to temperature variations and humidity changes caused by ON-OFF switching of the compressor, thus preventing the system from maintaining comfortable conditions.

Based on the results of the investigation, a new power saving control logic having the characteristics shown in Fig. 3 was adopted by changing the highest control temperature setting.

### 4. Power consumption measurement of air conditioning systems

The annual compressor power consumptions were measured for the AIRTREK's system, the original OUTLANDER's system, the OUTLANDER's system incorporating the new compressor, and the OUTLANDER's system with the new compressor plus the new power-saving control logic to verify the power saving performance of the last system (improved MAC system).

When these measurements are compared, the compressor of the original OUTLANDER's system annually consumes approximately 35 % less power than that of the AIRTREK's system; replacing the compressor of the original OUTLANDER's system with the new compressor further reduces the annual power consumption by approximately 7 %; when the OUTLANDER's system with the new compressor is controlled using the new power saving control logic, the annual power consumption is further reduced by approximately 18 % (Fig. 4). Overall, the combined effect of the new compressor and the new power saving control logic reduces the com-

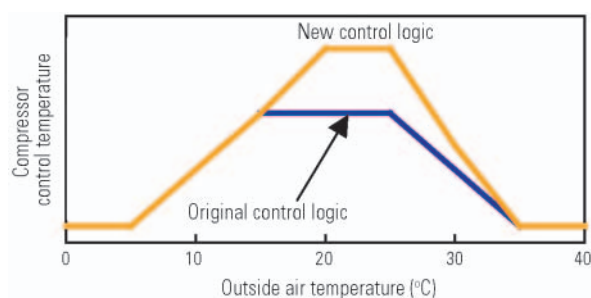


**Fig. 3 Compressor control temperatures (vs. outside air temperatures)**

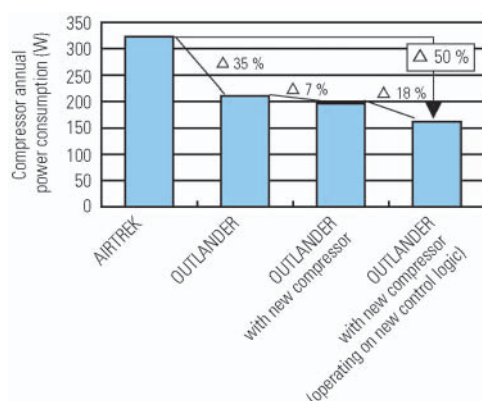


**Fig. 4 Comparison of annual total power consumed by compressor**

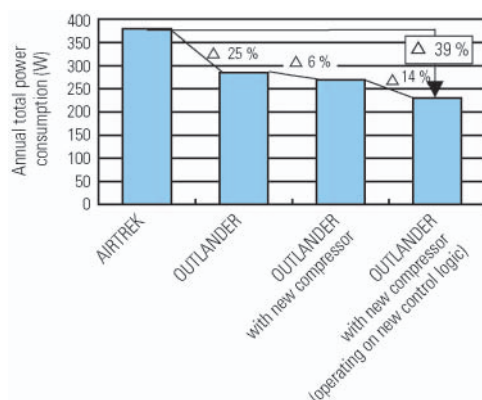


**Fig. 5 Comparison of annual total power consumed by MAC system**

pressor's annual power consumption by approximately 50 % compared with the AIRTREK's system.

**Fig. 5** compares the four air-conditioning systems in terms of the annual total power consumption obtained by calculating power consumptions of the cooling fan, etc. based on the annual power consumption by the compressor described above. As noted, the annual total power consumption of the original OUTLANDER's system is approximately 25 % lower than the AIRTREK's system; it is further reduced by approximately 6 % by the new compressor and by a further 14 % thanks to the new power saving control logic. The overall reduction

**Table 2 Average vehicle speed**

	Traffic jam	Urban road	Highway
Average vehicle speed	11.4 km/h	44.4 km/h	77.4 km/h

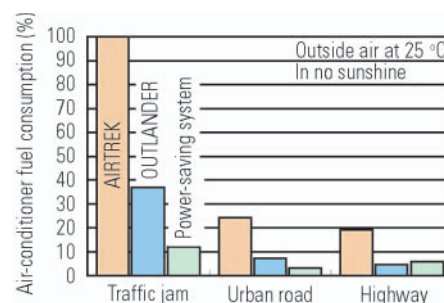


**Fig. 6 Comparison of fuel consumption of MAC systems**

in total power consumption compared with the AIRTREK's system is some 39 %, exceeding the 30 % target set at the beginning of the development<sup>(1)</sup>.

## 5. Measurement of actual fuel consumption

To verify the effect of the improved MAC system on the actual vehicle fuel consumption, a test was conducted on a chassis dynamometer to measure the fuel consumption.

Since it was impractical to exactly simulate the fuel consumption throughout the whole year on a chassis dynamometer, the test was conducted assuming conditions of an outside air temperature of 25 °C and no sunshine. Also, an operation pattern was assumed for the test, simulating three different traffic conditions, i.e., congested traffic, urban road driving and highway driving, to compare vehicle fuel consumptions with and without the air conditioning system in use. **Table 2** shows the average vehicle speeds when driving under the individual traffic conditions.

**Fig. 6** compares the fuel consumptions of the three air-conditioning systems under the three traffic conditions, assuming the fuel consumption of the AIRTREK's system under traffic jam condition as 100 for reference.

The fuel consumption of the OUTLANDER's system is 40 % lower than the AIRTREK's system. The fuel consumption of the improved MAC system incorporating the new compressor and control logic discussed in this paper is small, indicating that the influence of the use of this system on fuel economy is significantly small.

For highway driving, however, fuel consumption of the improved MAC system is a little higher than the original OUTLANDER's system. Although this difference is considered insignificant as there is little difference in vehicle fuel consumption at high vehicle speeds between using and not using the air conditioning system, further analyses will be conducted.

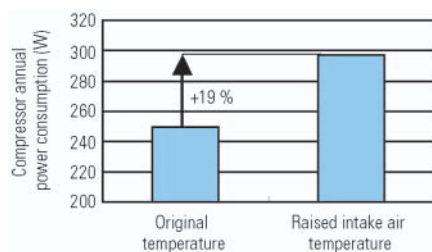


**Fig. 7** Impact of intake air temperature on annual total power consumption

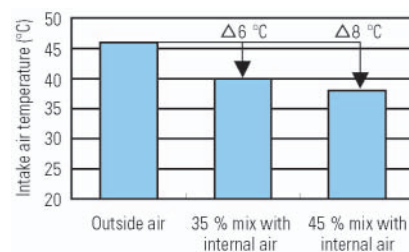


**Fig. 8** Effect of mixing inside air with introduced outside air

## 6. Future challenges

The temperature of the air taken into the air conditioning system has a significant influence on the compressor's power consumption and rate of operation.

Since the system intake air is mixed with the engine compartment air through a cowl-top drain hole and directly heated in the cowl-top, its temperature is higher than the outside air temperature. Especially during idling, the system intake air is more than 10 °C higher than the outside air, increasing the air conditioning system load and thus worsening the vehicle fuel consumption. If the system intake air temperature is lowered to around the outside air temperature, the compressor's power consumption and rate of operation can be significantly lowered, particularly in a traffic jam.

**Fig. 7** shows the results of a simplified bench test to examine the influence of the temperature of the system intake air on fuel consumption. The bench test used the OUTLANDER's system and measured the annual total power consumption of its compressor by raising the system intake air temperature from below 25 °C by 10 °C during idling and by 5 °C when driving at 20 km/h. These limited changes in condition resulted in a major power increase of about 19 %.

One way to reduce the system intake air temperature is to mix it with part of the inside air. **Fig. 8** shows a study on the effect of such air mixing.

When the intake air contains 45 % inside air, the temperature will be approximately 8 °C lower than the original temperature. Mixing with more inside air may increase the concentration of CO<sub>2</sub> in the cabin air.

The structure of the vehicle body needs to be studied further to lower the temperature of the system intake air and the effects of available methods should be clarified.

## 7. Conclusions

The improved MAC system which was developed to reduce the power consumed by the air conditioning system successfully achieved a 30 % reduction in annual total power consumed by the air conditioning system by using MHI's new compressor and revising the compressor control temperature logic.

For saving air-conditioning power, in addition to the successful improved MAC system, there are many areas remaining both in control method and vehicle body structure that can be improved without compromising comfort. To reduce the actual vehicle fuel consumption which is of growing interest to users, MMC will continue work on suppressing air-conditioning power consumption.

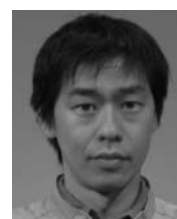
Finally, we thank MHI and MMC staff for their cooperation in the studies on air conditioning system power saving.

### Reference

- (1) Hideto Noyama and Kazumi Okinaka: Energy Efficiency Improvement of the MAC system with the New Development Scroll Compressor, presented at the SAE Automotive Alternate Refrigerant Systems Symposium held on June 27 – 29, 2006



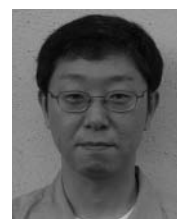
Kazumi OKINAKA



Akihisa YAMATANI



Masaru KADOI



Hideto NOYAMA

# Digital Evaluation Method with VR Technology

Kazushi MAEKAWA\* Masahiro YOSHIDA\*\* Yoshiaki ITO\*\*  
 Michitaka HIROSE\*\* Tomohiro TANIKAWA\*\*

## Abstract

Virtual reality (VR) technology made its debut more than 40 years ago, but it is only in the last decade or so that businesses, persuaded by the rapid advance of computer technology, have begun to seriously tap into the technology's potential in product development.

VR technology is considered capable of handling phenomena that act on human sensory organs. Therefore, it can be effectively used to develop products whose success depends heavily on sensory evaluation of customers, such as ergonomically designed easy-to-use controls.

Also, VR technology, when combined with physical simulation technology, would make it possible to perform repetitive verification trials in complex and changing external conditions with elements intricately affecting each other and to conduct virtual experiments and analyses based on visualizations of vast amounts of numerical calculations. This will lead to innovative product development techniques.

This presentation describes the application of VR technology that we undertook, namely the ergonomic verification as a part of packaging development, which is the basis of vehicle development, and the prediction of flow field in aerodynamic development that affects exterior styling. These efforts were supported by advice from Professor Michitaka Hirose and Lecturer Tomohiro Tanikawa, both from the University of Tokyo and authorities on VR technology with numerous academic achievements in the field.

**Key words:** *Visibility, Driving Simulator, Computer Graphics (CG), Aerodynamics, Computational Fluid Dynamics (CFD)*

## 1. Introduction

Initially a technology for drawing, computer graphics have evolved sufficiently to enable any optical phenomena in the real world to be simulated (Fig. 1). Based on this image processing technology, VR technology has been developed to achieve synthesis with the real world.

There are numerous types of image processing tools and software that could be categorized as VR technology in the broad sense of the term, so we decided to carry out our study in a clearly defined environment.

The goal of this study was to establish a method for dynamic simulation and sensory evaluation corresponding to real test driving. We therefore defined "VR technology" as that having the following image processing functions.

- (1) Function of visualization for three-dimensional stereovision
- (2) Function of own-self inspection in full scale corresponding to real test driving
- (3) Function of real-time display and adjustment for evaluation

In line with this goal, we chose to study an immersive multi-projector display based on IPT (Immersive Projection Technology) which produces wide-field, high-resolution interactive images. Specifically, we

were kindly permitted to use the following equipment:

- SCABIN (Small CABIN): Installed at the Hirose-Tanikawa Laboratory of the University of Tokyo. (Fig. 2).
- CABIN (Computer Augmented Booth for Image Navigation): Installed at Intelligent Modeling Laboratory (IML) of the University of Tokyo (Fig. 3).

## 2. Utilization of VR for Package Engineering

### 2.1 Background and issues

In the 1990s, digital tools for vehicle development were widely used for a range of structural analysis and product design, primarily for numerical verification.

In comparison, verifications in sensory areas were conducted solely with physical models, and simulations of moving objects were carried out only after a test vehicle had been fabricated.

Efficiency and frontloading in development processes have been improved thanks to advanced computer technology. However, technology has not been widely used to judge product viability, because technology proposals may differ from the real product due to insufficient display accuracy and presence. Nevertheless, evaluations using physical models or test vehicles make it difficult to improve merchantability and to reduce the number of test models and vehicles. Therefore, it is

\* Package Engineering Dept., Development Engineering Office

\*\* The University of Tokyo

\*\* Function Testing Dept., Development Engineering Office



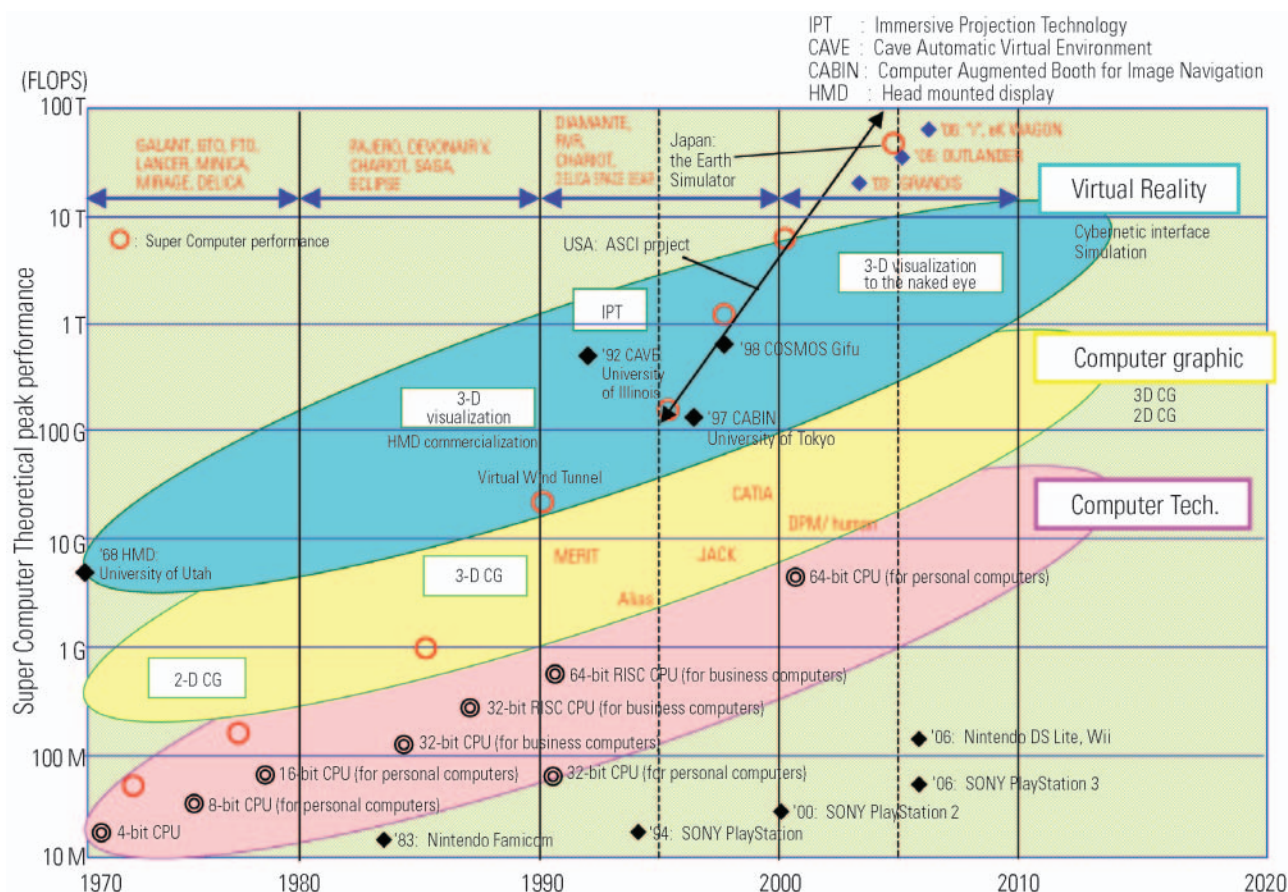


Fig. 1 Development of digital technology and VR



Fig. 2 SCABIN

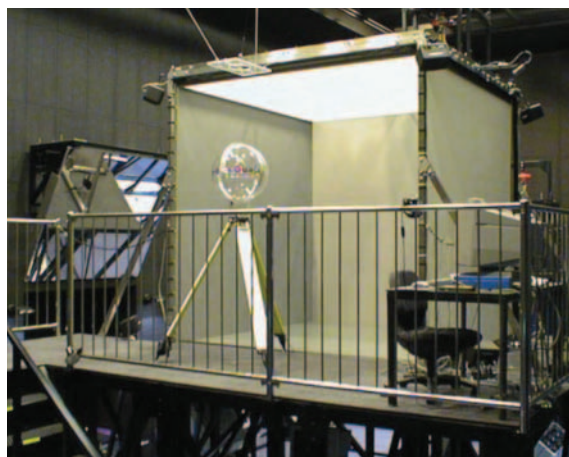


Fig. 3 CABIN

necessary to perform the sensory and dynamic (equivalent to test driving) verifications from the stage of producing design data, and to address such barriers to development. This is where VR technology is useful.

## 2.2 Assignment

We made our target as "Development of Simulation Method for Preventing Sight Hindrance of the Driver." Specifically, we aimed to construct a visual simulation

system using VR technology corresponding to real test driving (for direct and indirect sight simulation on urban road, winding road and free way) to explore the additional technical factors and output affecting the simulation method.

### 2.2.1 Construction of visual simulation system by using VR technology corresponding to real test driving

A simulator based on a test vehicle was developed for visual simulation using VR technology.



Fig. 4 Full-scale driver's seat model

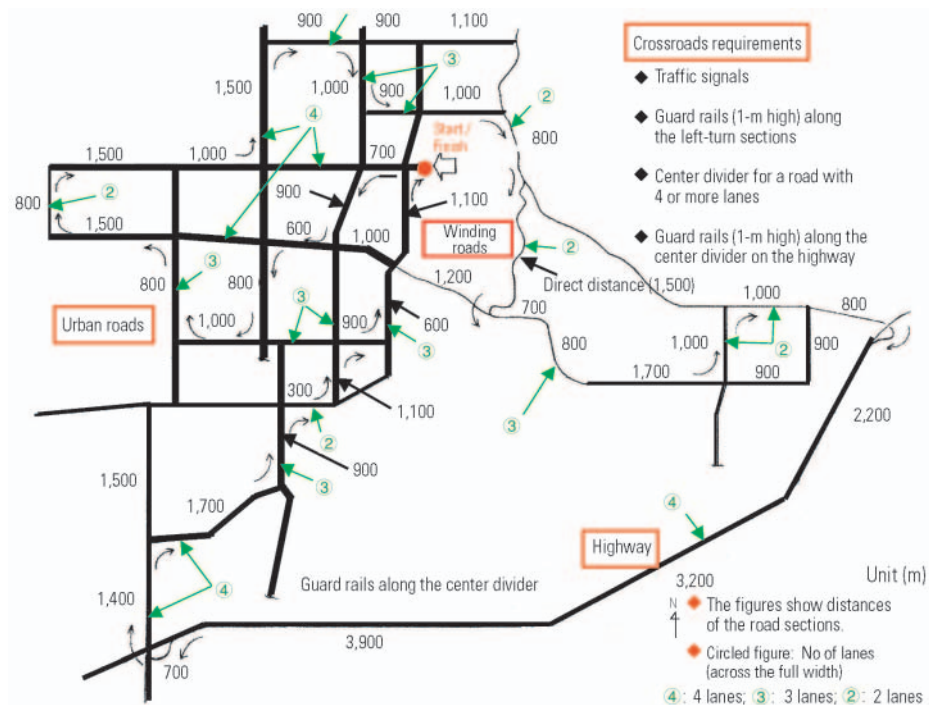


Fig. 5 Driving test course

(1) The setting of driving position

A full-size driver's seat model was developed and outputs from the accelerator pedal, brake pedal and steering wheel were loaded into a personal computer. The data were then transferred to a VR imaging system. The seat adjustable range was set up to correspond to those of minicar and ordinary vehicles (Fig. 4).

(2) The setting of VR display items

The following four items were incorporated into the VR imaging system to create a driving environment for the sight verification simulation.

- ① The environment of driving test course: A driving test course corresponding to real test driving was set up (Fig. 5).

- ② The traffic environment: Traffic patterns on every section of the test course were established based on videos that had been shot of an actual vehicle driving the course. The patterns included oncoming vehicles, pedestrians and vehicles that suddenly come out into the way (Fig. 6).

- ③ Vehicle kinematic performance: Vehicle kinematic performance on turns that correspond to real test driving was programmed in the simulation.

- ④ Display: Information available to the driver was set up (speed, reference distance, and test course navigation).

To display real-time imaging of the above items, a

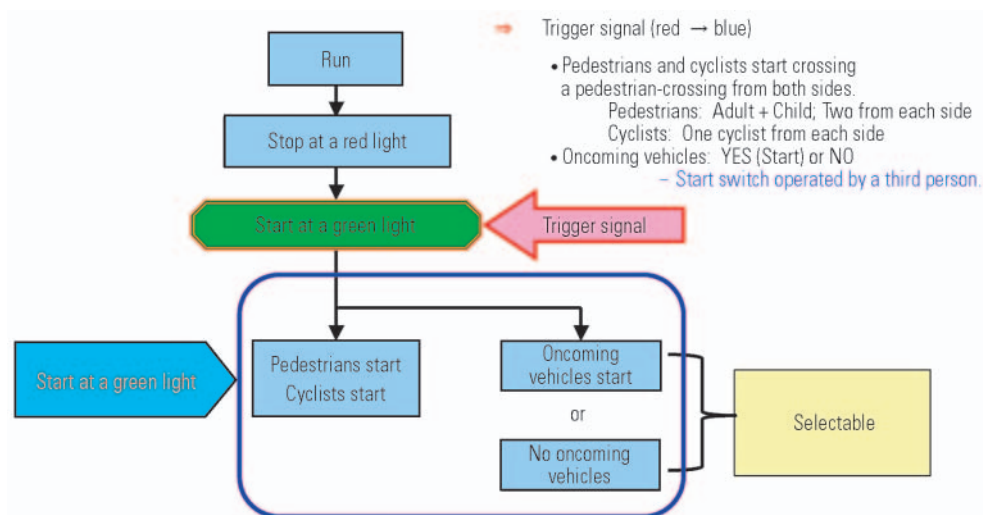


Fig. 6 Traffic pattern (e.g. Flowchart at the time of turning right)

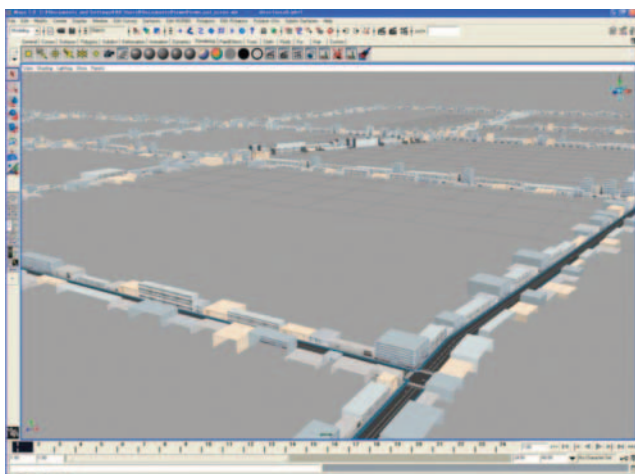


Fig. 7 3-D urban road model data in the VR space

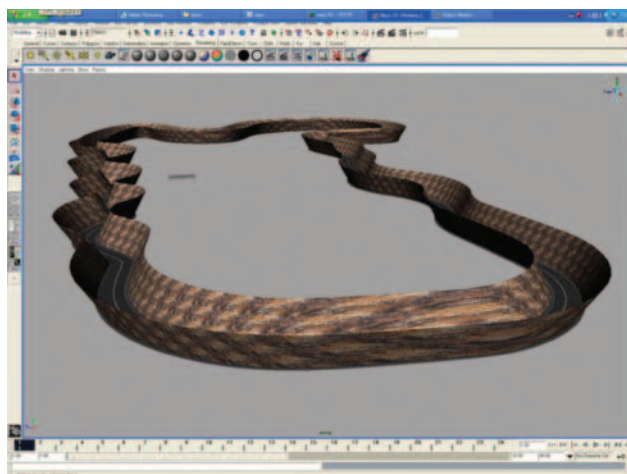


Fig. 8 3-D winding road model data in the VR space

three-dimensional (3-D) space model was developed that accommodated the imaging machine's computing performance limitations (Fig. 7 and Fig. 8).

### (3) VR imaging system

The SCABIN is a cubic display device of approximately 2-m side length. It has three screens, one in front, another on the right-hand side, and a third on the bottom. Three-dimensional stereovision images are projected from the projectors onto the backs of the front and RH side screens while a third projector located above and forward projects images down onto the bottom screen. It has a maximum angular field of display of 158°.

The CABIN is a five-screen cubic display device of approximately 2.5-m side length. In addition to the screens in front, on the right-hand side and on the bottom, it also has top and left-hand side screens. Images are projected onto the backs of all of the screens, which makes the entire facility fairly large, measuring 11 m (overall length) x 7.9 m (overall width) x 7.3 m (overall

height). It has an angular field of display of 270°, which should be enough for image reproduction seen from the driver's seat.

Inputs from the sensors on the accelerator pedal, brake pedal and steering wheel are converted into the corresponding values of movement. Based on these values, the VR imaging system projects the next image frames onto the screens.

Using liquid crystal shutter glasses, the driver can see the projected image stereoscopically. This is made possible by synchronizing the changeover of the right-eye image and left-eye image on the screen with the alternate release of the right and left shutters of the glasses using the infrared rays from the IR emitter installed at the image presentation area.

On the glasses, a three-dimensional electromagnetic position sensor is also installed to track the wearer's eye point so that stereovision images presented to the wearer follow his/her movement.

By integrating items (1) to (3) described above, we





Fig. 9 VR test driving: Panoramic view at right turn

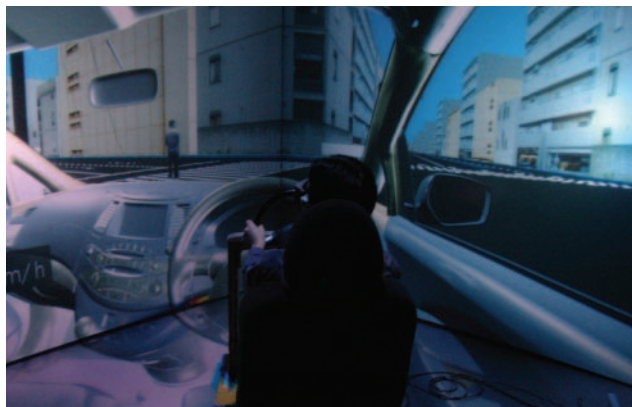


Fig. 11 VR test driving: Panoramic view at left turn



Fig. 10 VR test driving: Driver's view at right turn



Fig. 12 VR test driving: Driver's view at left turn

constructed a VR environment corresponding to real test driving.

### 2.2.2 VR imaging system operation

The driver wears the aforementioned glasses and sits in the driver's seat. The driver then adopts his/her preferred driving position and starts driving just as if driving a real vehicle.

Image data items of "driving test course environment," "traffic environment" and "vehicle kinetic performance" are converted into stereovision-enabled data before being projected onto the screens.

This enables the driver to drive the test vehicle along the driving test course freely as if actually driving a real vehicle in an VR environment corresponding to real test driving. Examples of the VR test driving are shown in the following figures.

- (1) VR test driving: Right turn at the urban crossroad (Fig. 9 and Fig. 10)
- (2) VR test driving: Left turn at the urban crossroad (Fig. 11 and Fig. 12)
- (3) VR test driving: Winding road (Fig. 13 and Fig. 14)

## 2.3 Evaluation result

By using the VR imaging system, the following

results were obtained.

### 2.3.1 Required environment for evaluation

- (1) Relative comparison evaluation in VR space is possible by calibrating the road and traffic environment to real test driving.
- (2) The VR space needs to be constructed with many different elements so as to sufficiently resemble the real world. To achieve this, image processing should use photographed images as much as possible.
- (3) It is important to incorporate moving human figures in the VR space to offer the feeling of being at the scene.

To achieve human figure representation as close to live humans as possible, a method using a video avatar capture system was adopted. This system, designed to incorporate various real-world objects into a VR space, has a total of 18 CCD cameras arranged at 20° intervals around the 360° circumference of a cylinder with a blue background inner wall (Fig. 15 and Fig. 16). In our study, live-action videos of real humans were shot, which were then projected in the VR space as pedestrians.

- (4) The system can store and reproduce the driving



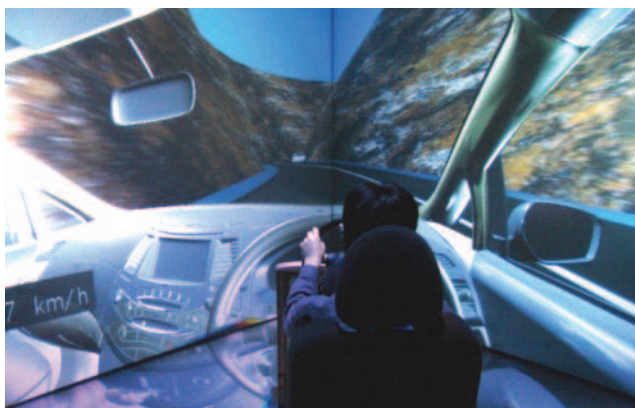


Fig. 13 VR test driving: Winding road – 1



Fig. 14 VR test driving: Winding road – 2

paths and eye movements of a number of drivers. A person can experience various eye movements of persons of different build, fields of view of different age, and different eyesight.

- (5) The simulation clarified the mutual relation between reality and VR images concerning distance and precision. A real 1 m-long rod and a virtual 1 m-long rod produced by CABIN were compared to verify whether the projected data agree with the dimensions in the real world. From the view point of the driver, they agreed with each other completely (Fig. 17).
- (6) A meteorological influence function (for any given region, time and weather) will need to be added to help improve the accuracy of the reproduced environment corresponding to real test driving.
- (7) A sound effect function will need to be added as vision can be influenced by sound.

### 2.3.2 Function of VR imaging system

- (1) The immersive multi-projector display based on Immersive Projection Technology (IPT) has boundaries of illuminance between adjoining screens. The boundary and its impact on sensory evaluation will need to be clarified.
- (2) To offer real-time display, the level of computational complexity that can be processed by the imaging



(a) External view

(b) Internal view

Fig. 15 All-around capture system for video avatar

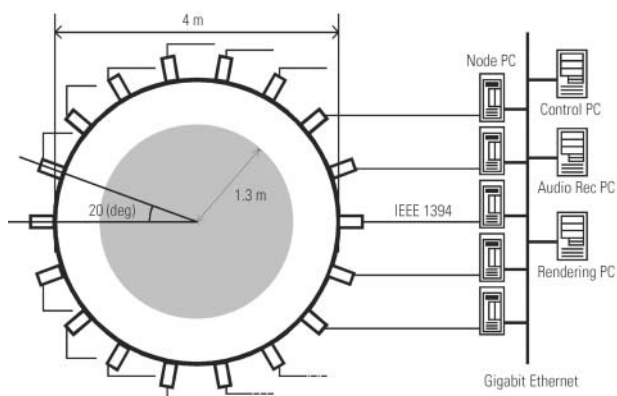


Fig. 16 All-around capture system layout for video avatar

machine will need to be respected.

The relationship between the data capacity that produces the feeling of being at the scene and the performance of the imaging machine will need to be clarified.

- (3) When modeling simulated objects (pedestrians, etc.), it will need to be clarified whether it is shape or movement that the driver recognizes.

## 3. Utilization of VR for Aerodynamics

### 3.1 Background and issues

Today, global warming has become an urgent issue for humankind, and the auto industry is being urged to reduce the running resistance of vehicles and improve fuel economy, thereby cutting carbon dioxide emissions. Air drag accounts for a majority of the resistance of a vehicle moving at high speed, so it is important to reduce the air drag coefficient ( $C_D$ ) of the vehicle.

In order to reduce the  $C_D$  of vehicles, auto manufacturers have been working hard to aerodynamically improve the body shape even before prototypes are completed, by conducting wind tunnel experiments using scale models and through computational fluid

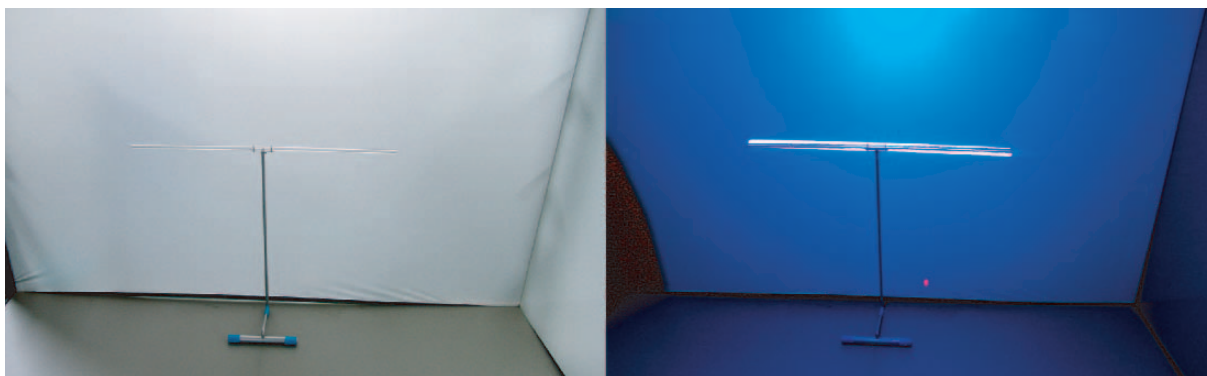


Fig. 17 Verification of VR display accuracy

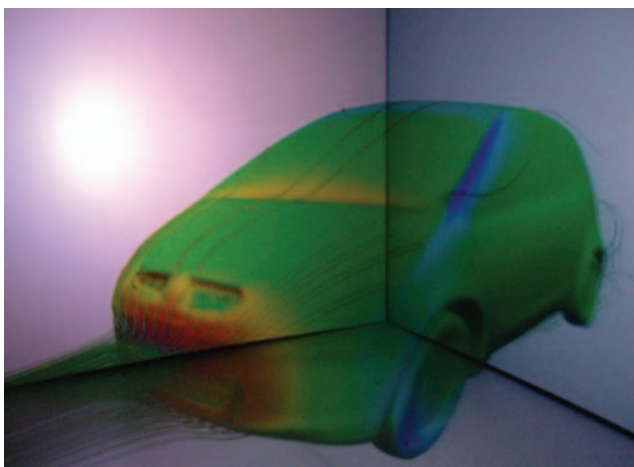


Fig. 18 Display of CFD analysis result in VR space  
(The particle path around the vehicle)

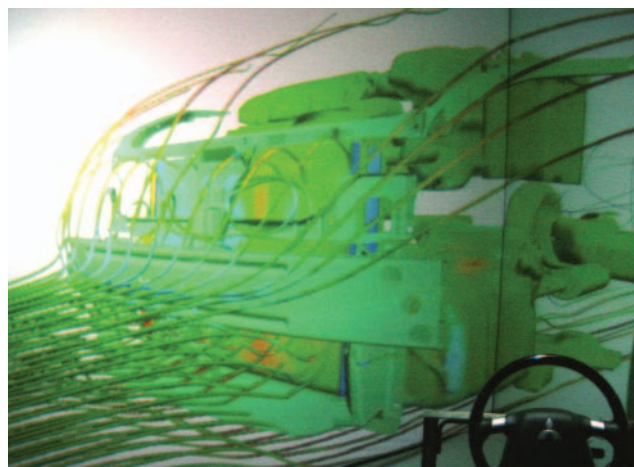


Fig. 19 Display of CFD analysis result in VR space  
(The particle path in the engine compartment)

dynamics (CFD) simulations. And yet as auto manufacturers must still promptly release products that meet diversifying market needs, the development time needs to be reduced significantly. Digital systems such as CAD and CFD have thus become indispensable for vehicle development.

In aerodynamics-related development, VR technology is expected to offer clearer insight into various aerodynamic phenomena on prototype vehicles before they are actually made and to help identify potential problems swiftly so that important decisions on improvements can be made faster.

In addition, VR technology is expected to help engineers make their ideas more specific through visualization and to present their ideas to the relevant people.

### 3.2 Visualization of CFD analysis result in VR space

Fig. 18 and Fig. 19 show SCABIN displays (See 2.2.1 (3)) of CFD analysis results factoring in cooling air into the engine compartment. This modeling enables diagnoses of whether the opening areas for cooling in the front bumper are at appropriate positions and whether there is an efficient flow rate of cooling air to the radiator.

The body model shown here is a polygonized model of the one used in CFD analysis, and the shape has been somewhat simplified. Some of the parts in the engine compartment are, however, polygonized based on CAD data, which is more detailed than CFD data models. This combination of CFD data models and CAD data models enables a more realistic analysis.

In VR space, the display scale is adjusted so that the image of the vehicle is in the same size as seen in the real world. Flow fields such as particle path and pressure distribution on the surface of the vehicle seen through liquid crystal shutter glasses are surprisingly as realistic as in the real world. In addition, as three-dimensional position sensors installed on the glasses keep track of the wearer's head position and direction of gaze, the wearer's vision changes whenever moving his/her head, just like in the real world. This enables the wearer to observe the flow field change while looking into the engine compartment or looking up at the bottom of the vehicle from under, just like on a real vehicle (Fig. 20). While two-dimensional images displayed on a CRT monitor can still allow sufficient understanding of equivalent three-dimensional flow, the VR space offers a very different level of reality compared to two-

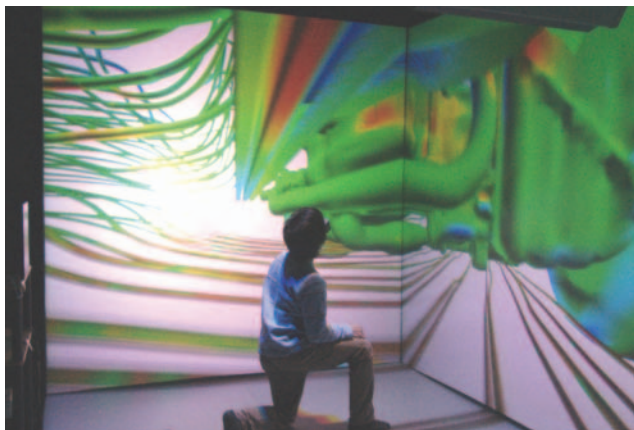


Fig. 20 Observation of CFD in VR space

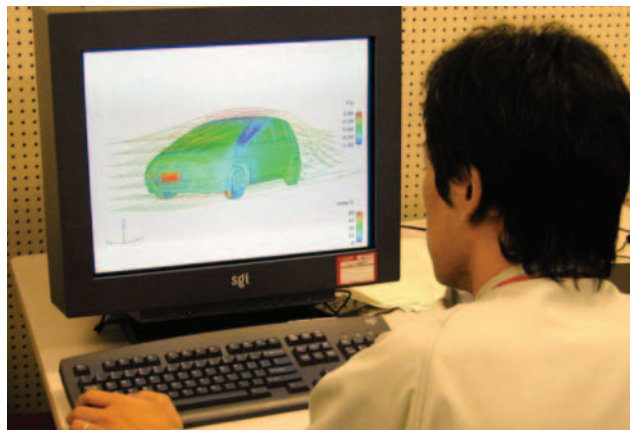


Fig. 21 Normal CRT monitor display

dimensional images (Fig. 21). This feeling of reality appears to be closely related to the synchronization of bodily movement with visual change.

### 3.3 Outlook for the future

In our study, analysis results that had been computed earlier were then visualized in the SCABIN. In a design process, however, there should be on-the-spot feedback and an understanding of how changes made to shape parameters alter the flow field. Immediate results should help in more intuitive understanding, and correction if needed. Currently, fluid analyses typically require several hours of computation to obtain results. Ultimately, this should be improved so that any corrections made on the spot to aerodynamic analysis results will immediately be reflected in subsequent images.

## 4. Conclusion

In this paper, we started out by defining VR technology based on the currently available knowledge about existing technologies and then looked into ways to use VR technology in digital evaluation by package engineers. VR technology continues to evolve, so we will flexibly choose themes for future study even if the scope of study goes beyond the definitions established earlier.

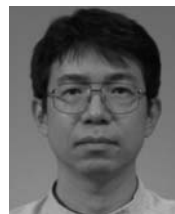
Our advisers, Professor Michitaka Hirose and Lecturer Tomohiro Tanikawa, both of the University of Tokyo, have pointed out that the scope of application of our study should be extended beyond the physical and

technical fields to include psychology and cognitive science. It has also been shown that, in expanding our study into active safety and function prediction, it will be necessary to develop innovative methods not based on conventional ideas.

Finally, we would like to thank Professor Michitaka Hirose and Lecturer Tomohiro Tanikawa, both of the University of Tokyo, and the staff of their laboratory; Mitsubishi Motors staff who helped to produce the study data; and everybody at UT Research Institute for helping to make this joint study possible.



Kazushi MAEKAWA



Masahiro YOSHIDA



Yoshiaki ITO



Michitaka HIROSE



Tomohiro TANIKAWA



# Quick Heating Rear Heater System for the New DELICA D:5

Motoaki SUGIHARA\* Takahide YAMAMOTO\* Tomonori HARADA\*  
Tomio KIMURA\*\* Hiroki SETO\*\* Fumihiko HONMA\*\*

## Abstract

Comfortable and quick heating from the heater is demanded by every vehicle occupant regardless of seating location. The Quick Heating Rear Heater System developed for the New DELICA D:5 uses a positive temperature coefficient (PTC)<sup>(Note)</sup> heater with excellent quick-heating characteristics. The PTC heater is integrated in the heater duct that runs from the 1st to 3rd rows in order to offer comfortable warmth to every seat. This PTC heater has enabled the heater unit to be made smaller and so installed underfloor (under-carpet), for an interior layout with no compromise on space. The system is also cost-effective. This paper outlines the technical features of the Quick Heating Rear Heater System.

**Note:** The PTC heater automatically regulates its heating power (self-temperature control capability). It increases thermal output when the ambient temperature is low and limits the heating power at higher ambient temperatures.

**Key words:** Air Conditioning, Heater, Control, Blower, Temperature, PTC

## 1. Introduction

Conventional rear heater systems typically come as either a "hot water system" (Fig. 1 (a)) or a "full-duct system" (Fig. 1 (b)). The hot water system provides rear heating by circulating heated engine coolant through a heater core located in the rear section of the vehicle. The full-duct system supplies warm air delivered from the front heater system through a duct running from the front to the rear while distributing warm air to all foot areas from the 1st-row seats to the 3rd-row seats.

The heating efficiency of the hot water system is very high as long as the engine coolant stays hot enough for heating but it has the following disadvantages:

- Today's high-efficiency engines run with coolant at lower temperatures.
- In low ambient temperatures, the coolant loses its heat as it runs through underfloor piping, which necessitates the system to take longer before it can give off comfortably warm air from the rear heater core.

The full-duct system, on the other hand, costs less since it simply distributes the air heated by the front heater system to all seating places, but it has the following problems:

- Required level of heating to every seating place cannot be assured unless the system has sufficiently large draft capacity.
- Air loses its heat as it flows through the long duct running from the 1st to 3rd rows due to radiation of heat from the duct surfaces. The air temperature, therefore, is cooler at the 2nd-row vents than at the 1st-row vents, and becomes even cooler at the 3rd-row vents.

- Air is distributed to the 3rd-row seating area even when there are no occupants there, wasting heat that could otherwise be used for the 1st- and 2nd-row seats.

Since both types of rear heater systems share the heat source with the front heater system (in the form of heated coolant or heated air), their heating performance for different seating places is affected by change in engine coolant temperature, the system's draft capacity, and the balance of distributed air to different seating places.

## 2. Solution to the problems in the conventional systems

The new rear heater system was developed to solve the above-mentioned conventional systems' problems and is basically a less costly full-duct system but incorporates a PTC heater and a shutoff door, and so offers better rear heating performance and functionality than conventional full-duct rear heater systems (Fig. 1 (c)).

### 2.1 Increase in airflow to foot areas and determination of airflow distribution to seating places

#### 2.2.1 Increased airflow to foot areas

The front heater system of the New DELICA D:5 was developed assuming shared use with the OUTLANDER. For its application to the New DELICA D:5, it was necessary to raise the airflow to foot areas to a level high enough to assure sufficient volume of warm air to the 3rd-row seats while ensuring sufficient airflow to the 1st- and 2nd-row seats, so the target airflow to foot areas for the New DELICA D:5 was set at least 10 % higher than that for the OUTLANDER. Reduction in airflow resistance of the foot ducts and rear heater duct

\* Interior Design Dept., Development Engineering Office

\*\* Function Testing Dept., Development Engineering Office



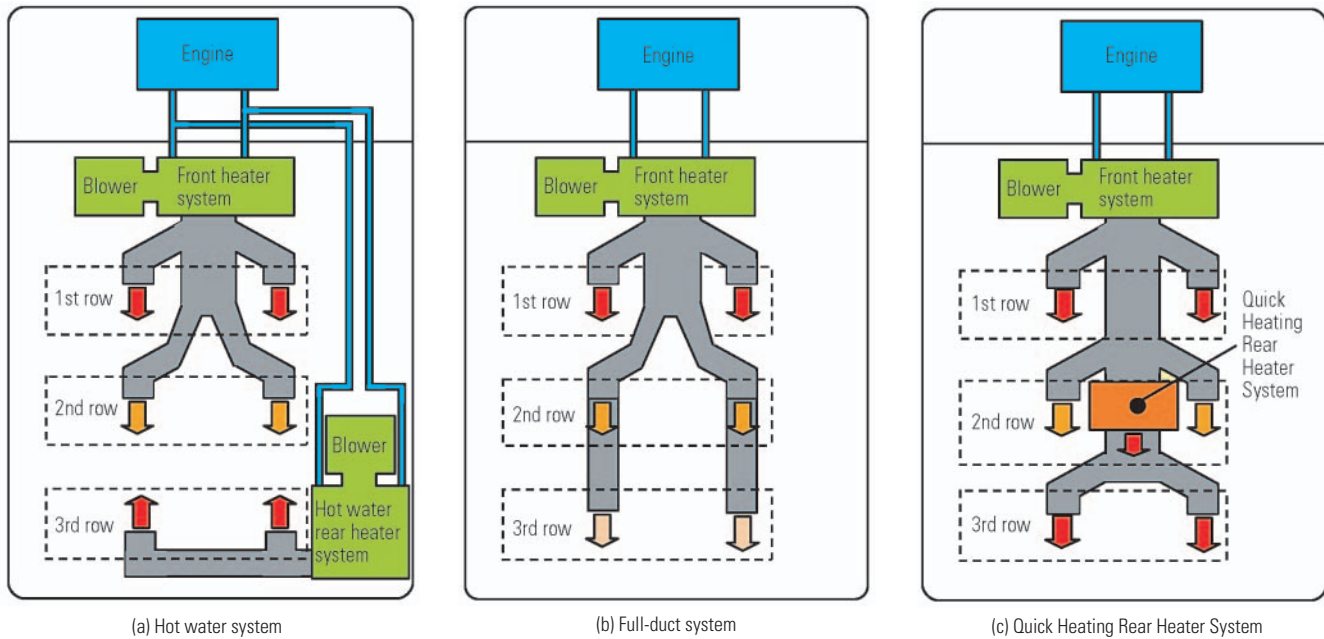


Fig. 1 Heater systems

was selected as a strategy for achieving the target. First, airflow resistance matching the target airflow level was estimated based on characteristics data of the front heater blower (Fig. 2) and then a CAE analysis was conducted on the foot and rear heater ducts as part of the study for determining the duct layout. Using the data derived from the above, fine-tuning was carried out for the required duct cross-sectional areas and duct branching profiles. These efforts successfully achieved the target airflow resistance.

### 2.2.2 Determination of airflow distribution to seating places

When determining the factors for airflow distribution to different seating places, the target was to ensure that the occupants in every seat could feel the same level of warmth. As a result of tests conducted on airflow distribution including benchmark testing compared with several competing one-box vehicles, the target factors of airflow distribution to foot areas were determined as 4:3:3 for the 1st-, 2nd- and 3rd-row seats, respectively, in consideration of the requirement to supply ample airflow even when the blower is set at the low-speed position.

In addition to the CAE analysis of airflow resistance described above, another CAE analysis was conducted on air vent size and duct branch location. Application of the analysis results enabled the target airflow distribution ratio to be achieved (Fig. 3).

## 3. Outline of the quick heating rear heater system

### 3.1 Incorporation of the shutoff door

Conventional full-duct systems blow warm air through the 3rd-row vents whenever in operation even when there are no occupants there. This wastes heat

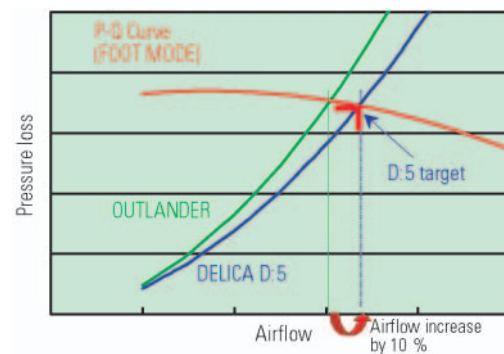


Fig. 2 P-Q curve and duct pressure loss

that could otherwise be used for the 1st- and 2nd-row seats. The new system prevents this loss by means of a shutoff door provided in the rear heater duct (Fig. 4). The door closes the duct to stop airflow to the 3rd-row seats when they are not occupied, thus making the entire airflow available to the 1st- and 2nd-row seats.

### 3.2 Heater control from the rear seats

The hot water system controls the rear heating via a switch that is used by rear seat passengers to change the speed of the rear blower. However, this method of controlling heat is not possible with the full-duct system, which has no rear blower. Although rear heating can be adjusted by changing the front heater blower speed, this causes a significant change in airflow to the 1st- and 2nd-row seats. The new system therefore provides a control so the occupants in 3rd-row seats can adjust the airflow by selecting the shutoff door position and blower speed combination as described below.

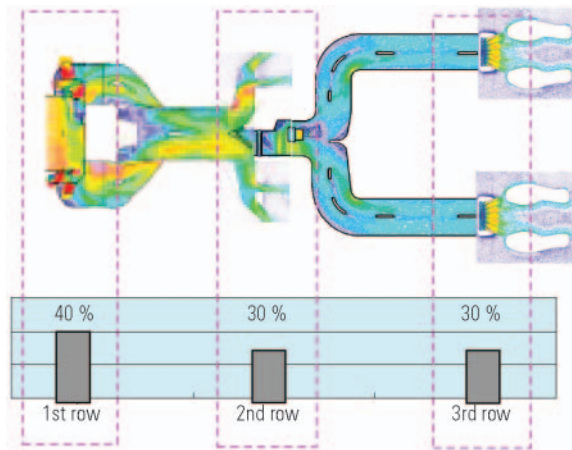


Fig. 3 CAE analysis of airflow distribution through ducts

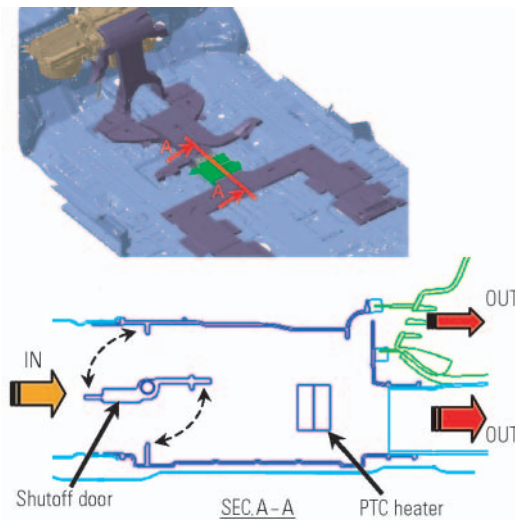


Fig. 4 Quick Heating Rear Heater System

### 3.3 Airflow adjustment

See the airflow adjustment strategy diagram in Fig. 5.

- Operation of the airflow control switch by an occupant in a 3rd-row seat changes the blower voltage of the front heater system, which changes the draft capacity of the heater system.
- Airflow distribution between the 1st/2nd rows and the 3rd row is regulated by the shutoff door in the rear heater duct that operates in coordination with the blower speed position selected by the rear heater airflow control switch as follows: closed in the OFF position; half-open in the Lo and Me positions; fully open in the Hi position.
- The PTC heater operates when the "Me" or "Hi" blower speed is selected by the rear airflow control switch to blow air of a higher temperature than when the "Lo" position is selected.

These strategies give the new system functionality that assures the same level of controllability and comfort as the hot water system. Namely, it is possible to change both the temperature and amount of air to the

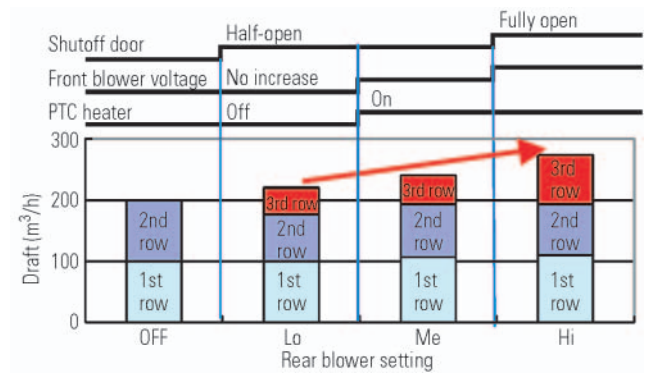


Fig. 5 Airflow control strategies

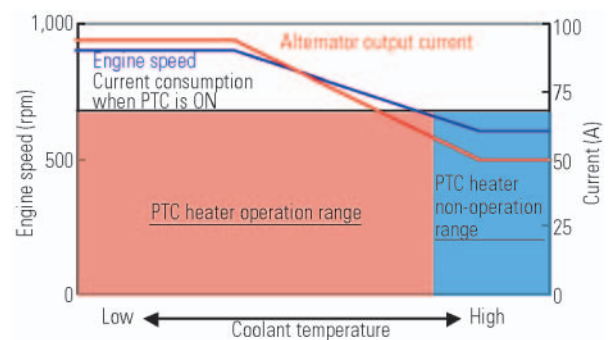


Fig. 6 PTC heater control strategies

foot areas of the 3rd-row seats in multiple steps without compromising heating performance for the occupants of the 1st- and 2nd-row seats.

### 3.4 Control of PTC heater

Under low ambient temperature and consequent low coolant temperature conditions, the PTC heater should run at full power for the quickest heating. However, the PTC heater running at full power draws considerable current, which may affect other devices which consume electric power in the vehicle. To prevent such problems, the range of conditions in which the PTC heater is allowed to operate was established as shown in Fig. 6.

More specifically, some conditions that exist when the vehicle is stationary with the engine idling are excluded from the PTC heater operating range and other conditions are included in the range depending on whether or not the alternator-generated current is limited, using the following criteria:

- At "low coolant temperatures" (and thus quick heating by the PTC heater is necessary), the engine is controlled at a raised idling speed, which means that the alternator assures sufficiently large current for the PTC heater to operate. This condition is included in the PTC heater "operating range".
- At "high coolant temperatures", quick heating by the PTC heater is not needed, as the air from the front heater system is warm enough to heat the inte-

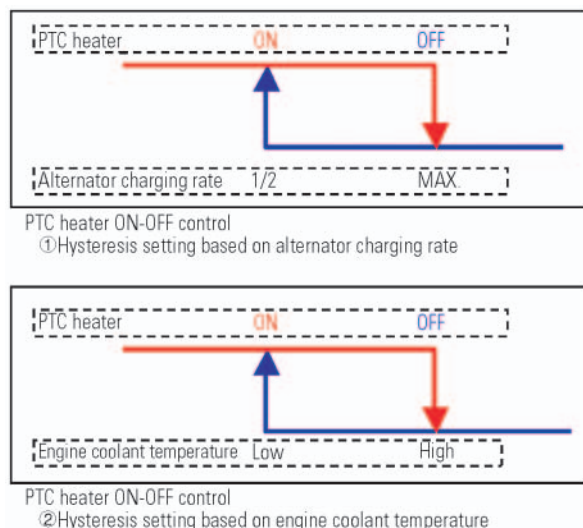


Fig. 7 PTC heater ON-OFF control strategies

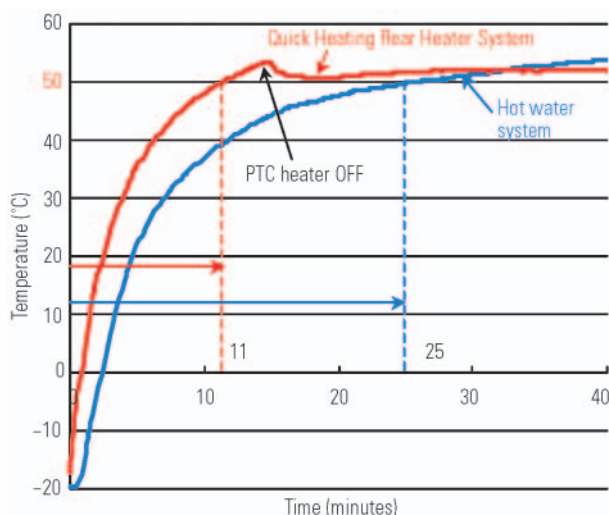


Fig. 8 Rise in air temperature at 3rd-row vents after system startup

rior. The engine, on the other hand, is then controlled at a low idling speed, causing the alternator to generate smaller current. This condition is included in the PTC heater “non-operating range”.

These PTC heater operating and non-operating ranges were adopted as the basis for the PTC heater control, i.e. the PTC heater turns off when the coolant temperature is high or a preset alternator charging rate is exceeded (Fig. 7).

These control strategies enable the PTC heater to operate most efficiently, allowing the heater to turn on under certain alternator output level conditions and to turn off automatically when not needed. Overall, the system consumes less power.

## 4. Evaluation of the system

### 4.1 Results of evaluation tests on actual vehicle

As part of the evaluation tests conducted, the quick

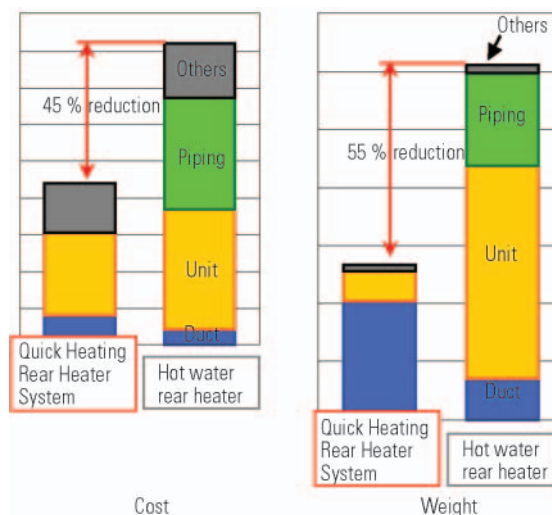


Fig. 9 Cost and weight – Quick Heating Rear Heater System vs. hot water rear heater system

heating rear heater system installed on an actual vehicle was tested to evaluate the rise time of vent air temperature after system startup. The results showed that the system took less time than the hot water system before the outlet air temperature rose to a certain level, meaning that the new system has excellent quick heating performance (Fig. 8).

The test results also proved that the blower speed control allows the desired airflow and temperature to be controlled from the 3rd-row seats without affecting the heating performance for the 1st- and 2nd-row seats. In addition, non-use of the rear blower reduced noise and improved comfort for passengers.

### 4.2 Cost and weight reduction

The new system is 46 % cheaper and 56 % lighter than the conventional hot water system. These reductions were achieved by not using the rear blower and underfloor piping and replacing the hot water heater with the PTC heater (Fig. 9).

## 5. Summary

The Quick Heating Rear Heater System was developed to assure the comfort of every seat occupant and improve the quick-heating performance. It successfully achieved the following:

- By increasing the draft capacity to foot areas and using the shutoff door, multiple-stage control of airflow was possible.
- The PTC heater operating range control system depending on the coolant temperature and alternator output level simultaneously assured the necessary heating performance and reduced the electricity consumption.
- The PTC heater reduced the size and production cost of the heater unit.
- Mitsubishi dealers highly evaluated the quick heating and well-balanced airflow distribution characteristics of the system, which they said were better

than those of the hot water type rear heaters on competing vehicles.

The system will be deployed on other three-row seat models in the future to improve quick heating performance for every seat.

Finally, the authors sincerely thank everyone within and outside Mitsubishi Motors Corporation (MMC) who assisted in the development of the new heater system.



Motoaki SUGIHARA



Takahide YAMAMOTO



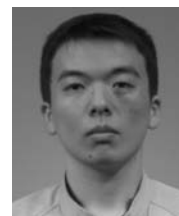
Tomonori HARADA



Tomio KIMURA



Hiroki SETO



Fumihiro HONMA



# Comprehensive ECU Testing Using Simulation Tools

Kunihiro SAKAI\* Yukihiro NISSATO\* Masahiro KANEDA\*

## Abstract

Automotive onboard electronic control units (ECU) need to be exhaustively tested for performance in a dynamic environment corresponding to the actual vehicle-mounted condition before starting mass production. On the other hand, there is a growing need to develop highly reliable software in a shorter time to reduce the development period. To meet these needs, we have introduced the Hardware In the Loop Simulation (HILS) in testing processes.

By implementing a Vehicle model into an HILS environment, it is possible to conduct integrated network testing corresponding to the actual vehicle-mounted condition in a bench test environment. Also, with the automatic test programming software embedded in HILS, it is possible to not only conduct functional testing, but also automatically carry out systematic real-time simulation of troubleshooting on open circuits and other electrical faults as well as abnormal communication.

**Key words:** HILS, Integrated Network Testing, Automatic Test

## 1. Introduction

Electronic control of automobiles using ECUs is becoming increasingly complicated and diverse. Onboard electronic control systems are playing an ever-greater role and this trend is expected to continue. It is therefore imperative to radically improve the efficiency of software verification processes in order to be able to quickly assure the quality of ECU software. This paper describes a HILS-based test environment that we have developed for efficient ECU software verification and validation.

## 2. System architecture

The HILS environment was developed based on the electronic platform of the OUTLANDER and in consideration of future scalability. The OUTLANDER employs more than 20 onboard ECUs, so a total of five racks were prepared and each rack was connected to an ECU being tested (**Fig. 1**). The operating environment for each of these ECUs can be tailored by incorporating an appropriate I/O board and an FIU (Failure Insertion Unit) that generates open and short circuits into the rack. The racks were connected with each other via optical cables, and real-time processors mounted on the racks enabled high-speed communication between the racks. The HILS structure described above represented a virtual vehicle.

The HILS is controlled by a personal computer (PC). Simulation data generated by the control PC are calculated by a processor board on which the vehicle model is embedded, and an I/O board sends and receives signals to/from the ECUs. In this HILS environment, the ECUs operate in the same way as those mounted on a real vehicle, and the operations are monitored by the control PC (**Fig. 2**).

## 3. Features of the HILS

### 3.1 Automatic testing

The greatest benefit of the HILS is automatic testing. Test procedures that have conventionally been performed manually by test engineers are compiled into a program, which can then be run automatically by simply pressing the execute key on the control PC. Automatic testing offers the following benefits.

- Efficient stress test for software
- More efficient analysis
- Application to regression test
- Unmanned long-running test

Software testing requires numerous input/output combinations and precise operating conditions. With the HILS, test programs can be completely sequenced in various ways and so stress tests with complicated subroutines and long-running repetitions can be run automatically and efficiently. Test programs that have been produced are stored in a test-project database and can be retrieved and re-run when needed, which substantially improves the efficiency of related analyses.

When large-scale software has been modified, regression testing must be conducted to find out whether the change may have caused unexpected impacts elsewhere. In this case, test programs managed by HILS can be used to efficiently complete the required regression tests. Numerous test programs need to be run in development projects. As HILS can perform the unmanned long-running testing, it helps minimize the work load on test engineers. The automatic test programming software embedded in HILS allows test engineers to construct complicated sequences on the graphical user interface, and so do not need to write the program code themselves. This also improves testing efficiency (**Fig. 3**).

\* Electronics Engineering Dept., Development Engineering Office



Fig. 1 External view of HILS

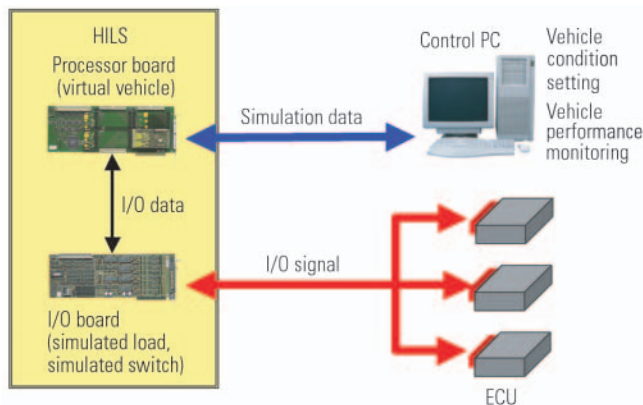


Fig. 2 System overview

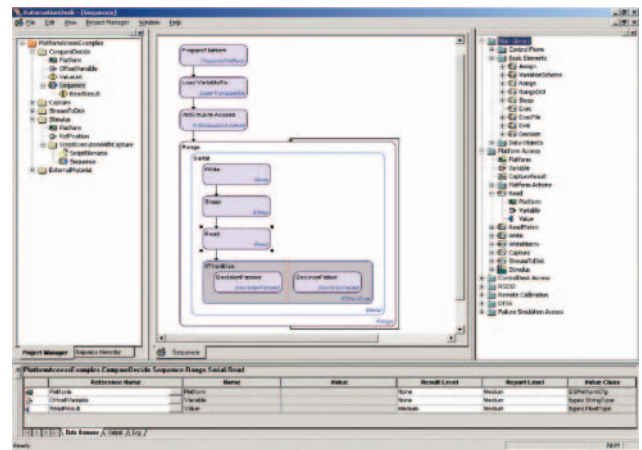


Fig. 3 Automatic test programming software (Automation Desk by dSPACE GmbH)

### 3.2 Supply voltage fluctuation simulation using a power source simulator

ECU faults tend to occur more often during supply voltage fluctuations. To simulate supply voltage fluctuations corresponding to those in a real vehicle, we employed a dedicated power source simulator and linked it with the HILS to generate desired voltage waveforms. This offers a HILS option in which a lot of different supply voltage wave forms can be automatically generated for simulation.

### 3.3 Open/short circuit simulation using FIUs

In recent years, a range of failsafe functions and DTCs (Diagnostic Trouble Codes) have been embedded in ECUs to offer more sophisticated diagnostic capabilities. Therefore, we developed an HILS architecture capable of monitoring ECU operation during fault occurrence and checking for fault codes generated. This was done by incorporating FIUs (Failure Insertion Units) into the HILS. FIUs are capable of automatically

generating electrical faults, such as an open circuit of a signal line and a short circuit to ground or power source (Fig. 4).

To enable fault code monitoring, dedicated diagnostic tool was linked to the HILS, by which fault codes can be read automatically from ECUs.

### 3.4 Communication simulation using CAN gateway

The diagnostic feature embedded in ECUs can detect not only hardware faults but also communication errors. Therefore, it is necessary to check the behavior and fault codes of ECUs when an unusual data is received. For this purpose, a gateway unit was incorporated in the HILS for intentionally altering the data communicated between the ECUs to simulate abnormal communication (Fig. 5).

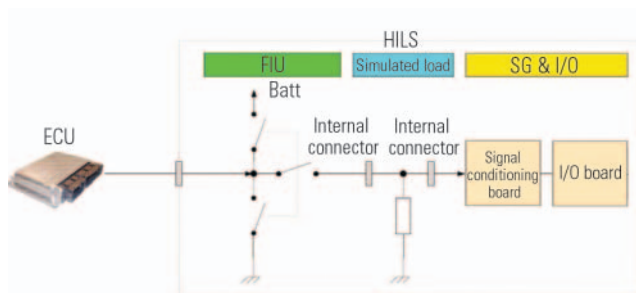


Fig. 4 Failure Insertion Unit (FIU)

## 4. The future

The HILS architecture capable of conducting simulated comprehensive ECU testing in a bench test environment better than that on an actual vehicle was developed. The automatic test programming software embedded in the system, however, has been produced in accordance with the conventional test standards and needs to be reviewed from new perspectives. In other words, software test methods that are built along software test standards need to be introduced in the HILS to cover all software codes being tested entirely with fewer test cases.

## 5. Conclusion

Real-time simulation on a virtual vehicle offers benefits of improved efficiency of testing and lower development costs. CAE systems are an example of this, and are indispensable for the development of vehicle control technologies. In order to help ensure the quality of complicated, large-scale software, we will make further

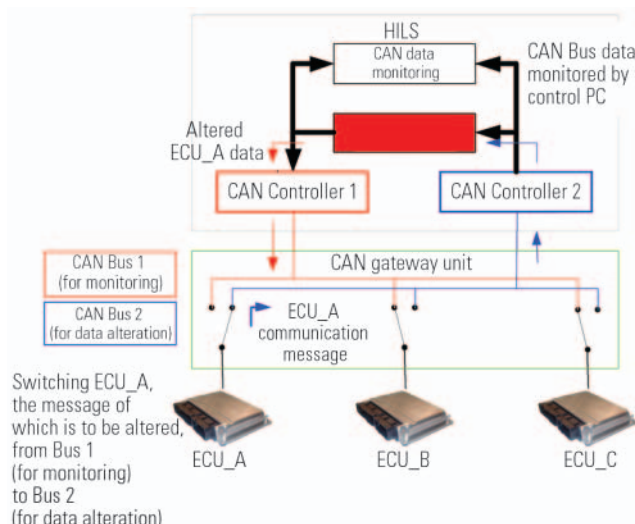


Fig. 5 CAN gateway

efforts to develop new HILS-based test methods based on test strategy and thus improve the reliability of ECUs.

Finally, we sincerely thank all those within and outside of Mitsubishi Motors Corporation (MMC) who assisted the development of our system.



Kunihiro SAKAI



Yukihiro NISSATO



Masahiro KANEDA

# Development of High-Grade Sound System for Minicars

Toshifumi OHBA\* Masayuki MIYATA\* Makoto ARAKAWA\*\*

## Abstract

We have developed a high-grade sound system as optional equipment for the new eK WAGON, eK SPORT and "i". This is the first high-grade system in the minicar segment. We aimed to attain a high-quality sound unprecedented in minicars with the least modification to the vehicle. This goal was attained not only by improving the performance of the tweeters, speakers, amplifier and other components, but also by using a non-communicative-type power amplifier and a waterproof film with sound-insulator.

**Key words:** High-Grade Sound System, High Quality Sound, EPDM, DSP (Digital Signal Processor)

## 1. Introduction

Mitsubishi high performance sound systems for passenger cars, including the Premium Sound System on the new OUTLANDER, have been well received by the market. In the minicar segment, too, there has been a steady growth in demand for higher sound reproduction quality. To meet these needs, we have developed the High-grade Sound System, as described below.

To achieve a high-quality acoustic environment unprecedented in minicars with the least modification to the car, we developed the following items:

- (1) Amplifier separate from audio/navigation unit (non-communication type)
- (2) Waterproof film integrated with sound insulating material (EPDM<sup>\*1</sup>)
- (3) Add-on tweeter

<sup>\*1</sup> EPDM: Ethylene propylene diene monomer

## 2. System configuration

The High-grade Sound System for the new eK WAGON and the "i" features a total of eight speakers in six positions (**Fig. 1**).

- Tweeters

New eK WAGON – below the A-pillar: 3.5-cm balanced dome tweeter (dedicated to high frequency reproduction)

"i" – above the instrument panel: 3.5-cm balanced dome tweeter (dedicated to high frequency reproduction)

- Front doors: 16-cm mid-bass speaker (dedicated to mid/low frequency reproduction)
- Rear doors: 16-cm coaxial 2-way full range speaker (for full frequency range reproduction)

While the standard package uses an audio/navigation unit incorporating a 140-W amplifier, the optional High-grade Sound System features a separate 360-W (MAX) amplifier, the first of its kind in minicar OEMs, to sufficiently drive all of the speakers. The amplifier is located under the front passenger seat on the eK WAG-

ON and behind a rear quarter trim on the "i".

The combination of the above amplifier and the front- and rear-door speakers and the tweeters offers clear sound reproduction. While the system does not use any subwoofer, deep bass is compensated to a certain degree by the front- and rear-door speakers. The DSP (Digital Signal Processor) integrated in the amplifier allows sound reproduction to be tuned to match the acoustic characteristics of the passenger compartment of the eK WAGON or the "i", offering a level of acoustic quality unprecedented in the minicar segment.

## 3. Technical features

### 3.1 Separate amplifier (non-communication type)

With the Premium Sound System offered on the OUTLANDER and the new PAJERO, sound quality and acoustic field are adjusted by two-way communication between the audio/navigation unit and the amplifier (**Fig. 2**). To realize this on the "i" which has an exclusive audio/navigation unit, it requires major modification to the audio/navigation unit's hardware and software.

The High-grade Sound System features a non-communication type amplifier separate from the audio/navigation unit. The separate amplifier and the audio/navigation unit do not communicate with each other for adjustment of sound quality or acoustic field, but the amplifier is tuned to bring out the best sound characteristics of the exclusive audio/navigation unit. Thanks to this technique of acoustic adjustment solely by the power amplifier, the separate power amplifier can be tuned and combined with any audio/navigation unit for better sound characteristics (**Fig. 3**).

Like the OUTLANDER, the amplifier of the new system incorporates a DSP (Digital Signal Processor). Its parametric equalizing function<sup>\*2</sup> tunes the frequency characteristics of the amplifier output so as to offer deep bass reproduction richer than that of the standard system (**Fig. 4①**), and flat and smooth high frequency reproduction (**Fig. 4②**) (<sup>\*2</sup>: The parametric equalizing

\* Electronics Engineering Dept., Development Engineering Office

\*\* Mitsubishi Automotive Engineering Co., Ltd.



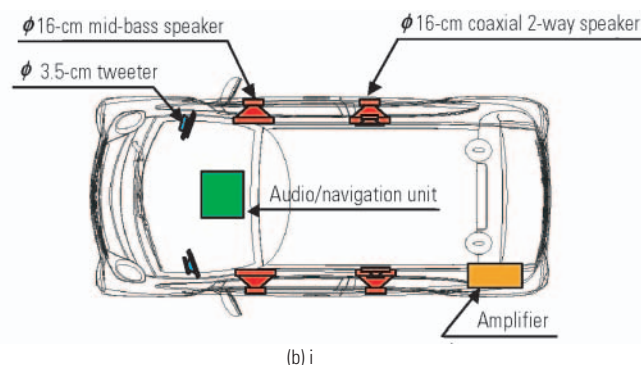
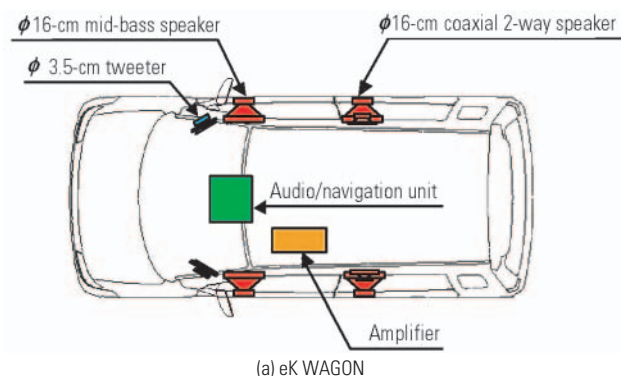


Fig. 1 Layouts of the high-grade sound system components

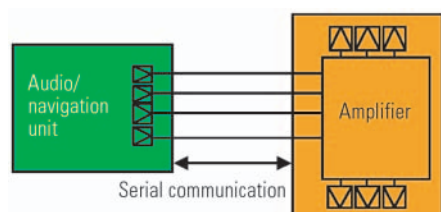


Fig. 2 Construction of the premium sound system on the OUTLANDER

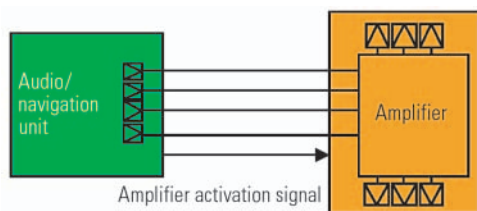


Fig. 3 Construction of the high-grade sound system

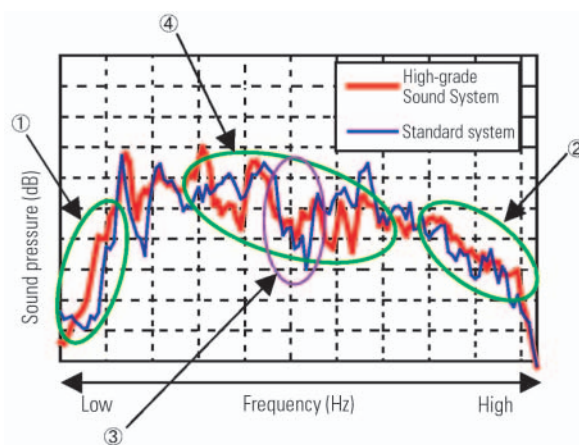


Fig. 4 Frequency characteristics of the eK WAGON

feature corrects the frequency ranges of reproduced sound that are amplified or attenuated by the specific shape, material and other characteristics of the particular passenger compartment in which the sound is reproduced). In mid frequency reproduction, the High-grade Sound System is free of any substantial drop in sound pressure like that of the standard system (Fig. 4③), achieving highly uniform sound pressure levels over the entire mid frequency range (Fig. 4④). This shows that the High-grade Sound System offers better audio balance than the standard system in the mid frequency range, too. The time alignment feature, which corrects distortion of the sound image caused by the difference of distance between a listener and speakers, tunes the outputs of the speakers on the time axis to offer a clear stereo acoustic environment with a good feel.

### 3.2 Waterproof film integrated with sound insulating material (EPDM)

With the OUTLANDER, the access holes in the door inner panels are closed off with sheet metal or resin

parts to stiffen the speaker mounting surface and to turn the doors into speaker boxes. With the High-grade Sound System, waterproof film integrated with EPDM (sound insulation material) is used (Fig. 5), the first such film to be employed in Mitsubishi Motors Corporation (MMC), to achieve high quality sound reproduction with the least modification to the car.

The integral film is made by cutting out the access hole positions of a waterproof film and welding EPDM to these holes. The EPDM is a dual-layer sheet with wavy surface (cross-section) (Fig. 6). The outside layer has a closed-cell structure and is waterproof as is the waterproof film. The inside layer has an open-cell structure and a wavy surface, which makes the layer a sound insulator/absorber. Fig. 7 shows the results of an experiment in which 1,000 Hz, 2,000 Hz and 4,000 Hz sine waves were fed to a speaker in the RH front door lined with integral EPDM/waterproof film and with only a waterproof film. As indicated by the graphs, the sound pressure of reverberation is lower with the integral film, which therefore has higher sound insulating performance. Thus, the integral film effectively prevents sound from the back of the speaker from leaking to the front and interfering with the sound from the front of the speaker.



**Fig. 5 Waterproof film integrated with EPDM sound insulator for “i”**

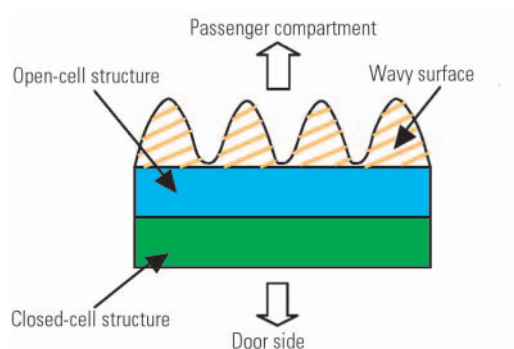


**Fig. 6 Dual-layer EPDM with wavy section**

The waterproof film can generate rattling noise if ① the film vibrates, ② a harness running nearby vibrates and comes into contact with the film, or ③ the door panel (trim) vibrates and comes into contact with the film. With the High-grade Sound System, cause ① has been eliminated by cutting out functionally unnecessary portions of waterproof film and filling them with EPDM, while causes ② and ③ have been minimized because most of the possible contact areas of the film have been replaced with EPDM.

Furthermore, the integral film takes only the same amount of time to install as a waterproof film.

### 3.3 Add-on tweeter

High quality acoustic reproduction has been achieved by parametric equalization of the DSP in the amplifier and the time alignment feature. However, the speaker layout is also a contributing factor, especially the uniquely shaped tweeter of the eK WAGON.

The tweeter, which is offered only on the High-grade Sound System of the eK WAGON, has a unique shape as shown in **Fig. 8**. Because of the unique shape, the tweeter projects high frequency sound straight to the driver and the front passenger irrespective of the shape of the A-pillar and other constraints.

If the tweeter were embedded in the A-pillar, the pillar trim could, depending on the shape and angle of the pillar, partially block the sound from the tweeter. With this unique design of the tweeter, however, obstruction is minimized to offer high quality sound.

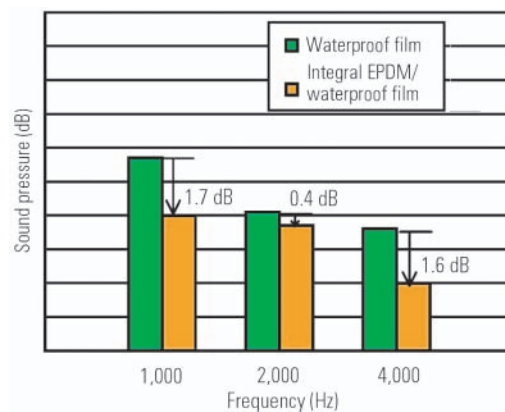


**Fig. 7 Sound insulating performance of waterproof film with EPDM sound insulator**



**Fig. 8 Add-on tweeter**

## 4. Conclusion

Using a non-communication-type amplifier, integral EPDM/waterproof film and other techniques, a high-quality acoustic environment unprecedented in minicars has been achieved with the least modification to the car.

We envision extending the system to other car models while best utilizing the features of the system.

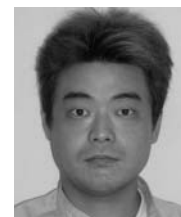
Finally, we express our appreciation to all those within and outside MMC for their help with this project.



Toshifumi OHBA



Masayuki MIYATA



Makoto ARAKAWA

# Development of High-Quality 5.1-channel Theater Surround System

Akihiro OKADA\* Atsushi GOMI\*  
Hidekazu ISHIWATA\* Shigeaki ASANO\*

## Abstract

We adopted a 5.1-channel theater surround system combined with the Rockford Acoustic Design premium sound system on the new PAJERO. This is the first introduction of the 5.1-channel theater surround system in Mitsubishi Motors Corporation (MMC) and the first introduction of Rockford Acoustic Design brand components in Japan. In the related development process, we aimed to deliver outstanding sound quality and presence not available with existing genuine audio systems. This goal has been achieved by not only improving the individual performance of speakers, amplifier and other components, but also by optimizing the speaker mounting condition to maximize speaker performance and employing the excellent digital signal processor (DSP) tuning technique.

**Key words:** Air Conditioning, Heater, Control, Blower, Temperature, PTC

## 1. Introduction

In developing the new theater surround system, we aimed to achieve high quality sound reproduction not available with existing genuine audio systems, and to create a surround system that offers the same feel of reality as in a movie theater. Specifically, we set the following targets:

- (1) Reproduction of high definition sound
- (2) Reproduction of strong and punchy deep bass
- (3) Surround system that offers the feel of reality

To achieve these targets, not only the performance of individual components such as speakers and amplifier needed to be improved, but especially the system tuning technique to reproduce the 5.1-channel audio source optimally and efficiently in a passenger compartment is required. This paper describes the process of developing the new theater surround system, highlighting the tuning (mixing) techniques employed.

## 2. System components

The Rockford Acoustic Design Premium Sound System offered on the new PAJERO features 12 speakers in 12 positions (Fig. 1).

- Passenger compartment side of the door mirrors: 3.5-cm soft dome tweeter (dedicated to high frequency reproduction)
- Front doors: 16-cm mid-bass speaker (dedicated to mid/low frequency reproduction)
- Upper portion of the rear doors: 3.5-cm soft dome tweeter (dedicated to high frequency reproduction)
- Lower portion of the rear doors: 16-cm mid-bass speaker (dedicated to mid/low frequency reproduction)
- Rear gate: 8-cm mid range speaker (dedicated to mid frequency reproduction)

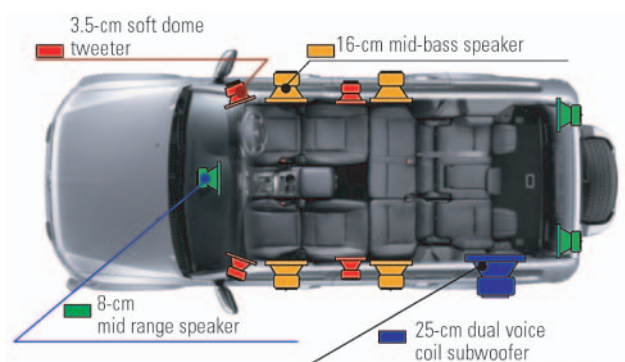


Fig. 1 Layout of speakers on the new PAJERO

- In the center of the instrument panel top: 8-cm mid range speaker (dedicated to mid frequency reproduction)
- Left rear quarter trim: 25-cm dual voice coil subwoofer (dedicated to deep bass reproduction)

To drive all of these speakers easily, an 860 W (MAX) 11-channel high power amplifier is provided behind the subwoofer box.

The system uses a DSP (Digital Signal Processor), which tunes the output signals of the amplifier to match the specific characteristics of the new PAJERO's interior to achieve a highly realistic sound field.

## 3. Product features

### 3.1 Reproduction of high definition sound

For a 5.1-channel surround system to achieve high definition reproduction, each speaker needs to output high definition sound, and the following requirements relating to the mounting of speakers must also be met:

- (1) Stiffening the speaker mounting surfaces of the

\* Electronics Engineering Dept., Development Engineering Office



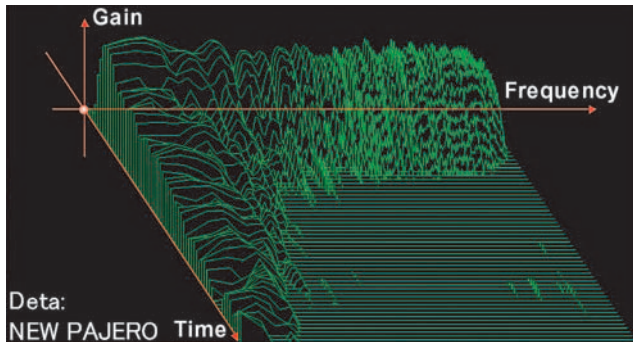


Fig. 2 Damping characteristics on the new PAJERO

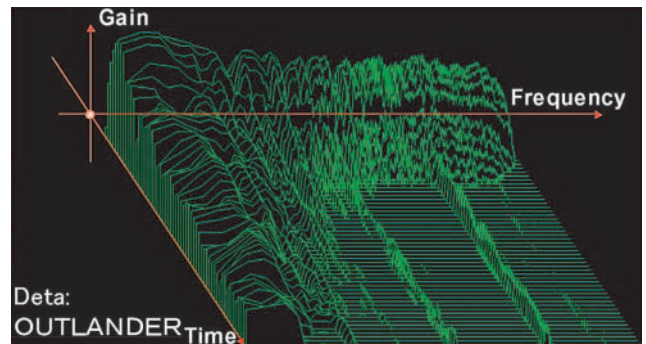


Fig. 3 Damping characteristics on the OUTLANDER

doors

(2) Turning the doors into speaker boxes

As described in our previous paper on the Premium Sound System of the OUTLANDER, if the speaker mounting surface is not stiff enough, the energy of reproduced sound will be converted to vibrational energy of the sheet metal, reducing the reproduction efficiency of the speakers and generating unwanted distortion. Therefore, to achieve high definition sound reproduction, the door panels need to be stiffened with sheet metal or other means, and the doors need to be turned into a speaker box. If the access holes in the door inner panel are left open, sound in front of and behind the speaker cancel each other out through these holes, so the holes need to be closed off.

The stiffness of the speaker mounting surfaces of the PAJERO and the OUTLANDER were compared acoustically.

Fig. 2 shows the damping characteristics across the entire frequency range of the instantaneous output of a 16-cm speaker mounted on a door of the new PAJERO.

Fig. 3 shows the corresponding results with the OUTLANDER.

As shown in these figures, the OUTLANDER has slightly inferior damping in the mid frequency range, but the new PAJERO does not. In the deep bass range, moreover, the PAJERO has a slightly better damping factor than the OUTLANDER. The doors of the new PAJERO thus have extremely favorable acoustic characteristics.

These results proved that the new PAJERO had, without stiffening, clear high-definition sound reproduction characteristics, so it was decided to stiffen the doors of the new PAJERO with sheet metal, etc. as was done on the OUTLANDER.

Next, we compared the frequency characteristics of when the access holes in the door inner panel were left open and when they were closed off with sound absorbing material (Fig. 4).

As shown in the figure, in the low frequency range, the door with closed holes has higher sound pressure than that with open holes. This appears to be because closing the holes with sound absorbing material excluded the interference of the antiphase waveform from the back of the speaker to the correct phase waveform from

the front of the speaker, resulting in more efficient sound reproduction.

With its doors having sufficient stiffness in acoustics as described above, it was possible to reproduce on the new PAJERO highly efficient, high definition sound by just adding sound absorbing material (Fig. 5).

### 3.2 Reproduction of punchy deep bass

As described in our previous paper on the OUTLANDER, the entire frequency range of a source CD needs to be reproduced to achieve high definition sound representation. For a 5.1-channel surround system, the reproduction of punchy deep bass is the key factor in creating a realistic, thrilling feel. The automobile interior, however, poses a great challenge in reproducing deep bass, and currently almost no automobiles offer a punchy deep bass audio environment. This area is a challenge for the premium sound system, and approaches include the following:

- (1) Large diameter subwoofer
- (2) Optimally designed subwoofer box

Without going into detail, the new PAJERO features a 25-cm subwoofer and a 20-liter enclosure box for the subwoofer (Fig. 6), allowing the new PAJERO to deliver the same level of deep bass reproduction as that offered on the OUTLANDER.

### 3.3 Surround system that offers the feel of reality

There are three important elements to realistic reproduction of surround sound:

- (1) Optimum time delay for each speaker
- (2) Optimum frequency characteristics of each speaker
- (3) Optimum assignment of reproduced sound components (mixing)

Each of these elements is described below.

#### 3.3.1 Optimum time delay

Unlike a home audio environment, listeners' positions in an automobile are usually offset to the left or right. Time delay can be used to meet this challenge.

Time delay enables an acoustic space to be formed at the optimum position for each listener sitting offset relative to the audio components, thus offering a good-sounding stereo sound. Time delay can also be used to form a sound image at a higher position above the speakers, helping to create a highly realistic acoustic



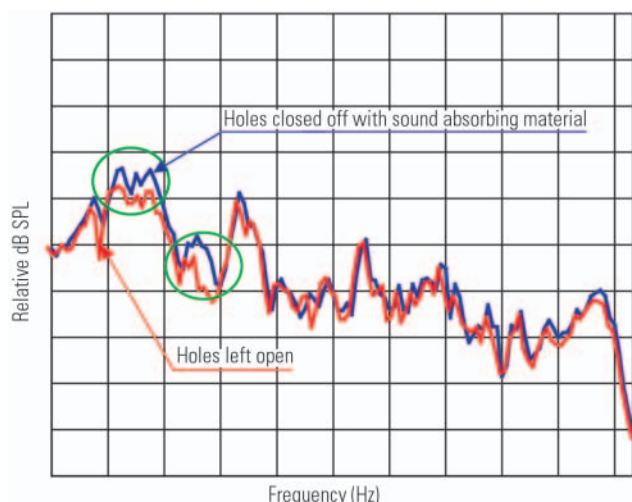


**Fig. 4** Frequency characteristics when door inner panel holes are closed by sound absorbing material and when they are left open

space. With a 5.1-channel surround system, the feel of reality is a function of various elements including the location of the sound source and the position of the sound image. By optimizing these attributes, the surround sound environment can be made truly realistic.

### 3.3.2 Optimum frequency characteristics

A speaker simply installed to an automobile door has some undesirable frequency characteristics due to the structure and stiffness of the door. This can be corrected by DSP.

**Fig. 7** shows acoustic A-weighting correction of output frequencies. The blue line represents the corrected frequency profile while the red line shows the original frequency profile.

As can be seen from the graph, if a speaker is installed in a special environment such as an automobile interior and is simply driven to produce the sound of a flat frequency spectrum, the intended sound output is disturbed by the specific characteristics of the interior such as the speaker mounting condition and the aperture ratio of the garnish. DSP corrects such disturbance to optimize the output so that it is acoustically flat as represented by the blue line of the graph. Output of even higher definition can be achieved by performing this optimization for each speaker. For example, the center speaker is carefully tuned so that the speaker produces highly realistic human voice when playing DVD movies. Likewise, by tuning the frequency spectrum of each of the 12 speakers to match the source sound being played, it is possible to produce a highly realistic sound field.

### 3.3.3 Mixing for optimum sound image and reality

To further enhance the feel of reality of surround sound, mixing is needed in addition to the set of tuning described above. Mixing means setting a ratio according to which the 5.1-channel output of a DVD is assigned to each of the speakers (center, right front, left front, right rear, left rear + subwoofer).

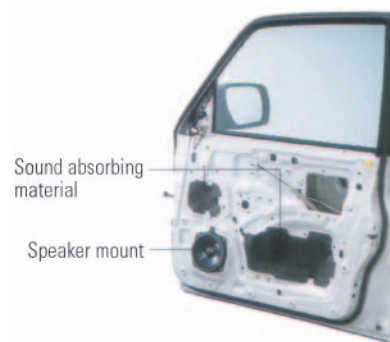


**Fig. 5** Door structure



**Fig. 6** 25-cm dual voice coil subwoofer with 20-liter enclosure box

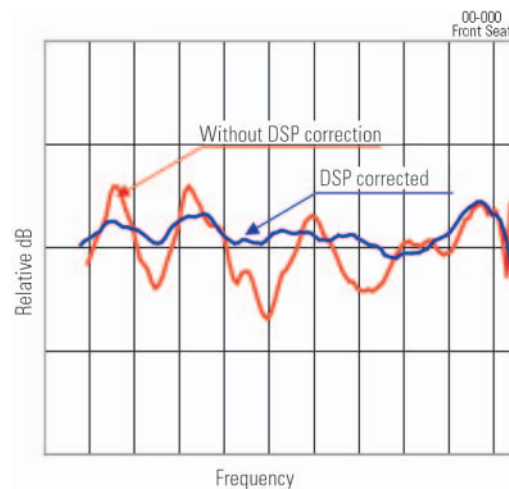


**Fig. 7** Before and after DSP (A-weighting) tuning

The effect of mixing is so great that it can produce a sound field within the automobile as realistic as that of a home audio system.

For example, you sit in the second row of seats of a car and watch a movie (**Fig. 8**). You cannot properly hear the sound output including human voice from the center speaker because it sounds rather far away if mixing has not performed on the system. To improve this, the sound components of the center speaker are mixed with those of the other speakers. This results in a surround sound field that feels pleasant and realistic.

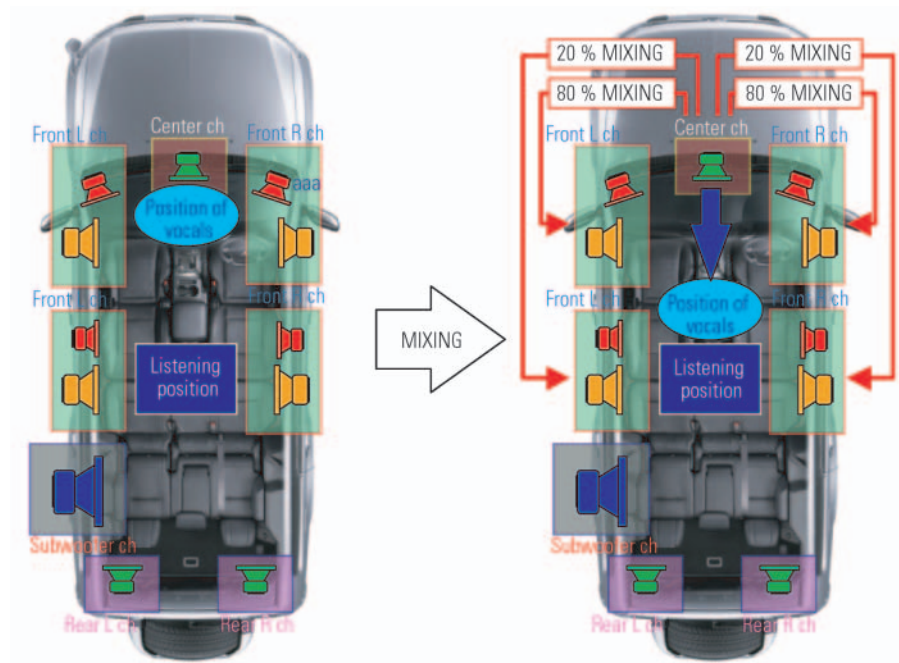


Fig. 8 Effect of mixing

The 5.1-channel surround system that we have developed offers a variety of selections, including 1st-row mode, 2nd-row mode and all-row mode. In every mode selected and no matter where you sit, the optimum sound is ensured by mixing.

#### 4. Conclusion

We have successfully developed a 5.1-channel theater surround system that exceeds customer expectations. This was achieved by focusing on the performance of individual speakers, optimizing aspects such as the door structure and sound system layout, and the superb DSP tuning technique. The quality of reproduced sound of the new PAJERO has been highly rated by specialized magazines and commentators, just as the OUTLANDER did. Building upon the techniques developed in the project, we will strive to offer premium sound systems that are more innovative and have even higher performance.

Finally, we would like to thank Mr. Yoshimura, acoustic engineer, of the Engineering Department of Foster Electric Company, Limited for assisting the acoustic quantification measurements and analyses for this project.



Akihiro OKADA



Atsushi GOMI



Hidekazu ISHIWATA



Shigeaki ASANO

# “Car School” – Sporty Driving Course

Tetsushi MIMURO\* Yoshihiro GOI\*\*  
Tsuneaki NISHIDA\*\*

## 1. Introduction

Mitsubishi Motors Corporation (MMC) offers “Car School” driving lessons to help enable customers to enjoy driving their cars in safety. Most of the lessons are aimed at beginners, but on October 15, 2006, MMC gave, for the first time, a sporty driving course for intermediate and advanced drivers at its R&D Center – Okazaki. The sporty driving course was attended by 24 course participants and their companions. Development personnel at the Technical Center served as instructors with support from other MMC employees.

## 2. Content of course

### Lecture: Basic knowledge about correct driving

This lecture covered the correct driving position, the correct ways (based on vehicle motion dynamics) to use the accelerator, brakes, transmission, and steering wheel, and the benefits of four-wheel drive and limited-slip differentials.

### Practical skills 1: Precision driving

A gymkhana-style session was conducted to enable course participants to sense how controlled, precise acceleration, steering, and braking translate into safe, smooth performance driving (**Photo 1**).

### Practical skills 2: Acceleration and braking

Course participants gained a correct understanding of cars’ braking performance by experiencing hard, full-force braking from high speeds using an antilock braking system (ABS) (something they would rarely be able to experience in real-world driving situations) and by being coached on the way to predict differences in stopping distances depending on speed. In the intervals between training runs, the participants were given a tour of the MMC test courses in their own cars.

### Practical skills 3: Vehicle control on a slippery surface

On the slippery surface of a skid pad, course participants were given a chance to feel how braking and steering performance differed with and without ABS operation (**Photo 2**). The participants also accompanied the instructors on demonstration runs.

In the intervals between training activities, a well-



Photo 1 Gymkhana session



Photo 2 Skid pad session

known rally driver delighted the course participants with demonstrations of a LANCER EVOLUTION WR car.

### Tour of facilities

Companions of the course participants were given a tour of the test courses, wind tunnel, electromagnetic wave testing laboratory and other development facilities and the Mitsubishi Auto Gallery. In addition, all the participants and companions watched a crash test conducted on a vehicle under development. Although they were able to see that the dummies inside the vehicle were well protected from the severe impact, the crash test was a sharp reminder of the importance of safe driving (**Photo 3**).

\* Advanced Vehicle Engineering Dept., Development Engineering Office

\*\* Development Planning Dept., Development Engineering Office

\*\* Function Testing Dept., Development Engineering Office





Photo 3 Observation of crash test

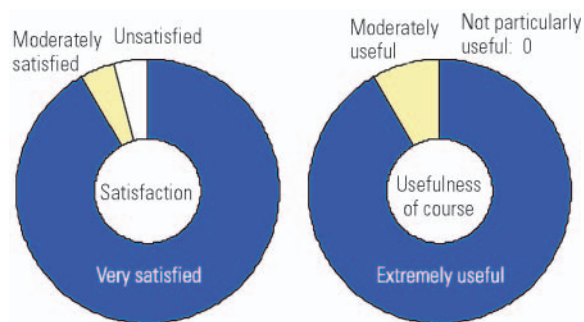


Fig. 1 Questionnaire results



Photo 4 Course participants, instructors, and volunteers

### 3. Impression meeting

After the course, each participant was given a completion certificate and asked to maintain a close focus on safe driving. The participants also filled in a questionnaire, the results of which reflected a high level of satisfaction with the course (Fig. 1).

### 4. Conclusion

Development engineers rarely have direct contact with customers, so being able to directly interact with customers by serving as instructors was of an experience of great value for future vehicle development

(Photo 4). MMC's development personnel plan to continue helping customers to drive safely through activities like this.



Tetsushi MIMURO



Yoshihiro GOI



Tsuneaki NISHIDA



# Construction of Large Anechoic Chamber

Atsuhiko KAWANO\* Wataru KATSUNO\*

## Abstract

In recent years, with the growth in the number of electrical/electronic components installed in vehicles and the degradation of the electromagnetic environment surrounding vehicles, regulatory requirements relating to the vehicle's electromagnetic compatibility (EMC) are becoming increasingly stringent worldwide.

To comply with future regulatory requirements and to accommodate the electromagnetic environment caused by the rapid increase of wireless systems such as mobile phones and digital terrestrial broadcasting, in August 2006 we constructed a large anechoic chamber and other facilities and equipment to improve and upgrade the EMC tests.

**Key word:** EMC

## 1. Introduction

The Commission Directive 2006/28/EC of January 2006, the first major amendment in approximately ten years, demands more stringent methods for testing a vehicle's immunity against incoming electromagnetic interference and for measuring electromagnetic emission from the vehicle. Because our previous anechoic chamber was too small and the related test facilities and equipment were not expected to meet the requirements of the new directive, we constructed a large anechoic chamber and installed upgraded facilities (**Photo 1** and **Photo 2**).

These facilities enable us to carry out efficient and comprehensive tests including homologation test for Directive 2006/28/EC and development test, in addition to the tests for Directive 95/54/EC.

For not only more high-frequency, complicated and powerful electrical/electronic components installed in vehicles but also for the EMC environment of the vehicle including the high-frequency radio emission from medical equipment like CT systems and cellular phone, complicated modulation radio emission from cellular phone and internet security system, and intense radio emission from air traffic control radar, we installed the facilities to upgrade accuracy and functions for EMC tests.

## 2. Overview of the large anechoic chamber

### 2.1 Test items

The large anechoic chamber is applied to two types of testing: immunity tests and emission tests for vehicles.

The immunity test checks whether the components of the vehicle relating to driving, turning and stopping function normally when the vehicle is exposed to intense radio waves such as from the antenna of a broadcasting station while driving nearby. We can per-



**Photo 1** Electromagnetic wave testing laboratory (seen from the west)

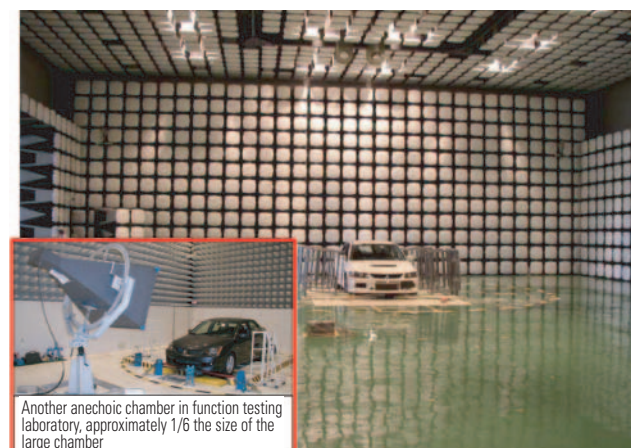


**Photo 2** Large anechoic chamber

form the vehicle test for electrical disturbance from off-vehicle radiation source conforming to ISO standards in the large anechoic chamber.

The emission test checks whether the electromagnetic energy emitted from the vehicle causes interference to radio or TV reception in the residential environ-

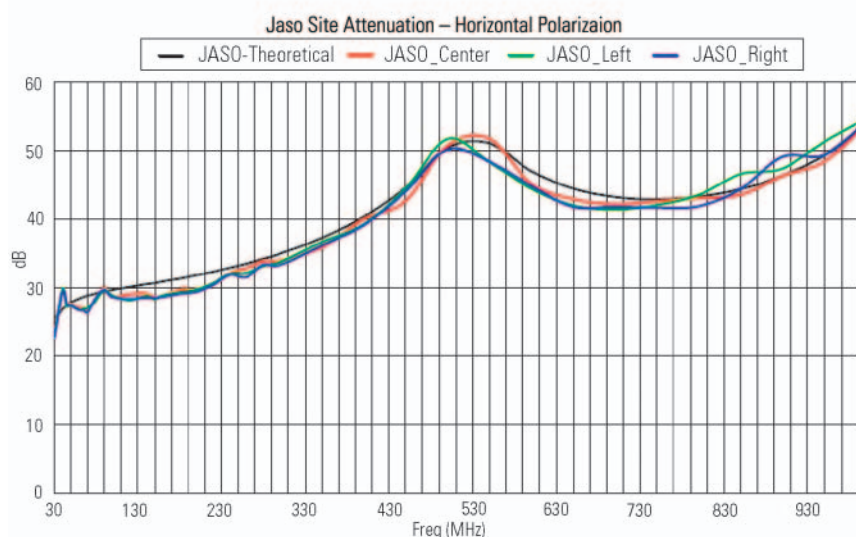
\* Electronics Engineering Dept., Development Engineering Office

**Table 1 Shielding performance**

Room	Frequency range	Component	Attenuation (dB)
Anechoic chamber	14 kHz – 30 MHz	Magnetic field	80 or more
Measuring room	14 kHz – 30 MHz	Electric field	100 or more
Amplifier room	20 MHz – 1 GHz	Plane wave	100 or more
C/D control room	1 – 18 GHz	Plane wave	100 or more

**Table 2 Field distribution uniformity performance**

Applicable standard	Measuring method
IEC61000-4-3	20 MHz – 2 GHz Within 0 – 4 dB at 12 of 16 points tested by the IEC standard
ISO11451-2 (2006/28/EC)	In the frequency from 20 MHz – 2 GHz, at frequency points of more than 80 % of the total, within –6 – 0 dB in 0.5 m horizontally to each side from the base point.

**Fig. 1 Site attenuation performance****Photo 3 RF immunity test**

ment. In the large anechoic chamber, we can perform the 10-m test of CISPR (Comité international spécial des perturbations radioélectriques) and the initial step of Directive 2006/28/EC ANNEX V.

## 2.2 Shielded rooms (Table 1)

The large anechoic chamber has enough space to carry out 10-m test. All six sides (the floor, walls and ceiling) of the chamber is covered with steel plates to prevent radio waves from leaking out. The measuring

room, the amplifier room and the chassis dynamometer (C/D) control room are also shielded in a similar manner.

To minimize the reflection of radio waves within the large anechoic chamber, the ceiling and walls are covered with ferrite hybrid absorbers, while the floor is covered with ferrite tiles. The chamber has site attenuation performance conforming to JASO D002-2004 standard and field uniformity performance conforming to ISO standard (Table 2 and Fig. 1).

## 2.3 Test equipment

### 2.3.1 Intense electric field generator

The generator installed in the large anechoic chamber consists of four antennas and three amplifiers, and the intense electric field of 200 V/m from 100 kHz to 2 GHz (not all frequencies in the range available) is generated onto the vehicle (Photo 3).

To help improve the efficiency of testing, the following can be remotely performed from the measuring room: switching between the amplifiers/antennas; adjustment of the antennas' height and angle; and selection of polarization.

### 2.3.2 Emission measuring device

The emission measuring device installed in the large anechoic chamber consists of a bilog antenna for measuring broadband noise and a pneumatically driven



Photo 4 Chassis dynamometer



Photo 6 Actuators for accelerator, brake and clutch pedal

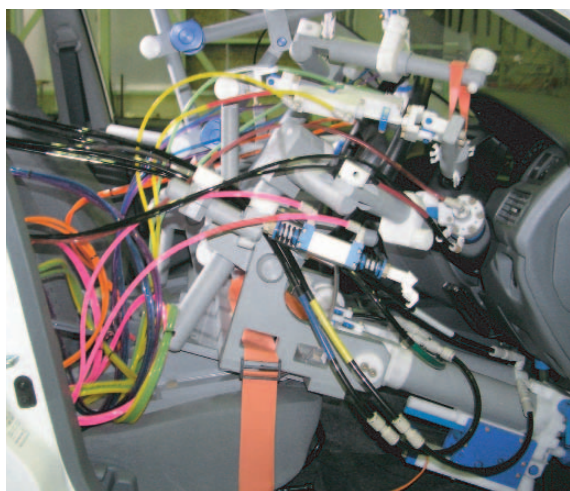


Photo 5 Actuators



Photo 7 Ignition switch actuator

antenna mast. This eliminates antenna replacement and polarization selection. By operating the turntable in a coordinated manner with the measuring device, it is possible to continuously measure broadband noise emitted from both sides of the vehicle, thus improving efficiency.

### 2.3.3 Chassis dynamometer (Photo 4)

Using the chassis dynamometer installed in the large anechoic chamber, it is possible to continuously run the vehicle at up to 100 km/h or to carry out test on ABS system under low  $\mu$  condition. The chassis dynamometer can be operated using either the controller in the large anechoic chamber or remotely on a PC in the measuring room. This improves test efficiency.

### 2.3.4 Vehicle operation actuators (Photo 5)

In the anechoic chamber, an intense electric field is generated onto the vehicle, so actuators are used to operate the vehicle on behalf of humans. Besides the actuators for the accelerator, brake and clutch pedals, we developed actuators for the ignition key switch, column switch and other switches for the new facilities. These improve test efficiency and expand the scope of tested components.

- Actuators for foot-operated controls (**Photo 6**)

The accelerator pedal actuator can control vehicle speed. A displacement sensor is installed at the end of the actuator cylinder and the vehicle speed data is taken from the chassis dynamometer. Based on these data, the actuator cylinder is extended or retracted to obtain the required vehicle speed.

The brake pedal actuator can control the pedal stepping force at a high or low level, and it can operate ABS system. The clutch pedal actuator can release the clutch pedal at 10 different speeds.

- Actuators for hand-operated controls

The ignition switch actuator can operate the switch through the entire sequence from engine start to stop: OFF → START → IG → ACC → PUSH → STOP (**Photo 7**).

The column switch (straight line) actuator can move a column switch between three positions, i.e. up, neutral and down, or forward, middle and rearward. This can be used, for instance, to operate the turn signal (right → cancel → left) or flash the headlamp main beams.

The column switch (rotational) actuator can rotate a switch between two positions such as ON and OFF. It can, for example, turn on and off the headlights. The



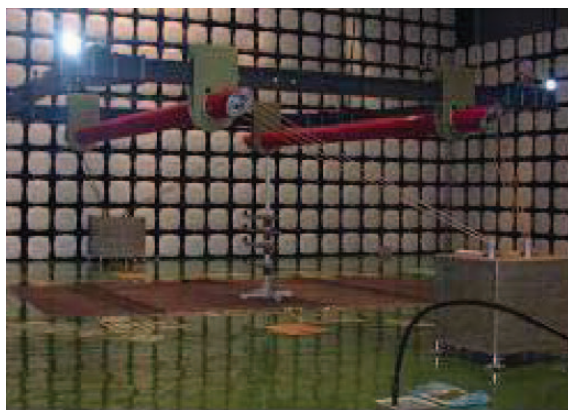


**Photo 8 TLS Antenna**

actuator can also push a switch at the end of a column switch to inject windshield washer.

The air conditioner / audio switch (straight line) actuator can push a switch ON and OFF, such as the switch of the air conditioner, audio or hazard warning lamp.

The air conditioner / audio switch (rotational) actuator can rotate a switch between two positions, such as ON and OFF.

The power window switch actuator can move the switch to open and close the power windows: open → stop → close.

## 2.4 Safety systems

The large anechoic chamber is equipped with an interlock system that disables radio wave radiation when the shielded door is open, and an emergency button to stop radio wave radiation and chassis dynamometer in emergencies.

The chamber is also equipped with safety sensors for fire, high CO concentration, fluid leakage and earthquake, and give optical and acoustic warnings.

## 3. Technical features of the new TLS antenna

### 3.1 Overview

TLS (Transmission Line System) antennas can generate electromagnetic field of relatively low frequency of 100 kHz – 30 MHz or so-called LF, MF and HF bands. The new TLS antenna consists of a base, a balun, radiation elements, a load and cables that connect these components (Photo 8).

### 3.2 Background and purpose of the installation

In the ISO11451-1 (3rd 2005) on immunity test, its required frequency ranges 0.01 – 18,000 MHz. Of that range, this facility can cover 0.1 – 30 MHz frequency test. The installation is aimed at checking for electrical disturbance from AM radio stations, motors, etc. One example of electrical disturbance with our retailed cars is: an aftermarket product that the customer installed on his car generated noise in a band around 125 kHz, which was also used by the immobilizer, causing the

immobilizer to malfunction. Our new facilities are expected to eliminate such malfunctions.

### 3.3 Brief description of the TLS antenna

The base, which is stowed just below the ceiling of the anechoic chamber, is lowered to the work position by four winches housed behind the ceiling. With the base lowered, the elements are then installed in position for testing. The elements can be moved horizontally by the air pump mounted on the base. The antenna is operated on the controller installed in the anechoic chamber. The winches and air pump are operated through TLS antenna controller.

From a PC in the measuring room, GPIB signals are sent to the balun to switch the direction of electromagnetic field (Vertical: E mode; Horizontal: H mode).

For safety, the base is equipped with four drop-prevention belts in case the cable breaks. Three height limits for the base (lowest, highest with cables on, and highest) are programmed in the system. As the base is raised or lowered, the program works according to the operation of the rotary encoders, each of which is installed on a winch. These encoders also monitor the inclination of the base. If the data difference between the encoders exceeds the preset level, the limit function intervenes.

### 3.4 Mechanism of electric field generation

Signals are generated by a signal generator, and are then amplified to a maximum of 10 kW by the amplifier in the underground amplifier room. The amplified signals are then sent to the balun where the signals are divided to the core side and the ground side of the coaxial cables. The elements are on the core side while the floor is on the ground side. This creates a potential difference between the elements and the floor, generating vertical electric fields (E mode) (Fig. 2). With the newly installed TLS antenna, it is possible to connect the core side of the coaxial cables to one element and the ground side of the coaxial cables to the other element. In this case, TLS antenna generates horizontal electric fields between the elements while also creating vertical magnetic fields (H mode) (Fig. 3).

### 3.5 TLS antenna performance

It has been verified that the TLS antenna can generate 200 V/m in a 100 kHz – 30 MHz range when the elements are arranged 2 m apart at a height of 2 m (E mode).

### 3.6 TLS summary

- The TLS antenna generates electric fields in low frequency bands.
- Vertical (E mode) and horizontal (H mode) electric fields can be generated.
- This is the first large-scale electromagnetic field generation facility covering below 20 MHz frequency for vehicles in Mitsubishi Motors Corporation (MMC).
- Four anti-drop belts (similar to seat belts) are fitted for safety.



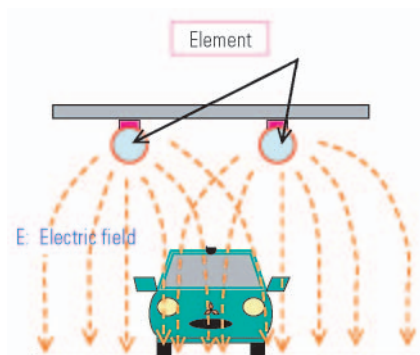


Fig. 2 E mode (vertical electric fields)

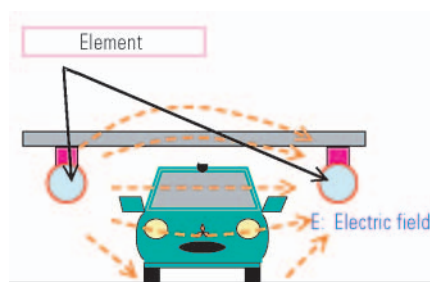


Fig. 3 H mode (horizontal electric fields)

#### 4. Conclusion

The new large anechoic chamber is constructed on many years of experience of all those concerned. We believe that full utilization of this state-of-the-art facility will help us to develop even higher quality, higher performance cars.

Finally, we sincerely thank everyone at and outside MMC for helping to construct the anechoic chamber.



Atsuhiko KAWANO



Wataru KATSUNO

Mitsubishi Motors Corporation (MMC) launched the new eK WAGON and eK SPORT, which have unique features including a diverse range of handy storage spaces and a power sliding door – the first on a bonnet-type passenger minicar – on 13 September 2006.

## 1. Targets

In developing the new, second-generation eK WAGON and eK SPORT, MMC sought to create a superior mini-wagon series that carries forward the qualities that established the first eK generation as a new minicar standard and enables convenience, peace of mind, and a feel-good factor to be experienced not only by drivers but also by passengers.

## 2. Features

### 2.1 Design

#### 2.1.1 Exterior

The body inherits the distinctive semi-tall, long-roof proportions of the first-generation eK WAGON, but it offers a new blend of casual individuality and contemporary urban quality thanks to simple, elegant design features that include taut-looking contours, unique, new-accent front graphics, and clear-lens rear combination lamps that convey a sense of innovation and self-assurance.

#### 2.1.2 Interior

The interior design blends household-appliance familiarity with a sense of digital-device precision within a contemporary two-tone\*<sup>1</sup> environment that creates optimal visual contrasts and offers a new kind of relaxation together with a pleasant sense of tension.

Operability and functionality are enhanced by an instrument-panel-mounted shift lever and by center-meter instruments that are offset toward the driver for visibility. At the same time, utility is enhanced by increased storage capacity and by location of the audio unit near the top of the center stack. The result is a fusion of peace of mind, convenience, a feel-good factor, and enjoyment of using the car.

\*1: Two-tone coloring is used in the new eK WAGON.



ek WAGON



ek SPORT

### 2.2 Power sliding door

The body incorporates a power sliding door – the first on a bonnet-type passenger minicar. A unique MMC-developed mechanism positions the center rail inside the sliding door to create an adequate door-opening width of 530 mm. The sliding door can be opened provided there is clearance of about 200 mm on the outside, so it permits easy ingress and egress in narrow parking spaces. It can be opened and closed using a keyless-entry key, using a switch on the left-hand center pillar, and using a switch in front of the driver's seat.





### 2.3 Useful storage spaces

Storage convenience is enhanced by increased storage capacity and by the addition of a lid to the mini trash box. Each seat has a cupholder, and an innovative Multi-Position Utility system allows users to customize the interior space by attaching or moving around various amenity items among attachment points that share the same mode of attachment.

### 2.4 Collision safety

For safety in the event of a collision, the eK WAGON and eK SPORT each have a RISE<sup>\*2</sup> body combining a high-energy-absorption front structure and a high-rigidity cabin structure. Collision safety is further enhanced by measures that enable compliance with regulations on pedestrian safety, by neck impact reducing front seats that mitigate neck injuries in the event of a rear impact, and by front seatbelts that each have a pretensioner and a force limiter. Also, hazard-evasion performance comparable with that of larger, compact cars is realized by technologies that include an antilock braking system (ABS) with electronic brake-force distribution (EBD)<sup>\*3</sup>. The overall result is high performance in terms of both active safety and passive safety.

\*2: Reinforced Impact Safety Evolution

\*3: The ABS with EBD is an option with certain grades.

### 2.5 Clean-running, fuel-efficient powertrain

All new eK WAGON grades and the new eK SPORT 'X' grade have a 4☆ low-emission-vehicle rating by virtue of exhaust emissions that are 75 % lower than those permitted by Japan's 2005 regulations. (The eK SPORT 'R' grade's exhaust emissions are 50 % lower than those permitted by Japan's 2005 regulations.)

Also, vehicles with two-wheel drive and a four-speed automatic transmission each deliver improved fuel economy thanks to the addition of a lockup mechanism to the torque converter.

### 2.6 Enjoyable handling and a quiet cabin

MMC improved the suspension tuning and suspension mounting rigidity by conducting mechanism analysis and structure analysis using computer-aided engineering technologies, thereby combining a smooth ride with low-roll handling stability. Newly added bulkheads behind the front fenders help to keep engine-compartment noise out of the cabin. They're complemented by other noise- and vibration-suppressing details including sound-absorbent material in the dash pad. Idling vibration, running vibration, and high-speed noise are significantly reduced, resulting in one of the best levels of cabin quietness in the class.

### 2.7 A wide range of colors

To accommodate diverse preferences and give customers the enjoyment of making color choices, all new eK WAGON grades are available in a range of 11 colors. The new eK SPORT is available in a range of six carefully selected colors including the new Dawn Silver Metallic, which projects a steely look of strength. MMC's choice of 'theme' color for the new eK WAGON is Pearl Beige Solid, which conveys a sense of calmness and amicability.

## 3. Major specifications

Major specifications are shown in the following table.

## NEW PRODUCTS

Specifications			Model	eK WAGON				eK SPORT		
				M		MS	G	GS	X	R
				2WD/4WD						
				5 M/T	3 A/T		4 A/T			
Dimensions and weights	Overall length		(mm)	3,395						
	Overall width		(mm)	1,475						
	Overall height		(mm)	1,550					1,570	
	Wheelbase		(mm)	2,340						
	Tread	Front	(mm)	1,300					1,295	
		Rear	(mm)	1,295						
	Minimum ground clearance		(mm)	140					160	
	Interior length		(mm)	1,895						
	Interior width		(mm)	1,275						
	Interior height		(mm)	1,290		1,265	1,290	1,265	1,290	
	Vehicle weight		(kg)	800/850	810/860	830/880		850/900	840/890	870/920
	Seating capacity		(persons)	4						
	Minimum turning radius		(m)	4.4						
Engine	Model			3G83					3G83 I/C T/C	
Chassis	Steering			Rack and pinion (with power assistance)						
	Suspension	Front		MacPherson-strut						
		Rear		Torque-arm (three-link)						
	Brakes	Front		Disc (13-inch)					Ventilated disc (14-inch)	
		Rear		Leading/trailing drum (7-inch)						
	Tires			155/65R13					165/55R14	

(Mini Car Product Development Project, Product Development Group Headquarters: Morii, Seko)



Mitsubishi Motors Corporation (MMC) unveiled the new, fourth-generation PAJERO – the flagship model of Mitsubishi’s sport utility vehicle (SUV) – at the Paris Motor Show in September 2006 and launched it in Japan on 4 October 2006.

## 1. Targets

In developing the new PAJERO, MMC sought to refine and enhance the reliability, durability, and all-round SUV driving performance that have been inherited by successive PAJERO generations. With the interior, MMC sought to create a refined interior design reflecting a shift from a main focus on functionality to the combination of functionality with refinement. And with a view to meeting the needs of customers around the world, MMC maintained the choice of two body types: 5-door and 3-door models.

## 2. Features

### 2.1 Exterior design

An exterior design inherited from that of earlier PAJERO generations makes the new model instantly recognizable. The headlights have a cat’s-eye shape with a wildcat motif. At the rear, the PAJERO identity is expressed by an externally mounted spare-wheel (a hallmark feature of all PAJERO models) that has a simple, tough-looking, functional design.

On the 5-door model, a handsome, simple contour running from the rear door to the rear quarter window on each side conveys a sense of refinement. The three-way, two-tone body colors available on certain grades of 5-door model are also an important design cues.

On the 3-door model, the rear wheel arches have a dynamic design that gives a sense of sportiness.

### 2.2 Interior design

The interior design reflects a shift from the functional, tough image of earlier PAJERO models to a focus on creating an environment that combines functionality with refinement. MMC carefully scrutinized every interior component beginning with the materials, selecting shapes that reflect attention to craftsmanship and quality but have a simple look that users will find consistently appealing over time. For example, the instrument panel, door trim, and center console are made using a new IMD (In-mold decoration) technique; aluminum-look panels in the cabin are finished with aluminum evaporated film; and gravure printing is used to create



New PAJERO – 5-door model



New PAJERO – 3-door model

hairlines in a way that yields a better texture than is possible with earlier techniques.

The meter cluster contains two circular diver’s-watch-motif meters that have high-contrast dials for superior legibility and sequential lightup and indirect illumination for a look of refinement.

There are two available interior color schemes: a beige one (available with the 5-door model version only) that helps to make the cabin look light and spacious, and a sportier black one.

### 2.3 Packaging

The new PAJERO inherits its predecessors’ highly praised all-round-SUV packaging, which gives drivers a superior field of vision and enables them to easily ascertain the surrounding road conditions. Short front and rear overhangs put the new PAJERO on a par with the third-generation model in terms of the large approach angle, departure angle, and ramp breakover angle that are crucial for off-road driving. For further convenience, the third-row seat is a bench type that can be folded completely into the floor.



Beige interior for 5-door model



Black interior for 5-door and 3-door models

## 2.4 Performance

### 2.4.1 Engines

As with the third-generation PAJERO, there are two engine choices: 3.8 L and 3.0 L.

The 3.8 L engine incorporates MIVEC (Mitsubishi Innovative Valve timing Electronic Control system) technology and detail improvements that contribute to maximum output of 185 kW (252 PS) with the 5-door model and 183 kW (249 PS) with the 3-door model for class-topping performance. Further, its torque and power levels are high across the rev range for excellent driveability.

The 3.0 L engine is based on that of the third-generation PAJERO but incorporates extensive improvements that yield better fuel economy and emissions

performance. In terms of exhaust emissions, it has a Japanese 3☆ rating, which requires emission levels 50 % lower than those permitted by 2005 regulations.

On automatic-transmission vehicles with either engine, an automatic transmission fluid (ATF) warmer further enhances fuel economy.

### 2.4.2 Handling stability and ride comfort

In line with the AWC (all wheel control) concept, MMC enhanced the off-road performance that's essential in a true all-round SUV while increasing high-speed handling stability and ride comfort to meet the expectations of today's users.

An increased number of spot welds contributes to enhanced body rigidity, and the suspension springs and shock absorbers have newly optimized designs that keep body roll significantly smaller than that of the third-generation PAJERO. Handling stability and ride comfort at high speeds are concomitantly superior.

For off-road driving, the new PAJERO has the Super Select 4WD II four-wheel driveline, which was highly praised in the third-generation model. Also, the driver can freely select ASTC (Active Stability & Traction Control) or a rear-differential lock for greatly enhanced performance in sand and mud.

## 2.5 Premium sound system

The new PAJERO (5-door model only) has a premium sound system by Rockford Acoustic Design™, a new brand from top US car-audio manufacturer Rockford Corporation which produced the highly praised system in the OUTLANDER. The new system was jointly developed by Rockford Acoustic Design and MMC with a focus on premium sound for jazz and classical music to satisfy 'grown-up' PAJERO users. It incorporates 12 optimally positioned speakers and an 860 W amplifier for a distortion-free, high-quality listening environment.

Also, the sound system in vehicles equipped with the MMCS (Mitsubishi Multi Communication System) is the first from MMC to have 5.1-channel Dolby Digital/DTS surround audio functionality, which creates a soundstage with powerful bass and a rich presence.



Rockford Acoustic Design Premium Sound System

## 2.6 Safety and environmental performance

A RISE (Reinforced Impact Safety Evolution) body structure is complemented by newly adopted safety features including side and curtain airbags and pedals whose structure limits their rearward movement in a frontal impact, so the new PAJERO offers occupant protection (as determined in MMC tests) equivalent to a maximum, 6☆ JNCAP (Japan New Car Assessment Program) crashability rating. Also, the new PAJERO incorporates compatibility features that help prevent it from riding up onto the other vehicle in the event of a vehicle-to-vehicle collision.

The paints and solvents used on components of the new PAJERO contain reduced quantities of toluene, aldehydes, and other VOC (volatile organic compounds)

that are believed to cause sick house syndrome. Also, the air filter in the automatic air conditioner and the liner on the roof have an odor-removing function that enables them to adsorb VOC together with odors to help realize a comfortable interior environment. The new PAJERO achieves early compliance with the JAMA (Japan Automobile Manufacturers Association) Voluntary Vehicle Interior VOC Reduction Initiative.

## 3. Major specifications

Major specifications of the new PAJERO (for Japan) are shown in the following table.

Specifications			Model		5-door model					
					Mitsubishi CBA-V93W				Mitsubishi CBA-V97W	
			Super Select 4WD II							
			ZR		ZR-S		EXCEED	EXCEED-X	SUPER EXCEED	
			LNUV	LRUV	LNUV1	LRUV1	LRHV	LYHY	LYXY	
Dimensions and weight	Overall length (mm)		4,900							
	Overall width (mm)		1,845		1,875					
	Overall height (mm)		1,870							
	Wheelbase (mm)		2,780							
	Tread	Front (mm)	1,560				1,570			
		Rear (mm)	1,560				1,570			
	Minimum ground clearance (mm)		225							
	Interior length (mm)		2,535							
	Interior width (mm)		1,525							
	Interior height (mm)		1,235							
	Vehicle weight (kg)		2,060		2,070		2,140	2,190	2,210	
Seating capacity (persons)		7								
Performance	Minimum turning radius (m)		5.7							
	10-15-mode fuel economy (km/L) (as verified by Ministry of Land, Infrastructure and Transport)		8.6	8.3	8.6	8.3		7.6		
	Major fuel economy enhancing measure		—	ATF warmer	—	ATF warmer		Valve timing electronic control system and ATF warmer		
Engine	Model		6G72 (ECI-MULTI)				6G75 (MIVEC)			
	Valve mechanism and number of cylinders		SOHC, 24-valve, V6							
	Maximum output (net) {kW (PS)/min <sup>-1</sup> }		131 (178)/5,250				185 (252)/6,000			
	Maximum torque (net) {N·m (kgf·m)/min <sup>-1</sup> }		261 (26.6)/4,000				338 (34.5)/2,750			
Transmission	Transmission type		5 M/T	INVECS-II Sports Mode 4 A/T	5 M/T	INVECS-II Sports Mode 4 A/T		INVECS-II Sports Mode 5 A/T		
Chassis	Steering		Rack and pinion (with power assistance)							
	Suspension	Front	Independent (double wishbones and coil springs)							
		Rear	Independent (multilink; double wishbones and coil springs)							
	Brakes	Front	16-inch ventilated discs (2-pot)				17-inch ventilated discs (4-opposed-pot)			
		Rear	16-inch ventilated discs (1-pot)				17-inch ventilated discs (1-pot)			
	Tires		265/70R16			265/65R17		265/60R18		

## NEW PRODUCTS

Specifications			Model	3-door model		
			Mitsubishi CBA-V83W		Mitsubishi CBA-V87W	
			Super Select 4WD II			
			VR-I		VR-II	
			MNUV		MRUV	
Dimensions and weight	Overall length (mm)		4,385			
	Overall width (mm)		1,845		1,875	
	Overall height (mm)		1,850			
	Wheelbase (mm)		2,545			
	Tread	Front (mm)	1,560			
		Rear (mm)	1,560			
	Minimum ground clearance (mm)		225			
	Interior length (mm)		1,830			
	Interior width (mm)		1,525			
	Interior height (mm)		1,225			
	Vehicle weight (kg)		1,900		2,010	
Seating capacity (persons)		5				
Performance	Minimum turning radius (m)		5.3			
	10-15-mode fuel economy (km/L) (as verified by Ministry of Land, Infrastructure and Transport)		8.9	8.6		7.9
	Major fuel economy enhancing measure		—	ATF warmer		Valve timing electronic control system and ATF warmer
Engine	Model		6G72 (ECI-MULTI)		6G75 (MIVEC)	
	Valve mechanism and number of cylinders		SOHC, 24-valve, V6			
	Maximum output (net) {kW (PS)/min <sup>-1</sup> }		131 (178)/5,250		183 (249)/6,000	
	Maximum torque (net) {N·m (kgf·m)/min <sup>-1</sup> }		261 (26.6)/4,000		338 (34.5)/2,750	
Transmission	Transmission type		5 M/T	INVECS-II Sports Mode 4 A/T		INVECS-II Sports Mode 5 A/T
Chassis	Steering		Rack and pinion (with power assistance)			
	Suspension	Front	Independent (double wishbones and coil springs)			
		Rear	Independent (multilink; double wishbones and coil springs)			
	Brakes	Front	16-inch ventilated discs (2-pot)			
		Rear	16-inch ventilated discs (1-pot)			
	Tires		265/70R16		265/60R18	

(RV1 Product Development Project, Product Development Group Headquarters: Tanaka, Nishioka, Sato)



The new Mitsubishi DELICA D:5 is a monobox type minivan that's unique in that it combines the sturdiness of a sport utility vehicle (SUV) with the user-friendliness of a minivan and is based on the same platform as the OUTLANDER. Representing a proposal for a vehicle that supports knitting family or relatives and amusing with nature, it was launched on 31 January 2007 in Japan market.

## 1. Targets

In developing the new DELICA D:5, the main target was set active families who spend their leisure time outdoors with relatives or friends. Amid diversification of customer priorities, Mitsubishi Motors Corporation (MMC) focused on relax, high quality and symbiosis. While carrying forward the highly regarded all-terrain performance of the previous model, DELICA SPACEGEAR, MMC developed the new DELICA D:5 with an emphasis on the following product features:

- comfort during both long journeys and city trips
- equipment that delivers relax and peace of mind to all passengers
- ecology and safety devices

## 2. Features

### 2.1 Exterior design (Figs. 1 and 2)

Eighteen-inch alloy wheels that accentuate the vehicle toughness are located in the corners of the simple and solid shape body, with the result the vehicle communicates high level of dynamism and mobility. While the straight-line-themed body design will remain freshness to users over long period, the headlamps and rear combination lamps are precisely crafted to convey a sense of sophistication.

The new DELICA D:5 is available in seven two-tone body color schemes and seven monotone body colors including a newly introduced Jade Green Mica.

### 2.2 Interior design (Figs. 3 and 4)

The two resin overhead garnishes and the pillar trims form a rib-frame-look figure that visually conveys a sense of shelter to protect occupants. The indirect lighting illuminations using 13 LED lights including that incorporate in the overhead garnishes (5 LED in case of sunroof model) realize a unique interior appearance both in daytime and night.

Multi-use hooks are provided at many positions in



Fig. 1 Exterior: Front view



Fig. 2 Exterior: Rear view

the cabin, to allow users to customize the space using accessories according with their idea.

There are two interior color choices: dark gray, which convey a sense of functionality, and beige, a sense of sophistication.

### 2.3 Packaging

For superior all-terrain performance, the minimum ground clearance (210 mm) and large approach, ramp-breakover and departure angles realize underbody clearance comparable with that of SUVs.

A high eye point and large front quarter windows gives the driver good visibility in the A-pillar areas. Also, the 340 mm fore-aft slide range for each of separate (left- and right- hand) third row seats with the long wheelbase that's 180 mm longer than that of OUTLANDER makes ample luggage area capacity and ample foot space for third-row passengers available.



Fig. 3 Instrument panel design

## 2.4 Strong, gentle performance

The new DELICA D:5 has an electronically controlled four-wheel drive (4WD) system based on that of the OUTLANDER. MMC refined the software from the OUTLANDER as follows:

- 4WD mode: In accordance with the different wheel-base and vehicle weight, the proportion of torque directed to the rear wheels is greater during uphill driving and smaller during steering maneuvers. The results are better hill-climbing performance and cornering stability.
- LOCK mode: The system senses when wheels on diagonally opposite corners are in danger of spinning without traction during vehicle operation at low speeds. It responds by activating a brake traction control function at lower speeds than the system in the OUTLANDER, thereby improving all-terrain performance at low speeds.

New 225/55R18 tires were specially developed for the new DELICA D:5. The tires help to realize high handling stability despite the vehicle's tall monobox proportions, and they realize a soft, smooth ride despite their low profile.

## 2.5 Strong body structure

A tall monobox minivan body with large door openings typically suffers from low body rigidity, which adversely affects handling stability and ride comfort and tends to detract from the fit of the doors over time. To minimize such problems with the new DELICA D:5, MMC enclosed the entire body within a ring-like frame by adopting the following measures:

- Larger under-floor cross-members
- More rigid joints between the pillars and roof
- A closed-section structure around the entire body

The results are greatly improved body rigidity and concomitantly improved handling stability, ride comfort, and durability.



Fig. 4 Interior design

## 2.6 Healthy "cocochi-interior"

With "clean", "stress-free", and "restful and safe" as its key words, MMC introduced a unique "cocochi-interior" concept to give the new DELICA D:5 a healthy, comfortable interior environment.

Specific equipment items include a deodorizing roof liner; an odor-removing air filter; water- and oil-repelling seat fabric; ultraviolet- and heat-blocking windshield glass; and water-repelling door-window glass.

The deodorizing roof liner and odor-removing air filter help to reduce volatile organic compounds (VOC) in the cabin.

The water- and oil-repelling seat fabric enables ketchup, for example, to be wiped off easily if it is spilled on the seats.

The ultraviolet- and heat-blocking windshield glass absorbs infrared radiation at certain wavelengths, so it can reduce the painful burning sensation that front-seat occupants experience on their skin. It also absorbs ultraviolet radiation, so it can prevent sunburn.

The water-repelling door-window glass (not applicable to certain grades) keeps the door mirrors and other exterior objects visible through the front door windows in rainy weather, so it can reduce stress for drivers.

By incorporating these equipment items in a well-balanced manner, MMC realized a cabin environment that's both healthy and comfortable.

## 2.7 Environmental performance and safety

The engine in the new DELICA D:5 is the 4B12 (2.359 L, DOHC, MPI) MIVEC\* model that's also used in the OUTLANDER. It has variable valve timing on the intake and exhaust sides for high performance and low fuel consumption.

As in the OUTLANDER, the exhaust system is positioned at the rear of the engine. The exhaust layout combines with a double-skin structure for the exhaust manifold and front pipe to hasten the post-startup rise in exhaust temperature for quick catalyzer activation. All DELICA D:5 grades qualify for Japan's "green" tax

reductions by virtue of exhaust emissions that are 75 % lower than those permitted by Japan's 2005 regulations and 10-15-mode fuel economy 10 % better than that required by Japan's 2010 standards.

To protect occupants in the event of a collision, the seatbelts for the driver and front passenger each have a pretensioner and a force limiter. To further enhance safety, all DELICA D:5 grades have front airbags for the driver and front passenger and a knee airbag for the driver. Curtain airbags that cover all three rows of seats are optional. Comprehensive safety equipment also includes a skid-preventing Active Stability Control (ASC) system, which is standard in all grades.

\*: Mitsubishi Innovative Valve timing Electronic Control system

### 2.8 Other features

Other features of the new DELICA D:5 include light-weight and highly dent-proof plastic fenders; Active Cornering Lamps (ACL), which promote nighttime visibility; a Multi Around Monitor, which reduces blind spots around the vehicle; a rear quick heater system, and a high-performance 5.1-channel theater surround system, which delivers powerful, clear sound. For details of the surround system, please refer to the "Development of High Quality 5.1-channel Theater Surround System" in this publication.

### 3. Major specifications

Major specifications are shown in the following table.

## NEW PRODUCTS

Specifications			Model	Mitsubishi DBA-CV5W				
				4WD				
				M	G	G POWER Pkg.	G NAVI Pkg.	G PREMIUM
Dimensions and weights	Overall length	(mm)	4,730					
	Overall width	(mm)	1,795					
	Overall height	(mm)	1,870					
	Wheelbase	(mm)	2,850					
	Tread	Front	(mm)	1,540				
		Rear	(mm)	1,540				
	Minimum ground clearance	(mm)	210					
	Interior length	(mm)	2,915					
	Interior width	(mm)	1,505					
	Interior height* <sup>1</sup>	(mm)	1,310					
	Vehicle weight* <sup>2</sup>	(kg)	1,770* <sup>3</sup>		1,780		1,800	
	Seating capacity	(persons)	8					
Gross vehicle weight* <sup>2</sup>	(kg)	2,210* <sup>3</sup>		2,220		2,240		
Performance	Minimum turning radius	(m)	5.6					
	10-15-mode fuel economy (as verified by Japan's Ministry of Land, Infrastructure and Transport)	(km/L)	10.4					
Engine	Model		4B12 D4 MIVEC					
	Valve mechanism and number of cylinders		DOHC; 16 valves; four cylinders					
	Bore x stroke	(mm)	88.0 x 97					
	Displacement	(cc)	2,359					
	Compression ratio		10.5					
	Maximum output (net)	{kW (PS)/min <sup>-1</sup> }	125 (170)/6,000					
	Maximum torque (net)	{N·m (kgf·m)/min <sup>-1</sup> }	226 (23.0)/4,100					
	Fuel supply		MPI					
	Fuel		Unleaded regular gasoline					
Fuel-tank capacity	(L)	66						
Chassis	Transmission		INVECS-III six-speed continuously variable transmission					
	Steering		Rack and pinion (with power assistance)					
	Suspension	Front	MacPherson-strut					
		Rear	Multilink					
	Brakes	Front	Ventilated disc (16-inch)					
		Rear	Drum in disc (16-inch)					
	Tires		215/70R16	225/55R18				

\*1: With triple sunroofs, the interior height is 1,275 mm.

\*2: Triple sunroofs add 30 kg to the indicated weight. Curtain airbags add 10 kg to the indicated weight.

\*3: Left and right powered sliding doors and a powered tailgate add 10 kg to the indicated weight. A high-grade audio system adds 10 kg to the indicated weight.

(C-seg Product Development Project, Product Development Group Headquarters: Nomura, Yamamoto, Yamauchi, Watanabe)



## LANCER EVOLUTION IX MR and LANCER EVOLUTION WAGON MR



Fig. 1 LANCER EVOLUTION IX MR



Fig. 2 LANCER EVOLUTION WAGON MR

The LANCER EVOLUTION IX MR and LANCER EVOLUTION WAGON MR (Figs. 1 and 2) are the latest models in the continually evolving LANCER EVOLUTION series, which has established an unmatched track record in top international and Japanese motorsport events including years of dominance in the World Rally Championship since the launch of the first-generation LANCER EVOLUTION in October 1992. These models represent the culmination of the third LANCER EVOLUTION generation and are the last to be powered by the famed 4G63 2L DOHC intercooled turbo engine.

Mitsubishi Motors Corporation (MMC) launched both models on 29 August 2006.

### 1. Targets

In developing the new models, MMC sought to create a further-elevated 'premium-sports' identity by using know-how gained in motorsport participation to deliver superlative levels of on-road sports driving performance and by revising the exterior and interior designs for a stronger sense of quality.

### 2. Features

#### (1) Exterior and interior



Fig. 3 Piano-black panel

On the exterior, a newly designed front airdam creates a tougher, more aggressive appearance and improves aerodynamic performance by reducing air resistance and front lift. Also, the trunk lid carries a glossy red 'MR' emblem to indicate the MR designation that MMC gives only to its most prominent sports vehicles. As a factory option, both models can be ordered with BBS forged-aluminum wheels, which have a metallic-texture paint that further enhances the premium look.

In the cabin, the instrument panel is finished with piano-black paint that gives it a look of depth. Each front door opening has an aluminum scuff plate bearing the 'LANCER Evolution' logo. Also, the front RECARO seats and rear seat are upholstered with a combination of leather and Alcantara with red stitches for an even stronger 'premium sports' identity (Figs. 3 and 4).

#### (2) Improved 4G63 engine

A reduced diameter for the turbocharger's compressor inlet combines with newly fine-tuned MIVEC\*<sup>1</sup> valve-timing control for improved throttle response.

With the sedan GSR and RS grades and the wagon GT grade, a change in the standard material for the turbocharger's turbine wheel from Inconel(R) (a nickel-chrome alloy) to a titanium-aluminum alloy realizes a further improvement in response. Maximum output



Fig. 4 Scuff plate

and maximum torque are unchanged in numerical terms, but off-the-line acceleration is better than that of the previous models.

For the sedan GSR and RS grades, a high-performance turbocharger with a magnesium-alloy compressor wheel is available as a factory option.

\*1: Mitsubishi Innovative Valve timing Electronic Control system

### (3) Suspension and four-wheel drive (4WD) systems

A reduction of 10 mm in ride height realizes superior handling stability on tarmac. Also, Eibach coil springs (**Fig. 5**), which offer a supple ride and are widely used in Formula One and other forms of motorsport, are employed in the suspension system.

Handling performance and ride quality are further enhanced by revised spring rates and optimized Bilstein shock absorbers.

In the sedan, improved cornering performance is realized by a 10 % increase in the amount of torque that can be transferred between the left and right wheels by the 4WD system's Super Active Yaw Control (AYC) function. Also, the control effected by the Active Center Differential (ACD) is newly fine-tuned to match the new suspension settings. (The AYC function is standard with the GSR grade and optional with the RS grade.)

## 3. Models and grades

The LANCER EVOLUTION IX MR is available in two grades: the GSR, which has a six-speed manual transmission and is designed for excellence in everyday con-



**Fig. 5 Suspension system**

ditions and in sports driving, and the RS, which has a five-speed manual transmission and is stripped down for motorsport competition. The LANCER EVOLUTION WAGON MR is also available in two grades: the GT, which has a six-speed manual transmission that allows users to enjoy sports driving to the fullest, and the GT-A, which has a five-speed automatic transmission with sports mode for flexibility in a wide range of scenarios from easygoing driving to sports driving.

## 4. Major specifications

Major specifications are shown in the following table.

Specifications			Model		LANCER EVOLUTION IX MR		LANCER EVOLUTION WAGON MR						
					Mitsubishi GH-CT9A		Mitsubishi GH-CT9W						
					Full-time 4WD								
					GSR [6 M/T]		RS [5 M/T]		GT [6 M/T]		GT-A [5 A/T]		
Seating capacity			(persons)		5								
Dimensions	Overall length		(mm)		4,490			4,520		4,530			
	Overall width		(mm)		1,770								
	Overall height		(mm)		1,440		1,450		1,480				
	Wheelbase		(mm)		2,625								
	Tread	Front	(mm)		1,515		1,500		1,515				
		Rear	(mm)		1,515		1,500		1,515				
Minimum ground clearance			(mm)		130		140						
Engine	Model			4G63 with MIVEC and turbocharger							4G63 with turbocharger		
	Valve mechanism and number of cylinders			DOHC; 16 valves; variable valve timing; four in-line cylinders							DOHC; 16 valves; four in-line cylinders		
	Displacement			(cc)		1,997							
	Maximum output (net)			{kW (ps) /min <sup>-1</sup> }		206 (280)/6,500					200 (272)/6,500		
	Maximum torque (net) {N·m (kgf·m) /min <sup>-1</sup> }					400 (40.8)/3,000		407 (41.5)/3,000		392 (40.0)/3,000		343 (35.0)/3,000	
	Fuel supply			ECI-MULTI (electronically controlled fuel injection)									
Chassis	Steering			Rack and pinion (with power assistance)									
	Suspension	Front	MacPherson-strut										
		Rear	Multilink										
	Brakes	Front	Ventilated discs (GSR: 17-inch; RS: 15-inch)					Ventilated discs (17-inch)					
		Rear	Ventilated discs (GSR: 16-inch; RS: 15-inch)					Ventilated discs (16-inch)					
	Tires					235/45ZR17		205/65R15		235/45R17 93W			

(C-seg Product Development Project, Product Development Group Headquarters: Watanabe)

## INTERNATIONAL NETWORK

### **Mitsubishi Motors North America, Inc. (MMNA)**

6400 West Katella Avenue Cypress,  
California 90630-0064, U.S.A.  
Phone: 1-714-372-6000  
Fax: 1-714-373-1020

### **MMNA (Manufacturing)**

100 North Mitsubishi Motorway Normal,  
Illinois 61761, U.S.A.  
Phone: 1-309-888-8000  
Telefax: 1-309-888-8154

### **Mitsubishi Motors R&D of America, Inc. (MRDA)**

3735, Varsity Drive, Ann Arbor, Michigan  
48108, U.S.A.  
Phone: 734-971-0900  
Fax: 734-971-0901

### **Mitsubishi Motor Sales of Canada, Inc.**

2090 Matheson Blvd. E., Mississauga,  
ON L4W 5P8  
Phone: 1-888-576-4878

### **Mitsubishi Motor Sales of Caribbean, Inc.**

Road 2 Km. 20.1 Candelaria Ward Toa Baja,  
Puerto Rico 00949  
(P.O. Box 192216 San Juan, PR 00919-2216)  
Phone: 1-787-251-5591  
Fax: 1-787-251-2953

### **Netherlands Car B.V. (NedCar)**

Dr. Hub van Doorneweg 1,  
6121 RD Born, THE NETHERLANDS  
Phone: 31-46-489-4444  
Fax: 31-46-489-5488

### **Mitsubishi Motors Europe B.V.**

Beech Avenue 150 1119 PR Schiphol-Rijk,  
THE NETHERLANDS  
(P.O. Box 22922, 1100 DK Amsterdam Zuidoost)  
Phone: 31-20-4468111  
Fax: 31-20-4468143

### **Mitsubishi Motor Sales Nederland B.V.**

Beech Avenue 150, 1119 PR Schiphol-Rijk,  
THE NETHERLANDS  
(P.O. Box 22934, 1100 DK, Amsterdam Zuidoost)  
Phone: 31-20-8512277  
Fax: 31-20-6541485  
email: klanteninfo@mmsn.nl

### **Mitsubishi Motors Deutschland (GmbH)**

Philipp-Reis-Strasse 4, 65795  
Hattersheim, GERMANY  
Phone: 49-6190-9260  
Fax: 49-1805-747329222

### **Mitsubishi Motor R&D of Europe GmbH (MRDE)**

Diamant-Strasse 1 65468 Trebur 2  
FEDERAL REPUBLIC OF GERMANY  
Phone: 49-6147-9141-0  
Fax: 49-6147-3312

### **Mitsubishi Motors Corporation France SAS**

9 Chausse Jules Csar, BP 10051 OSNY, 95521  
CERGY PONTOISE Cedex, FRANCE  
Phone: 33-1 34 35 84 00

### **Mitsubishi Motors Belgium N.V.**

Uitbreidingsstraat 2-8,  
2600 Berchem, BELGIUM  
Phone: 32-3-280-8484  
Fax: 32-3-280-8485

### **Mitsubishi Motors de Portugal, S.A.**

Rua. Dr. Jos-Espirito Santo, 38, 1950-097 Lisboa,  
PORTUGAL  
Phone: 351-218-312-100  
Fax: 351-218-312-232

### **Mitsubishi Motors Australia, Ltd. (MMAL)**

1284 South Road, Clovelly Park  
South Australia, 5042, AUSTRALIA  
(P.O. Box 8, Melrose Park SA 5039)  
Phone: 61-8-82757111  
Fax: 61-8-82756841

### **Mitsubishi Motors New Zealand, Ltd.**

Private Bag 50914, Porirua, NEW ZEALAND  
Phone: 64-4-237-2439  
Fax: 64-4-237-4495

### **Mitsubishi Motors (Thailand) Co., Ltd. (MMTh)**

88 Mu 11, Phaholyothin Road, Klongneung,  
Klongluang, Phatumthani Province Thailand 12120  
Phone: 66-2-908-8000  
Fax: 66-2-908-8285

### **Mitsubishi Motors Philippines Corporation (MMPC)**

Ortigas Avenue Extension, Cainta, Rizal,  
PHILIPPINES  
Phone: 63-2-658-0109  
Fax: 63-2-658-0671

# MITSUBISHI MOTORS CORPORATION

- **Head Office**  
33-8, Shiba 5-chome, Minato-ku, Tokyo 108-8410, Japan  
Phone: +81-3-3456-1111  
Telefax: +81-3-6852-5420
- **Design Center**  
**Tama Design Center**  
1-16-1, Karakida, Tama-shi, Tokyo 206-0035, Japan  
Phone: +81-423-89-7307
- **Engineering Offices**  
**Research & Development Office**  
1, Nakashinkiri, Hashime-cho, Okazaki-shi, Aichi Pref. 444-8501, Japan  
Phone: +81-564-31-3100  
[Tokachi Proving Ground]  
22-1, Osarushi, Otofuke-cho, Kato-gun, Hokkaido 080-0271, Japan  
Phone: +81-155-32-7111
- **Plants**  
**Nagoya Plant**  
1, Nakashinkiri, Hashime-cho, Okazaki-shi, Aichi Pref. 444-8501, Japan  
Phone: +81-564-31-3100  
**Powertrain Plant**  
[Powertrain Plant – Kyoto]  
1, Uzumasa Tatsumi-cho, Ukyo-ku, Kyoto-shi 616-8501, Japan  
Phone: +81-75-864-8000  
[Powertrain Plant – Shiga]  
2-1, Kosuna-cho, Konan-shi, Shiga Pref. 520-3212, Japan  
Phone: +81-748-75-3131  
**Mizushima Plant**  
1-1, Mizushima Kaigandori, Kurashiki-shi, Okayama Pref. 712-8501, Japan  
Phone: +81-86-444-4114
- **Pajero Manufacturing Co., Ltd.**  
2079, Sakagura, Sakahogi-cho, Kamo-gun, Gifu Pref. 505-8505, Japan  
Phone: +81-574-28-5100

We welcome e-mail inquiries about this publication at:  
[technicalreview.et@mitsubishi-motors.com](mailto:technicalreview.et@mitsubishi-motors.com)



